Protein Surface Recognition by Polymers

Dissertation

by

Wei Sun

Essen, 2009

Protein Surface Recognition by Polymers

Dissertation

by

Wei Sun

Birth Place: Shenyang / China

In Partial Fulfillment of the
Requirements for the Degree
Doctor of Chemistry
(Dr. rer. nat.)

Department of Chemistry
University Duisburg-Essen

January, 2009

This work is submitted at 30th January, 2009 and is accepted at 24th February, 2009 by the department of chemistry in the university of Duisburg-Essen in Germany. The oral defence is at 24^{t}h March, 2009.

Chairman: Prof. Dr. Stephan Shulz
Reviewer: Prof. Dr. Thomas Schrader
Reviewer: Prof. Dr. Mathias Ulbricht

To my family

This work was performed during the period from October 2005 to August 2006 at the institute of organic chemistry, University Marburg, and from September 2006 to January 2009 at the institute of organic chemistry, University Duisburg-Essen, under the supervision of Prof. Dr. Thomas Schrader.

I declare that this dissertation represents my own work, except where due acknowledgement is made.

Wei Sun

Eidesstattliche Erklärung

Hiermit versichere ich, die vorliegende Arbeit mit dem Titel

„ Protein Surface Recognition by polymers „

selbst verfasst und keine ausser den angegebenen Hifsmitteln und Quellen verwendet zu haben.

Zudem erkläre ich, dass ich die Arbeit in dieser order ähnlicher Form bei Keiner anderen Fakultät eingereicht habe.

Essen, im Janur 2009,

Wei Sun

Acknowledgement

A number of colleagues, friends, and family members are instrumental in helping me complete my Ph.D. research and deserve proper thanks. First and foremost, I would like to pay my gratitude to Prof. Dr. Thomas Schrader for providing this interesting project and for his supervision. His kind support in other parts of life is also, highly acknowledged.

I am thankful to Prof. Dr. Mathias Ulbricht for reviewing my thesis.

I am also indebted to all members of my research group for their friendship and help. Especially, I would like to thank Christian Renner, Kirstian Wenck, Marc Blecking, Caroline Breitkreuz, for their kind suggestions in my work and friendly help during my living in Marburg and Essen. I would also like to thank Heinz Bandmann and Dr. Torsten Schaller for the NMR measurement; Heike woell for the HPLC, Film balance measurement and peptide synthesis; Ingeborg Reiter for her kind advices and help; Klaus Kowoski for the ITC measurement.

I would like to thank all the technical departments in the university of Duisburg-Essen, especially the MS department for the mass spectrum measurement, and Dieter Jacobi for the GPC measurement. The same thank goes to all the technical departments in the University of Marburg for their help during my first year Ph.D study there.

I would like to thank Prof. Dr. Börje Sellergren and Dr. Eric Schillinger for their kind cooperation.

Last but not least, I would like to thank my family, especially my wife, Jing Xu. Without their loving guidance, encouragement, and support, I would certainly not have been capable of enduring a Ph.D. degree program.

Abstract

Recognition of protein surfaces using synthetic receptors is an effective strategy for providing access to enzyme inhibitors, protein antagonists, and diagnostic biosensors. In the artificial protein receptors, polymers represent promising fields due to their sizes (commensurate with proteins) and the ability to tailor a wide range of functionalities. Furthermore, the ability of polymers to adapt their conformations to protein surfaces renders them attractive candidates for protein surface binding.

This work emphasized firstly on the synthesis of functional monomers which are specific for the amino acid residues on protein surfaces, and then on the development of polymers which can recognize protein surfaces in aqueous solution tightly and selectively.

Eighteen monomers were prepared by multi-step synthesis. The interactions between their functional groups and amino acid residues covered several binding motifs in molecular recognition: hydrogen bond, electrostatic, hydrophobic, metal-ligand and π-cation interaction. For the later polymerization, these functional groups were incorporated with polymerizable structures. Thirteen of them were based on methylacylamide, and the other five were based on a 10, 12- tricosadiyne structure.

Functional monomers based on methylacrylamide were polymerized by radical polymerization under heat or UV light in organic solvent or aqueous solution, with AIBN, V-50, benzophenone or ammonium persulfate as initiators. In some cases polymer lengths were controlled by RAFT method with water-soluble *S, S´*-bis(α,α'- dimethyl-α''acetic acid)-trithiocarbonate as the chain transfer reagent (CTA) in aqueous buffer. Functional monomers based on a 10, 12-tricosadiyne structure composed of two parts: a polar functional headgroup and a hydrophobic tail containing the diacetylene moiety. The polymerization could proceed without any initiator, only when the diacetylenes were arranged in a lattice with appropriate geometry, ex., at water-air surface or in the form of liposome.

In this work, polymers were prepared mainly in several forms: dendrimers, linear polymers, grafted polymers on PET membrane and crosslinked polymer materials. The binding events between these polymers and proteins were studied either in solution or at interface by fluorescence, UV, ITC titrations, BCA assay, HPLC and computer modeling.

To prepare the dendrimers, the lysine and arginine specific monomer, bisphosphonate dilithium salt, was incorporated on the periphery of different polypropyleneimine (PPI) generations by reductive amination with $NaBH_4$. They were purified with dialysis with a 1 KDa membrane. Their ^{1}H and ^{31}P NMR spectra in D_2O displayed clear sets of slightly broadened signals, however MALDI TOF-MS showed that the dendrimers were not monodisperse. The binding events between proteins/peptides and these dendrimers were studied in buffered aqueous solution by three different spectroscopic methods (PFGLED, UV/Vis, and fluorescence). Results showed that the single weak binder (Ka in pure water $<10\ M^{-1}$) was turned into powerful dendrimeric receptors for basic proteins (K_D <250 nM for the hexadecamer and histone H1), and the binding affinity and stoichimetry didn't only depend on the dendrimer size, but also on the size and distribution of basic domains on protein surfaces.

Series of linear copolymers were prepared with methylacrylamide based monomers by radical polymerization under 60°C with AIBN or V-50 as initiators. After preparation the polymers were purified by precipitation in ethylacetate and in some cases by dialysis. Several copolymers decorated with o-aminomethylphenylboronates for covalent ester formation and/or alkylammonium ions for noncovalent Coulomb attraction, showed exceptionally high affinities for a series of glycans: heparin, chondroitin-4-sulfate, hyaluronic acid and dextran. Heparin, a constant repeat of a 1, 4-glycosidic sugar dimer, carrying hydroxycarboxylates (iduronic acids) and hydroxysulfates (glucosamine), could be quantitatively detected with an unprecedented 30 nM sensitivity. One of these polymers was used to develop a fluorescence microplate assay for quantification of heparins and other sulfated carbohydrates by a cooperation group from Kiel, Germany. Based on these results, we proposed a new 7-member-ring binding scheme between the boronate and a sulfated ethylene glycol or aminoethanol unit, and this propose was studied by NMR titration and computer modeling

with D-glucosamine 2-sulfate sodium salt (a fragment of heparin) and 1:1 complex of phenylboronic acid and piperidine.

For the preparation of affinity membrane, track-etched PET400 membrane was grafted with a copolymer with 1:4 of bisphosphonate ester monomer and amino alcohol monomer via a synergist immobilization method from acetonitrile solution. In the synergist immobilization method, the synergist (tertiary amino groups) for photo-initiator benzophenone (BP) was introduced onto the membrane surface via an aminolysis reaction with diethylenediamine (DEEDA). The polymer formation was examined with solid state ^{31}P NMR spectrum, contact angle and water permeability measurements. The resulting affinity membrane showed high binding capacity for selected proteins. Especially, it was found that markedly higher binding capacity and affinity have been achieved for lysozyme than for cytochrome C, both proteins with similar pI value and protein size. With this affinity membrane, the protein separation has been realized in the 1:1 mixture solution of lysozyme and cytochrome C with a very high selectivity.

Crosslinked polymer materials for protein recognition and separation were developed in two ways, water-soluble microgels and MIPs (molecular imprinting polymers).

All microgels were prepared by radical copolymerization in dilute aqueous solution. A typical monomer feed composition consisted of 80 mol% *N*-isopropylacrylamide, 10 mol% of crosslinker methyl bisacrylamide, and 10 mol% of an anionic comonomer such as sodium methacrylate, tetrazolate or bisphosphonate. Polymerizations were carried out at 70°C in the presence of a surfactant (sodium dodecylsulfate) and an initiator (ammonium persulfate). Microgels were subsequently purified by ultrafiltration against deionized water, using cross-flow membranes with a 100 kDa and 2 mm cut-off, to remove low-molecular-weight impurities and macroscopic gel particles, respectively. ITC titrations showed that they could recognize protein guests in buffered aqueous solution at neutral pH with K_a values of up to 10^{11} M^{-1} (averaged affinity towards each single protein). Switching between the functionalities

allowed distinction between basic proteins of similar PI and size. Nearly all the other bindings was entropy driving.

The research of MIPs with IgG as the final recognition target is still being under research. In this thesis only a little finished part is introduced. In the previous work, an exposed 9-mer fragment from IgG C-terminal was used as a template, and for comparing imprinting effects, a shorter peptide with only six amino acids but having more effective binding sites with respective to my monomers, as the other template. MIPs were prepared with ethylenebisacrylamide (crosslinker), methacrylamide (comonomer) and functional monomers in 10 mM hepes buffer on a microplate with the aiding of a liquid-handling robot. Until now only one functional monomer was used for each MIPs. For each functional monomer, six polymers were prepared. Three of them were MIPs (with template in polymerization) with varied crosslinker percentages (20%, 50% and 70%), and the other three were corresponding NIPs (without template in polymerization) as references. After the preparation, polymers were washed with buffer and 10 nM HCl solution until no residue signal could be observed in HPLC measurement. The following rebinding experiments were performed at three concentrations, 50 μM, 500 μM and 5000 μM of the template. The total template amount in 5000 μM solution was same as the original used in MIPs preparation. Between each rebinding, polymers were washed as described above. All rebinding experiments were monitored by HPLC and BCA assay. Results showed that several monomers had comparatively good imprinting effects. The larger template showed a better effect than the shorter one. No apparent difference was observed for the three crosslinker percentages. These results provided us much information for the further development.

Contents

1 Introduction

Recognition of protein surfaces using synthetic receptors is an effective strategy for regulating protein-protein and protein-substrate interactions.[1] The successful development of these receptors can also provide access to new classes of enzyme inhibitors,[2] protein antagonists,[3] and diagnostic biosensors.[4] While designing ligands for a concave site of a protein is relatively easily conceived, design of molecules to recognize the solvent exposed surface area of proteins is challenging due to their large surface area,[5] and the presence of divergent functional groups on the surface of a protein. For efficient and selective molecular recognition processes on surfaces, nature often applies the concept of multivalency.[6]

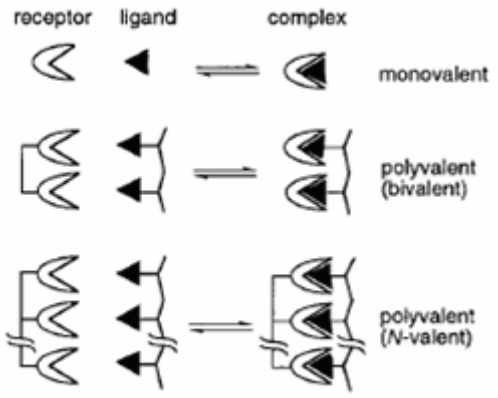

Figure 1.1 *Schematic monovalent and polyvalent interactions.*[5]

Multivalency (polyvalent interaction) is characterized by the simultaneous binding of multiple ligands on one biological entity (a molecule, a surface) to multiple receptors on another (Figure 1.1). These interactions have a number of characteristics that monovalent interactions do not. In particular, polyvalent interactions can be collectively much stronger than corresponding monovalent interactions, and they can provide the basis for mechanisms of both agonizing and antagonizing biological interactions that are fundamentally different from those available in monovalent systems.[6]

Polyvalent interactions have three types. A binding event is defined as positively cooperative with respect to a second interaction if its affinity is increased in the presence of that second interaction. Conversely, a binding event is negatively cooperative if its affinity is decreased in the presence of that second interaction (Figure 1.2). The third situation is non-cooperative if the two interactions don't affect each other. In protein surface recognition, the general

expectation for a positively cooperative binding event is the tightening of protein structure with a resulting gain in enthalpy and loss in entropy. An example is the formation of the biotin–streptavidin complex.[7] In negatively cooperative ligand binding, the interacting partners become more dynamic, with an associated loss in enthalpy and gain in entropy. Williams et al. show that O_2 binds to hemoglobin in a negatively cooperative manner.[8]

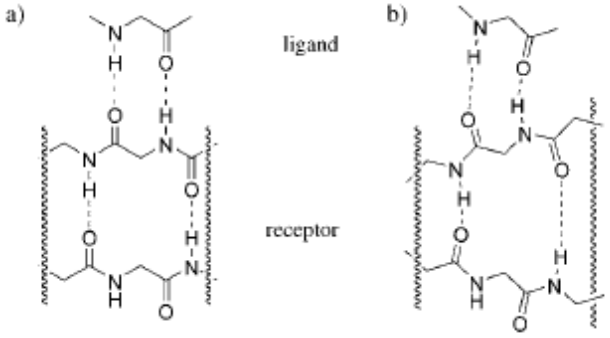

Figure 1.2 *Structural models for a) positive and b) negative cooperativity; the lower pair of hydrogen bonds is within a protein receptor and the upper pair of hydrogen bonds is formed upon the binding of a peptide ligand.*[8]

One example of the positively cooperative multivalency in nature is the recognition of a bacterium by a macrophage. Mannose residues on the tail of the antibody interact with mannose receptors (the Fc receptor) on the surface of a macrophage (a type of white blood cell important for clearing infectious particles). The interaction of a single Fc portion with its

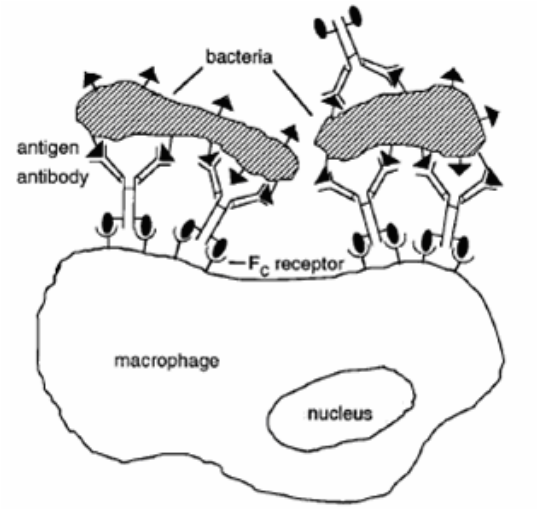

Figure 1.3 *Layered polyvalent binding of a macrophage to bacterium through antibodies;* ● *is the mannose residue.*[9]

receptor seems to be too weak to induce a response by the macrophage, however, multiple antibodies bound to the surface of an infecting particle do interact strongly with multiple receptors on the surface of the macrophage, and give a three-layered structure stabilized at both interfaces.(Figure 1.3).[9,10,11] Thus, polyvalency in this system permits stability and specificity of the recognition.

Multivalency has been also very often applied in artificial receptors. Large molecules with multipoint binding sites may be particularly valuable for cases in which protein surfaces do not possess clear binding sites that may allow high affinity association with small molecules.

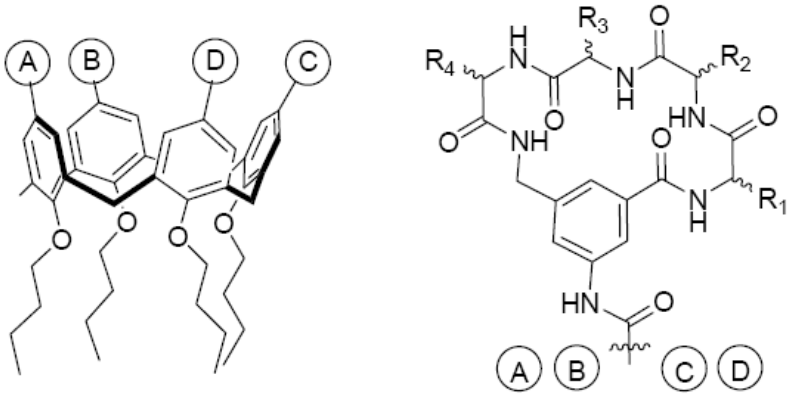

Figure 1.4 *General structure of the calix[4]arene-based antibody mimics.*[12]

An example is a calix[4]arene antibody mimic developed by Hamilton and coworkers.[12,2] The receptors are based on a design in which four peptide loops are arrayed at the upper rim of the calix[4]arene. This kind of receptor has a binding area bigger than 450 $Å^2$ (Figure 1.2). By varying the sequence of the loop regions, a range of differently functionalized receptors can be prepared, which can interact with basic residues on the surface of R-chymotrypsin. The most potent molecule shows slow binding kinetics in an analogous manner to several of the natural protein proteinase inhibitors. In addition, a competitive binding experiment shows that it is able to displace trypsin inhibitor from its 1:1 complex with R-chymotrypsin.

Similarly, Hamilton etl. have developed a receptor for cytochrome C.[13] In cytochrome C, the exposed surface of the heme edge is surrounded by a series of cationic residues. They have demonstrated that this surface can be recognized by receptors designed with tetraphenylporphyrin (TPP) as a scaffold bearing various amino acid and peptide derivatives

on its periphery. One out of them, which has a larger hydrophobic core than others and 16 charges on its periphery, exhibits the strongest affinity with a K_d value of 0.67 nm.

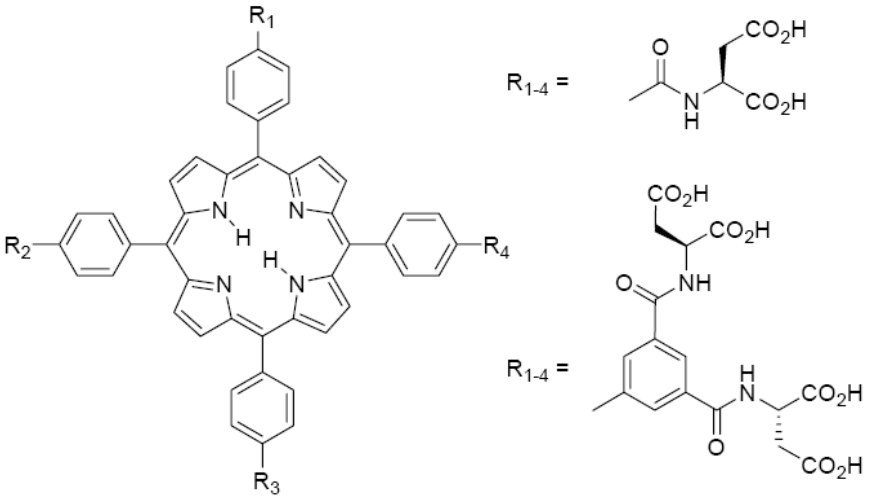

Figure 1.5 *TPP derivatives for the recognition of the exterior surface of cytochrome C.*[13] *Up: with aspartic acid functionalities (K_d = 160 nM). Bottom: a better receptor with biphenyl spacers (K_d = 0.67 nM).*

Hamachi and co-workers employed a related design concept for the recognition of Cytc.[14] A [Ru(bpy)$_3$] complex with carboxylate groups on its periphery was shown to form a complex with Cytc selectively over myoglobin, horseradish peroxidase, and cytochrome b562. This approach offers the advantage of the templating function of metal, with which molecular assembly can be carried out in a stepwise ligation of the individual bipyridine units. With this synthetic strategy, a series of unsymmetrically substituted receptors were prepared; compound 16 (Figure 1.6), the most symmetrical compound, showed the strongest binding. However, investigation of the photoreduction of Cytc catalyzed by these complexes showed 15 (Figure 1.6) to be the most efficient catalyst. This effect was attributed to a balance between the binding of the Ru complexes and accessibility to the sacrificial reducing agent.

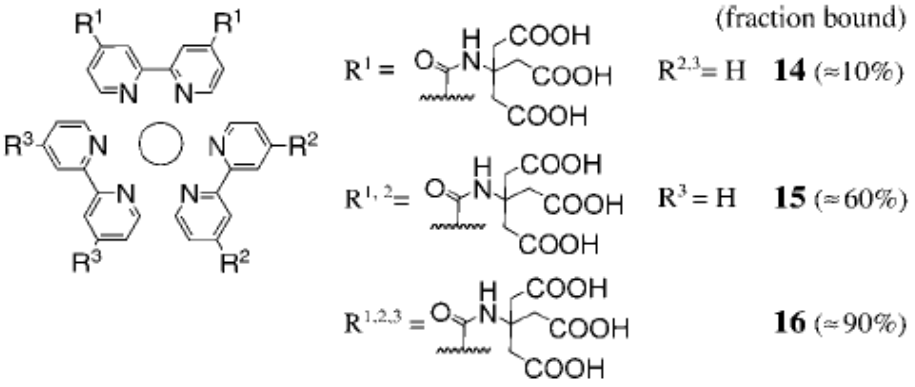

Figure 1.6 *[Ru(bpy)$_3$] complexes that recognize the surface of cytochrome C.*[14]

Polymers and nanoparticles represent promising fields[8] in the artificial protein receptors, due to their sizes (commensurate with proteins) and the ability to tailor a wide range of functionalities. Furthermore, the ability of polymers to adapt their conformations to protein surfaces renders them attractive candidates for protein surface binding.

Rotello and coworkers have developed mixed-monolayer protected gold clusters (MMPCs) functionalized with terminal anionic groups for recognition of the positively charged surface of a chymotrypsin (ChT) (Figure 1.7).[15] Later they found that the enzyme was inhibited by a two-step mechanism that comprised a fast, reversible inhibition step followed by a slower, irreversible process. ChT was released under elevated ionic strength with full enzymatic activity, suggesting a complete restoration of the native structure.[16]

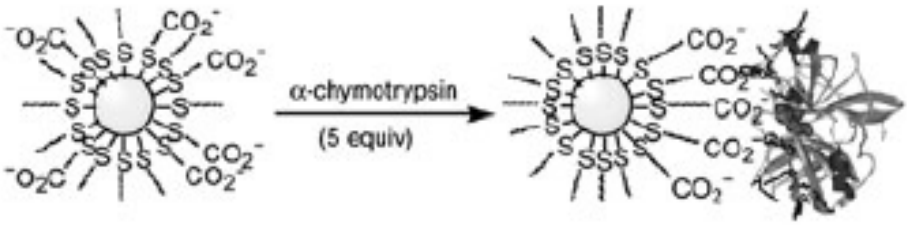

Figure 1.7 *Recognition of the surface of chymotrypsin by the nanoparticle receptor.*[15]

Later, Rotello and Thayumanavan have developed a homopolymer which can not only bind to chymotrypsin by electrostatic interaction with submicromolar affinities in aqueous solution, but also stabilize the native structure of the protein.[17] The binding significantly alters the

enzymatic efficiency of the protein, which is attributed to the fact that the patch with the appropriate charge complementarity is present near the active site of the protein. Also, the electrostatic interaction between the polymer and the protein was used to rescue the enzymatic efficiency by increasing the ionic strength or by releasing the enzyme through addition of a competitive cationic binder for the anionic polymer.

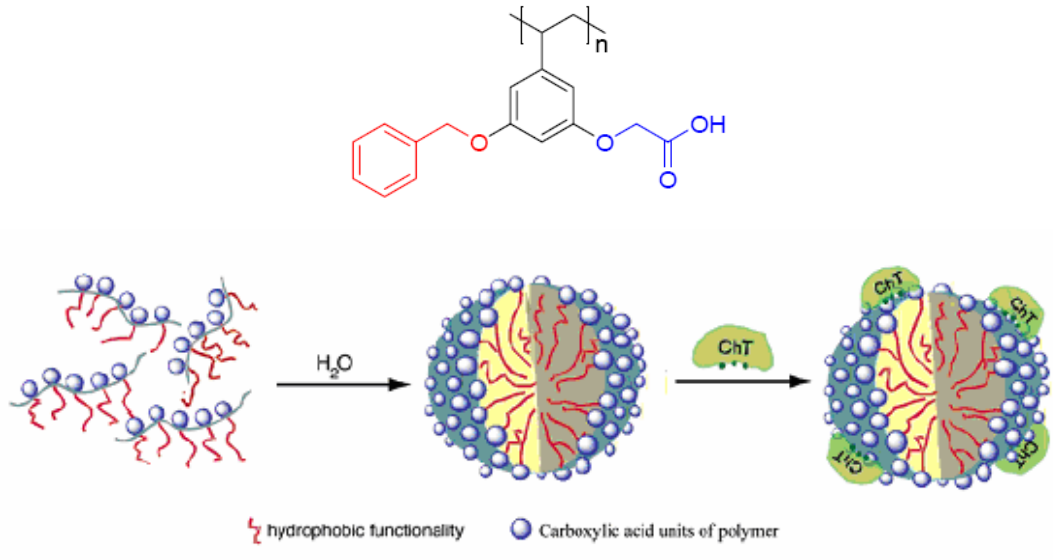

Figure 1.8 *Up: structure of the amphiphilic polymer from Rotello and Thayumanavan. Bottom: Schematic structures of the polymer in water and its complex with chymotrypsin.*[17]

Recently, a promising application of polymers has been developed by our group. C. Renner and S. Koch have turned linear copolymers into protein specific hosts.[18] Several polymers with different functional monomers and different monomer ratios are synthesized and their bindings to proteins are evaluated by fluorescent titrations and Reflectometric interference. Arginine-rich lysozyme is recognized by a bisphosphonate-rich copolymer with a remarkable K_d value of 25 nm, which is 100-times superior to cytochrome c with a comparable size and pI (Figure 1.9).

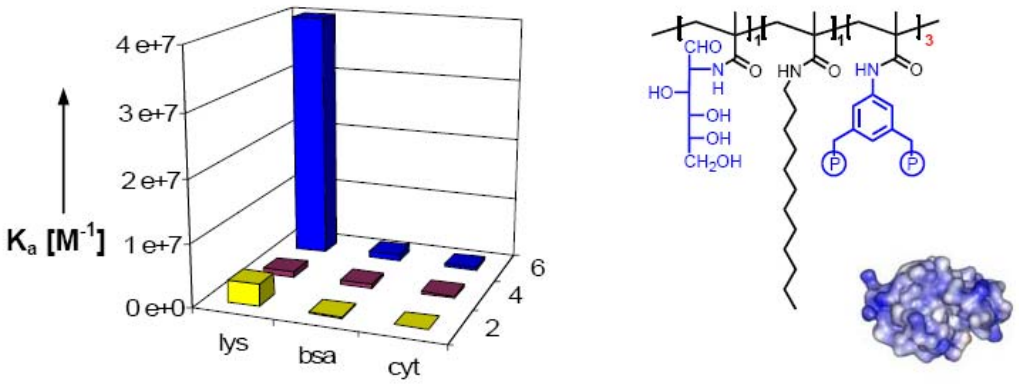

Figure 1.9 *Drastic selectivity of a copolymer to lysozyme. lys=lysozyme, cyt=cytochrome c, P=phosphonate.*[18]

Efficient artificial polymeric protein receptors could be prepared by the technology of molecularly imprinted polymers (MIPs). This interesting concept was proposed by G. Wulff in 1972.[19] Molecularly imprinted polymers (MIPs) are synthetic materials produced by the cross-linking of functional monomers or polymers in the presence of a template molecule. The template is subsequently removed, leaving cavities possessing size, shape, and functional group orientation which are complementary to the target molecule. Thus, the polymers can bind to the template molecule selectively (Figure 1.10).[20]

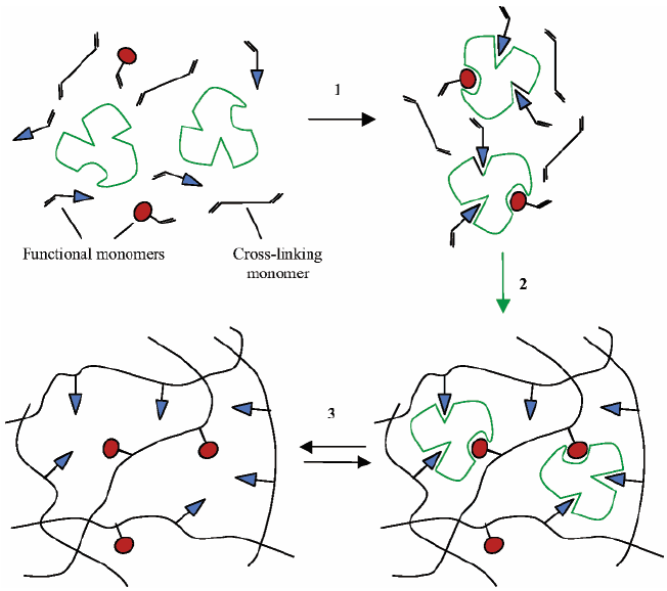

Figure 1.10 *Schematic presentation of MIPs. 1) formation of pre-polymerization complex; 2) polymerization; 3) template removal/rebinding.*[20]

Molecular imprinting is becoming a well-established technology in the field of synthetic molecular recognition, offering a generic, robust, and cost-effective alternative to existing techniques such as monoclonal antibodies. Despite the obvious advantages in the development of MIP systems, there is a paucity of literature on the development of MIPs for the recognition of proteins. When imprinting proteins there are a number of key issues to address that are largely absent when targeting small molecules and these are related to the molecular size, complexity, conformational flexibility, and solubility.[20] To overcome the problems, one proposed method of reducing the complications associated with the imprinting of proteins and peptides has been termed the "epitope approach".[21,22] In this technique, a small sequence of amino acids from the larger protein target molecule is used to create the imprint.

One example of the application of "epitope" methodology was done by Shea and coworkers. They have developed a selective protein capture by epitope imprinting on surface (Figure 1.11). The peptide epitope was covalently attached to a glass or silicon surface. Monomers were then polymerized on these surfaces to produce a molecularly imprinted polymer film. Following separation from the functionalized surface, the polymer film bound and captured the target protein from protein mixtures. The selective recognition of proteins with the special amino acid terminals used in the imprinting have been proved by SDS-PAGE and MALDI-MS.[23]

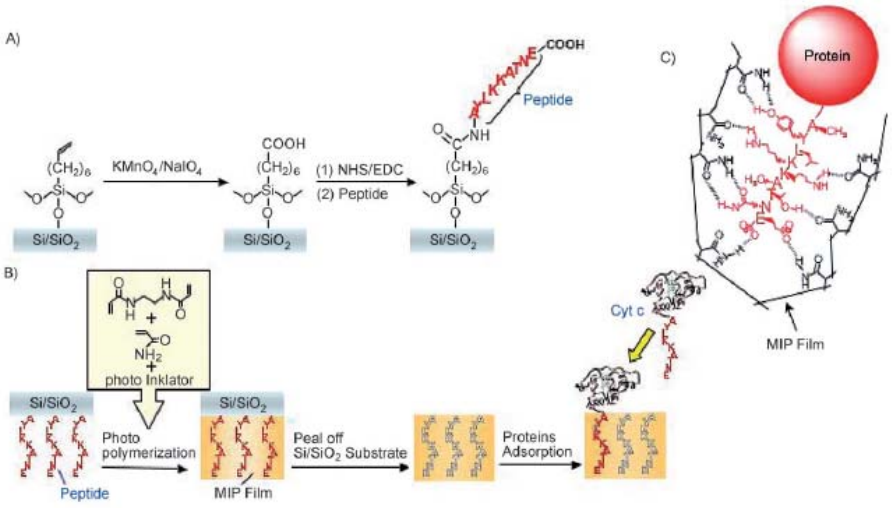

Figure 1.11 *Protocol for template imprinting with protein epitopes. A) Method for glass modification and peptide attachment. B) Illustration outlining MIP film*

fabrication and evaluation. C) Proposed mechanism for the target protein recognition of C-terminus peptide-sequence-imprinted surfaces.[23]

Although many successes have been achieved in the protein recognition, it remains a challenging research field. It is highly probable that a general solution to this protein surface recognition problem will involve molecules with a large surface area and multi-binding sites. Only in this way will the large number of weak interactions be available to overcome the highly solvated character of the protein surface.[1]

2 Objectives

With the concept of multivalency, the general objective of this work was to develop polymers which can recognize protein surfaces selectively and tightly. Good candidates should then be further developed into enzyme inhibitors, biosensors and materials for protein purification. Along this line, several projects were performed in my Ph.D. research.

- Objective 1: to develop dendrimeric bisphosphonates for multivalent protein surface binding.

In recent years our group introduced a m-xylylene bisphosphonate as a receptor unit for lysine and arginine. However, as the binding event relied mostly on electrostatic interactions, even in organic solvents the affinity dropped drastically with increasing solvent polarity. In water, almost no attraction of basic peptides occurred. The question of whether the original high affinity for basic amino acids could be restored in water by applying the concept of multivalency and at the same time impose specificity for accμmulated basic amino acids over isolated arginines or lysines therefore arose. This concept was already applied to make linear polymers by free radical polymerization. However, the polymers were polydisperse, rendering the characterization of the protein binding event problematic. With very uniform structures, dendrimers might be better choices than the above linear polymers. In addition, the control over size and shape provides dendrimers many interesting characteristics. In my work, the m-xylylene bisphosphonate functionality should be incorporated into dendrimers and the binding events between the dendrimers and a series of proteins should be examined.

- Objective 2: to prepare a linear polymer library with different functional monomers tailored for different amino acids, and then screen this library with proteins in order to find best protein binders.

The single binding event in the polyvalent complex between polymers and proteins is the interaction between the monomeric receptor and the amino acid residue. Because the amino acid sidechains existing on a protein surface are highly divergent in their chemical properties, to prepare polymeric protein receptors with significant affinity and good selectivity, there was

a demand to prepare a series of different functional monomers specific for amino acids. Considering the interaction types in molecular recognition, monomers tailored for glutamic acid and aspartic acid (electrostatic interaction), histidine (metal ligand interaction), diols in glycoproteins (covalent ester formation), hydrophobic amino acid residues (hydrophobic interaction) should be synthesized. Afterwards, based on these monomers, a linear copolymer library should be prepared with different monomer combinations. The polymers in the library should be screened with proteins quickly on a microreader plate in order to find the best binding pairs. Best polymer candidates should then be evaluated with enzyme assays, aiming to test their applications as enzyme inhibitors or protein sensors.

- Objective 3: to immobilize linear polymers on a substrate with keeping their affinities to proteins.

In the previous work, when we immobilized an anionic linear polymer to a substrate covered by a cationic polyethyleneimine layer, we observed that the binding on this surface was always weaker (2-3 magnitude order) than that in the solution. In free solution, the long copolymer chain could wind around one or several protein targets, and undergoes an extensive induced-fit procedure on their surfaces to maximize favorable binding interactions. However, on the polyethyleneimine layer, the anionic polymer didn't not only lose a fraction of its binding sites for the immobilization, but also became confined to a two dimensional flat arrangement, which reduced the accessibility of globular proteins from all sides. Therefore we start to think how to immobilize our highly selective linear polymer system on the surface with keeping the affinities.

- Objective 4: to make crosslinked polymer materials to recognize immunoglobulin G by the so called "epitope" molecular imprinting technology.

Recently, molecularly imprinted polymers (MIPs) have been used for the recognition of peptides and proteins. However, functional monomers used in most of the applications were weak binding sites, which were less likely to produce a highly specific MIP and tend to favor nonspecific binding. Moreover, in most cases only one functional monomer was used together with the comonomer and the crosslinker to make the polymeric scaffold. With a variety of effective functional monomers prepared before, MIP libraries should be prepared in aqueous media and with IgG as the final recognition target. To overcome the problems existing in

protein imprinting, the so-called “epitope” method should be used. Followingly, the libraries should be screened, in order to find best functional monomers and their combinations.

3 Monomer design and preparation

The surface of a protein offers an array of charged, polar, aliphatic and aromatic groups that can be targeted by surface recognition agents. While there are hundreds of amino acids in nature, only 20 of them are commonly found in proteins and each of them has its unique property (Table 3.1). Each of our monomers is therefore designed and synthesized aiming at one or one kind of the amino acids.

Amino acid	3-Letter	1-Letter	Polarity	Acidity or basicity
Alanine	Ala	A	nonpolar	neutral
Arginine	Arg	R	polar	basic(strongly)
Asparagine	Asn	N	polar	neutral
Aspartic acid	Asp	D	polar	acidic
Cysteine	Cys	C	nonpolar	neutral
Glutamic acid	Glu	E	polar	acidic
Glutamine	Gln	Q	polar	neutral
Glycine	Gly	G	nonpolar	neutral
Histidine	His	H	polar	basic(weakly)
Isoleucine	Ile	I	nonpolar	neutral
Leucine	Leu	L	nonpolar	neutral
Lysine	Lys	K	polar	basic
Methionine	Met	M	nonpolar	neutral
Phenylalanine	Phe	F	nonpolar	neutral
Proline	Pro	P	nonpolar	neutral
Serine	Ser	S	polar	neutral
Threonine	Thr	T	polar	neutral
Tryptophan	Trp	W	nonpolar	neutral
Tyrosine	Tyr	Y	polar	neutral
Valine	Val	V	nonpolar	neutral

Table 3-1 *Twenty nature amino acids and their symbols, polarities and basicities or acidities.*

3.1 Monomer synthesis

3.1.1 Monomers based on methylacrylamide

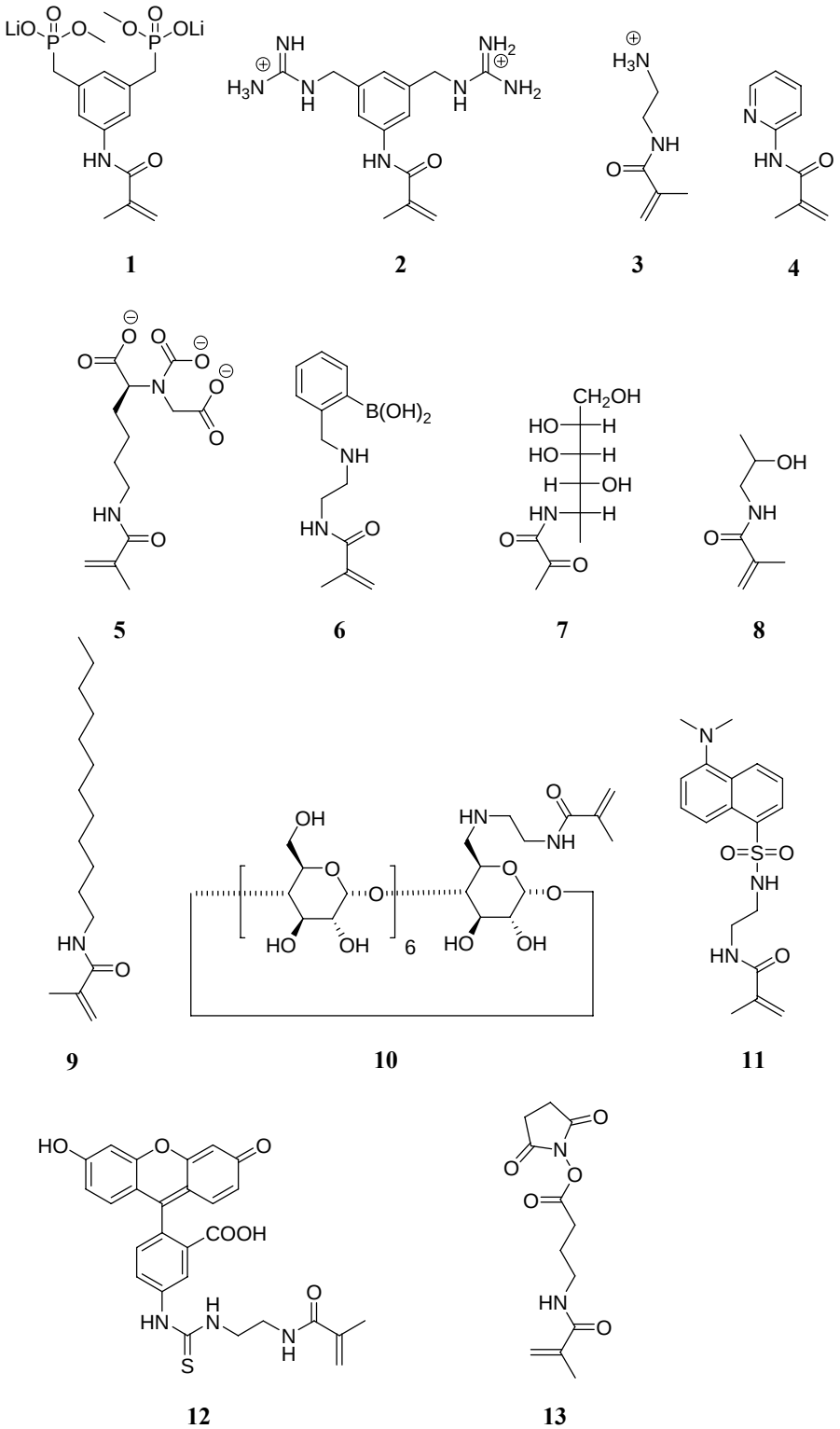

Figure 3.1 *Monomers prepared in this work.*

3.1.1.1 Monomer 1 for basic amino acids

Several years ago, it was discovered in our group that small bisphosphonate dianions (Figure 3.2) bind to arginine and lysine residues in a peptidic environment with remarkable affinity, while almost other amino acid side chains are rejected.[24] Its binding constants to argine and lysine were 86000 M^{-1} and 4000 M^{-1} in DMSO respectively, and the recognition process relied mainly on electrostatic attraction, enforced by π-cation attraction.

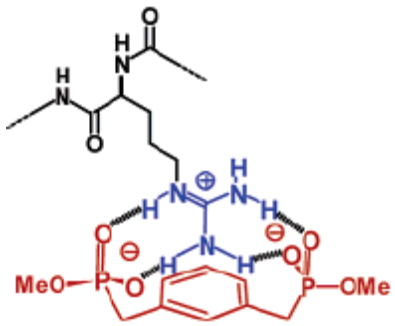

Figure 3.2 *Arginine residue embraced by bisphosphonate dianion.*[24]

The synthesis of the bisphosphonate monomer **1** started from the preparation of 3, 5-dibromomethyl nitrobenzene (**14**). It could be obtained by from 3, 5-dimethylnitrobenzene, accompanied by many other bromination byproducts. The other more tedious route, however with a cheaper cost and higher yield, started from 5-nitroisophthalic acid. It was converted to the corresponding acid chloride with phosphopentachloride, flowingly reduced to a diol by sodiumborohydride and subsequently brominated to **14** by phosphotribromide. **14** was treated with 2.2 eq. of trimethylphosphite (Arbuzov reaction) to afford **15**, which was reduced with 10% Pd/C as a catalyst under 1 atm. hydrogen atmosphere to furnish an amine derivative **16**, whose coupling with methylacroyl chloride generated **17.** This molecule can only be polymerized in organic solvents; however it could be dealkylated by 2.2 eq. of lithium bromide in acetonitrile to afford **1**, which can be polymerized in aqueous solution (Figure 3.3).

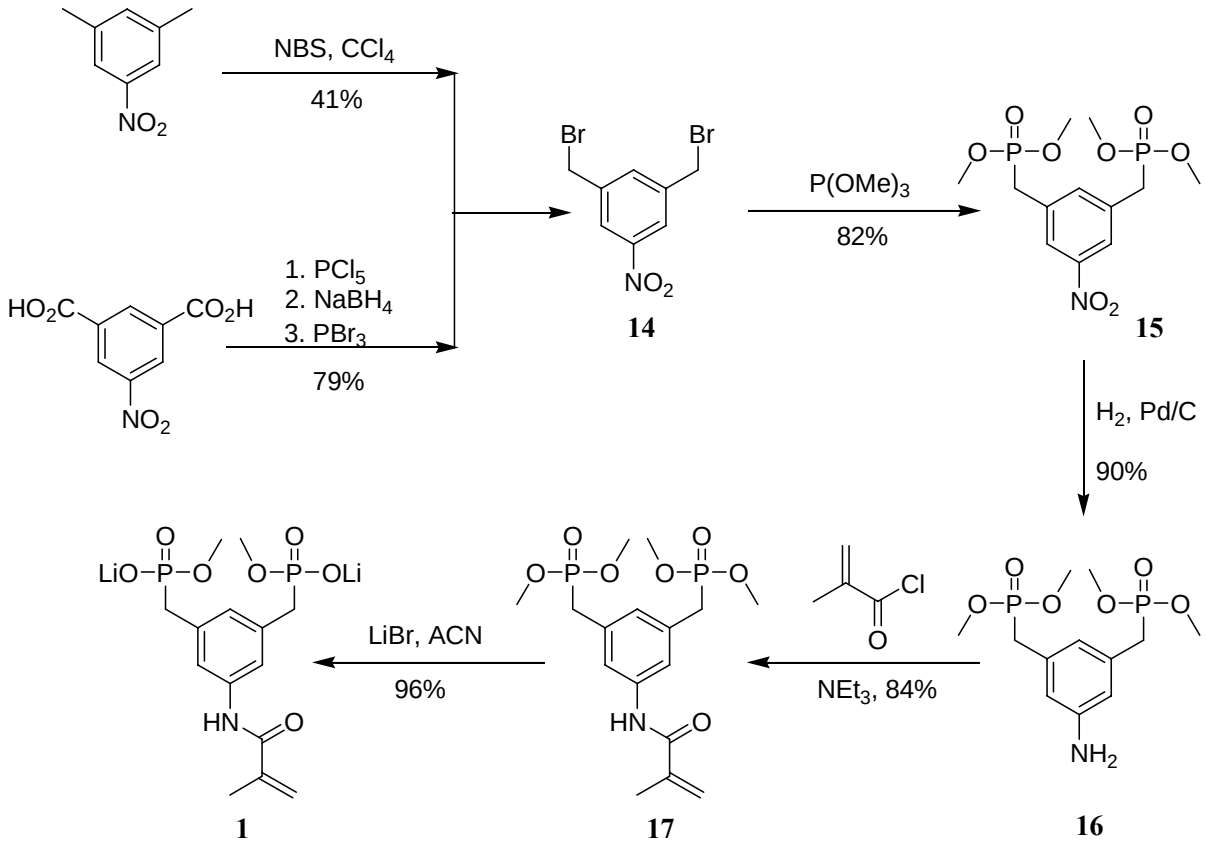

Figure 3.3 *Preparation of monomer 1.*

3.1.1.2 Monomer 2, 3 and 4 for acidic amino acids

Designed synthetic small molecules that bind carboxylic acids have been developed in a number of laboratories including those of Hamilton[25], Lehn,[26] Schmidtchen,[27] and Anslyn.[28] The majority of these incorporate either a 2-aminopyridine substructure or a guandinium moiety embedded in their structures. Here the guandinium monomer **2** (Figure 3.4), ammonium monomer **3** (Figure 3.5) and aminopyridine monomer **4** (Figure 3.7) were synthesized.

Monomer **2**, with a similar m-xylylene structure as **1**, was designed as a candidate for aspartic acid and glutamic acid, with two guandinium subunits as binding sites. N,N'-bis-Boc-2-methyl-2-thiopseudourea (**18)** was synthesized by keeping the solution of 2-methyl-2-thiopseudourea sulfate and di-*t*-butyldicarbonate stirred at room temperature for 5 days.

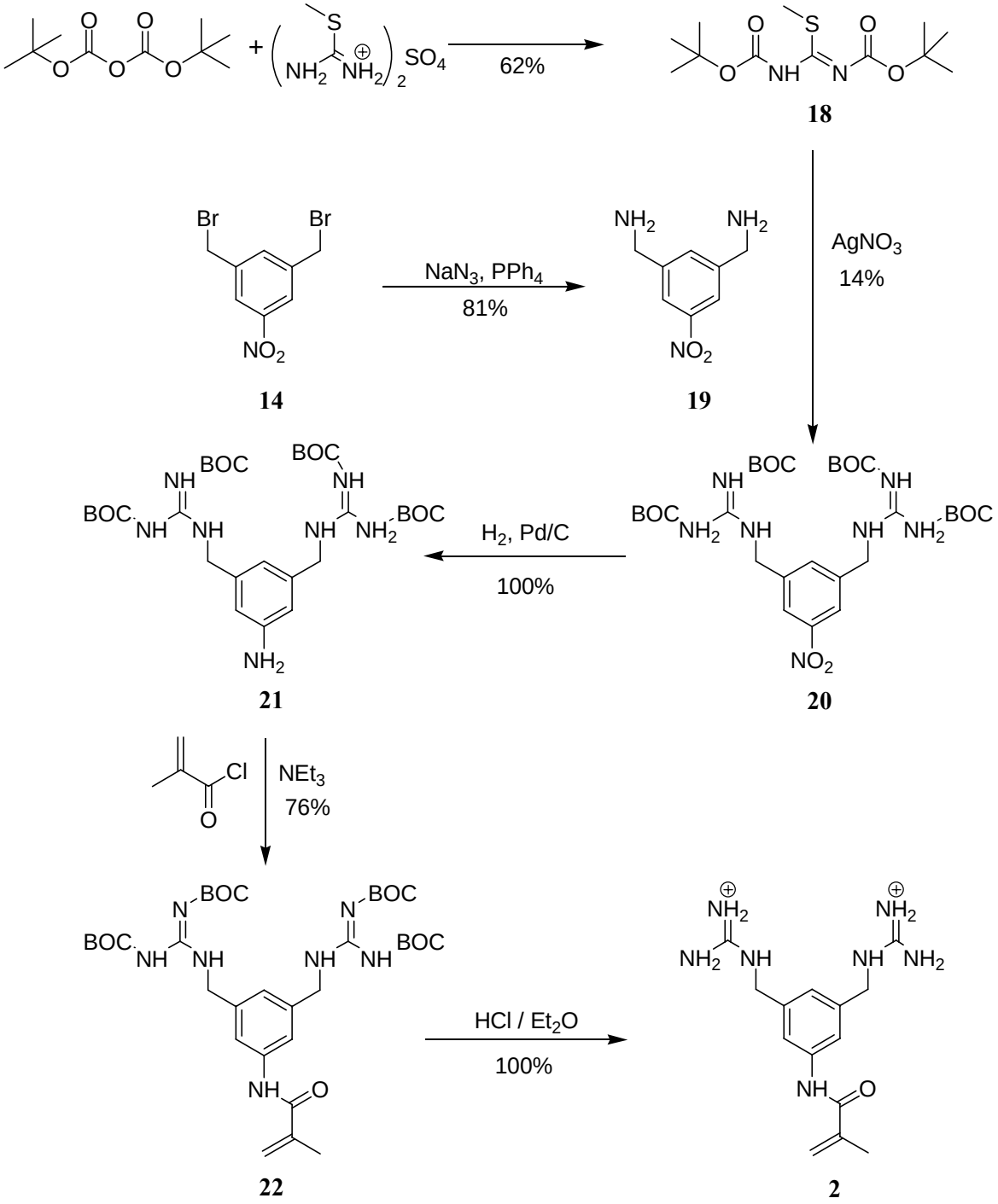

Figure 3.4 *Preparation of monomer 2.*

14 was converted to **19** by azide substitution, and subsequent Staudinger reduction. Direct conversion of halide to primary amine by Gabriel synthesis was not successful. **19** was treated with **18** under the assistance of silver nitrate to provide **20** as a white solid, whose nitro group was reduced by hydrogen over Pd/C to afford **21**. Its direct amidation with methacryloyl chloride afford the polymerizable molecule **22**. From **22** to monomer **2** was only the deprotection of BOC groups. Because it was found that **2** was unstable at temperatures above

30 ºC, 2M HCl in diethylether was used instead of traditional TFA. **22** was soluble in diethylether, while **2** precipitated from the ether solution as a white solid.

N-(2-aminethyl) carbamic acid *t*-butylester (**24**) could be prepared by two paths. In the first route ethylene diamine was bis-protected (**23**) and the subsequent mono-deprotection by HCl furnished **24**. It was also obtained by direct mono-protection. Compared to the first one, althogh the second route needed more purification work, the costs decreased a lot due to the small amount of di-*t*-butylcarbonate. Coupling of **24** with methacryloyl chloride and the following deprotection gave product **3** as a light yellow solid. Due to the monomer instability at room temperature, HCl in diethylether was used for the deprotection.

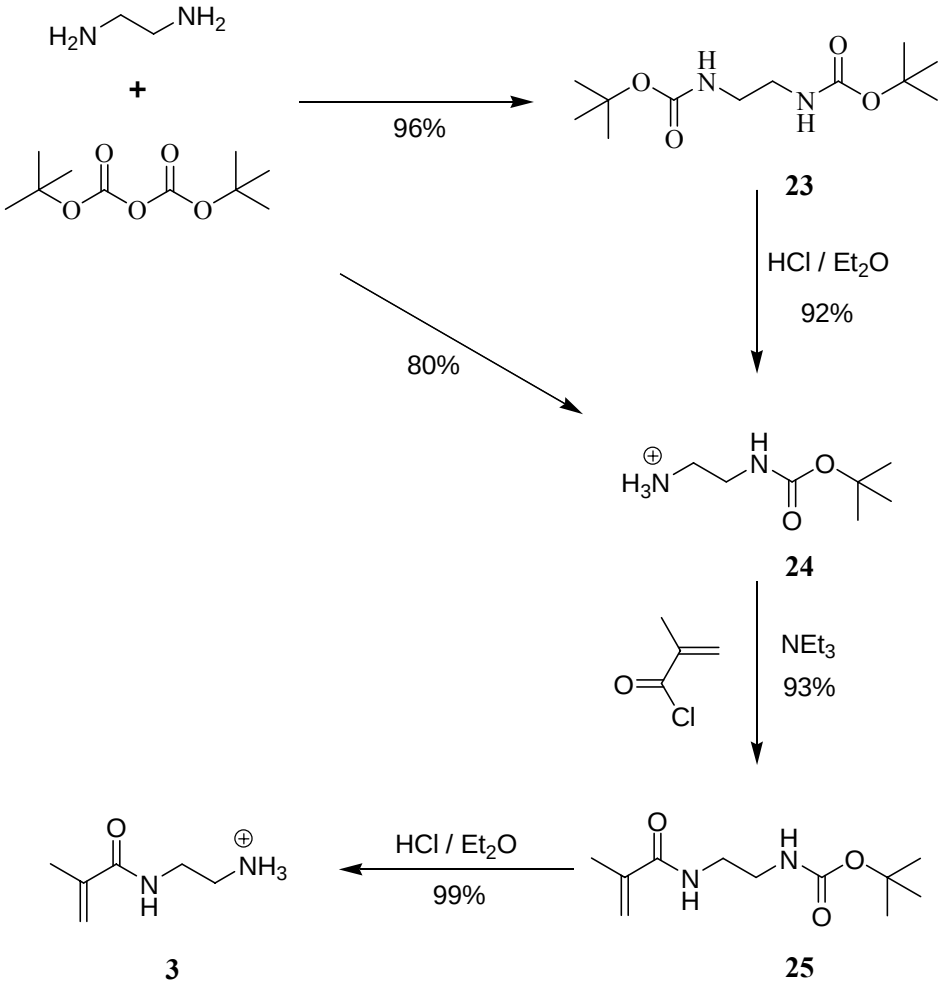

Figure 3.5 *Preparation of monomer 3.*

Monomer **4** was synthesized straightward by a condensation of methacryloyl chloride with 2-aminopydidine.

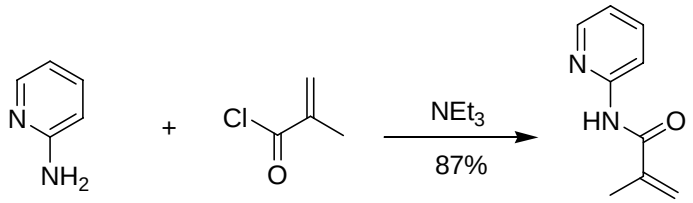

4

Figure 3.6 *Preparation of monomer **4**.*

3.1.1.3 Monomer 5 for histidine

Metal-ligand (M-L) interactions offer several advantages in recognition compared to hydrogen bonding, ion-pair or other interactions. M-L interactions are usually stronger in water compared to other noncovalent interactions.[29] The spectroscopic properties of the metal ions can further be used to monitor the binding process and to obtain structural information about the resultant complex.[30] Various transition metal ions (e.g., Cu^{2+}, Ni^{2+}, Zn^{2+} etc.) bind to the imidazole side chains of surface exposed histidines of proteins.[31] This coordination interaction (M^{2+}-His) has been used extensively for protein purification by immobilized metal affinity chromatography (IMAC),[32] protein targeting to a surface[33] and two-dimensional protein crystallization.[34]

Hochule et al. introduced an adsorbent, based on a Ni(II)-nitrilotriacetic acid (NTA) complex, for protein purification. NTA forms stable 1:1 complexes with Ni(II) with an association constant of over 10^{11} M^{-1}. This ligand occupies four positions in the octahedral coordination sphere of Ni(II), leaving the remaining two for selective interactions. They have proved that this Ni^{2+}-NTA is selective for proteins and peptides which contain histidines on the surface.[35]

The synthesis of monomer **5** started from Z-protected L-lysine methylester. Alkylation of this ester with 2.3 eq. of methyl bromoacetate afforded **26**, whose Z group was deprotected by hydrogenolysis with 10% Pd/C. **27** was acylated with methylacryloyl chloride to furnish **28.** In the literature saponification of **28** was performed with lithium hydroxide in acetone/water (4:1), however, this procedure didn't work in my case even increasing the amount of lithium

hydroxide to 20 eq. and extending the reaction time to 5 days. The final product monomer **5** was finally obtained by treating **14** with an excess amount of trimethylsilyl iodide in tetrachlorocarbon (Figure 3.7).

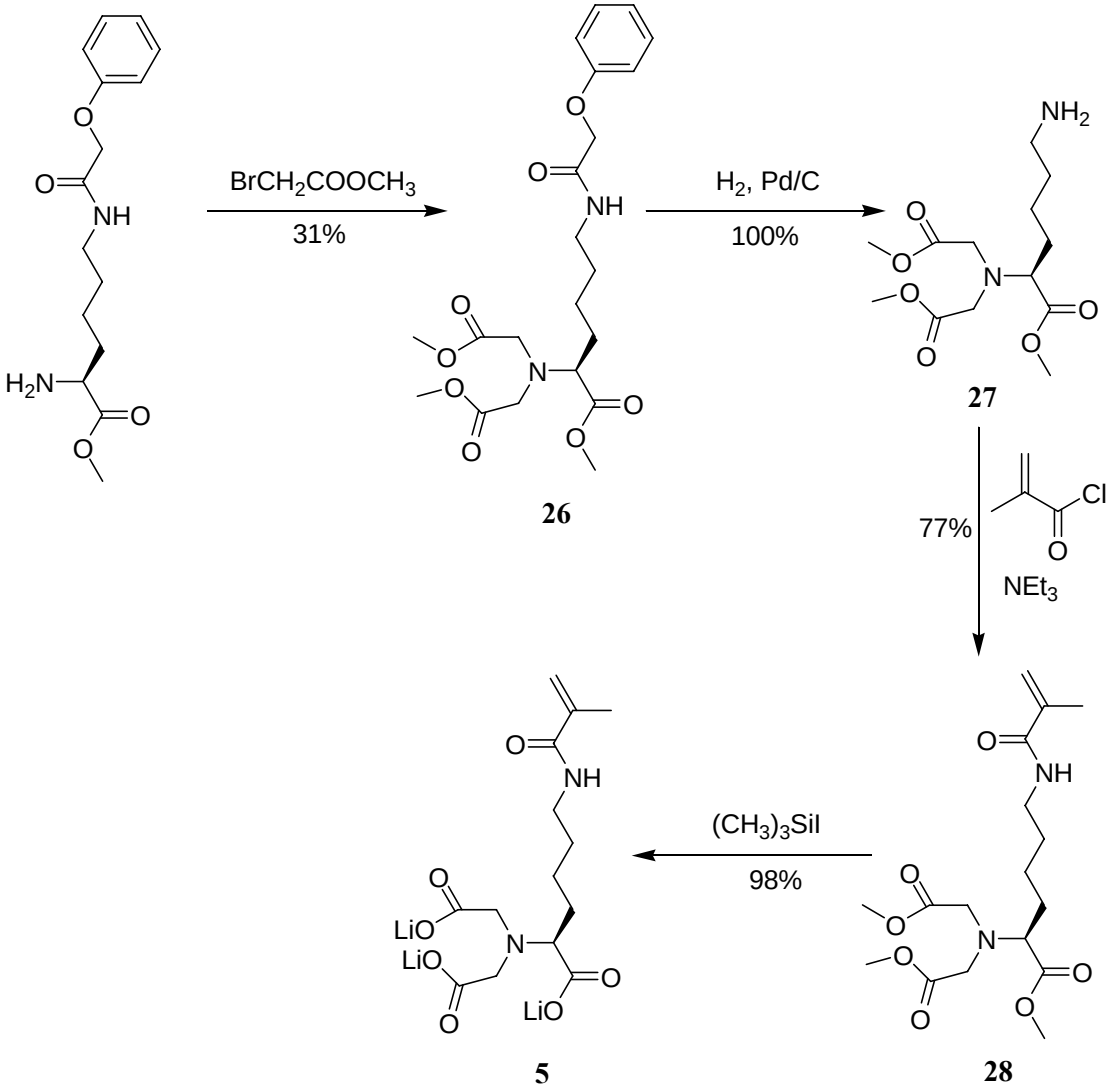

Figure 3.7 *Preparation of monomer **5**.*

3.1.1.4 Monomer 6 for diol

The use of boronic acids has advanced the molecular recognition of sugars in aqueous media, because boronic acids form reversible covalent linkages to 1, 2- and 1, 3-diols (Figure 3.8).[36] The formation of the boronate ester is faster when the boron is tetrahedral, which occurs at high pH. As it is not always desirable to work at high pH, Wulff demonstrated that a tertiary

amine adjacent to the boron can add to the boron center, creating a tetrahedral boron at neutral pH.[37] Recently, several groups pointed out that a-hydroxycarboxylates can also form cyclic boronate ester with boronic acids[38] and Strongin and Kataoka utilized this interaction to develop chemical receptors for neuraminic acid.[39]

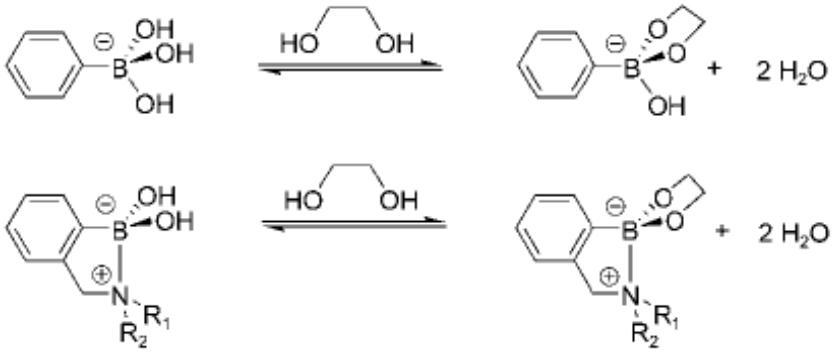

Figure 3.8 *Phenylboronate ester formation (up), Phenylboronate ester formation with aminomethyl group at O-position (bottom).*[36]

Based on above principles, monomer 6 was designed to bind glycoproteins. With 29 in hands, the SN2 substitution of this molecule by monomer 3 was tried firstly. Unfortunately this reaction didn't work. Monomer 6 was obtained finally by reductive amination between 3 and 2-formyl phenylboronic acid.[40] 2-formylphenylboronic acid was treated with exact 1 equivalent of 3, triethylamine and molecular sieves in dry methanol, and the formed imine intermediate was reduced by sodium borohydride to furnish 6 as a white solid. ESI-MS and NMR spectrum indicated that the crude product was nearly pure except of the existence of borotrimethylester and triethylamine. 100% pure product of 6 could be obtained by recrystalizing it for several times. Micheal Maue observed an intramolecular addition of the amide group to the imine in the intermediate,[41] which didn't happen in my system.

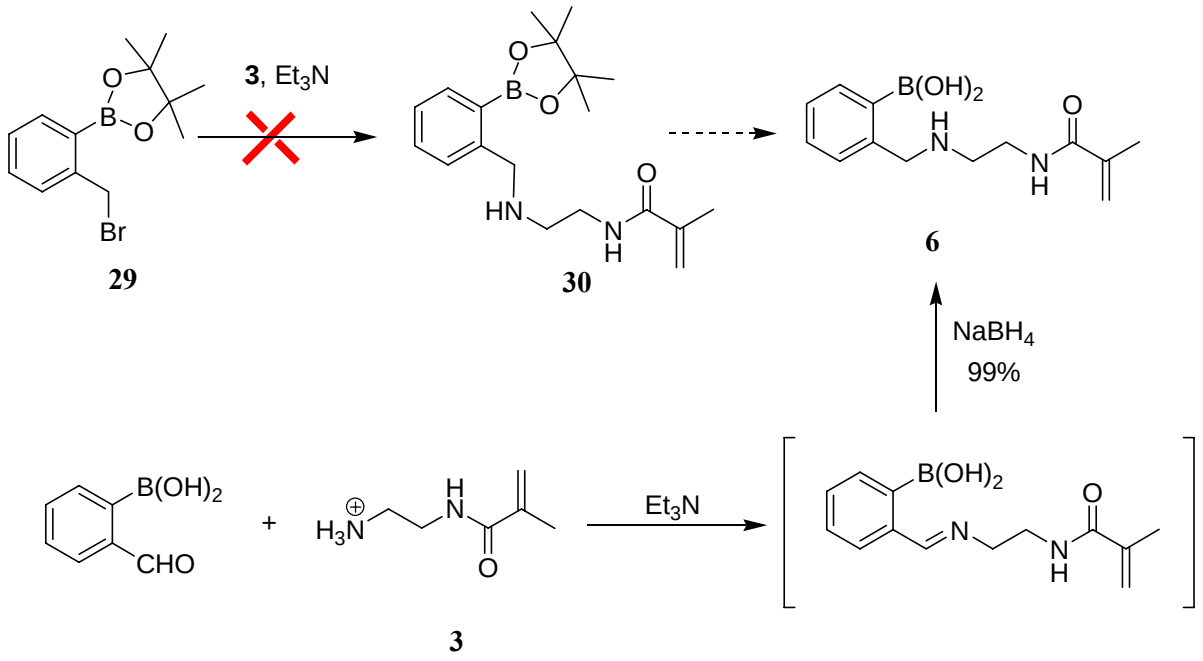

Figure 3.9 *Preparation of monomer* **6.**

3.1.1.5 Monomer 7 and 8 for solubility

Monomer **7** and **8** were used mainly to increase the polymer solubility in aqueous solution, and of course they could form hydrogen bonding with peptide backbones. Both of them could be synthesized by one-step amidation.

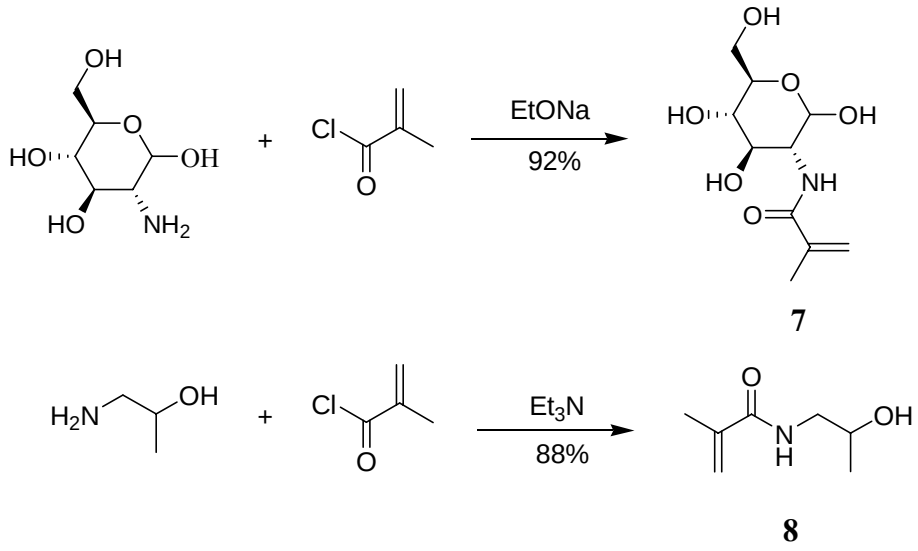

Figure 3.10 *Preparation of monomer 7 and 8.*

Monomer **7**, a glucose based methacrylate material, was used for carbohydrate protease conjugates (CPCs) and its polymerization feasibility was examined.[42] Its synthesis was not as easy as it looked like, because the product purity was highly required. In the starting molecule 2-deoxy-glucosamine, except of the amine group, hydroxyl groups could also react with metharyloyl chloride and thus formed multi-substituted byproducts. It was observed that when the product contained more than 1% of multi-substituted byproducts, the solubility of polymers formed by monomer **7** could become worse in aqueous solution due to crosslinking. Therefore, the solution pH during the reaction was strictly controlled in a range between 8 and 9 to avoid side reactions between hydroxyl groups and metharyloyl chloride.

3.1.1.6 Monomer 9 and 10 for hydrophobic amino acid residues

Monomer **9** and **10** were used as binding sites which could hydrophobically interact with some amino acid sidechains on protein surfaces. With a flexible dodecyl chain, **9** was proved to be a better hydrophobic monomer than a cyclohexyl one in linear polymers.[19] Its synthesis was very simple: after the condensation of dodecylamine and methacyloyl chloride, the product could be purified by chromatography.

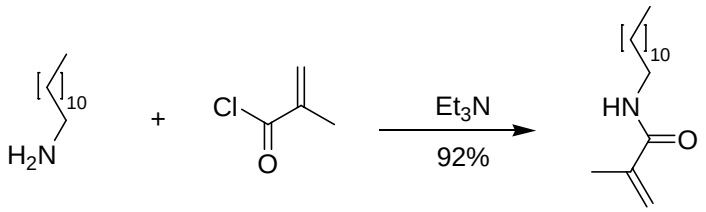

9

Figure 3.11 *Preparation of monomer 9.*

Monomer **9** could only be used in organic solvents, while **10** could be used in polar organic solvents and aqueous solutions. ß-cyclodextrin was the functional group of **10**. ß-cyclodextrin can be topologically represented as a toroid with the larger and the smaller openings of the toroid exposing to the solvent secondary and primary hydroxyl groups respectively (Figure 3.12). Because of this arrangement, its interior is not hydrophobic, but considerably less hydrophilic than the aqueous environment and thus able to host other hydrophobic molecules. In contrast, the exterior is sufficiently hydrophilic to impart cyclodextrins or their complexes

water solubility. ß-cyclodextrin has a hole with 6.0 Å in diameter and 7.9 Å in height.[43] It has previously been shown to be capable of binding amino acids with decreasing binding constants from tryptophan, leucine, tyrosine to phenylalanine.[44]

The synthesis of monomer **10** included three steps (Figure 3.13). The 6-OH position of ß-cyclodextrin was tosylated to furnish mono-substituted product **31** with comparatively good regioselectivity. The di-substituted byproduct observed in MS and NMR was less than 5%. Higher purity could be obtained by using Cu^{2+} in the synthesis, because the secondary 2 and 3-OH could form chelatcomplex with this metal ion,[45] and therefore are blocked during the tosylation. The tosylate group was substituted by much excess of ethylene diamine to keep a high conversion of **31** to **32**. In the point view of later purification, excess amount of methacryloyl chloride was used in the third step and the byproduct could be purified by being precipitated from water with adding ethanol, or even by dialysis if needed. The final product **10** was a slurry solid with a pale yellow color.

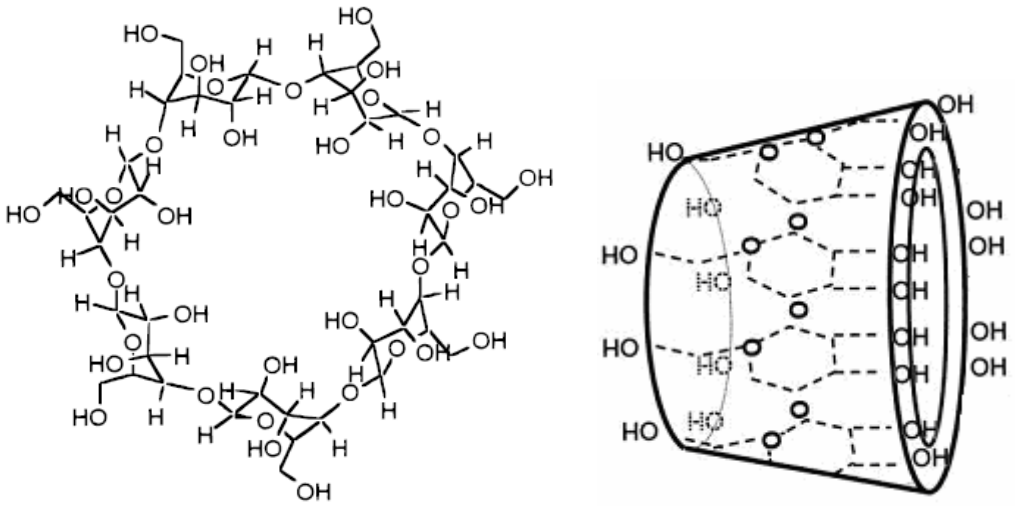

Figure 3.12 *a) ß-cyclodextrin, b) schematic structure of ß-cyclodextrin.*

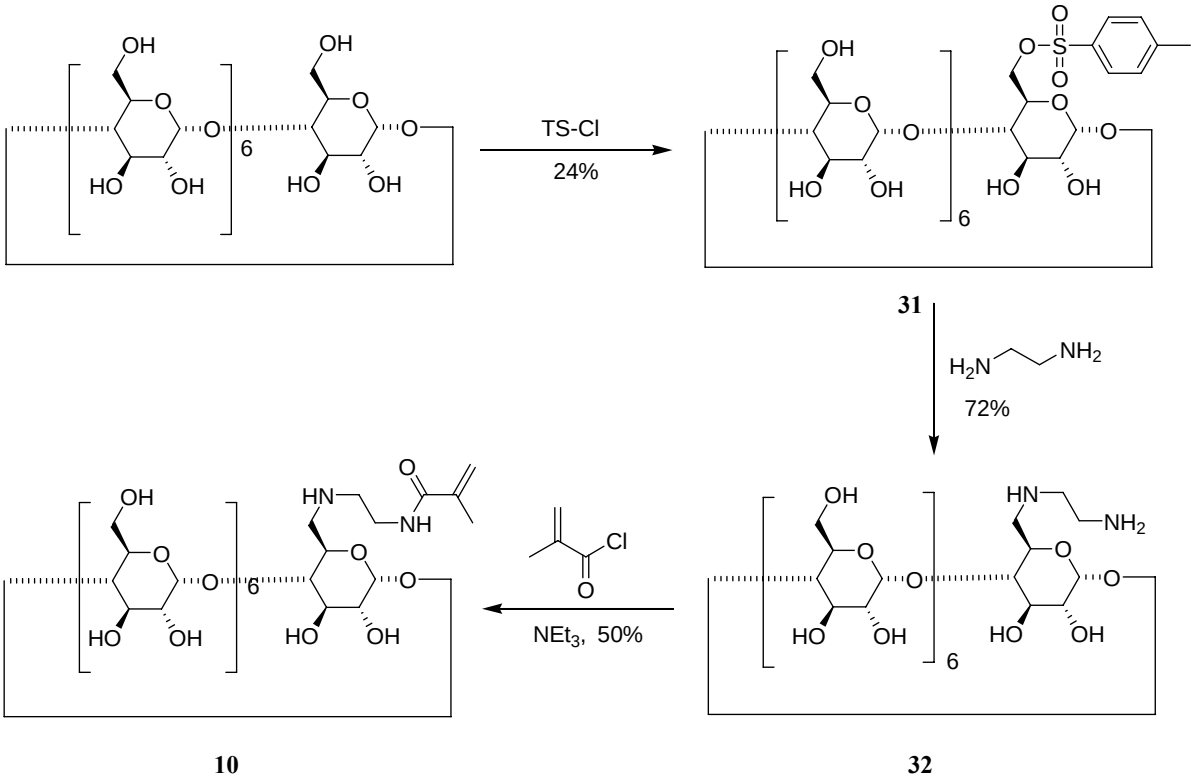

Figure 3.13 *Preparation of 10.*

3.1.1.7 Monomer 11 and 12 as fluorescence labels

In the next chapter most of the interactions between polymers and proteins were studied by fluorescent titrations, hence, it was required to have fluorophores in polymers. Monomer **11** and **12** were synthesized for this purpose, albeit they could also provide hydrophobic interactions (Figure 3.14). Except of the optical difference, their solubilities were also different. **11** was soluble only in unpolar organic solvent. **12** was initially designed to be used in aqueous solutions, but in fact it was only slightly soluble in aqueous solutions, and well soluble in polar organic solvent or mixtures of them and water, e.g., 20% methanol in water.

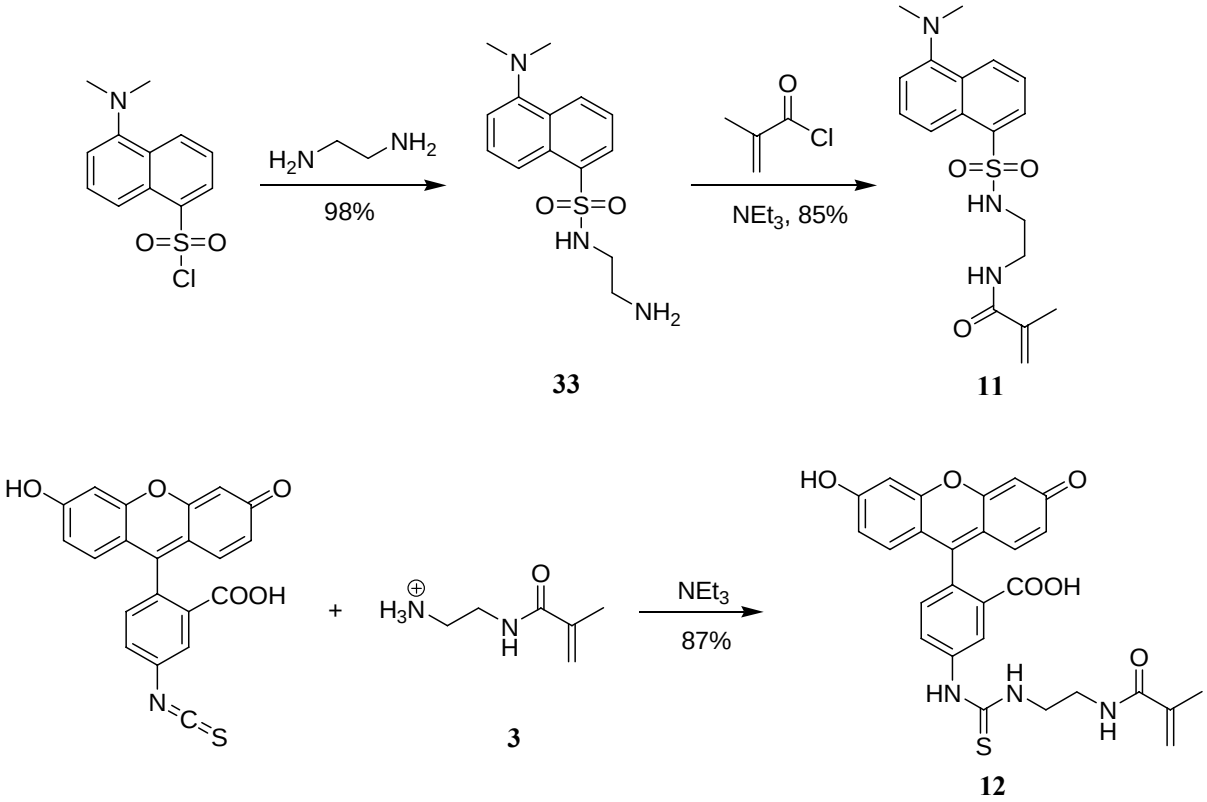

Figure 3.14 *Preparation of monomer 11 and 12.*

The fluorescence of the dansyl group is widely used in protein sequencing and amino acid analysis, [46] and http://en.wikipedia.org/wiki/Dansyl_chloride - cite_note-1it is also known to be very sensitive to changes in media polarity and has been previously used for the investigation of polymer structure.[47] Normally it has an absorption at about 340 nM and emission at about 520 nM. [48, 49] In the later work this fluorophore in polymers was excited at 330 nM and the emission was at about 530 nM. **11** was synthesized in two steps. Dansyl chloride was treated with ethylenediamine to afford **33**, which was amidated with methacryloyl chloride yielding the product as a green solid.

Fluorescein has an absorption maximum at 490 nm and emission maximum of 520 nm in water. Fluorescein has a pK_a of 6.4 and its ionization equilibrium leads to pH dependent absorption and emission over the range of 5 to 9. There are many fluorescein derivatives, for example fluorescein isothiocyanate, often abbreviated as FITC. It and a succinimidyl ester functional group attached to the fluorescein core, are common amine reactive fluorescein derivatives. They are often used to label and track cells and many other biologically active molecules. The synthesis of **12** was only an acylation of FITC with **3**, and the product could be purified by chromatography.

3.1.1.8 Monomer 13 for polymer immobilization

Polymers containing monomer **13** could be immobilized on a substrate with amine groups on the surface. The first step of the monomer synthesis was a coupling of methacryloyl chloride with γ-amino butyl acid,[50] followed by the activation of N-γ-macrylamidobutyric acid with NHS and EDC (Figure 3.15).

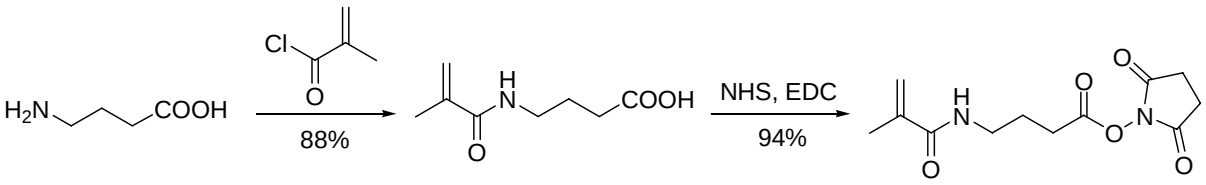

13

Figure 3.15 *Preparation of monomer 13***.**

3.1.2 Monomers based on a diacetylene structure

Polydiacetylene (PDA) is a conjugated polymer with interesting and useful optical properties. It was firstly prepared by Wegner in 1969.[51] The monomeric PDA acid could be synthesized based on an asymmetrical Chodkiewicz coupling of a 1-iodoalkyne and an alkynoic acid.[52] With a commercial available monomeric PDA acid, TRDA (10, 12-tricosadiynoic acid), in hands, our monomers **14-18** were prepared by the amidation of this acid with amines.

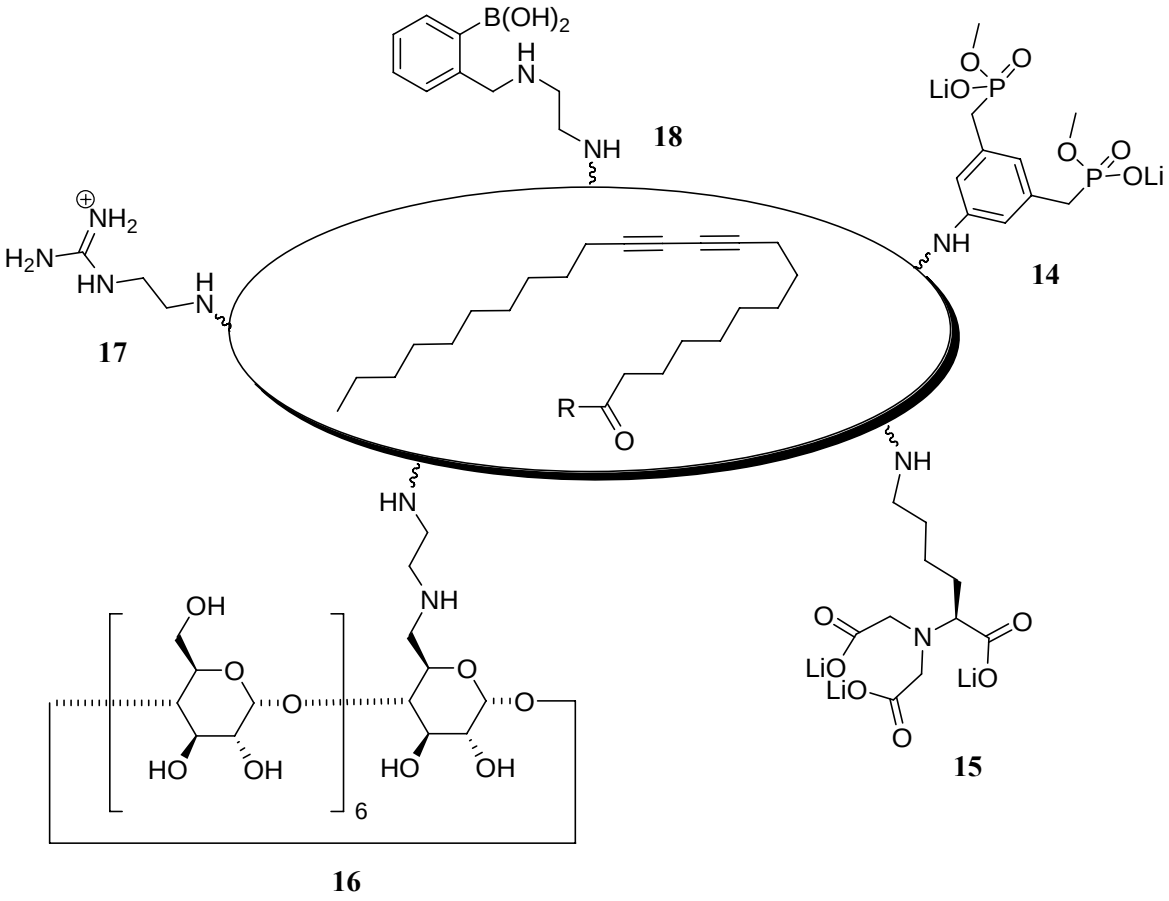

Figure 3.16 *Different functionalities incorporated on 10, 12- tricosadiyne structure.*

3.1.2.1 Preparation of PDA monomers

The synthesis of PDA monomers was nearly same as those monomers based on methylacrylamide. However, due to the highly sensitivity of the diacetylene group to light, the synthesis of PDA monomers were more complicated than the monomers based on

methacrylamide. What should be mentioned is that, it is better to keep all the PDA monomers in solutions instead of as solids, because these substances are in more ordered lattice as solids and therefore easier to be polymerized by light.

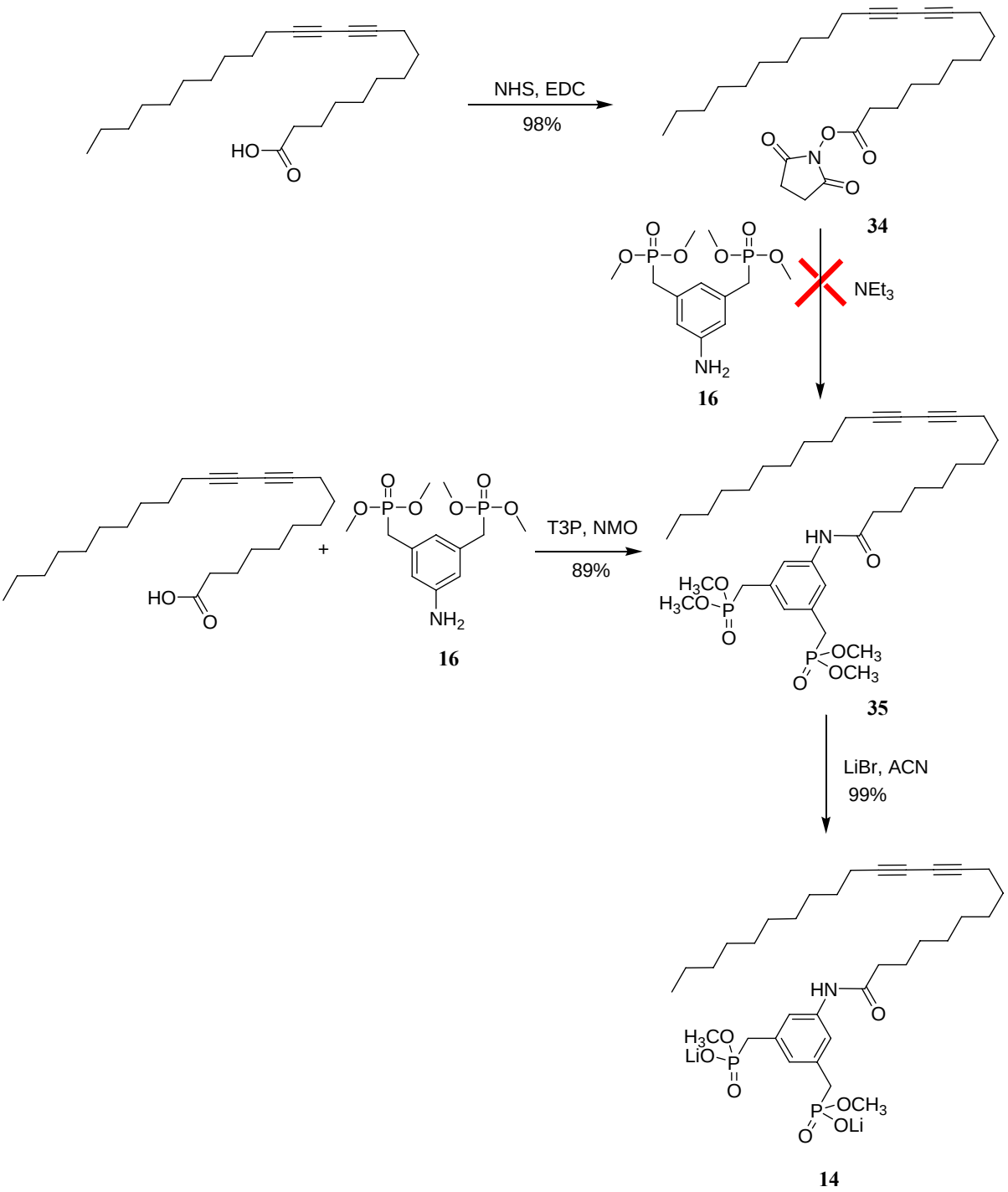

Figure 3.17 *Preparation of monomer 14.*

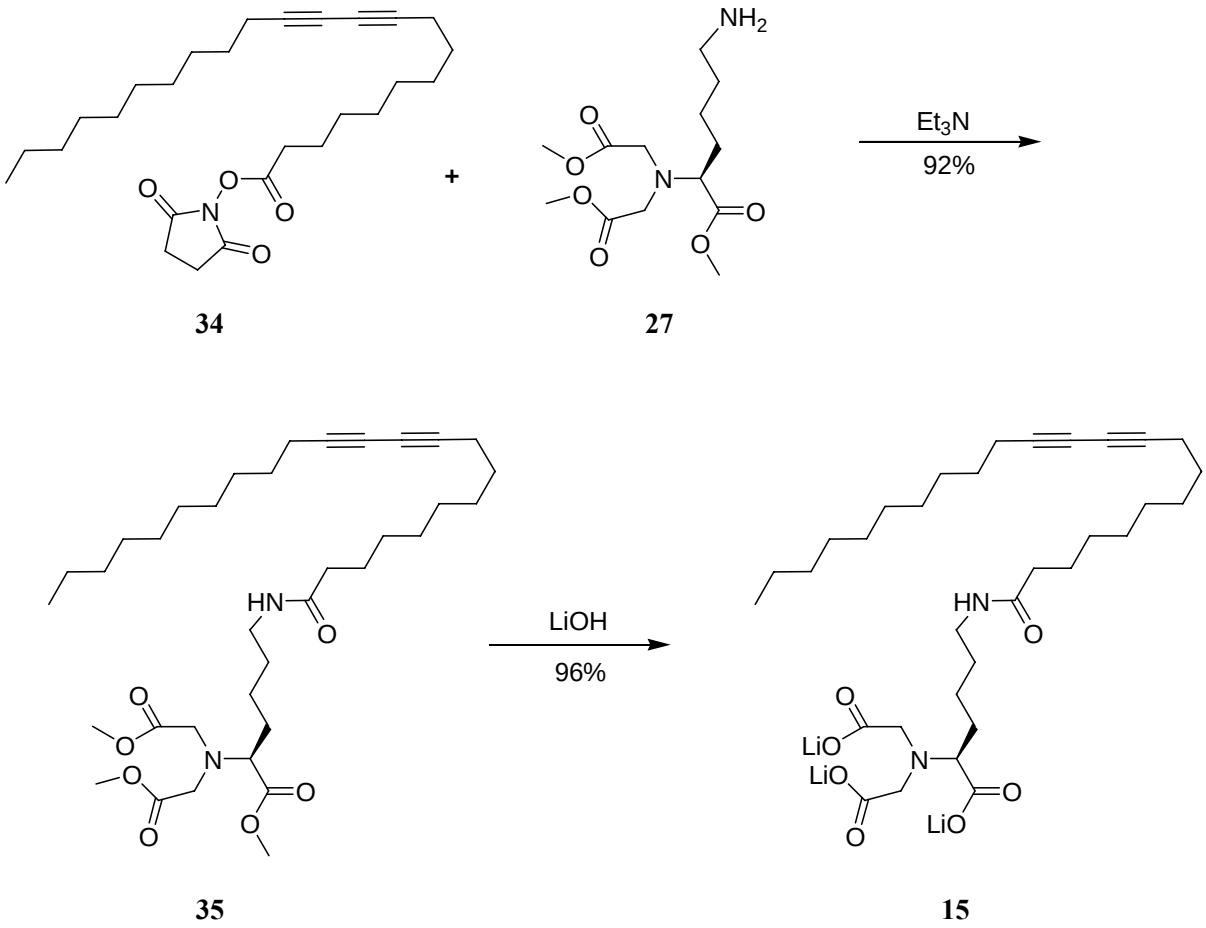

Figure 3.18 *Preparation of monomer 15.*

Prior to use, TRDA needed to be purified to remove polymers formed during store. It was dissolved in chloroform and filtered through Nylon membrane filters (0.8 μM, Whatman), and then the filtrate was condensed to afford a white powder. TRDA molecule could be kept in the refrigerator at - 20 ºC under argon and could also be kept at room temperature in its NHS ester (**34**) state. This ester was obtained by treating TRDA acid with N-succinimide and DDC/EDC as coupling reagents. The crude product produced with DCC needed to be purified by chromatography, but **34** was found unstable in the column. EDC was a better choice than DCC. Because byproducts produced with EDC were soluble in water, the product in diethyl ether could be easily purified by being washed with water.

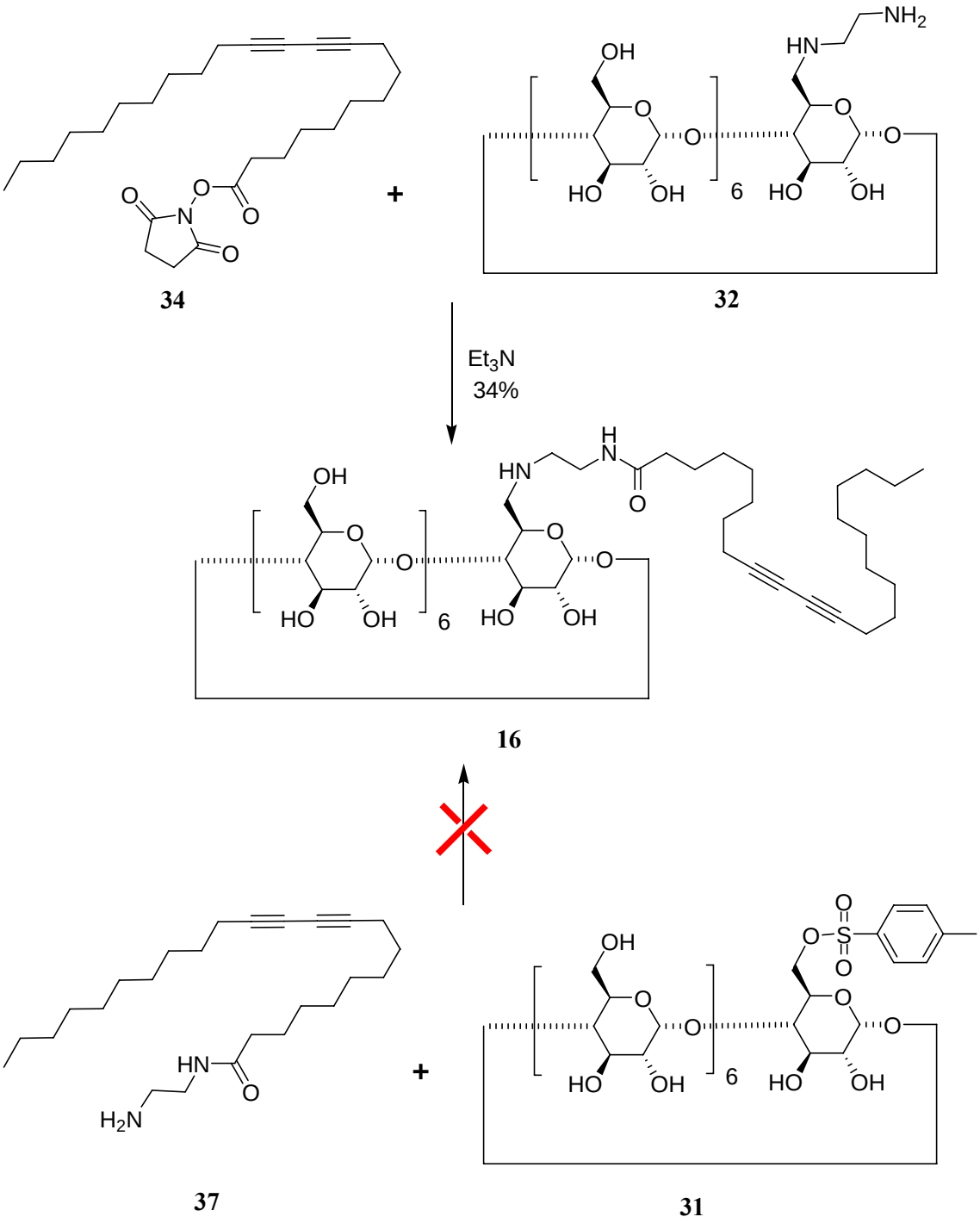

Figure 3.19 *Preparation of monomer 16.*

The coupling reaction between **16** and **34** didn't work, which could attributed to the weak basicity of the aniline group. **35** was obtained by the coupling reaction of TRDA and **16** by using T3P and N-morpholine in THF. Subsequent ester saponification with LiBr in acetonitrile at 70 °C didn't affect the diacetylene group and finally gave the monomer **14** (Figure 3.17). **34** reacted with **27** to afford **35**, which was dealkylated by lithium hydroxide in acetone/water (4:1) to give **15** (Figure 3.18).

16 was obtained by a substitution between **34** and **32**. Due to their different solubility, several solvents were tried to make the reaction and DMF was considered as the best choice. **34** was well soluble in DMF and **32** was only suspended in it at the reaction beginning. After the mixture was kept stirred for several hours, the solution became clear. It was an indirect indication that the reaction went on at this condition. The substitution of the tosylate group on **31** by the primary amine on **37** didn't work. The very different solubility of them was believed to be the reason (Figure 3.19).

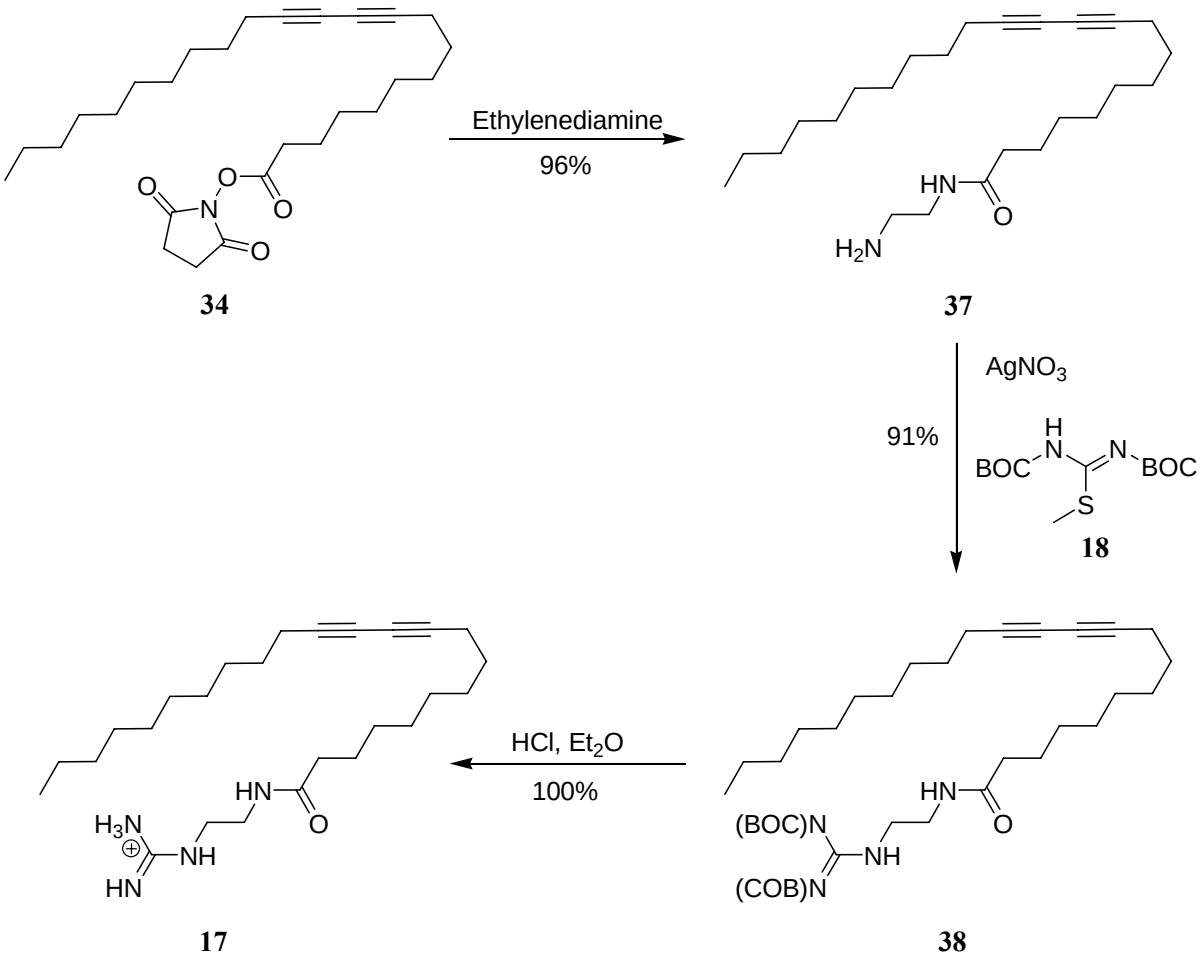

Figure 3.20 *Preparation of monomer 17.*

With much excess of ethylenediamine, **34** could be converted to **37** with a high yield in dichloromethane at room temperature. The product precipitated out of the solution after several hours without a need for further purification. **37** could be converted to **38** with **18** under the assistance of silver nitrate. Subsequent Boc-deprotection of **38** by HCl at 0 ºC furnished an effective carboxylate binder **17** (Figure 3.20). Both **17** and **37** were very unstable. **17** was stored in the more stable stage **38,** and deprotected just before use.

Monomer **18** was recrystalized from methanol as a white solid, after the reductive amination of **37** with *o*-formylphenylboronic acid (Figure 3.21).

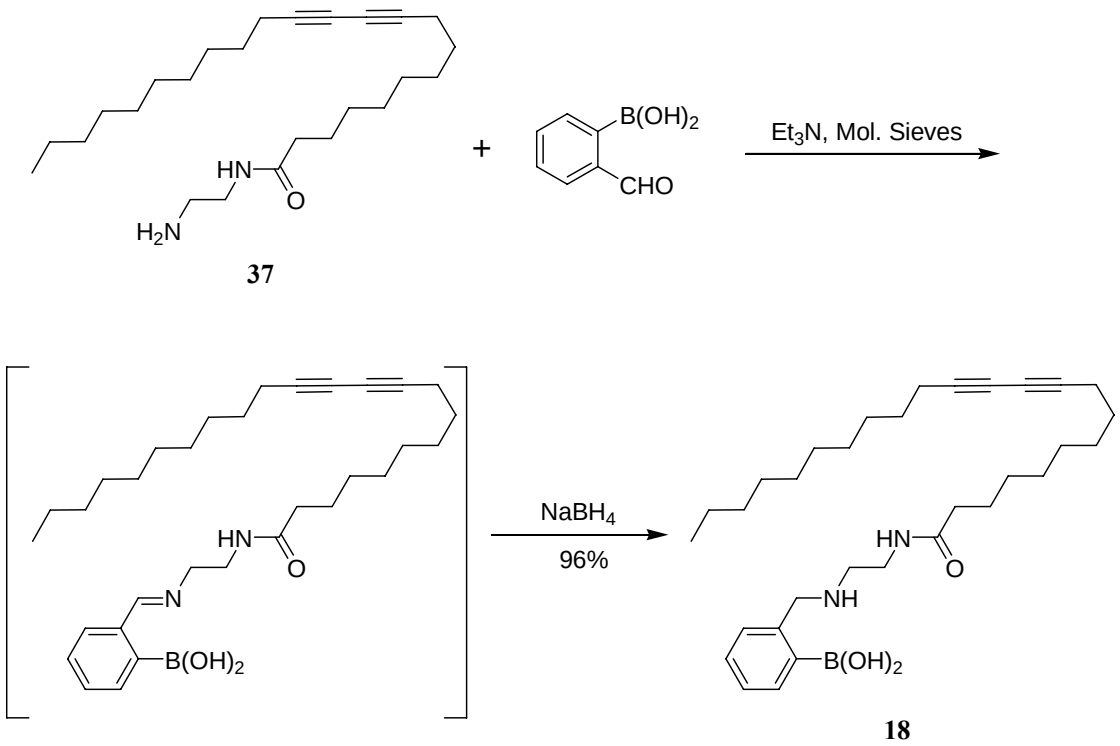

Figure 3.21 *Preparation of monomer **18**.*

3.1.2.2 Monolayer and polymer formation of monomer 14 at air-water interface

The surface properties of one sample monomer, **14**, were evaluated with pressure-area isotherms measured by a filmbalance (NIMA, 601BAM). All measurements were performed with a compression speed of 50 cm^2/min.

To prepare a monolayer, 50 µL of 3.5 mM stearin acid in chloroform was injected into water. Followingly, 3.5 mM of **14** dissolved in a mixture of chloroform and methanol (1:9) was added stepwisely. It could be observed that with the addition of **14**, surface area of the monolayer increased at pressures below 20 mN/m, and this monolayer reach a very compressed sate at a larger surface area compared to pure sterinacid. The more **14** was added, the more obvious this phenomenon is. All of these proved that molecule **14** went to air-water surface to form a monolayer with sterinacid (Figure 3.22 a).

To test the sensitivity of the monolayer to a guest, a solution of spermidine in water was added into the subphase of a monolayer formed by sterin acid and **14** with a ratio of 1: 0.6. Because the bisphosphonate dianion headgroup of **14**, could attract sperimidine (an amine) from water to the surface, surface area increased largely at a fixed pressure with the addition of sperimidine (Figure 3.22 b). In some cases (0.4, 0.6 and 0.8 eq. of sperimidine), the surface area could not be measure at low pressures due to the area limitation of the balance.

At last the pure monolayer of **14** was exposed to UV light and the isotherms were measured after 0.5, 1.5, 2.5 and 3.5 hours to observe the polymerization feasibility of this monolayer. The results were showed in figure 3.22 c, and indicated that the polymerization almost finished after half an hour of exposure and no obvious change happened any more after longer time. Due to the covalent linkage of **14** on the surface, surface area decreased a lot at a pressure after polymerization.

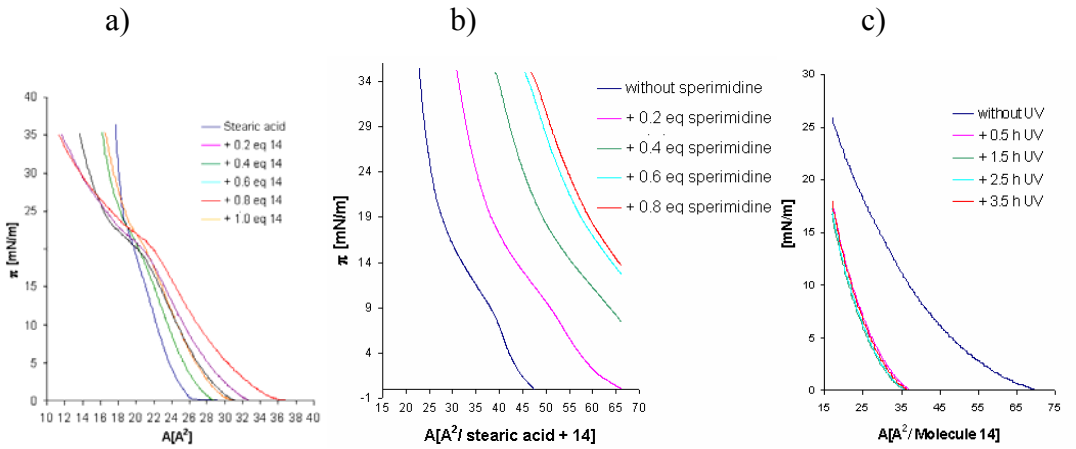

Figure 3.22 *a) Isotherms of the stearic acid monolayers with different content of monomer 14; b) Isotherms of the monolayer of stearic acid and 0.6 eq. of monomer 14 with the addition of spermidine; c) Polymerization of the pure monomer 14 monolayer under UV light. All the measurement is performed at 20 ^{o}C.*

4 Protein recognition and separation with polymers

4.1 Protein surface analysis

The nature of protein-protein interfaces has been the focus of investigation for some time. A recent important breakthrough has been the identification of "hot spots" on protein surfaces. A hot spot is a defined locale of ca. 600 $Å^2$ on the surface of a protein at or near the geometric center of the protein-protein interface. Residues that comprise the hot spot contribute significantly to the stability of the protein-protein complex. Surrounding the hot spot is an area of residues that contribute slightly less to the stability of the complex. This outer area has been compared to an O-ring that excludes solvent from the protein-protein interface, stabilizing the complex (Figure 4.1).[53]

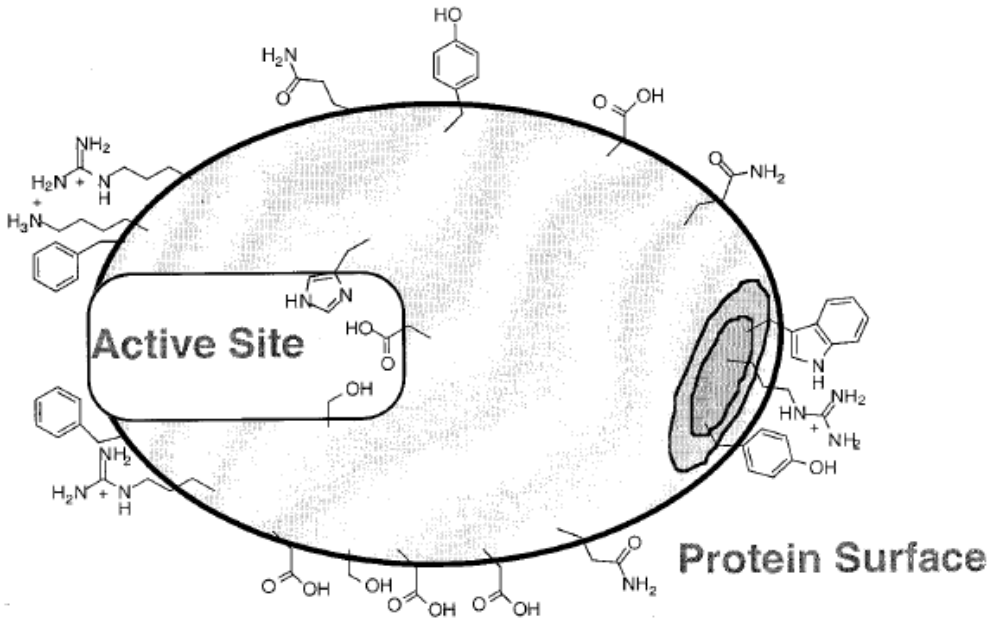

Figure 4.1 *Schematic protein surface.*[53]

Each protein has its unique pattern of amino acid residues on the surface, to distinguish proteins of similar sizes and pI values, but of different biological functions, an artificial host must be able to recognize this special pattern, that is, the topology, polarity, as well as the electrostatic potential of a protein surface. This information can be roughly estimated by several means.

Amino acids existing on a protein surface could be calculated by an online program *PROVE* (protein volume evaluation, http://biotech.eml-ebi.ac.uk:8400/ (EU) or http://biotech.pdb.bnl.gov:8400/ (USA)),[54] with the protein crystal structure. Furthermore, the surface area of a protein could also be estimated by using this online program.

In a statistical *PROVEOUT* result (Table 4-1) amino acid residues are represented by special symbols. NC3 represents the SP3 nitrogen connected to three hydrogens in a charged group (lysine); NC1 represents the SP2 nitrogen connected to one hydrogen in a charged group (arginine). Other amino acids which don't have an unique atom can't be distinguished from each other, but could be calculated in a group, e.g., OC represents the SP2 oxygen with a net charge on Glutamic acid and aspartic acid; CR6 represent the SP2 carbon without hydrogen in six atom rings (phenylalanine and tyrosine).

**SURFACE AREA STATISTICS FOR STRUCTURE
CALCULATED WITHOUT WATER based on chemical type

CHEMICAL TYPE	SURFACE AREA		AVE AREA	TOTAL NUMBER OF OBSERVATIONS		
	TOTAL	PERCENT	PER TYPE	ALL	BURIED	SURFACE
C	345	5.2	2.1	166	72	94
CH1	436	6.6	3.0	144	77	67
CH2	1544	23.4	10.0	155	43	112
CH3	647	9.8	10.6	61	22	39
CR15	24	0.4	3.0	8	3	5
CR16	317	4.8	6.2	51	24	27
CR5	1	0.0	0.2	7	5	2
CR56	12	0.2	1.0	12	7	5
CR6	9	0.1	1.0	9	6	3
N	1	0.0	0.3	2	0	2
NC1	103	1.6	9.4	11	0	11
NC2	755	11.4	34.3	22	1	21
NC3	246	3.7	35.2	7	0	7
NH1	106	1.6	0.8	126	79	47
NH2	430	6.5	25.3	17	1	16
NR15	38	0.6	5.4	7	3	4
NRD5	12	0.2	11.5	1	0	1
O	1078	16.3	7.4	145	55	90
OC	313	4.7	15.7	20	2	18
OH1	178	2.7	8.9	20	5	15
S	14	0.2	1.8	8	7	1
SH1	0	0.0	0.1	2	1	1
TOTAL	6610	100.0	6.6	1001	413	588

Table 4-1 *Part of the Proveout result of lysozyme 1HEL.*

	PI	MW (KD)	Arg/ Lys	Asp, Glu/	Phe, Tyr	Try, His	Asn, Gln	Ser, Thr, Tyr	PDB No.
Histone H3	11.5	15	10/8	8	3	1	6	12	1HQ3
Histone H1	10.4	22	12/17	6	3	3	9	29	1HUM
Cyto. C	9.2	12	2/19	11	3	0	10	13	1CCR
Lysozyme	9.3	14	11/7	9	3	2	16	15	1HEL
Trypsin	8.3	23	2/14	9	11	2	24	48	1AUJ
Chymotrypsin	8.2	25	3/16	15	5	1	18	43	1GMD
Proteinase K	7.7	29	9/7	13	16	1	20	53	
Hemoglobin	6.8	64	9/48	63	2	22	24	55	1A3N
HSA	5.8	66	22/41	81	19	13	30	56	1BJ5
Ferritin	5.4	440	10/10	26	6	4	16	19	1IER
Ovalbumin	4.6	44	10/17	35	7	4	26	50	1OVA
Trypsin inhibitor	4.5	21	8/6	19	7	1	11	15	1AUV
Carbonic anhydrase	4.5	31	14/37	54	4	11	42	54	1V9E
Amylo-glucosidase	3.5	97	7/28	38	16	5	26	35	1LF6
Pepsin	1.0	34	5/11	26	9	3	30	47	1AM5

Table 4-2 *Properties of the proteins used in this research: PI, molecular weight, amount of some amino acid on the protein surface and the PDB number.*

Crystal structures of the proteins used in this research are available in *PDB* bank (Protein Data Bank), and the presence of their surface amino acids is calculated and given in table 4-2. PI values and molecular weights of these proteins could also be calculated by software "*Editseq"* with the *Fasta sequences* from PDB.

Except of above information, the amino acid distribution on a protein surface is also a key point for the recognition. A direct imaging with color could be obtained by using software "*Pymol"*. In such a picture, we always color the basic amino acids with blue and the acidic amino acids with red (Figure 4.2).

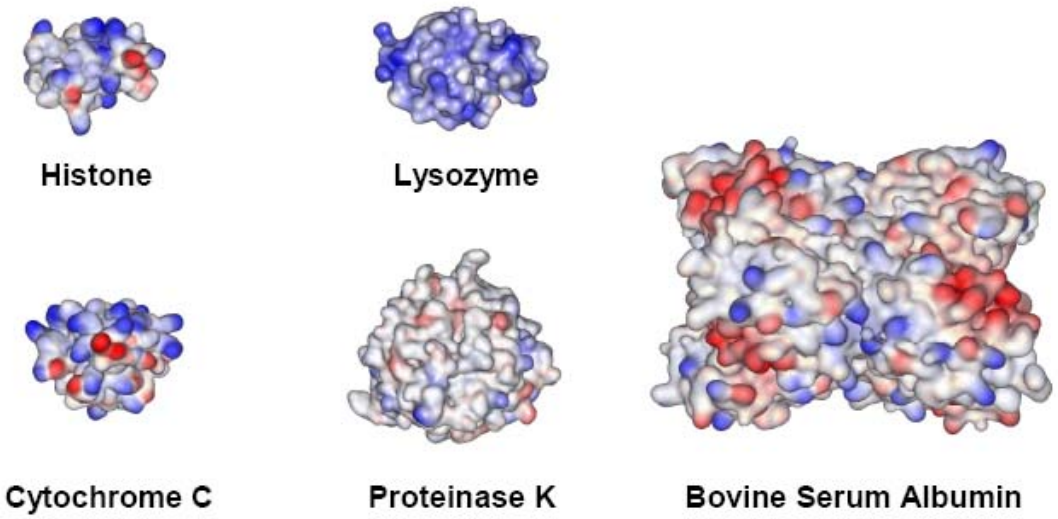

Figure 4.2 *Example proteins are patterned with the electrostatic surface potential (ESP), showing basic (blue) and acidic domains (red) on the protein surfaces.*

4.2 Protein recognition with dendrimers

The word *dendrimer* originates from the Greek (combining "Dendron" meaning tree or branch, and "*meros"* meaning part) and refers to a class of structurally-perfect branched macromolecules.[55] Dendrimers are spheroid or globular nanostructures that are precisely engineered to carry molecules encapsulated in their interior void spaces or attached to the surface. Size, shape, and reactivity are determined by generation (shells) and chemical composition of the core, interior branching, and surface functionalities. Traditionally dendrimers are constructed through a set of repeating chemical synthesis procedures that build up from the molecular level to the nanoscale region. The dendrimer diameter increases linearly whereas the number of surface groups increases geometrically. Dendrimers are very uniform with extremely low polydispersity, and are commonly created with dimensions incrementally grown in approximately nanometer steps from 1 to over 10 nm (Figure 4.3, right). The control over size, shape, and surface functionality makes dendrimers one of the "smartest" or customizable nanotechnologies commercially available.

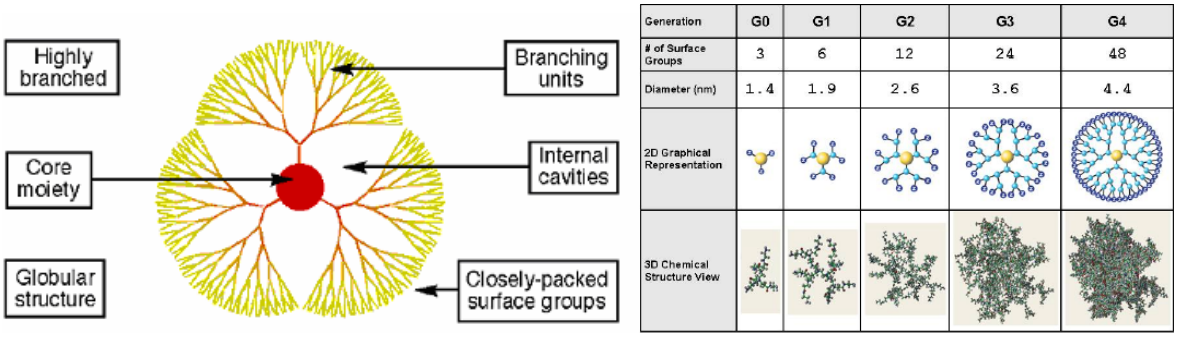

Figure 4.3 *Left) schematic dendrimer structure; right) sizes, 2D and 3D views of several generations of PAMAM dendrimers.*[56]

A dendrimer contains three areas where fascinating chemistry can occur (Figure 4.3 left). The first area, the encapsulated core, can harbor chemical species that show unparallel properties due to the special microenvironment created around them by the dendritic branching. The second area, the tailored sanctuary created within the voids of the flexible branches, can provide a refuge from the outside world. Finally, the third area of a dendrimer, its multivalent surface, can accommodate a very large number of functionalities that interact with the bulk,

thereby defining the dendrite's macroscopic properties.[1] Many research have been made in all these three areas.

In this research our attention concern on its third advantage: using its multivalent functionalities to recognize protein surface. With the m-xylylene bisphosphonates receptors in hand we have developed several generations of dendrimers based on PPI (polypropyleneimine) backbones and studied their bindings to the proteins with different PI and sizes. The complexation event is studied in buffered aqueous solution by three different spectroscopic methods (PFGLED, UV/Vis, and fluorescence). We have proved that a single weak-binding event is multiplied into an efficient receptor site for protein surfaces (from $<10^2$ to $>10^6$ M^{-1} in buffered aqueous solution) in a biomimetic fashion. An illustration of the binding between our dendrimers and proteins is shown in figure 4.4.

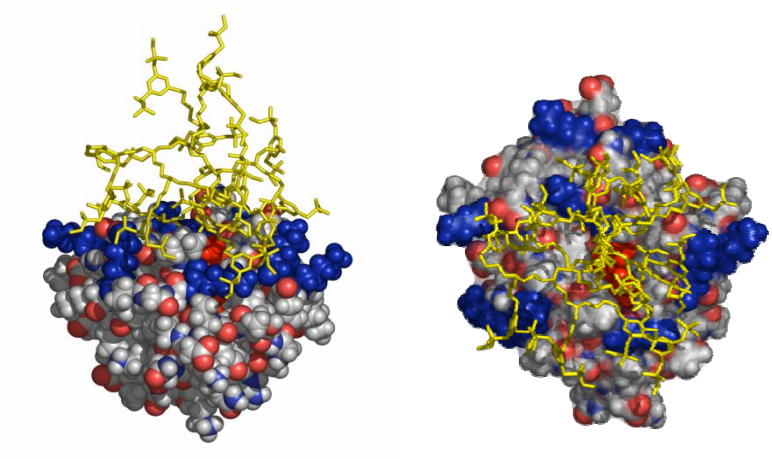

Figure 4.4 *Minimized 1:1-complex between cytochrome c (C:grey, O:red, N:blue, lysines around the active site: blue) and the hexadecamer dendrimer (yellow, SYBYL 6.9, MMFF94). Left) side view; right) top view (protein with transparent connolly surface and buried heme group in red, arrow).*

4.2.1 Dendrimer synthesis

Traditionally dendrimers are synthesized by a fully controlled step by step approach, but a stepwise construction of large molecules suffers from a clear disadvantage in synthesis economy. This difficulty can be circumvented by starting from dendrimer cores and simultaneously attaching binding sites to their periphery.[57] Polypropyleneimine (PPI)

dendrimers are commercially available in various generations and offer a similar number of bridging atoms between their amine end groups. Moreover, initial modeling experiments suggested that in spite of their dendritic nature, almost every binding site can find its arginine counterpart on a flat surface, such as the one of a protein.[58]

In addition, the conventional synthesis of higher oligomers proved problematic in this research, because even with alkylphosphonate protecting groups the products are water-soluble and cannot be chromatographied over silica gel nor over RP phases. An ideal solution would directly furnish the free phosphonate salts in quantitative yield. However, to date, only few organic reactions are known involving multiply charged ionic species in highly polar solution. Kießling et al. developed the Staudinger reaction for native chemical peptide ligation;[59] von Kiedrowski et al. used acylhydrazone formation for the construction of DNA hybrids,[60] and Sharpless et al. achieved covalent modifications of biomolecules in living systems with "click chemistry".[61] With the PPI dendrimer polyamines at hand, we examined a multiple reductive amination sequence (Figure 4.5).[62]

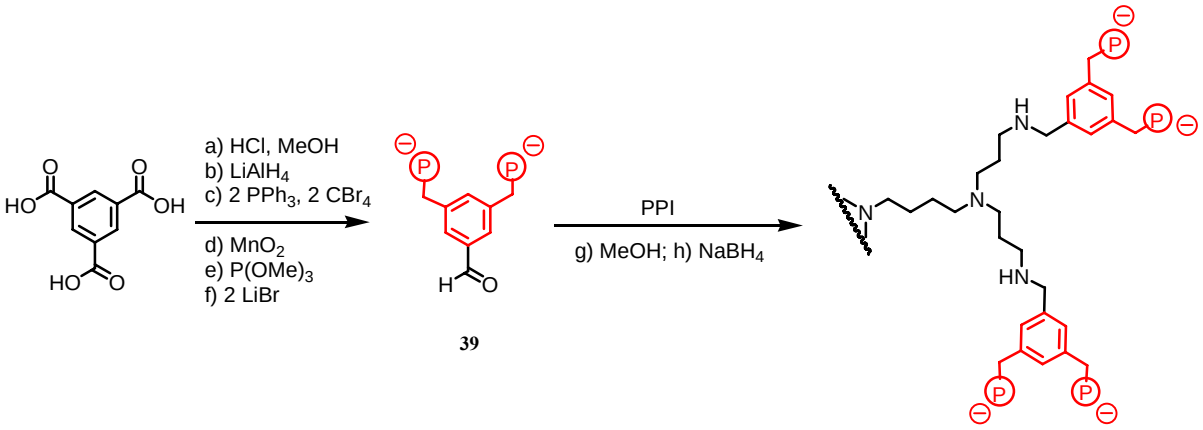

Figure 4.5 *Synthesis of the ionic bisphosphonate building block and subsequent one-pot reaction with PPI core by a multiple reductive amination sequence. Yields: a) 98%; b) 81%; c) 60%; d) 95%; e) 95%; f) 92%; g) 99%; h) 98%.*

Benzene-1, 3, 5-tricarboxylic acid was converted into its trimethyl ester, which was reduced into the corresponding triol by lithium aluminum hydride. With two eq. of *Appel* reaction reagent, two of the three hydroxyl groups were substituted by bromides. The other one was oxidized to aldehyde with a mild oxidant, MnO_2. By Arbuzov reaction and the following ester bis-dealkylation, 39 was obtained. This building block was dissolved in methanol and reacted in a 1:1 ratio with each primary amine end group of the PPI. Subsequent treatment with

$NaBH_4$ in the same pot converted the unstable *Schiff* base into the stable benzylamine. In order to remove an excess of borate salts, the dendrimers were also purified over RP-HPLC. ^{1}H and ^{31}P NMR spectra in D_2O displayed a clean set of slightly broadened signals, but MALDI TOF-MS showed that the dendrimers were not monodisperse, for example the octamer contained 5-8 mers and hexadecamer contained 12-16 mers (Figure 4.6).

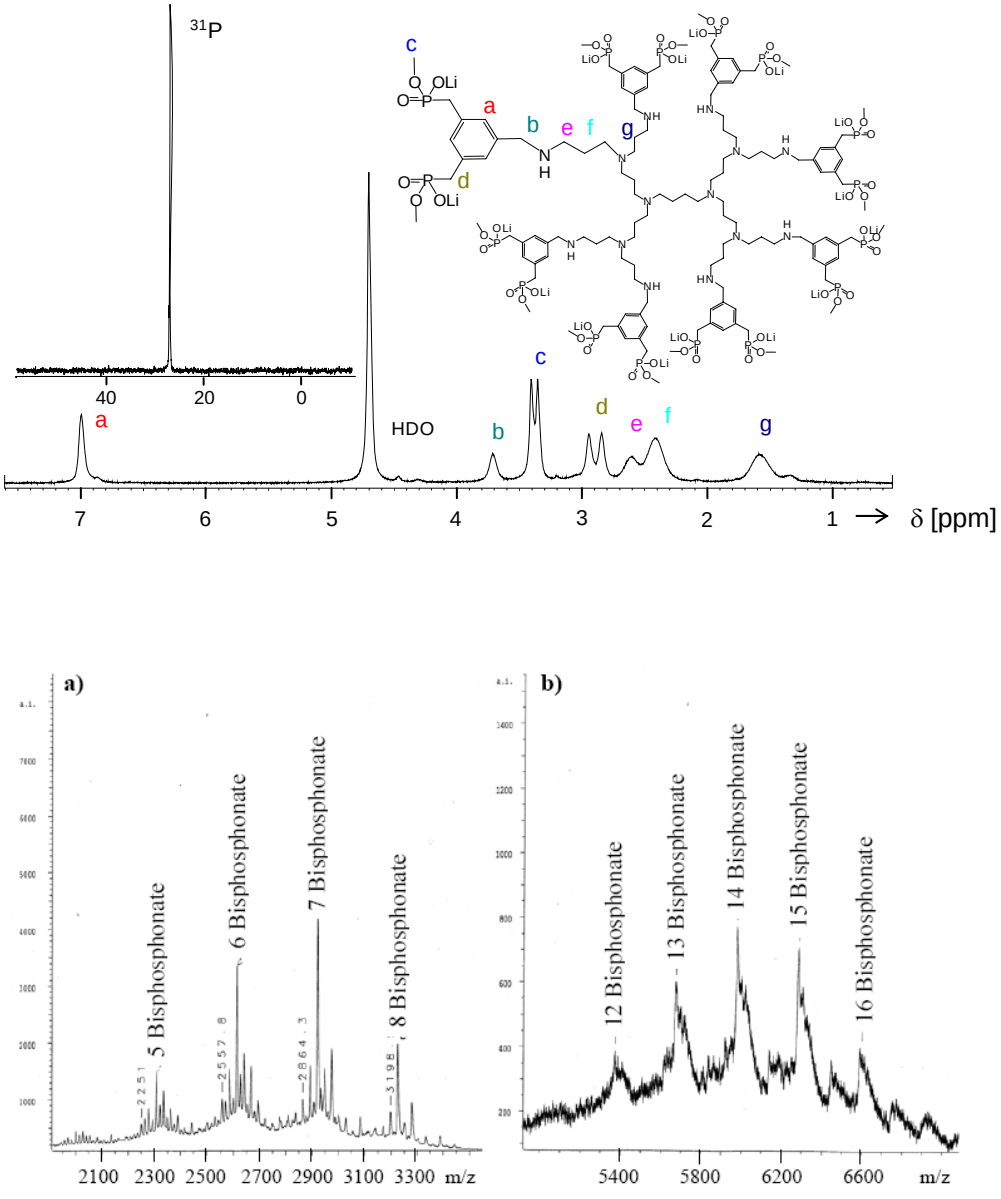

Figure 4.6 *Up) ^{1}H and ^{31}P NMR show a clean set of signals for the octamer; Down) MALDI-TOF MS spectra of octamer (a) and hexadecamer (b) indicate that the dendrimers are not monodisperse.*

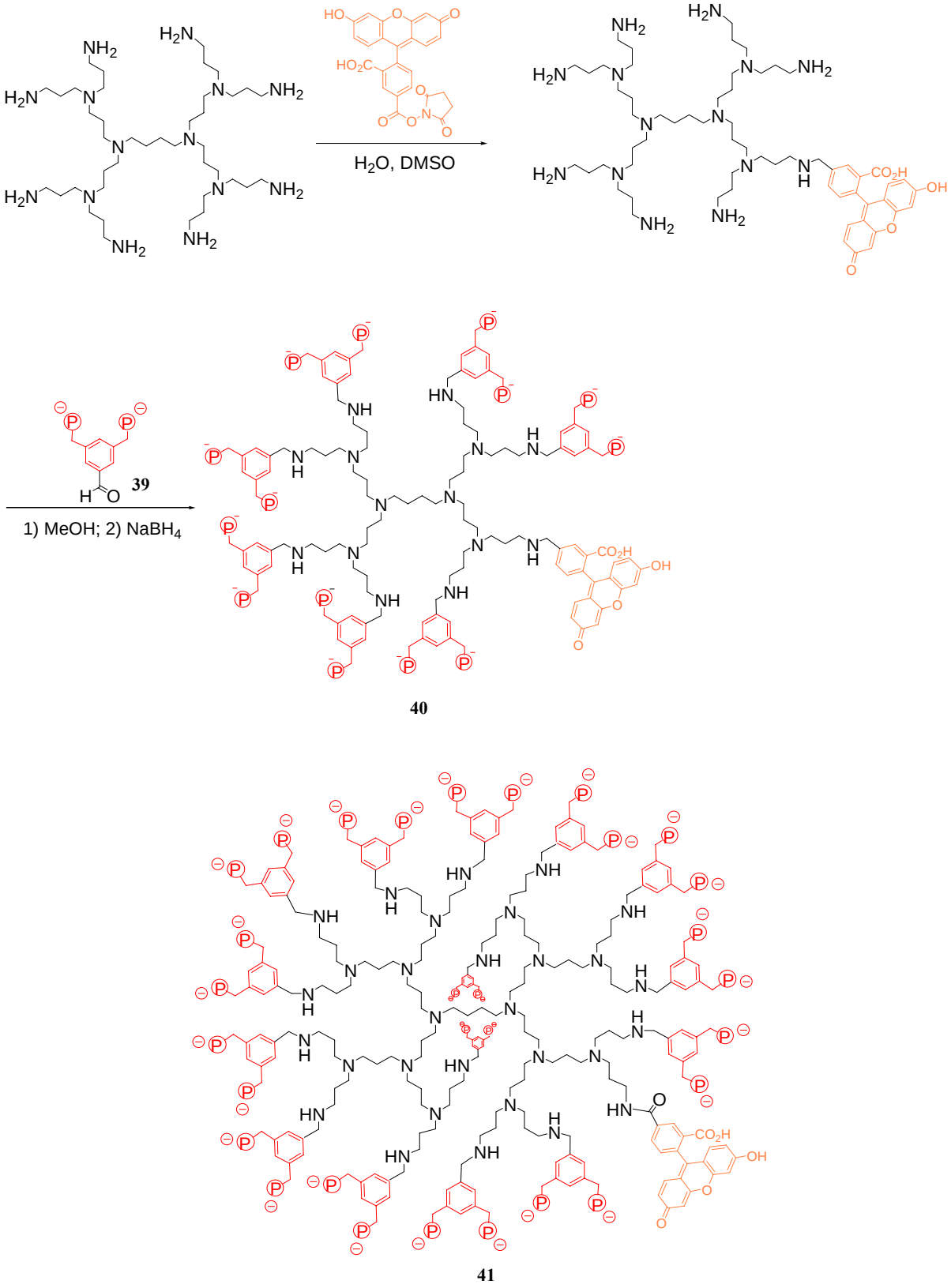

Figure 4.7 *Synthesis of fluorescein labeled octamer (40) and hexdecamer (41).*

For the later fluorescent titrations, dendrimers with the fluorescein label were also synthesized in the similar way as the non-fluorescent ones (Figure 4.7). A mixture of PPI octamer (1.0 equiv) in water and fluorescein, activated as N-hydroxysucciimide ester (1.3 equiv) in DMSO, was incubated for 4 h. The solvent was removed, and 3, 5-bis(methoxyphosphorylmethyl) benzyl aldehyde dilithium salt (39) was added to the residue. The mixture was dissolved in anhydrous methanol and stirred under argon with molecular sieves at ambient temperature. After 24 h, sodium borohydride was added, and the solution was stirred for another 24 h. The crude solid was purified by dialysis (MWCO with pore size 1000 g/mol) with water for 4 times and each time for 1 day. Under such condition the small molecules whose molecular weights are smaller than 500 could diffuse out of the dialysis membrane. Afterwards the purified product solution in the membrane was dried to afford a light yellow solid.

In this way fluorescein labeled octamer and hexdecamer were prepared. Their MALDI TOF-MS were measured. Although no spectrum with good resolution was got, it could be observed that the octamer was not monodisperse and contained 6, 7, 8 mers. Anyway the ^{31}P and ^{1}H seemed good: there was only one peak in ^{31}P spectrum at about 26.5 ppm; in the ^{1}H spectrum the signals in the aromatic range at about 7.2 ppm showed nearly 6 protons more than those in the non-labeled dendrimers, which came from the fluorescein.

4.2.2 Binding study

Before the binding study *Markus Arendt* had proved that there was no back folding occurs in the zwitterionic dendrimer by dilution experiments, which means that the dendrimers didn't self-associate between the phosphonate negative charge and positive charge on the backbone, and thereby bisphosphonate functionalities at the periphery of the dendrimers were free for binding to the basic amino acids on the surface of proteins. He used diffusion experiments, UV titrations and fluorescence titrations between labeled proteins and polymers to evaluate the bindings, but all of these three had their shortages. Diffusion measurement is only suitable for small molecules compared to proteins, because hydrodynamic volumes of larger molecules approaches that of the proteins and leads to large intrinsic errors. In our case only tetramer was small enough to produce a significant difference in diffusion coefficient D compared to a basic protein such as cytochrome C. UV titration could only be used for the proteins with natural chromphore such as cytochrome C and hemoglobin. Fluorescence

titrations between labeled proteins and polymers also had problem. Changes in fluorescence intensity were in most cases very small, thus precluding an exact quantitative evaluation. A possible explanation is the location of the N terminus in these proteins: if the dendrimer binds to the basic domain far from the fluorescence label attached to the N terminal of the protein, the binding will fail to give an efficient fluorescence signal (Figure 4.8). This phenomenon precluded an exact quantitative evaluation and therefore fluorescent labeled dendrimers were synthesized.

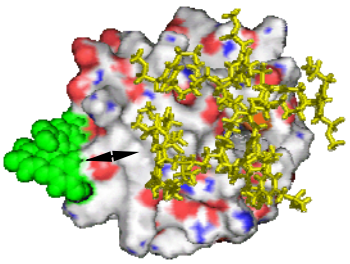

Figure 4.8 *A dendrimer (yellow) binding to the active site of cytochrome C is far from the fluorescence label (green) and fail to give an obvious fluorescence change while binding.*

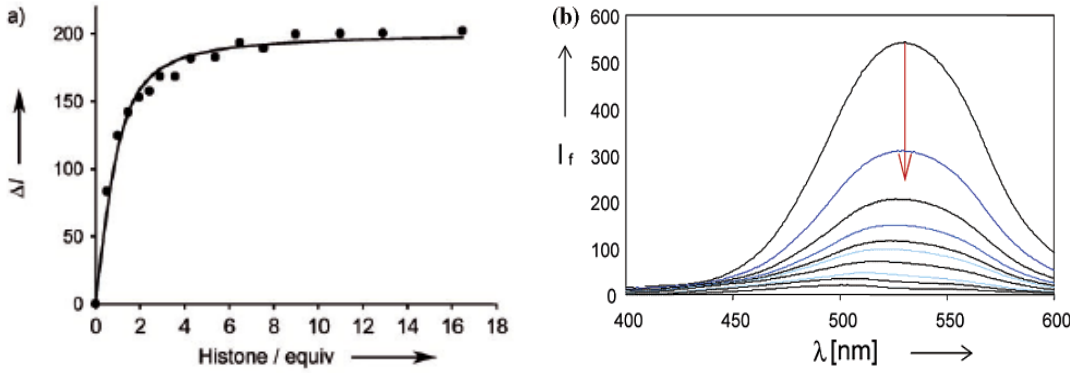

Figure 4.9 *A typical fluorescence titration curve obtained from complex formation (left), and fluorescence intensity change (right).*

Fluorescence titrations with fluorescent-labeled dendrimers and proteins were performed in Hepes buffer (10 mM, pH 7.0) (Table 4-3). In some cases, to reveal the effect of different buffers, the Hepes buffer was replaced by sodium phosphate buffer (10 mM, pH 7.1) or treated with sodium chloride (150 mm). Compared to the changes in fluorescence emission

intensity between non-fluorescent dendrimers and labeled proteins, those between the new fluorescent dendrimers and proteins became much more impressive (Figure 4.9).

Table 4-1 *Association constants and stoichiometries for complex formation between fluorescein-labeled dendrimers and native proteins of varying pI and size, according to fluorescence titrations in buffered aqueous solution at 25°C.*

Proteins and Peptides					Octamer 40		Hexadecamer 41	
Protein	pI	MW	Arom[a]	lys/ar[a]	K_a[b]	ratio	K_a[b]	ratio
Histone H1	10.4	22K	3.3%	17/12	1e+6 M^{-1}	1:1	-	
Histone H3	11.5	15K	3.3%	13/18	1e+5 M^{-1}	1:2	2e+4 M^{-1}	1:2
Cytochr C	9.2	12K	2.5%	16/2	2e+4 M^{-1}	1:1	no effect	-
Lysozyme	9.1	14K	5.5%	7/11	8e+3 M^{-1}	1:1	no effect	-
Hemoglobin	8.8	31K	5.8%	48/9	7e+3 M^{-1}	2:1	-	-
Trypsin	8.3	22K	5.7%	14/2	1e+6 M^{-1}	1:1	2e+6 M^{-1}	1:1
Chymotryp	8.2	25K	3.9%	6/8	no effect	-	5e+5 M^{-1}	1:1
Proteinase K	7.7	29K	8.7%	7/9	7e+4 M^{-1}	1:2	-	-
BSA	5.8	66K	4.0%	41/22	-	-	3e+4 M^{-1}	1:2
Ovalbumin	5.3	44K	2.0%	66/38	no effect	-	-	-
Carb. Anhyd.	4.5	50K	4.4%	37/14	no effect	-	-	-
Lys_4	9.5	0.9K	0%	4/0	6e+4 M^{-1}	1:1	2e+5 M^{-1}	1:1
Arg_4	12.0	1.2K	0%	0/4	6e+5 M^{-1}	1:1	1e+5 M^{-1}	1:1

[a] the percentage of aromatic area and the numbers of lysine and arginine residues on the protein surface were calculated with the *atomic volume analysis option* in the software PROVE; [b] *K*a determinations in selected cases produced experimental errors below 30%.

Generally octamer bind most of the basic proteins following roughly the pI scale except of trypsin, and have no effect to the acidic proteins such as ovalbumin and carbonase anhydride. For most proteins with pI values above 7, binding isotherms could be fitted to a 1:1 or 1:2 binding model. In some cases the dissociation constant dropped into micromolar regime, especially with small lysine-rich proteins (histone 1 and trypsin).

It was a surprise that the lysine rich histone H3 had better affinities than arginine rich histone H1, which was contrast to our arginine selectivity of the bisphosphonate binding site and our linear polymers. The other lysine rich protein, trypsin, also had a stronger affinity than others with a higher PI value but low lysine content on the surface. A possible explanation for this

unprecedented potential lysine selectivity involves unfavorable Coulomb repulsion between arginine's approaching guandinium cation and the unique secondary benzylammonium group (Figure 4.10 a), which is present only in the dendrimers due to the reductive amination step. Transition from the octamer to the much larger hexadecamer did not lead to a drastic affinity increase and in some cases, K_a values were even smaller (histone H3, Arg_4) or no obvious effect could be observed on protein addition to the hexadecamer (cyt c, lysozyme). Assuming a globular dendrimer topology for both, the hexadecamer is clearly more rigid, rendering its induced fit onto a flat protein surface more problematic as well as limiting its total contact area. Another factor contributing to enhanced protein affinity seems to be the additional hydrophobic interaction between the extended π-face of the fluorescein label and aromatic residues on the protein surface (trypsin: 10^4 M^{-1} - unlabeled dendrimer vs. 3×10^5 M^{-1} - labeled dendrimer).

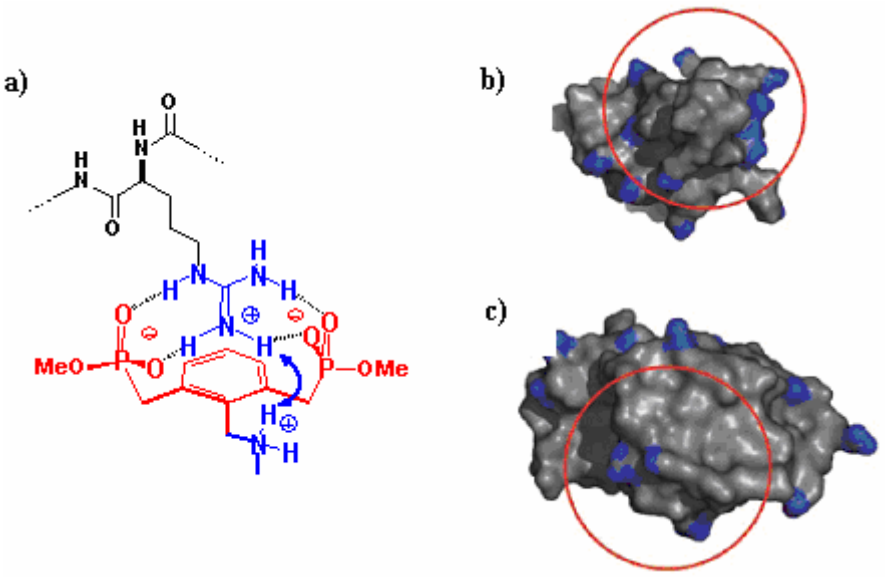

Figure 4.10 *a) Diagram shows the repulsive guaidnium/ammonium interaction preventing formation of the p-cation-stabilized arginine–bisphosphonate complex within the dendrimer. Highest density of basic residues on a connolly surface for histone (b) and lysozyme (c). The estimated contact area of the hexadecamer dendrimer is depicted in red. Note that histone is lysine-rich, whereas in lysozyme, arginines prevail.*

Finally, a close inspection of EPS (electrostatic potential surface) patterns now offers a plausible explanation for the sensitive discrimination ability between proteins of similar pI and size (Figure 4.10 b and c). Only a fraction of both the dendrimer's and the protein's

(roughly globular) surfaces is available for close intermolecular contact. For efficient binding it is therefore mandatory to ensure a high local density of basic amino acids within this critical cross-section. This holds especially for the relatively small octamer; its contact area is about 8 Å wide. Consequently, arginine residues on Lysozyme surface, which are on average 12 Å apart from each other, cannot be simultaneously covered by the same ligand. By contrast, histone is densely packed with lysines, and trypsin has a pronounced basic domain at its *N*-terminal end, ideally suited for multivalent dendrimer docking. We believe that a favorable combination of the above-detailed factors inevitably leads to efficient and selective protein surface recognition by bisphosphonate dendrimers. Trypsin, e.g., is bound more than a hundred times more tightly than lysozyme or cytochrome C, in spite of its lower pI.

Interestingly the binding stoichimetry determined by means of Job plots for the octamer and hexadecamer and basic proteins were all 1:1 or 1:2, with the exception of large hemoglobin accommodating two octamer molecules. The highly possible reason is that, the dendrimers search for domains of high positive surface charge in order to exploit multivalent electrostatic attraction and therefore the stoichimetry depend mainly on the size and distribution of the basic domain on the protein surface.

In three cases (histone H3, proteinase K, BSA), one dendrimer could hold two protein molecules; this is surprising, especially in view of the considerable protein size of BSA, but may be connected with local basic domains of high surface charge. Separate calculation of both association constants [63] reveals a distinct preference for the first binding event (negative cooperativity), most likely due to mutual electrostatic repulsion between both protein guests in the second binding step. The results are summarized in table 4-4.

Protein	Dendrimer	K_1 [M^{-1}]	K_2[M^{-1}]
Histone H3	40	1.4E05	4.2E03
Histone H3	41	4.8E05	1.5E03
Proteinase K	40	1.8E05	1.2E03
BSA	41	6.9E05	5.1E03

Table 4-4 *Binding constants calculated separately for three proteins involved in 1:2 complexes.*

Basic peptides are also strongly bound (Table 4-4, last two rows). Even small Arg4 almost

reaches micromolar affinity in buffer towards the octamer. This finding holds strong promise for immobilization of dendrimers on solid support for a potential development of new affinity chromatography material for Arg-tagged recombinant proteins.

4.3 Protein recognition with linear polymers

As said at the beginning, large molecules such as polymers may be particularly valuable for cases in which protein surfaces do not possess clear binding sites. In this line our group has developed linear copolymers for protein recognition. The concept is the following: for a given protein target, we choose from a preformed set of polymerizable binding sites those that match the majority of amino acid residues dominating the surface character of the protein. By copolymerization, a flexible copolymer is produced that is capable of performing an extensive "induced-fit" procedure on top of the respective protein surface, and therefore reaching maximal attractive (non)covalent interactions. No cross-linking is employed to guarantee perfect water solubility; no imprinting technique is used because the linear polymer is expected to adapt its shape to flat and rugged surface topologies.

Pioneering works have been done successfully in our group by Christian Renner and Sebastian Koch. C. Renner has used free radical polymerization to turn weak arginine binders into powerful polymeric protein receptors, and S. Koch has found a copolymer mainly based on a bisphosphonate monomer (**1**) is selective to lysozyme. These results give us a hint, that we could optimize the above introduced modular concept by creating diverse copolymer libraries with a representative pool of binding monomers for all important interactions occurring in protein recognition events.

4.3.1 Polymer synthesis

With the monomers described in chapter 3, a small polymer library containing 20 polymers was prepared for test in order to find a general protocol for polymer libraries. Most of the 20 polymers were highly fluorescent powders with good water solubility, and could be characterized by ^{1}H NMR and ^{31}P NMR spectroscopy in some cases. Their molecular weights could be obtained by GPC measurements (standards: polyethylene oxide, polyethylene glycol) in water or DMF. All structural elements were visible in their ^{1}H NMR and afford nearly same integrals as initial adding ratios. In selected cases, *Christian* has determined copolymerization parameters by the Fineman-Ross method[64] and found to be close to 1.0, [65] ensuring a statistical copolymerization.

	M1	M2	M3	M6	M7	M8	M9	M11	M12	M13
P1		1								
P2			1							
P3				1						
P4									1	
P5										1
P6				1		4		0.5		
P7		2		1				0.3		
P8		2		1		4		0.2		
P9		2		1		4	0.7	0.8		
P10		5		1			1	0.7		
P11	1			1				0.7		
P12	1			1			1	0.3		
P13	1					3		0.6		
P14	4						1	0.4		
P15	2						1	0.3		
P16	1				5		5	1		
P17	1					5	5	1		
P18	1	1						0.7		
P19		2.5				1		0.3		
P20		1			1		0.5	0.3		

Table 4-2 *Polymers synthesized in DMF by free radical polymerization.*

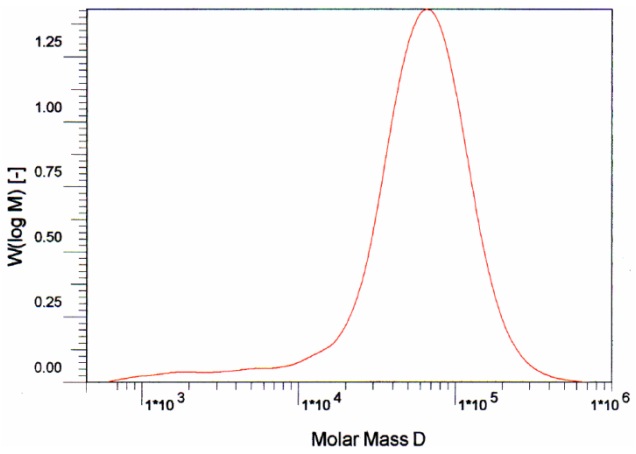

Figure 4.11 *A polymer GPC example.*

In these 20 polymers, P1, P2, P3, P4 and P5 (Figure 4.12) were synthesized to prove the polymerization feasibility of monomer **2**, **3**, **6**, **12** and **13**. (The polymerizable ability of other monomers is reported in literatures.[19, 41, 49, 61]). Other polymers were prepared with design and will be discussed in several groups based on main binding monomers.

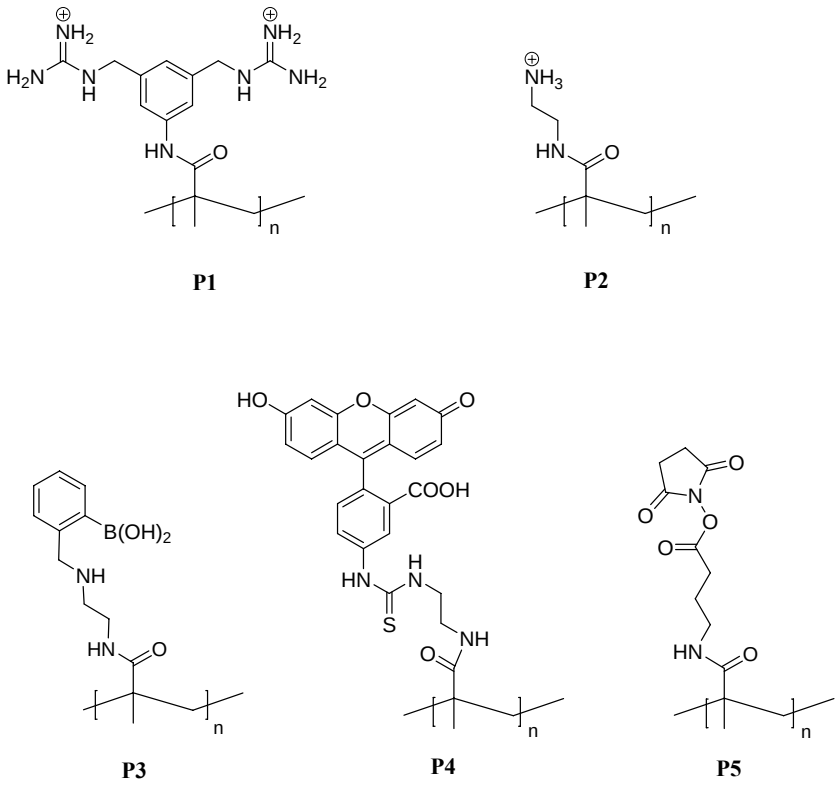

Figure 4.1 *Polymer structures of P1, P2, P3, P4 and P5.*

Polymers based on *o*-aminomethyl-phenylboronic acid monomer 6 (Figure 4.13): 6 was soluble in DMF, and after polymerization its homopolymer P3 precipitated from the solution and became not soluble in water, methanol and DMSO. P7 was prepared tightly packed with two comonomers, i. e., boronates and ammonium ions. It was designed to have a ratio of 1:3 between boronates and ammonium monomers. As a reference, a neutral polymer P6 was also synthesized, lacking any cationic group. Its affinity should reveal the importance of Coulomb attraction vs. boronate ester formation. P8 diluted both binding sites with an excess of amino alcohol groups with the aim of generating more selectivity. The glucose amide monomer **7** is not used for this kind of polymer because it might form complex with **6** internally. P9 incorporated the unpolar dodecyl tail, in order to probe the importance of hydrophobic interactions, but unfortunately it was insoluble in aqueous solution.

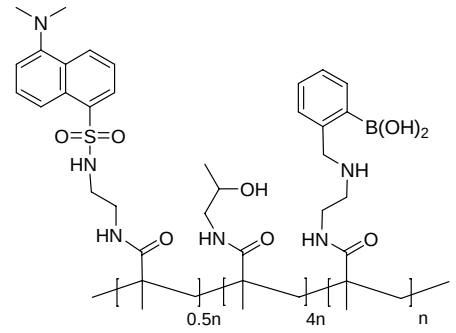

P6

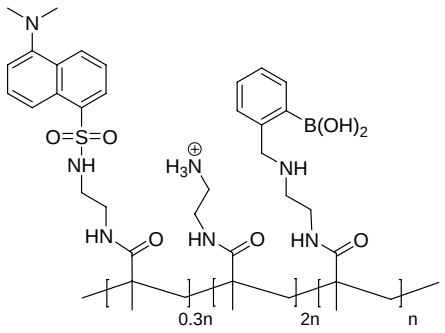

P7

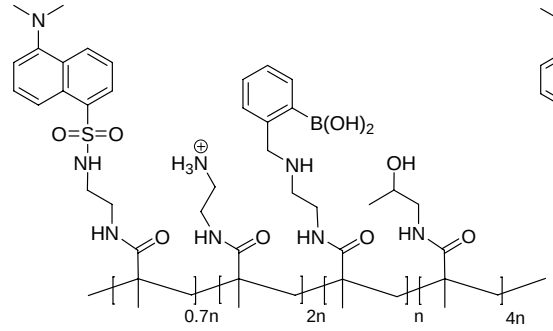

P8

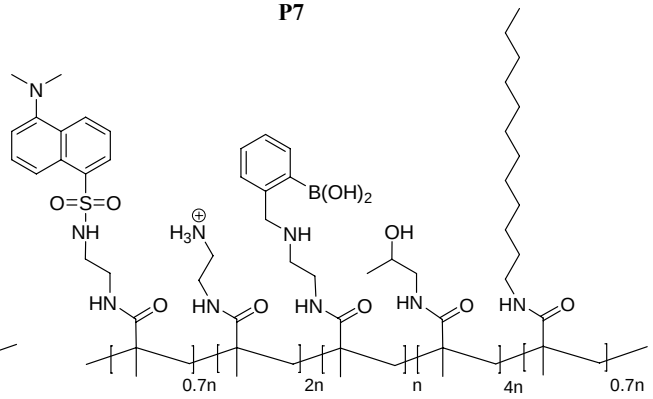

P9

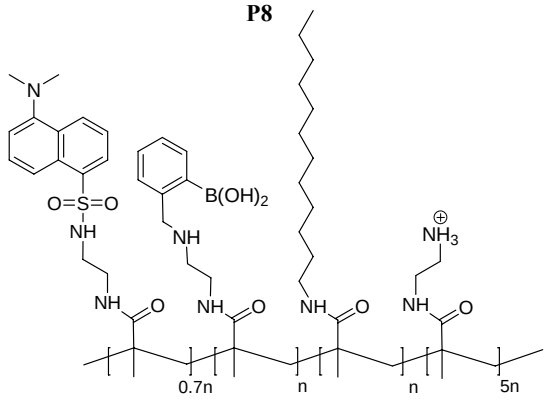

P10

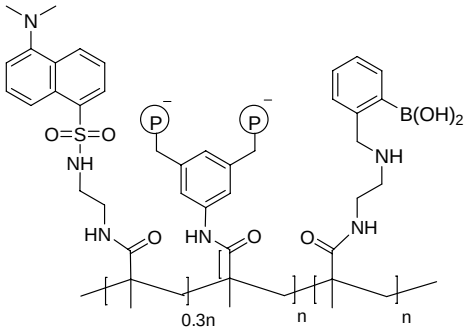

P11

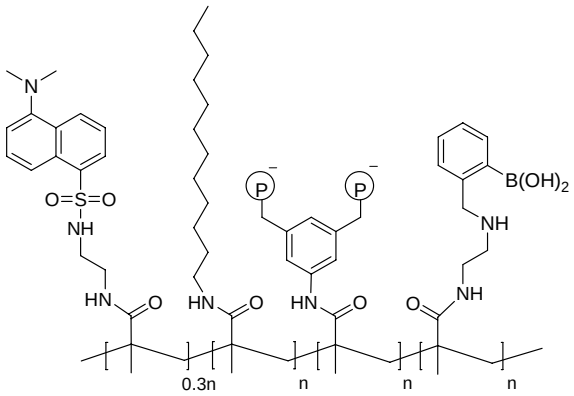

P12

Figure 4.2 *Copolymers mainly based on monomer 6.*

P10 contained more ammonium monomers to generate stronger electrostatic interaction than above ones. Different from others, P11 and P12 didn't contain cationic monomers, but the anionic **1**. P11 was still soluble in water, but after the dodecyl monomer was introduced into its structure, the generated P12 became insoluble in aqueous media.

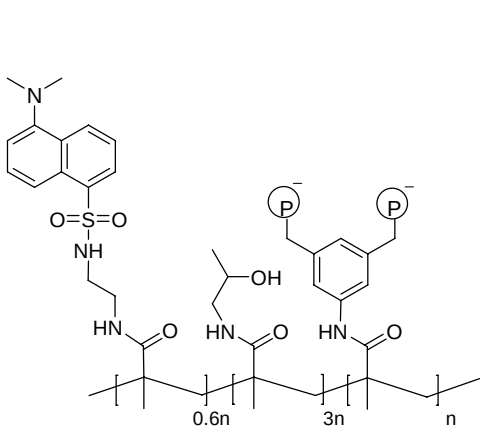

P13

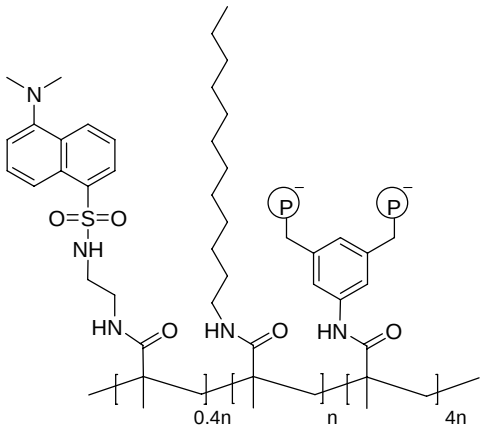

P14

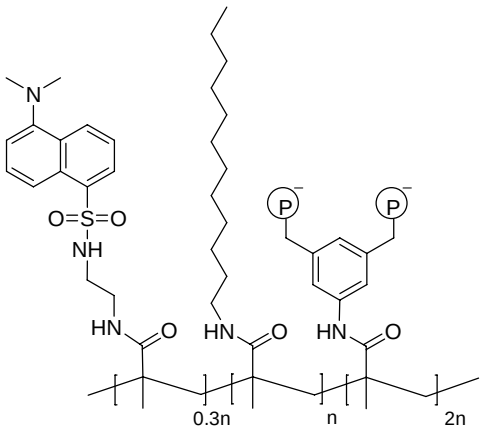

P15

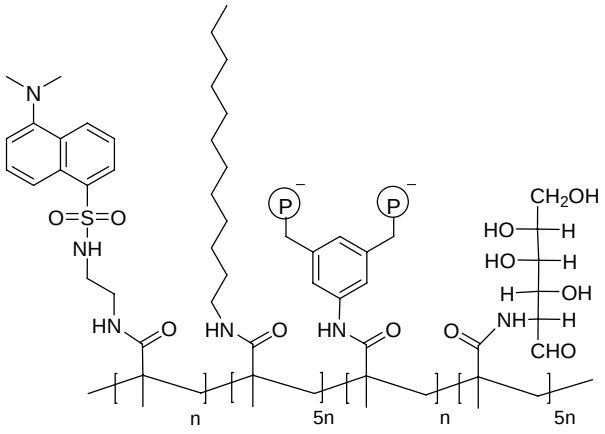

P16

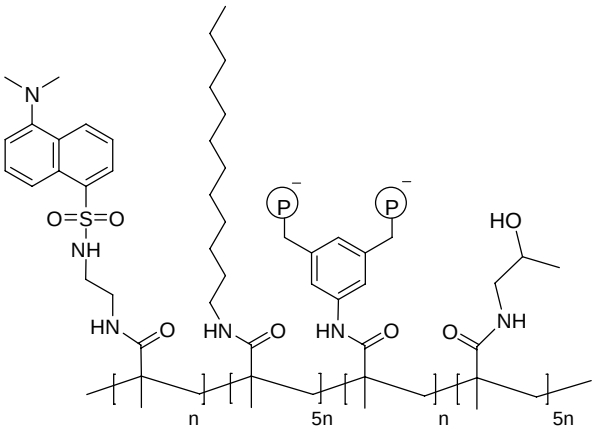

P17

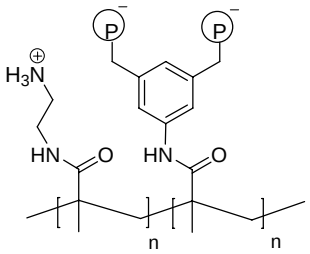

P18

Figure 4.3 *Polymer structures mainly based on monomer 1.*

Polymers based mainly on monomer 1 (Figure 4.14): Much pioneering work had been done based on this monomer and an important finding was the combination of it and hydrophobic monomer **9** with a 1:3 ratio. Here polymers with different monomer combinations were developed. In P13 monomer **1** was diluted with the amino alcohol monomer **7,** with the aim of generating more selectivity. P14 was designed to have 5eq. of **1** and 1eq. of hydrophobic dodecyl monomer **9**. From P14 to P17, binding sites for electrostatic interaction decreased and hydrophobic receptors increased, with an increasing content of monomers **7** and **8** for keeping solubility. The difference between P16 and P17 was only the monomer change from a glucose monomer **7** to the amino alcohol monomer **8**. P16 was poorly soluble in water, might due to the multi-methacrylate impurity from the glucose monomer **8**. Although dendrimers containing dianions at periphery and secondary amines at the backbone didn't show self-assembly,[66] polymer P17 was not soluble in any solvent, indicating a strong internal interaction.

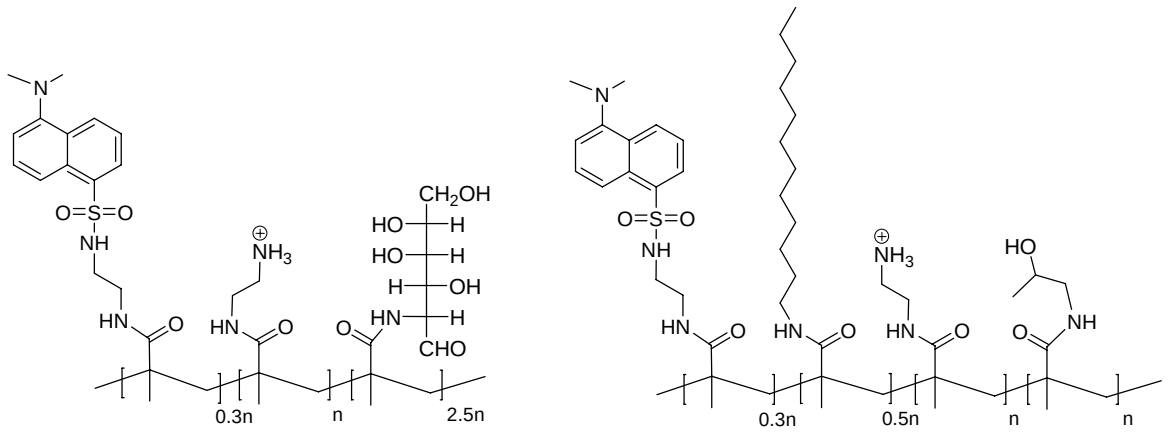

P19 **P20**

Figure 4.4 *Copolymer structures based on monomer 3.*

Polymers based on alkylammonium monomer 3 (Figure 4.15): in this series, **3** was used to prepare two polymers, P19 and P20, without any other strong binding sites. They could bind acidic proteins, and the comparison between them could provide us the information about the importance of coulomb attraction vs. hydrophobic interaction.

4.3.2 Binding study with microplate screening

With above polymers in hands we began to examine screening methods. In the previous work the binding affinities between polymers and proteins were measured by fluorescence titration in most cases. However, the normal titration takes several hours and become not accepted for a library screening. Fluorescence titrations on microreaders were therefore tested.

Two kinds of fluorescence microreaders were used. The first was an external demountable fluorescence microreader from JASCO. Because results measured from this reader had unacceptable reproducibility, later we changed to a standard fluorescence microreader (VICTOR). The reproducibility produced by the second reader was not bad, but the calculated binding constants had large errors, and therefore couldn't be used for comparison. The volume limitation could be the source of the errors.

In another try, some strong bindings were monitored by the solution optical density (OD). In polymers, monomer **1** and **3** was not only electrostatic binding receptors, but also responsible for the polymer solubility in somehow. After the polymers containing them formed complex with proteins, the solubility of the complex became worse than that of the polymers. In fact precipitation was observed in several cases with high binding affinities. Therefore, strong bindings might be monitored by the solution optical density (OD). UV microreader was utilized to evaluate OD changes. However, it was found that these results could only give us a qualitative, but not quantitative indication.

4.3.3 Binding study with normal-scale fluorescence titrations

Normal scale fluorescence titrations were performed in some cases. All the polymers based on monomer **1** (P13, P14, P15 and P16) showed strong affinities to basic proteins, and no binding to acidic proteins. P13, P14 and P15 had similar affinities to lysozyme and trypsin, and their affinities to histone were so strong that the complex precipitate from the solution and prevent quantitative evaluations. Due to the higher PI value of lysozyme and its more negative charge density on the surface, all polymers were selective to lysozyme compared to trypsin.

P10, P19 and P20 were polymers based on monomer **3**. P20 had nearly no affinity to acidic proteins, BSA and Pepsin, although it had more hydrophobic tails than P19. This revealed the importance of electrostatic interaction in the recognition. P10, containing more ammonium monomers (**3**) and more hydrophobic monomers (**9**) than others, showed high affinities to BSA and Pepsin. Its binding to pepsin couldn't be measured due to the complex precipitation. (Table 4-6).

	Glycan/protein				
	Histone	Lysozyme	Trypsin	BSA	Pepsin
P6	NA	NA	NA	NA	NA
P13	>1E+08	2E+06	1E+05	NA	NA
P14	>1E+08	9E+07	3E+06	NA	NA
P15	>1E+08	3E+06	8E+05	NA	NA
P17	1E+06	6E+05	6E+04	NA	NA
P10	NA	NA	NA	1E+06	>1E+08
P19	NA	NA	NA	5E+05	3E+07
P20	NA	NA	NA	NA	NA
	Dextran	Hyalur.acid	Chondroitin	Heparin	Ovalbumine
P6	<1E02	<1E02	6E03	4E05	2E04
	-	-	*1:4*	*1:5*	*1:2*
P7	3E03[a]	2E03	4E06	3E07	1E06
	1:2[b]	*1:9*	*1:7*	*1:6*	*1:3*
P8	<1E02	<1E02	2E06	2E07	7E04
	-	-	*1:10*	*1:8*	*1:5*

Table 4-3 *Association constants determined by fluorescence titrations in 25 mM aqueous HEPES buffer; a) Errors are standard deviations and were calculated at 7-59%; b) stoichiometries (in italics) from Job plots. NA means that no binding could be observed.*

Polymer P6 didn't show good affinities to the examined proteins. Later in a systematic study, it and other three similar polymers based on boronic acid monomers (P7, P8 and P9) were tested against a series of sugars (Figure 4.16) beginning with neutral dextran, and ending with ovalbumin, a typical glycoprotein. Intriguingly, the acidic protein produced substantial

fluorescence quenching, while most (albeit not all) sugar experiments lead to a marked increase in fluorescence emission intensity. Direct comparison thus yields the selectivity for heparin, which carries most sulfate groups (low molecular weight heparin LMWH was used in this study, with a mean mass of 3 kD).

4.3.4 Study of a polymer selective to heparin

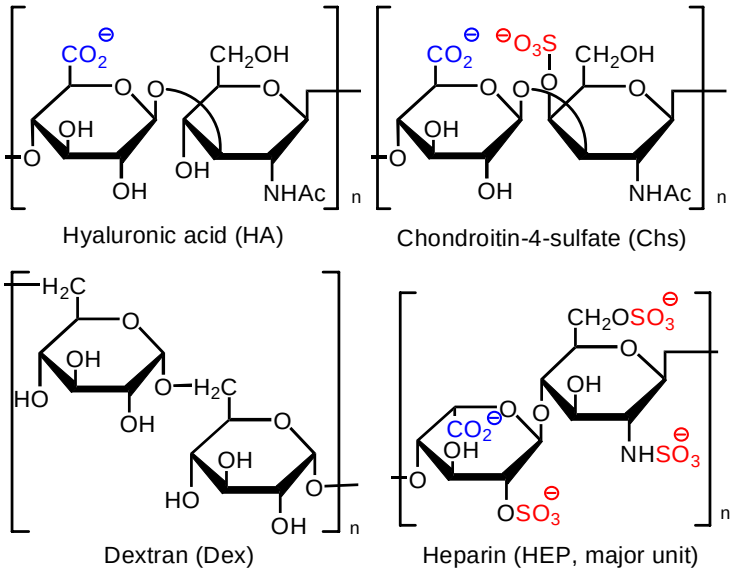

Figure 4.16 *Glycan structures: dextran, hyaluronic acid, chondroitin sulfate and heparin.*

Heparin's chemical structure, although of high polydispersity, is a constant repeat of a 1, 4-glycosidic sugar dimer, carrying hydroxycarboxylates (iduronic acids) and hydroxysulfates. In serum it is often accompanied with less sulfated anionic sugars, such as chondroitin sulfate and hyaluronic acid (Figure 4.17). Dextran, a simple polyhydroxyl sugar, was bound weakly, whereas affinities steadily rose with an increasing number of sulfate groups (Table 4-6). This trend was common for all polymers P6-P8. Heparin was always bound 1-5 orders of magnitude tighter than chondroitin sulfate or hyaluronic acid (with K_D values down to 30 nM). Comparison between polymer P6 and P7 which differ mainly in their cation content, reveals the importance of both binding sites for efficient sulfated sugar recognition. P6, without any cationic binding site, is still able to bind heparin with almost micromolar affinity; however, it loses all of its binding power if the sulfate groups are removed as in dextran. Contrary to P7, it is also much more selective with respect to chondroitin and ovalbumin.

Polymer P8 retains a high affinity towards heparin, but is much more selective than P7; thus confirming the dilution concept. The tight packing of cationic groups in P7 facilitates efficient Coulomb interactions with any anionic binding site along a saccharide strand or on a protein surface, whereas dilution with inert moieties forces both complex partners to an induced fit process in order to find complementary functionalities. Polymer P9 has bad solubility itself and produces insoluble complexes with most glucosaminoglycans, which precipitated from aqueous solution. The high affinity and selectivity of this kind of polymer are studied more in detail.

4.3.4.1 Binding model

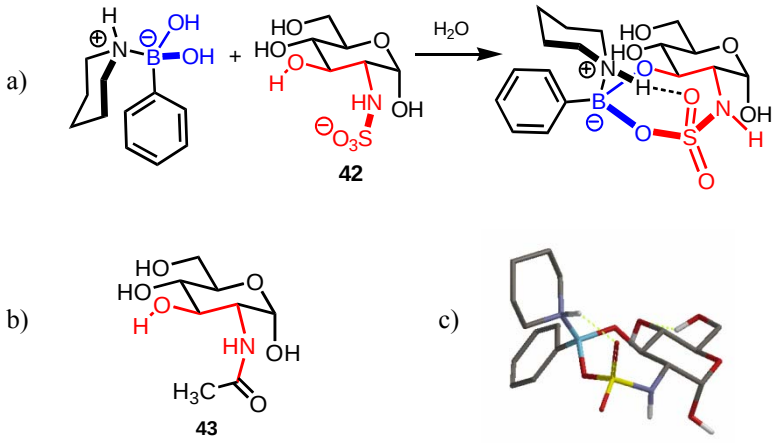

Figure 4.17 *a) Model complexation mixture, consisting of D-glucosamine 2-sulfate sodium salt (42) and the preformed 1:1 aggregate from phenylboronic acid and piperidine. b) Reference compound 43. c) Proposed structure of the preferred complex. Note that the boronic acid moiety (light blue) forms a 7-membered ring with the 3-OH group (red) and the 2-aminosulfate (yellow).*

In the past few years, the Anslyn group combined the *ortho*-aminomethyl-phenylboronate motif with alkylammonium groups for additional electrostatic interactions, and finally presented a heparin sensor fixed onto a wide aromatic platform.[67] This host molecule was shown to detect heparin in serum samples with very high affinity, down to 0.1 M concentrations. It was argued, that both the hydroxycarboxylates and the sulfates contribute to the binding event, with selectivity resulting from Coulomb attraction between sulfates and

ammonium ions, and an additional boronic acid ester formation, whose structural features were not specified.

From the above-detailed observations, we concluded, that a remarkably stable complex must be formed between a boronic acid and a sulfated aminoethanol or glycol. In order to gain deeper insight into this interaction, we examined the model compound **42**, a true heparin fragment, with a 1:1-complex of phenylboronic acid and piperidine (Figure 4.17).

Addition of increasing amounts of **42** to the tetrahedral boronic acid amine complex resulted in formation of a new set of ^{1}H NMR signals in the aromatic region, with considerable shift differences to the starting complex (*ortho*-protons 0.1 ppm upfield). This is typical for cyclic boronic acid esters, which are usually formed in a kinetically slow process on the NMR time scale.[68] In support of this assumption, ^{11}B NMR spectra furnished two new broadened signals at lower field (shifted from 5.8 to 9.3 and 11.7 ppm, respectively).[69] Interestingly, the sugar CH-region also displayed a new set of NMR signals, with large downfield shifts of 0.3-0.9 ppm. COSY experiments were very difficult to analyze unambiguously because of substantial overlap of cross peaks. However, a (small) new α-anomeric signal was found with a 0.4 ppm downfield shift, and at least one of the three methine protons was also drastically shifted downfield. By contrast, the closely related model compound **43** with an *N*-acetyl group instead of the sulfate did not produce significant complex peaks under the same conditions. Obviously, the sulfate is important for complexation, and the neighbouring hydroxyl groups participate in a cyclic ester formation. Although we were unfortunately not able to produce a clear NOE correlation due to the broadened complex peaks we tentatively suggest formation of the cyclic 7-membered ester depicted in figure 4.17. A molecular model can be constructed with small ring strain and a potential S=O$^{\cdots}$H^{+}-N stabilization. If this is correct, the 5-membered cyclic esters formed with α-hydroxycarboxylates can be extended to 7-membered cyclic esters likewise formed with β-hydroxyl amine sulfates.

A closer inspection shows, that the new CH-signals form $^{3}J_{H,H}$-couplings among each other and with non-shifted CH signals. Their distribution features all possible cyclic esters, although only the one depicted in figure 4.17 can exist in the heparin polymer. Each single species is present only in a relatively small amount (7-10%), and the signal ratio between **42** and all complexes furnishes a virtual association constant of <70 M^{-1}. However, the respective K_a value for cyclic boronic acid ester formation with α-hydroxycarboxylates is in the same

range (~ 300 M^{-1}). As a consequence, it must be assumed, that multiple ester formations between the polyboronate and heparin appear in a highly cooperative fashion, leading to the observed free binding enthalpy of about 7.5 kcal/mol. Anslyn et al. argue along the same lines, when they explain the drastic efficiency increase for their second generation heparin receptor with enlarged cavity.[67]

Based on the above monomeric model, it may be assumed that electrostatic contacts are most favourable at the isolated carboxylate or *O*-sulfate in the back of the heparin dimer at the 5-position, while the front with its hydroxysulfate prefers interaction with a boronic acid. Thus, we proposed a wrapping mechanism of the polymer around the sugar guest, assuring a maximum number of (non)covalent interactions, and thereby explaining the high stoichiometry factors of 5-8 LMWH molecules per polymer.

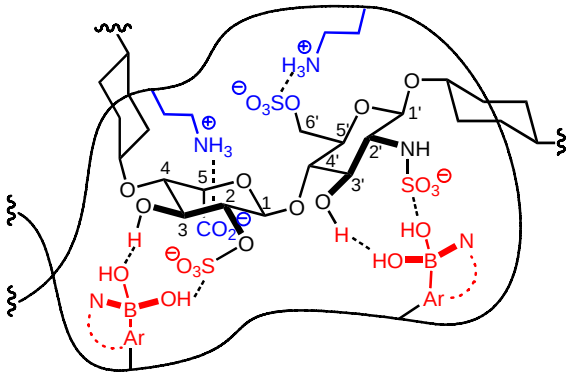

Figure 4.18 *Proposed wrapping mechanism with favourable interactions between polymer and heparin.*

4.3.4.2 Polymer as a heparin sensor

Heparin is widely known as anticoagulant because of its inhibitory complex formation with antithrombin III – it is therefore commonly used in surgery and in postoperative treatment.[70] Serum concentration must be monitored in submicromolar concentrations during cardiopulmonary surgery and even lower in long-term anticoagulant therapy of DVT (deep venous thrombosis: ≤ 0.1 M). Conventional methods involve the classical measurement of the activated clotting time (ACT), activated partial thromboplastin time (aPTT), potentiometric assays and protamine complexation.[71]

The biological effect of heparin can be reversed by addition of protamine, a cationic protein, which is known to sequester the anionic polysugar and release antithrombin III. In order to show that our heparin binding is also a fully reversible process in spite of the formation of covalent boronate ester bonds, we first prepared the complex between heparin and polymer P7 and subsequently added increasing amounts of protamine. Figure 4.19 demonstrates that the effect is completely reversed, and fluorescence emission intensity reaches the starting value. Consequently, our polymers imitate the reversible binding mode of heparin found in nature.

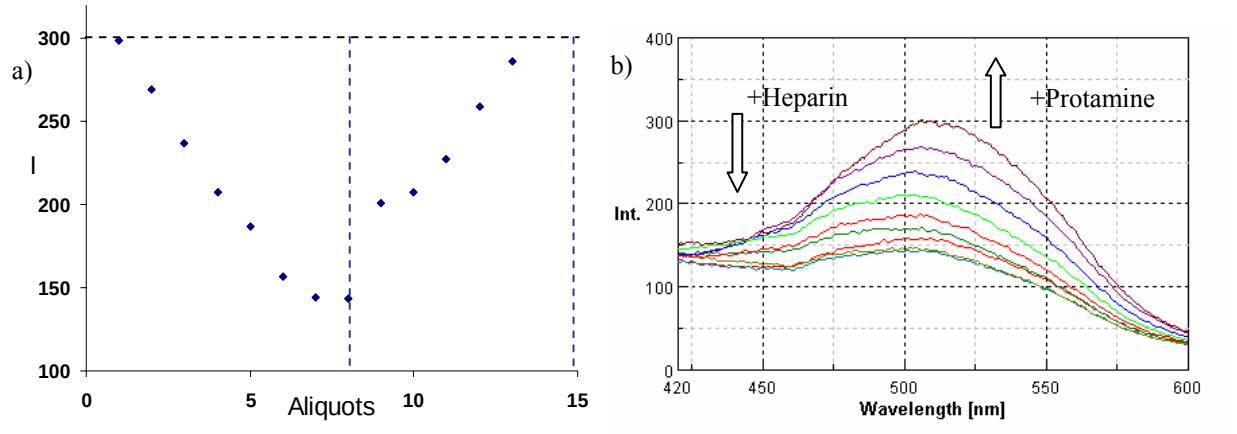

Figure 4.19 *Reverting heparin binding by P7 upon titration with protamine. a) Addition of 8 aliquots of heparin to polymer P7 (33 nM), followed by 5 aliquots of protamine, the fluorescence emission is fully restored. b) Fluorescence emission quenching of P7 via addition of increasing amounts of heparin (30-220 nM). Subsequent protamine addition restores the original emission intensity.*

The high sensitivity of P7 for heparin was used to generate a calibration curve for quantitative measurements (Figure 4.20). An almost perfect linearity was found for the concentration range from 30 nM to 220 nM heparin. This extends the values beyond the lower limits reported to date for artificial heparin receptors. Due to the built-in fluorescence label, the new polymers seem to be ideal materials for a heparin-quantification in medicinal samples. Intravenous or subcutaneous injection of heparin occurs at dosing levels as low as 2 UmL^{-1} (800 nM) in surgery or emergency DVT, and even reaches long-term levels of 0.2 UmL^{-1} (80 nM). Thus even the lowest clinically relevant dose can be quantitatively measured with a simple fluorescence assay using a cheap copolymer from readily available building blocks.

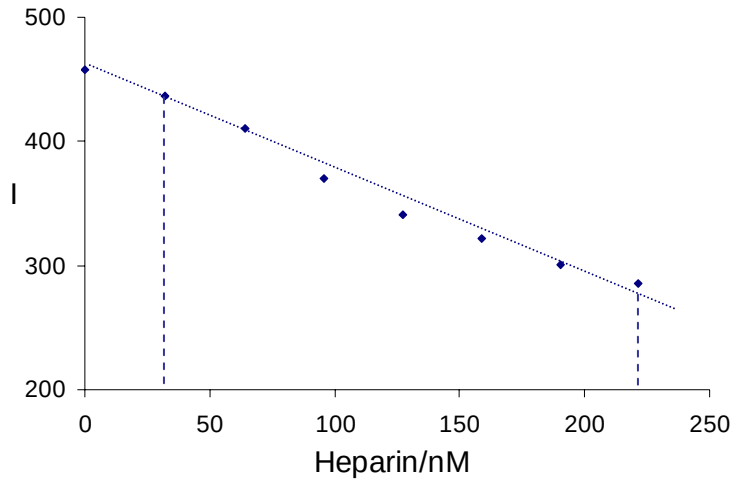

Figure 4.20 *Calibration curve displaying a linear correlation between fluorescence emission intensity and heparin concentration from 30 nM to 0.22 mM heparin (25 mM HEPES buffer).*

4.4 Protein recognition by polydiacetylene liposomes

The research in this chapter was a cooperation between us and the group of Raz Jelinek from Ben Gurion University, Israel. My contribution in this research was the preparation of five PDA monomers based on a 10, 12-tricosadiynene structure (showed in figure 3.16).

Polydiacetylene (PDA) is a polymer with built-in optical signal. The advantages of PDA materials for bio-detection applications arise from their fortunate conjunction of environmentally sensitive optical characteristics and easy formation in self-assembled systems. It is formed from the 1, 4-photopolymerization of diacetylene monomers, which are normally composed of two parts: a polar headgroup and a hydrophobic tail containing the diacetylene moiety. The polymerization only proceeds when the diacetylene are arranged in a lattice with appropriate geometry and the propagating species is believed to be an ene-yne, sometimes in resonance with a butatriene structure (Figure 4.21). [72]

The original color of PDA polymer is from blue to red to yellow, depending on the exposed time on UV lamp during polymerization. Changes in the absorption and emission spectra of the conjugated backbone are caused by its interaction with targets, which have been suggested that the effective conjugation length of the backbone is changed in the recognition by previous studies.[73]

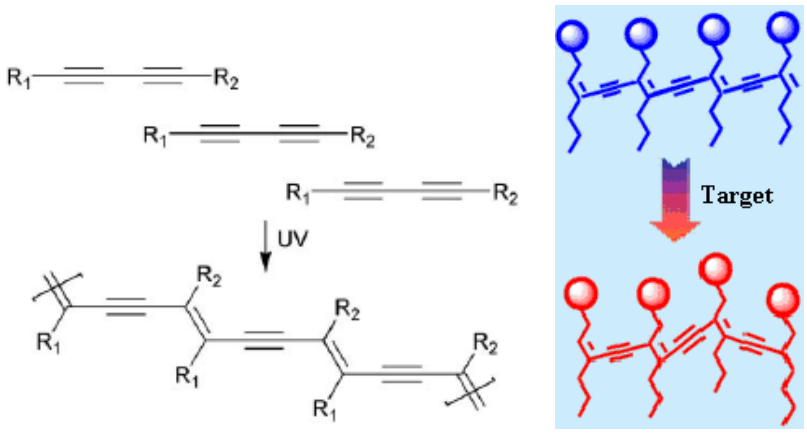

Figure 4.21 *Left) Photopolymerization of diacetylenes; right) schematic color change of PDA polymer caused by its interaction with targets.*[72]

The initial purpose of this cooperation was to make molecular imprinting PDA polymers in the form of liposome. This study is still under investigation, however, some monomer effects have been observed in the previous work, in which the synthesized monomer was incorporated with/without DMPC (Dimyristoylphosphatidylcholine) into the matrix formed by 10, 12-tricosadiynoic acid (Figure 4.22).

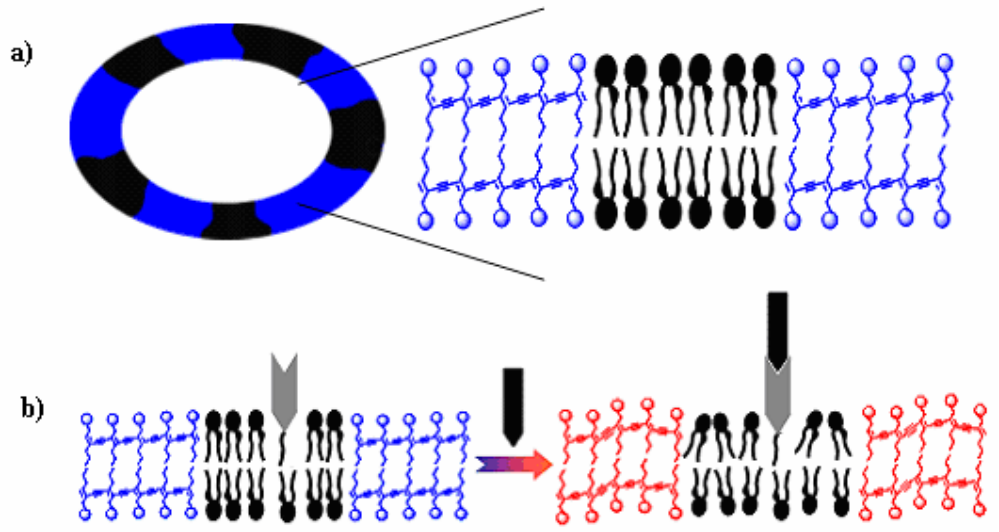

Figure 4.22 *a) Schematic structure of a liposome used in the measurement; b) Color response mechanism of the liposome.* *DMPC;* *polymer matrix formed by* 10, 12-*tricosadiynoic acid;* *synthesized PDA monomer;* *guest molecule.*

4.4.1 Target recognition with liposomes

A liposome was prepared with 50 mol% monomer **14** incorporated into 50 mol% polymerized 10, 12-tricosadiynoic acid (TRCDA). As a reference, the other liposome didn't include monomer **14**. The very interesting observation was that vesicles comprising 50 mol% **14** seemed to inhibit the chromatic transformations induced by positive small molecules (imipramine and propranolol), positive peptides (polyarginine, polylysine and polymyxin B), and basic proteins (histone, cyto C and albumine). This observation probably meant that the phenyl headgroup on **14** essentially captured the positive molecules, prevented them from interacting with the PDA surface, and thus led to less color change. The other interesting

thing was that, for more hydrophobic molecules (lidocaine, metoprolol, isopropylalcohol) the result was the opposite: the vesicle made of 50 mol% **14** had higher sensitivity than the reference. Furthermore, several basic proteins, cyt C, tripsinogen, Lysozyme (not shown), did not induce any signals in both vesicle types (Figure 4.23).

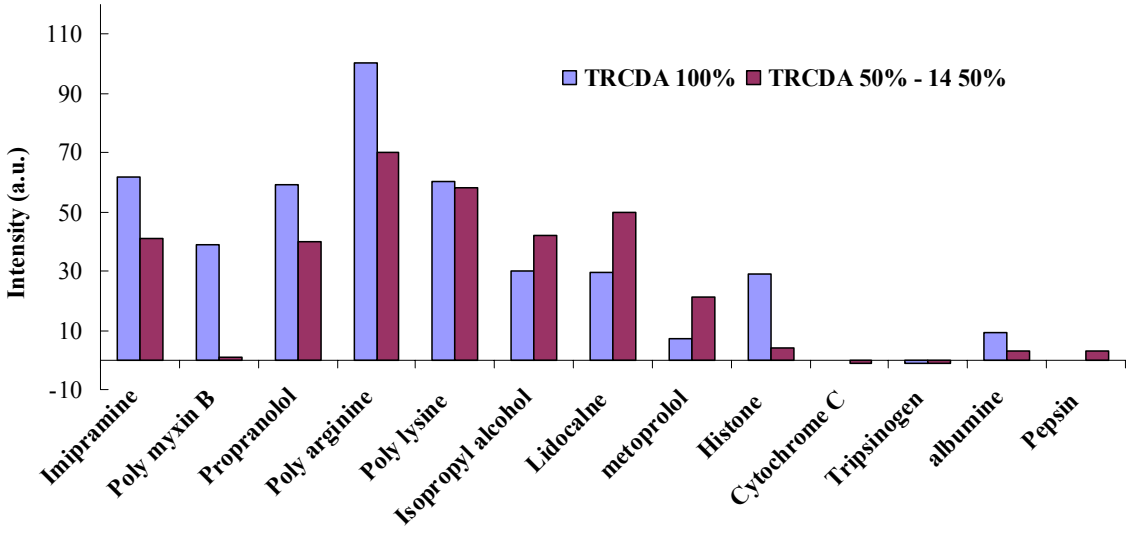

Figure 4.23 *Emission intensity change of liposome based on monomer 14 to targets.*

As shown in figure 4.24, 50 mol% **18** was added to polymerized 10, 12-tricosadiynoic acid (TRCDA) vesicles, followed by the addition of glycans. Figure 4.24 showed net color changes (after subtraction of background produced by TRCDA and polyglycans) were more pronounced for the interactions with polyglycans than small sugars, e.g., heparin and dextran compared to sucrose and glucose.

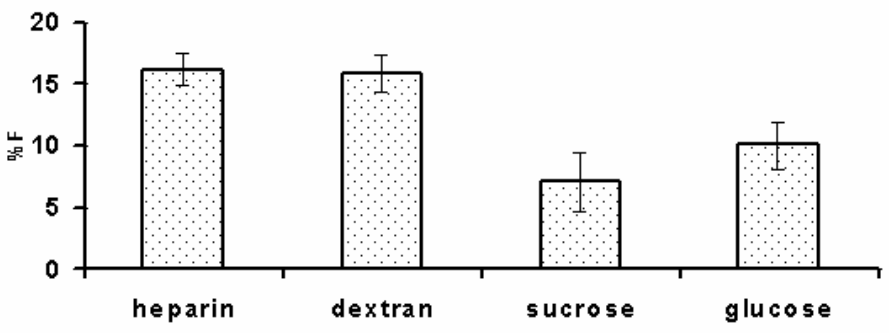

Figure 4.24 *Color responses of liposomes based on monomer 18 to targets.*

4.5 Grafted polymers on PET membrane

This research was cooperation between us and the group of *Ulbricht* from University Duisburg-Essen, Germany. In this work, my contributions were the preparation of monomers, dealkylation of neutral ester membranes with LiBr and their NMR characterizations, static binding studies between the grafted membranes and proteins and the affinity separation of lysozyme. *D.M. He* from the group of *Ulbricht* prepared the membrane and characterized them by contact angle and water permeability measurements.

In the previous work, when we immobilized an anionic linear polymer to a cationic polyethyleneimine layer on a substrate, we have observed that the binding on this surface is always weaker (2-3 magnitude order) than that in the solution.[65] In free solution, the long copolymer chain could wind around one or several protein targets, and undergoes an extensive induced-fit procedure on their surfaces to maximize favorable binding interactions. However, on the polyethyleneimine layer, the anionic polymer does not only lose a fraction of its binding sites for the immobilization, but also becomes confined to a two-dimensional flat arrangement, which reduces the accessibility of globular proteins from all sides ("horizontal architecture"). Therefore we start to think how to immobilize our highly selective linear polymer system on the surface with keeping the affinities.

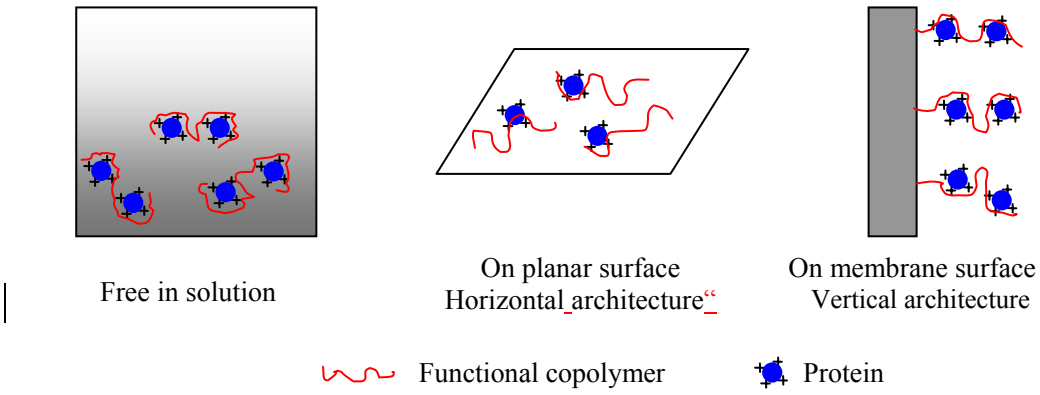

Figure 4.25 *Schematic protein recognition with arginine-selective copolymers: a) linear macromolecules free in solution; b) linear macromolecules immobilized on oppositely charged surface; c) end-grafted macromolecules covalently anchored on surface of large membrane pores.*

With the cooperation with the group of Prof. Ulbricht from University Duisburg-Essen, we have developed a relatively dense grafted functional copolymer layer inside cylindrical macropores. A "grafting-from" strategy is used to form macromolecule layers which are covalently anchored to the substrate.[74] One advantage of this type of immobilization ("vertical architecture") compared to the "horizontal architecture", is the more flexible conformation of the protein-specific macromolecules (Figure 4.25). At the same time, proteins can penetrate deeply into the polymer brushes and become surrounded by multiple binding sites. Both features could lead to a binding affinity similar to that in free solution. Another potential advantage when compared to the non-covalent route for immobilization of the affinity polymer is the higher stability of the composite, for example under high-salt conditions used for the elution of bound proteins.

4.5.1 Graft copolymer preparation

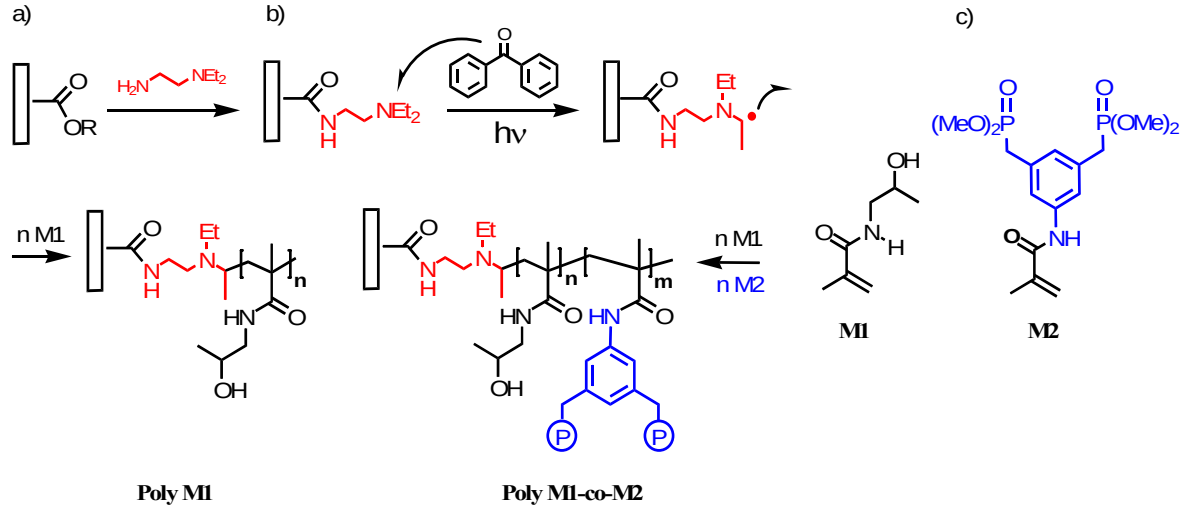

Figure 4.26 *Two-step polymer surface grafting process: a) aminolysis with DEEDA on PET surface; b) BP-sensitized photo-initiated radical graft copolymerization; c) structures of neutral comonomers used in the grafting process.*

Affinity membranes were prepared in two steps via the synergist immobilization method for "photo-grafting-from" (Figure 4.26).[75] Tertiary amino groups were immobilized on the PET membrane as a co-initiator of benzophenone and photo-graft functionalization. As described previously,[76] an aminolysis reaction of PET membrane was carried out with DEEDA (70 °C, 2 h), by which nearly full coverage of the PET surface with a monolayer of tertiary amino groups was achieved. Subsequently, the photo-graft polymerization of aminolysed

membranes preceded in acetonitrile solutions of functional monomers, containing 1.5 mmol/L of photo-initiator BP. Briefly, an aminolysed PET membrane sample with a diameter of 26 mm was immersed in 2.5 mL of monomer solution and fixed between two sheets of filter paper in Petri dishes (60 mm in diameter). 12 min UV irradiation followed after a few minutes of equilibration (the effective UV intensity was about 7.0 mW/cm^2). Afterwards, the grafted membranes were taken out immediately and washed 3 times with acetonitrile to remove the unreacted monomer, residual initiator and polymers formed in the solution. Then, the membranes were dried overnight *in vacuum* at 45 °C. A constant molar ratio of 4:1 between monomers M1 and M2 (Figure 4.27) was employed for the preparation of copolymer-grafted membrane poly M1-co-M2. For the conversion of the phosphonate methyl ester groups in the grafted copolymer to their respective Li salt, a polymer-analogous cleavage reaction was performed in 2 mL dry acetonitrile solution using 0.5 mmol/L lithium bromide (75 °C, 1 d). Stoichiometric ratio had been chosen based on the degree of grafting, so that only cleavage of two ester groups per molecule took place. As control samples, grafted membranes with M1 (poly M1-grafted membranes) have been also prepared under the same conditions. The degree of grafting (DG) was determined gravimetrically from the weight of each sample before and after modification through the following equation, where W_0 and W_1 represent samples' weights before and after modification, respectively, and $S_{spec.}$ stands for specific surface area of the membrane (1.7 m^2/g for the used membrane):

$$DG = (W_1 - W_0)/(W_0 \cdot S_{spec.}) .$$

4.5.2 Characterization of the grafted membrane

In order to confirm the composition of the grafted layers, the poly M1 and both copolymer grafted membranes (phosphonate ester and Li-salt) were analyzed by solid state ^{31}P-NMR spectroscopy on a Bruker Advance 400 instrument with phosphoric acid as external reference. As shown in figure 4.27, only a background signal at about 0 ppm was observed for the unmodified PET (not shown) and poly-M1-grafted membrane. By contrast, a strong and a weak signal additionally appeared at about 30 ppm and about 20 ppm in the spectrum of the neutral poly-(M1-co-M2)-grafted membrane, most likely corresponding to the neutral phosphonate methyl ester and its partially dealkylated phosphonate salt, respectively (in agreement with typical ^{31}P NMR chemical shifts in solution).[77] Experimental evidence was

thus produced for the copolymerization of M2 along with M1 on the membrane. The unwanted small amount of phosphonate salt can be tentatively explained by nucleophilic attack of the tertiary amines on the PET surface on the phosphonate esters of the monomer at elevated temperatures during UV irradiation, leading to quaternary ammonium phosphonate salts. Consequently, treatment with LiBr in a dipolar aprotic solvent, although performed on the grafted copolymer, almost completely generates the free lithium phosphonate salt, as indicated by its large ^{31}P NMR signal at 20 ppm, with only a trace of the neutral phosphonate ester as judged from the very small residual intensity at 30 ppm.

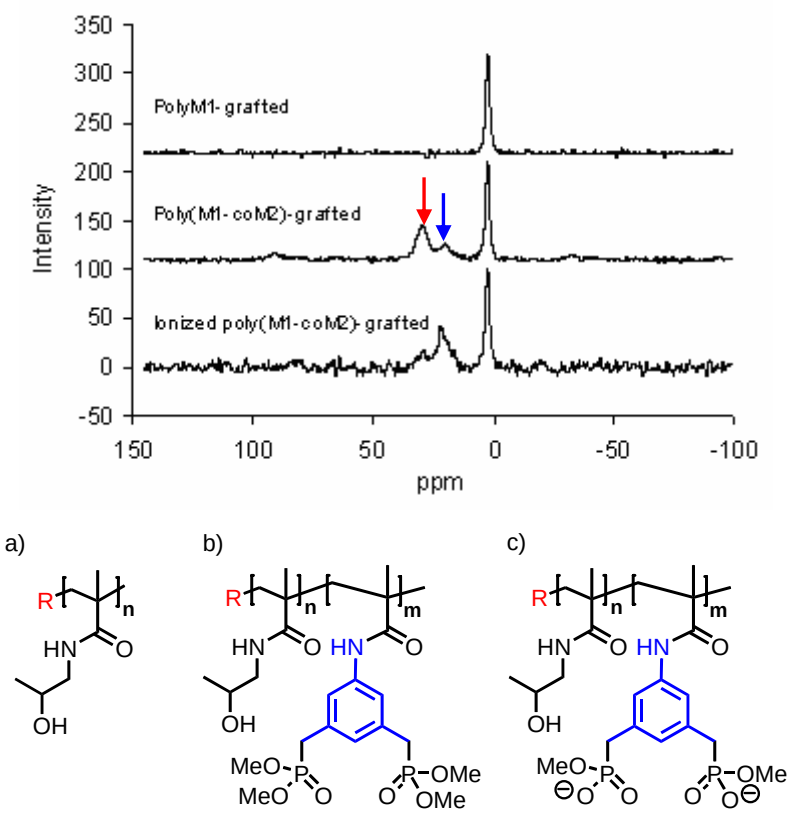

Figure 4.28 *Top: ^{31}P NMR spectra (MAS SS-NMR) of grafted membranes (red: phosphonate ester; blue: phosphonate salt). Bottom: structures of the grafted polymers: with a) polyM1, b) neutral poly(M1-co-M2), c) anionic poly(M1-co-M2).*

In addition, contact angle and water permeability have been measured for all stages of the grafting process. Contact angles were measured via the static sessile drop method using an optical contact angle measurement system (OCA 15 plus, Dataphysics, Germany). A drop of water (5 µL) was injected with a syringe onto the sample surface, and the data for 5 drops on

different locations were averaged to obtain the contact angle of one membrane sample. In water permeability measurements, the water flux of membranes was measured using stirred cells with 10 mL volume and 3.14 cm^2 effective membrane areas (Amicon Model 8010, Millipore). 0.2 bar transmembrane pressure was used by adjusting the nitrogen pressure from a gas flask.

As compared to the original aminolysed polymer surface, the hydrophilicity steadily increases on transition via grafted M1 homopolymer to the grafted M1/M2 copolymers. PET surface grafted with polyM1 has a contact angle which is typical for polymethacrylamide based hydrogels. Interestingly the introduction of only 20% of additional neutral phosphonate ester comonomer, however, greatly raises the polarity of the whole polymer and the subsequent dealkylation to the phosphonate anion has a smaller additional effect. Exactly the same trend is seen in the water permeability investigation. If the grafted polymer chains really grew from the inner wall of the large membrane pores, their increasingly polar chemical nature should be reflected in an increasing degree of polymer swelling, leading to an increasing degree of pore blocking. Data in table 4-7 demonstrate that this is indeed the case: Water permeability values drop in the same consecutive order as the respective contact angles, with the most significant jump occurring on introduction of the neutral phosphonate esters. As demonstrated before,[78] for PET membranes with cylindrical pores of very narrow size distribution, an estimation of effective grafted layer thickness on the pore walls by using the Hagen-Poiseuille law is well justified. For the PET membranes of the 1st batch, the pore diameter of the aminolysed membrane (700 nm) had been experimentally determined by using gas flow / pore dewetting[78]. Hence, the reductions of water permeability relative to this membrane (Table 4-9) correspond to reductions of pore radius (identical with effective thickness of the grafted layer on the pore walls) of ~40 nm for polyM1, ~180 nm for neutral poly(M1-co-M2) and ~240 nm for anionic poly(M1-co-M2). Because all three membranes had the same DG (i.e., mass of grafted polymer relative to the PET surface), this data can directly be related to the degree of swelling of the grafted polymer. Swelling increases by more than 4fold upon introduction of the phosphonate moieties into the already hydrophilic poly(2-hydroxypropyl)methacrylamide, the further increase after ionization is only by a factor of about 1.3. Obviously, already the neutral phosphonates dominate the surface and volume properties and render the whole polymer highly polar. In this respect, it should be kept in mind, that the formal P=O double bond displays only small -character, and should be more properly written as P^+-O^-.[79] Therefore, this can be used to explain the large increase of hydration of the grafted polymer relative to

the poly-M1 grafted membrane. Additional ionic effects onto swelling or water uptake by the polymer are also significant, as expected considering effects such as charge repulsion between grafted chain segments or osmotic pressure within the grafted layer.

Table 4-7. *Contact angle and water permeability of various membranes.*

	Membrane	Estimated DG ($\mu g/cm^2$)	Contact angle (^{0})	Water permeability (L/h bar m^2)
1	Aminolysed	-	48 ± 4	47,500 61,300*
2	PolyM1-grafted	2.3 3.5	36 ± 5	36,700 52,500*
3	Poly(M1-co-M2)-grafted	2.3 3.5	29 ± 5	10,600 25,400*
4	Before ionization After ionization	2.2 2.2	23 ± 7	6,600** 4,600**

*: 2nd batch of PET membrane with similar porosity to 1st batch, but somewhat larger pore size (about 760 nm). **: These two values have been measured for the same membrane sample, while other data in this row represent average values measured for 2 to 5 samples of the same membrane type.

Grafted poly(meth)acrylamides with sufficient molar mass (>50 kg/mol) are still in the "brush" regime even at a grafting density of as little as 0.05 chains per nm^2.[80] About 2 tertiary amino groups per nm^2 are introduced under the used aminolysis conditions as "synergist", i.e. potential starter sites for grafted chains. Considering the estimated layer thicknesses (cf. above), caused by coiled or partially stretched macromolecule chains and the large excess of potential grafting sites, the synthesized polymer layers will most presumably be in the "brush" regime. Consequently, protein binding from aqueous solutions will take place in relatively thick three-dimensional layers where the grafted functional macromolecules are immobilized in such a high density that their mutual interactions are also influenced by this confinement (especially leading to a more stretched conformation as compared to the same polymer free in solution).

4.5.3 Static binding capacity

In order to evaluate the protein affinities of the above-described new absorber materials, a series of proteins differing in pI and size were dissolved in hepes buffer (25 mM, PH 7) and equilibrated with the grafted membranes under exactly identical conditions. Figure 4.28 summarizes the results. Each protein was examined with all three membranes leading to a triad of capacity values; only trypsin, proteinase K and BSA were not tested against the lithiated poly (M1-co-M2) grafted membrane.

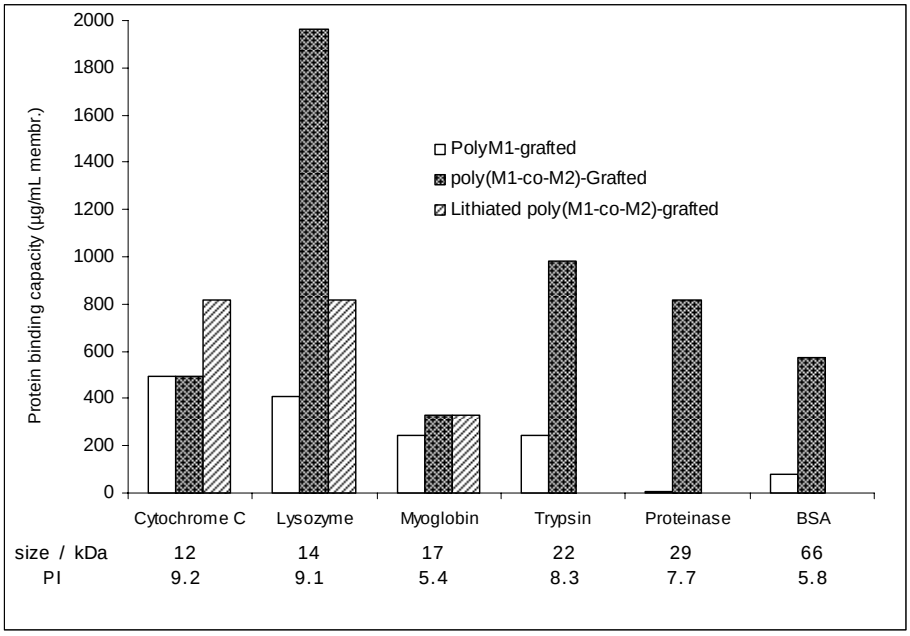

Figure 4.29 *Protein binding capacity of various grafted membranes. 50 µg/mL protein in buffer (pH = 7.1) was used.*

All proteins are listed according to increasing size (from left to right). Apparently, poly-M1-grafted membranes, which represent blank samples, exhibit a low, but non-negligible binding capacity for all six selected proteins. This is most likely due to formation of weak hydrogen bonds between methacrylamide backbone and hydroxyls in the side groups and the polar protein surfaces. This nonspecific effect is minimized as protein size increases, probably a size effect explained by their restricted penetration deeper into the grafted polymer hydrogel layer. This observation supports the assumption that such a high grafting density had been achieved, that the grafted macromolecule chains are in the “brush” regime.

In sharp contrast, the neutral poly(M1-co-M2)-grafted membrane binds much larger amounts of all basic proteins, with one notable exception, cytochrome C, while the acidic protein is bond in much lower amounts. The larger protein uptake as compared to the grafted polyM1 materials can be related to the much higher degree of swelling of the grafted M2copolymers, i.e. accessibility of the grafted layer for protein is better.

Although pI values definitely play an important role, especially the facile discrimination between two basic proteins of very similar pI and size deserves attention: The most striking difference between lysozyme and cytochrome C's basic amino acid composition is the drastic difference in surface arginine content: lysozyme carries 61% arginines, cytochrome C only 11%.[81] Detailed mechanistic investigations have revealed, that the *m*-xylylene bisphosphonate tweezer is arginine-selective already in its dianionic state. It was argued and experimentally verified that this selectivity stems from specific -cation interactions between the extended guandinium cation and the coplanar electron-rich *m*-xylylene host surface, while the ammonium ion mainly undergoes electrostatic interactions with the oppositely charged bisphosphonate.1 In our case, the charge component is missing and π-cation contributions become dominant, reinforced by NH $^{\sigma+}\cdots^{\sigma-}$O=P hydrogen bonds (Figure 4.29). In related studies with protein recognition in free aqueous solution by linear bisphosphonate-methacrylamide polymers, lysozyme was already bound one order of magnitude more tightly than cytochrome C. Obviously, the absence of negative charges on the bisphosphonate in our new grafted membranes greatly enhances their arginine over lysine preference. BSA carries distinct basic and acidic patches on its barrel-shaped surface, while myoglobin displays a large excess of aspartates and glutamates, explaining relatively small affinities towards the neutral grafted bisphosphonate polymer.

After dealkylation of the phosphonate esters, this pronounced selectivity is lost. Binding capacities are uniformly high for both basic proteins (lysozyme and cytochrome C) and much lower for the acidic protein of similar size (myoglobin); this behavior strongly resembles a traditional ion exchanger. In a related effort to prepare a protein adsorber, the dianionic bisphosphonate methacrylamide monomer was subjected to free radical polymerization in the presence of a high excess of crosslinking agent. Its elution profile in an attempted protein affinity chromatography, however, was undistinguishable from that of efficient ion exchangers.[82] We conclude that, grafted polymer membranes with charged bisphosphonates are much less selective than their neutral predecessors, probably because they rely mostly on

Coulomb interactions. In addition, the significantly different conformation of the grafted chains, i.e. a larger degree of stretching as compared with the neutral polymer, deduced from the permeability data (Table 4-7), may also contribute to a lower binding capacity at the same protein concentration in solution.

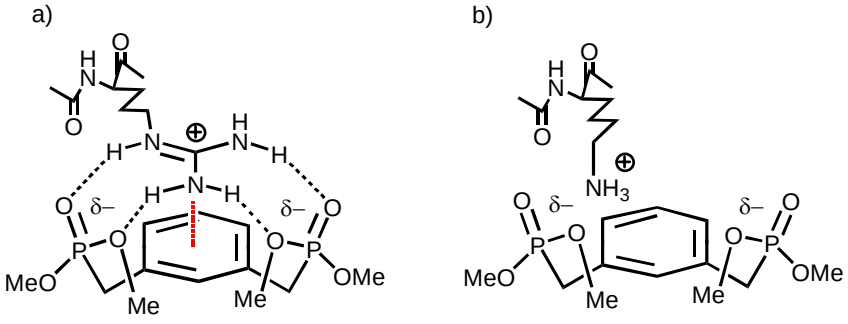

Figure 4.29 *Specific interactions between arginine or lysine residues and the neutral bisphosphonate moiety of the poly(M1-co-M2) grafted polymer.*

In order to directly prove the superior affinity of the neutral poly(M1-co-M2)-grafted membrane towards arginine-rich proteins, both lysozyme and cytochrome were chosen for the experimental determination of adsorption isotherm towards the adsorber material in batch experiments. Both adsorption curves could be roughly fitted to the Langmuir isotherm model (Figure 4.30). Saturation of protein recognition sites on the affinity membrane occurred for both basic proteins above 70 µg/mL. Maximam binding capacities reached about 2000 µg/mL membrane and about 800 µg/mL membrane for lysozyme and cytochrome C, respectively. The corresponding association constant is much greater for lysozyme (1.33×10^7 M^{-1}) than for cytochrome C (8.6×10^5 M^{-1}), confirming the proposed mechanism of binding. It is instructive to compare the order of K_a values in all the three mentioned regimes: The grafted membrane binds lysozyme more tightly than a related linear polymer in free aqueous solution (10^6 M^{-1}); this in turn is much more efficient than an immobilized linear polymer on an oppositely charged flat surface. Obviously, the highest gain of free energy is intimately connected to the complex topology, the grafted polymer architecture seems to combine flexibility and high local concentrations of specific binding sites. This is on one hand entropically favorable because no highly ordered complex structure has to be formed as in the case of a linear polymer chain winding around its protein guest in aqueous solution. On the other hand, no binding enthalpy is lost by electrostatic immobilization on oppositely charged surfaces as in the case of PEI-supported affinity polymers on glass. In addition, the "vertical architecture" of

the new grafted affinity polymer has also the advantage that protein binding to a solid support can take place in three dimensions.

The maximam binding capacity for lysozyme (expressed in mass protein per membrane volume) seems relatively small when compared to established affinity membrane adsorbers, but the porosity of the PET track-etched membranes (about 15%) is much smaller than that of typical commercial materials (75%). Indeed, when relating the bound mass of protein to the specific surface area of the PET membrane, about one densely packed monolayer of lysozyme (area per molecule 3×5 nm^2) [83] This impressively high value makes the new materials especially attractive because the used photo "grafting-from" method can easily be used to prepare membrane adsorbers also on base membranes with much higher porosity and specific surface area.[84] For potential practical applications, the reusability of neutral poly(M1-co-M2)-grafted membranes was tested in successive binding and rebinding experiments, with intermediate extensive HEPES buffer washing steps. The protein binding capacity started to decline after 3 repeated bind-wash-elute-regenerate cycles.

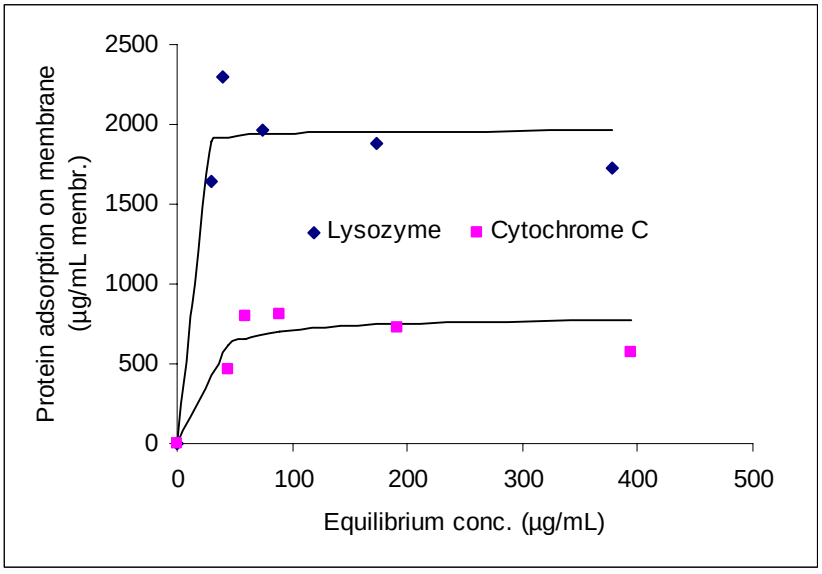

Figure 4.30 *Lysozyme and cytochrome C isotherm adsorptions for poly(M1-co-M2)-grafted membrane. The equations obtained from fitted Langmuir adsorption isotherm model are: A=1966*0.95*c/(1+0.95*c) [binding constant K=0.95 mL/µg (=1.33*10^7 M^{-1})] for lysozyme, and A=805*0.072*c/(1+0.072*c) [K=0.072 mL/µg (=8.6*10^5 M^{-1})] for cytochrome C.*

4.5.4 Affinity separation of proteins

Based on the distinct pattern among all obtained static binding capacities of various proteins on neutral poly(M1-co-M2)-grafted membranes and on the markedly different K_a values in the experiment with single protein, the resulting affinity membrane should display pronounced lysozyme selectivity and was expected to be able to separate this target from protein mixtures. Therefore, in this work a 1:1 mixture of lysozyme and cytochrome C was used, which is not easily separated by conventional techniques, due to the high degree of similarity in physical and chemical properties. Following the same protocol as in the previous static binding capacity measurements, a total protein binding capacity of about 1500 µg/mL total protein per membrane was determined for the mixture, which is comparable with the pure lysozyme binding capacity but much higher than for pure cytochrome C. To identify the composition of the bound protein, UV-Vis spectra were acquired of the pure components and the elute at the same concentrations (18 µg/mL). As shown in figure 4.31, the only visible eluent absorption peak was located around 280 nm, while no absorption peak was observed at 410 nm, indicating that no detectable fraction of cytochrome C was bound by the membrane.

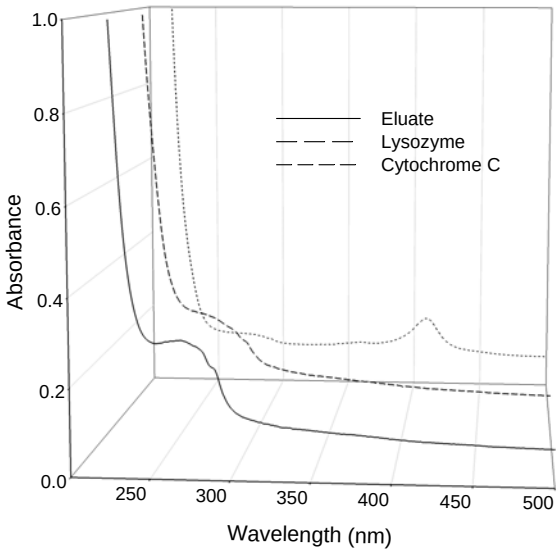

Figure 4.31 *Front: UV spectrum of the elute from a membrane grafted with poly(M1-co-M2), after its equilibration with a 1:1 mixture of lysozyme and cytochrome C (concentration of 35 µg/mL in buffer pH 7.1). Background: solutions of pure lysozyme and pure cytochrome C, all at a concentration of 18 µg/mL in buffer.*

4.6 Crosslinked water-soluble polymers: Microgels

Microgels used in this chapter were synthesized in the *Kraft* group at Heriot-Watt University, Edinburgh, Scotland. My contribution was the binding study with microcalorimetry between these microgels and a series of proteins.

Microgels are very large highly crosslinked discrete polymeric particles that have a size in the submicrometer range from *ca.* 0.1 μm to several μm and swell in a good solvent environment.[85] They are not only easy to be synthesized but also highly soluble in water. Contrary to macroporous polymers used for imprinting, microgels are completely translucent allowing for spectroscopic detection of binding events. Although their inner core is densely packed with crosslinked and backfolded polymer arms, their outer layers exhibit numerous large solvated pores, which could accommodate whole proteins (Figure 4.32). Noncovalent interaction between human serum albumin and poly-NIPAM microgels has been demonstrated by Linse and coworkers,[86] however, binding in these cases was essentially restricted to hydrophobic interactions.[87] The Kraft group recently reported that suitably designed microgels are capable of acting as supramolecular receptors for protonated amines in aqueous buffer at physiological pH and ionic strength with moderate affinities.[88] This work led us to anticipate that negatively charged microgels should promote electrostatic interactions in a multivalent fashion with positively charged residues on the surface of a protein.

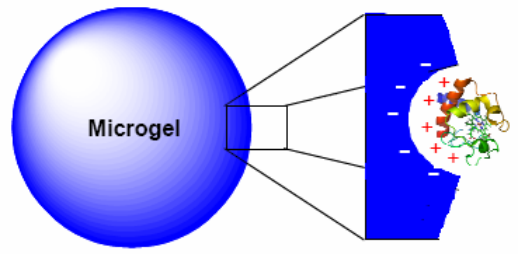

Figure 4.32 *Schematic illustration of the protein absorption of a microgel on its exterior pores.*

A typical monomer feed composition consisted of 80 mol% *N*-isopropylacrylamide (**44**), 10 mol% of crosslinker MDA, and 10 mol% of an anionic comonomer (Figure 4.33) such as sodium methacrylate (**45**), a polymerizable tetrazolate (**46**)[89] or bisphosphonate (**1**). Polymerizations were carried out at 70°C in the presence of a surfactant (sodium

dodecylsulfate) and an initiator (ammonium persulfate). Microgels were subsequently purified by ultrafiltration against deionized water, using cross-flow membranes with a 100 kDa and 2 μM cut-off, to remove low-molecular-weight impurities and macroscopic gel particles, respectively.

Isothermal microcalorimetry (ITC) measurements were then carried out to study the thermodynamic parameters of observed microgel–protein interactions. With a typical averaged molecular weight value of 2.5×10^9 g mol^{-1} for the microgels,[90] macroscopic binding constants could be calculated for the 1:1 complexes between each protein molecule and microgel (Table 4-8).[91] Each single protein displayed affinities towards the microgels between 10^8 and 10^{11} M^{-1}. In order to have a direct comparision between the monomers, the binding contant, binding stoichimetry and heat change were also calculated between the binding monomer and a protein, although the error was much bigger than that from a whole microgel.

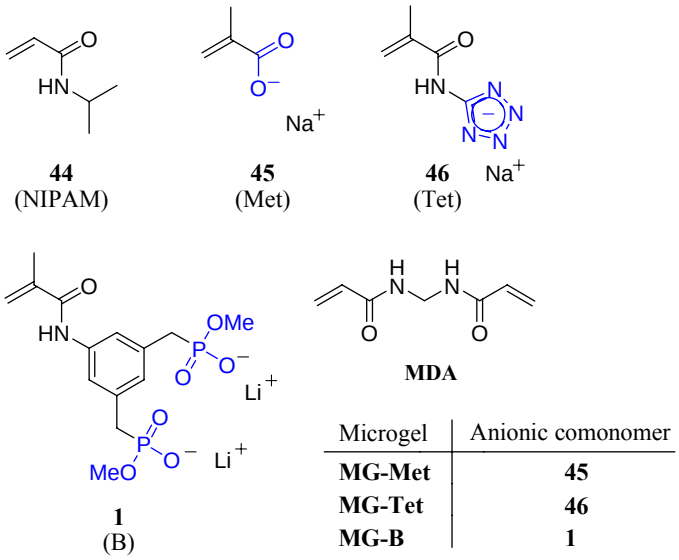

Microgel	Anionic comonomer
MG-Met	**45**
MG-Tet	**46**
MG-B	**1**

Figure 4.33 *Monomers used in the preparations of microgels: N-isopropylacrylamide (44), sodium methacrylate (45), sodium 5-(methacrylamido)tetrazolate (46), a polymerizable bisphosphonate (1), and N,N'-methylenebisacrylamide (MDA).*

Specially, it was verified, that Cytochrome C binds to MG-Met but not to MG-Tet. Hemoglobin was found to bind to MG-Tet and especially to MG-B whereas no binding was noted for MG-Met. These remarkable selectivities among basic proteins render MG-Met a cytochrome C selector, while MG-Tet picks Hemoglobin. Intriguingly, the doubly charged

bisphosphonate is superior to the carboxylate and its heterocyclic analog by one to three orders of magnitude, pointing to electrostatic attraction as a major driving force for association (Figure 4.34). Roughly, K_a values for MG-B follow the proteins' pI scale, with Lysozyme as a notable exception. This protein is very similar to Cytochrome C in basicity and size (pI 9.2, 14 kD), but is recognized much more efficiently by the bisphosphonate microgel, possibly reflecting its arginine preference. These effects are reminiscent of water-soluble related linear homopolymers.

Table 4-8 *Affinities and stoichiometries as well as thermodynamic parameters as determined by microcalorimetry.*

	Protein[1]	Macrosc. K_a / M^{-1}	Protein: Microgel	K_a per residue / M^{-1}	Monomer : protein	G[4] /kcal mol^{-1}	H /kcal mol^{-1}	TΔS / kcal mol^{-1}
MG-met	Cyt C	1E08	700	1×10^3	11 : 1	–4.3	+14.4	+18.7
MG-met	Hem	NA[2]	NA	NA	NA	NA	NA	NA
MG-tet	Cyt C	NA	NA	NA	NA	NA	NA	NA
MG-tet	Hem	3E08	16000	6×10^3	90 : 1	–5.1	+0.4	+5.5
MG-tet*[3]	Hem	3E07	66	3×10^2	210:1	–3.3	–22.0	–18.7
MG-B	His	1E11	2000000	-	-	-	-	-
MG-B	Lys	2E11	5000	-	-	-	-	-
MG-B	Cyt C	3E09	15000	3×10^3	6 : 1	–4.0	+2.7	+6.7
MG-B	Hem	2E10	1200	2×10^5	20 : 1	–7.3	+2.0	+9.3
MG-B	BSA	~ 1E09	-	-	-	-	-	-

[1] In the order of decreasing pI value; [2] NA indicates that no binding constant and thermodynamic data was attainable from microcalorimetry titrations, because heat changes were too small; [3] microgel with 15% cyclohexylmethacrylamide content; [4] ΔG, ΔH and TΔS for each binding monomer.

Most notably, all microcalorimetry measurements unanimously revealed that the binding event is endothermic and entropy-driven. Two effects may account fore this: unspecific Coulomb attraction releases well-ordered water molecules into the bulk solvent on ion-pair formation; a positive ΔH is also characteristic for the classical hydrophobic effect. Obviously binding does not only occur at the microgel's exterior, but also in macropores of the outer layers. Such endothermic binding processes are also well known for protein–protein interactions and protein–ligand systems when a structural rearrangement or closure of the

binding site is necessary.[92] The flexible structure of the microgels demands a significant degree of conformational adjustment upon binding to a protein.

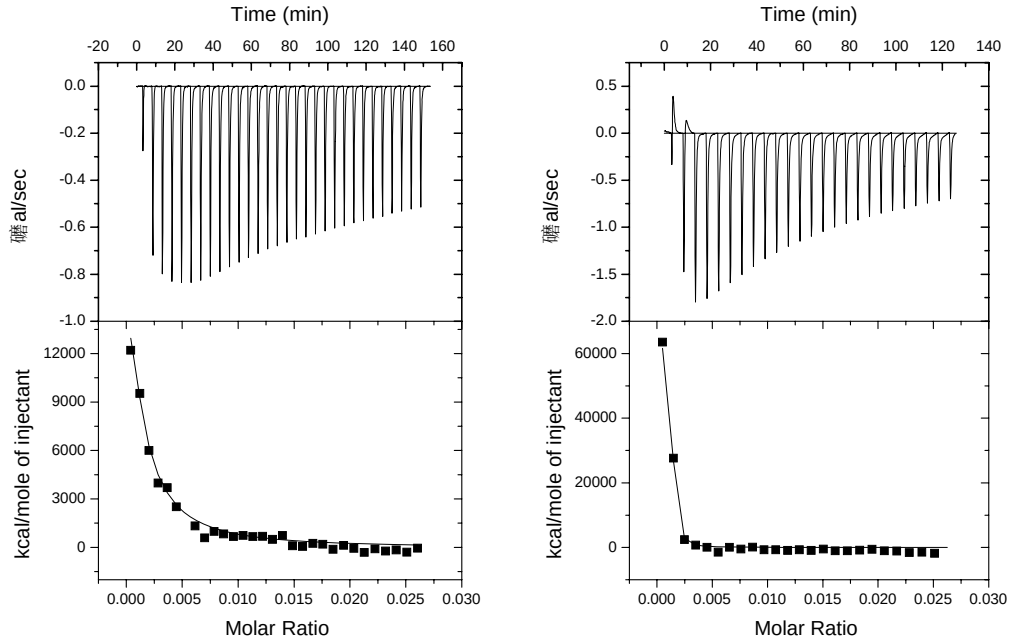

Figure 4.34 *ITC titration curves for MG-Tet and MG-B with Hemoglobin.*

In light of the above-discussed calorimetric data selectivities cannot be treated in terms of specific host-guest interactions; most likely, varying charge densities within the carboxylate, tetrazolate and bisphosphonate play a significant role. Since the binding units vary in size and degree of solvation, their accessability within the outer macropores will also determine the microgel's capability to distinguish between two basic proteins.

These findings have illustrated the enormous potential of microgels as supramolecular hosts for protein binding in a highly competitive aqueous environment. The major drawback seems unspecific binding; this could be overcome during the polymerization process by combining the bisphosphonate unit with other comonomers tailored for characteristic amino acid residues of the target protein. A first step into this direction was attempted by including unpolar cyclohexylmethacrylamide into the polymerization mixture of MG-Tet. Intriguingly, protein binding now became enthalpy-driven; however, the total free energy gain and hence K_a was lowered – presumably by entropy compensation. In the future, with a new series of more specific binding monomers we hope to increase both affinity and specificity of the protein recognition event.

4.7 Molecularly imprinted polymers (MIPs) in aqueous solution

The imprinting of organic polymers was first reported by the research group of Prof. Günter Wulff in 1972.[19] MIPs are synthetic materials produced by the cross-linking of functional monomers or polymers in the presence of a template molecule. The template is subsequently removed, leaving cavities possessing size, shape, and functional group orientation which are complementary to the target molecule. The size and shape of the cavity allow the target molecule or similar molecules to occupy the cavity space, while the functional group orientation within the cavity will preferentially bind in specific locations to only the target molecule and not to similar molecules (Figure 1.10).[93]

While MIPs have been prepared for a large number of target molecules and applications [3,94,95,96] over years, the majority of the template molecules studied have been characterized by organic small molecules. Much of the pioneering work in the molecular imprinting of peptides and proteins was conducted by Mosbach [97,98,99,100,101] using amino acid derivatives as template molecules, however the MIPs synthesized in these early studies were performed in organic solvents. Recently, many groups have studied the imprinting within aqueous solution with a variety of peptides and proteins[102,103,104,105,106,107,108], in which hydrophobic interaction are frequently employed.

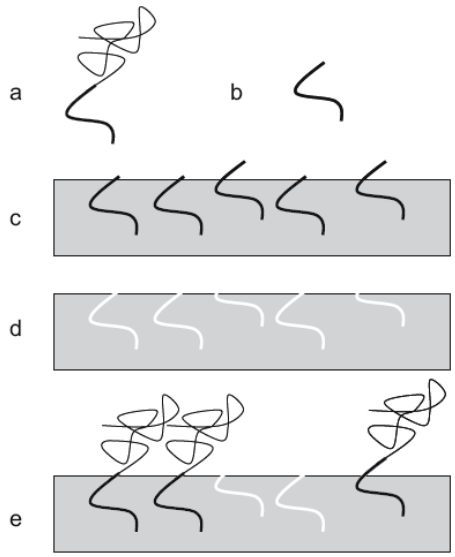

Figure 4.35 *Schematic of the "epitope approach" utilized for molecular imprinting of proteins and peptides. A) Target molecule, b) epitope (imprinted) portion of target molecule, c) epitope-imprinted polymer before template removal, d) imprinted polymer after template removal, with cavities that display shape which is complementary to the imprinted portion (epitope) of the target molecule, e) MIP subsequent to template re-binding. The MIP selectively recognizes the imprinted (epitope) portion of the target*

Despite the obvious advantages in the development of MIP systems for peptides and proteins, there are a number of key issues to address what are largely absent when targeting small

molecules. They are related to the molecular size, complexity, conformational flexibility, and solubility. [109] One proposed method of reducing the complications associated with the imprinting of proteins and peptides has been termed the "epitope approach" [2, 110,111,112] to molecular imprinting (Figure 4.35). In this technique, a small sequence of amino acids from the larger protein target molecule is used to create the imprint. When a protein containing this specific amino acid sequence is allowed to incubate in the presence of the MIP, the entire protein can thus be recognized and bound.

Due to the many parameters influencing the MIPs' properties at different length scales, as well as the absence of a clear understanding of how these parameters interplay, there are presently no well developed rules to follow for the design of materials exhibiting the desired recognition properties. Thus, combinatorial synthesis approaches, allowing the main factors to be rapidly screened, have offered valuable tools in the development of new MIPs. [113] Techniques allowing high-throughput synthesis and evaluation of molecularly imprinted polymer sorbents at a reduced scale (mini-MIPs) have been developed and used for the optimization of MIPs for recognition of target molecules in various environments. The most recent technique incorporates a liquid-handling robot for the rapid dispensing of monomers, templates, solvents and initiator into the reaction vessels of a 96-well plate (Figure 4.36).

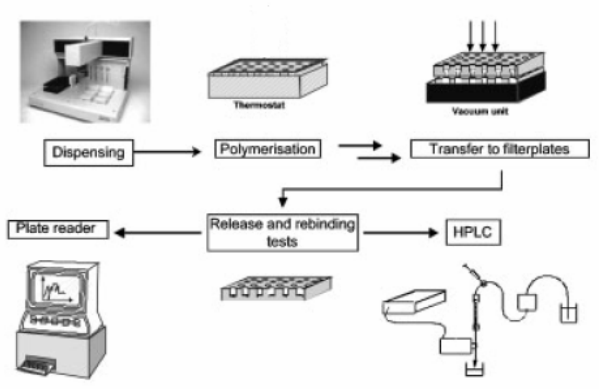

Figure 4.36 *Semiautomatic high-throughput procedure for the synthesis of mini-MIP libraries in a microtiter plate and evaluation of the library via serial (HPLC) or parallel (multifunctional plate reader) techniques.*[114]

Based on above two techniques, “epitope” and “liquid-handling robot”, MIPs was prepared in aqueous buffer with immunoglobulin G as the final recognition target. The main aim was to screen our 16 functional monomers and find best monomer combinations for MIPs. This research was cooperation between us and the group of *Sellergren* at University of Dortmund, Germany.

4.7.1 Design

4.7.1.1 Target molecules and choice of templates

IgG are large molecules of about 150 KD composed of 4 peptide chains. It contains 2 identical heavy chains of about 50 kDa and 2 identical light chains of about 25 kDa. The two heavy chains are linked to each other and to a light chain each by disulphide bonds. The resulting tetramer has two identical halves which together form the Y-like shape.[115]

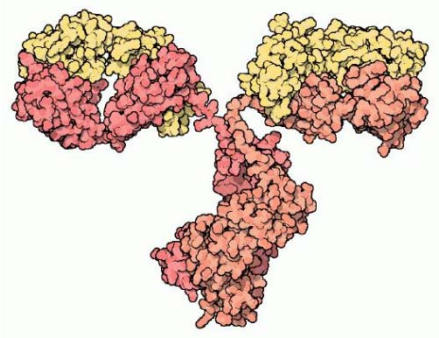

Figure 4.37 *Structure of the antibody IgG.*[74]

For the epitope imprinting, we need to know the exposed fragments of proteins. The information of the most accessible amino acid residues at IgG C-terminal is provided by *MIP Technologies AB* in Sweden. Values for relative accessibility (accessible surface area in the folded structure expressed as a percentage of the area if residue totally exposed) are shown in table 4-9. The first column is calculated for water accessibility by using a 1.4Å probe and the numbers in brackets are calculated with a 3Å probe. They are not that different. It seems likely that, except of the leucine 441, other 8 terminal residues SLSPG are very accessible. The two termini from heavy chains are quite a distance apart about 10Å between the two residues at position 443.

Residue	Abbreviation	Accessibility a	Accessibility b
Gly446	(G)	100%	(100%)
Pro445	(P)	100%	(100%)
Ser444	(S)	100%	(100%)
Leu443	(L)	65%	(83%)
Ser442	(S)	41%	(36%)
Leu441	(L)	7%	(1%)
Ser440	(S)	57%	(64%)
Lys439	(K)	42%	(50%)
Gln438	(Q)	42%	(43%)

Table 4-9 *The accessibility information of the IgG C-terminal. Accessibility-a is calculated with 1.4 Å probe and accessibility-b is calculated with 3 Å probe.*

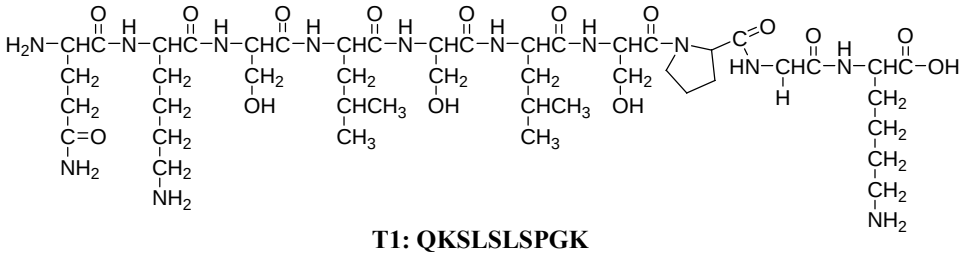

T1: QKSLSLSPGK

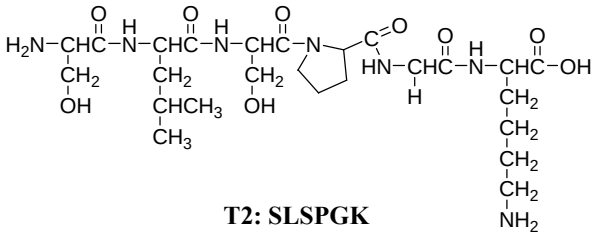

T2: SLSPGK

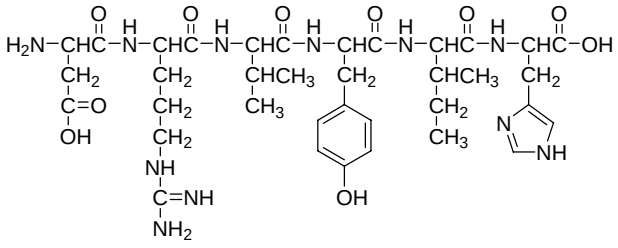

T3: DRVYIH

Figure 4.37 *Three peptide templates used in the imprinting.*

In the sequence, a lysine residue at the very terminal may be missing.[116] In protein data bank (PDB), IgG with the code numbers 2GJ7, 1T83, 1OQO, 1IIS, 2DTQ, 1HZH, 2J6E, 1E4K, 1IIX, 1H3T and 1ZA6 match best with the sequence QKSLSLSPGK, and out of them 1HZH and 1ZA6 contain x-ray structures of the complete sequence including the C-terminal lysine.

Based on above discussion, a consecutive exposed sequence SLSPGK was chosen as one template (Figure 4.38, T2). Although contacting the Leu441 might destabilize the core of the domain of IgG, a longer sequence QKSLSLSPGK (Figure 4.38, T1) was also used, with the consideration that imprinting with longer epitope peptides could provide better effects than shorter ones. At the same time, to investigate the monomer effect more detaily, I also chosen another template T3, a part of angiotensin II.[117] It contains three amino acid residues, arginine, tyrosine and histidine, for which my monomers were specific.

4.7.1.2 Choice of functional monomers

The guiding principle to choose functional monomers is functional group complementarities.[118] It is clear that forming imprints and using them for selective rebinding in aqueous systems is achievable in a variety of matrices using different forms of polymer/template interactions. Hydrophobic interactions have been shown to work, but this type of bond is non-directional. This may lead to lower specificity, especially when working with macromolecules with similar structure, as well as problems with solubility and conformation due to apolar effects. Polar interactions on the other hand are directed and therefore more favorable in obtaining specificity.[21] It has been proposed that binding in aqueous media can be enhanced by exploiting cooperative interaction effects and selecting proper hydrophobic microenvironments to create better receptors.[119] Studies on the combination of hydrogen bonding and hydrophobic interaction,[120] hydrogen bonding and electrostatic effects,[121] and hydrophobic and electrostatic interaction,[122] have been performed.

The water-solubility of monomers described in chapter 2 limited their utilizations. Out of them, monomer 1-5, 7, 8 and 10 were selected. Monomer 46 was from *Kraft* at Heriot-Watt University, Edinburgh. Monomer 51, methacyloyl acid, was commercial available. Monomers 52-57 were from *Sellergren* at Universität Dortmund, Germany. Prior to use, their water-

solubilties were tested (Table 4-10). Although monomer 4, 56 and 57 were badly soluble in water, they were still tested by being dissolved in DMF.

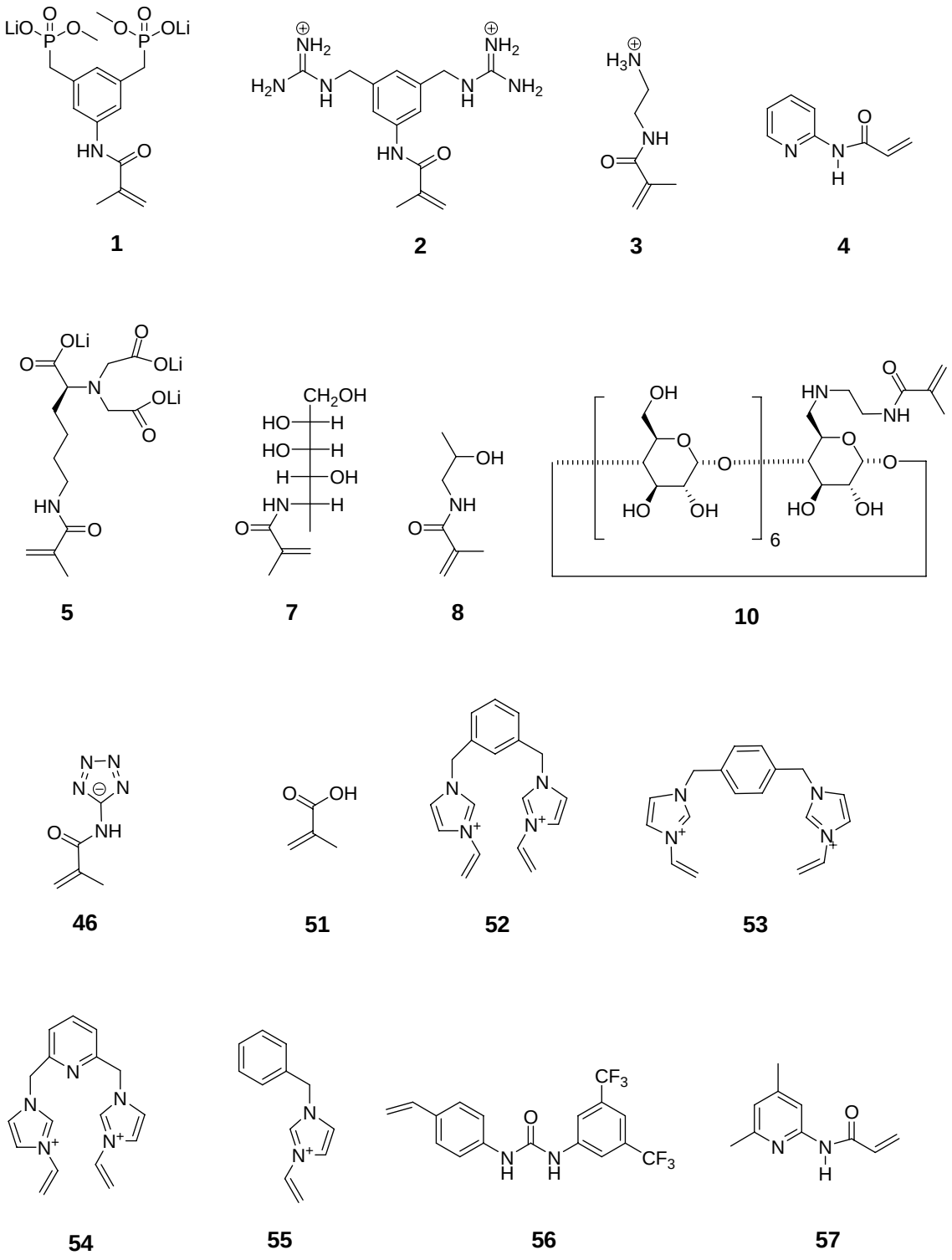

Figure 4.39 *Monomers used in the MIPs.*

Table 4-10 *Monomer solubility tests.*

Monomers	Weight /mg	solvent	Volume / μL
1	10	water	10
2	10	water	10
3	10	water	10
4	10	DMF	10
5	10	water	15
7	10	water	10
8	10	water	10
10	10	water	15
46	10	water	10
51	-	water	miscible
52	10	water	10
53	10	water	20
54	10	water	10
55	10	water	10
56	10	DMF	10
57	10	DMF	20

4.7.1.3 Choice of comonomer and crosslinker

Methacrylamide (MA), an often used co-monomer in MIPs, was selected due to its commercial availability, good water solubility and cheap price.

Several crosslinker were considered. Although previous works proved that ethyleneglycol dimethacrylate (EDMA), trimethylolpropane trimethacrylate (TRIM), methylenediacrylamide (MDA) and pentaerythritol trimethacrylate (PETRA) had their own advantage in MIPs,[29] a polar, more peptide-like ethylenediacrylamide (EDA) was chosen as the crosslinker. Methylenediacrylamide (MDA) was not selected, because its instability in the etching step on a silane surface which might be used in the future development.

The solubility of crosslinker EDA was tested: 10 mg of it could be dissolved in 80 μL of water, which was beyond our requirement for making mini-scale synthesis on a 96-well plate.

However, the mixture of EDA and comonomer MA had a better solubility (Table 4-11), and was added into the polymerization mixture together.

Percentage of EDA	EDA mg	MA mg	Water μL
20 mol%	100	169	300
50 mol%	100	42	350
70 mol%	100	18	450
80 mol%	100	10	600
100 mol%	100	0	800

Table 4-11 *Solubility tests of different crosslinker and comonomer compositions.*

4.7.1.4 Choice of buffer

In addition to the number of interactions which are possible between the template and the MIP receptor, the microenvironment surrounding the binding site can have a large role in determining how effective the MIP will be in recognizing its target molecule, because proteins can adopt a wide number of conformations depending on their environment. Since aqueous buffer is the reaction media, the effect of buffer composition and ionic strength are two variables will have a large effect on the MIP system. In a system several buffers have been studied to observe the effect of ionic strength and buffer composition on the binding capacity of the MIPs. All buffers examined resulted in a decrease in binding capacity of the MIP polymers and the smallest effect is observed for 10 mM HEPES and 10 mM phosphate buffers. A conclusion is that the ionic strength of the binding solution, not the buffer composition itself, plays a large role in determining the effectiveness of the MIP.[123] Based on above discussion, 10 mM Hepes (PH 7) was decided to be the buffer in this research.

4.7.1.5 Choice of temperature and initiator

Temperature is another affecting parameter for MIPs, because it can influence the stability of monomer-template assemblies.[21] In the case of electrostatic interactions, lower temperatures of polymerization are known to increase the stability of the assemblies. Therefore, low

temperature thermal initiators or photo-initiators are commonly used. APS is often used to catalyze the polymerization of acrylamides in making a polyacrylamide gel. It could be accelerated by TMEDA (tetramethylethylene diamine), with which the reaction rate could be three times faster as APS alone. APS just needs a mild reaction condition and is not as sensitive to the air as AIBN does.[34] The other important point is that the good water solubility of APS, 80g/100ml water, can satisfy our requirement.

Polymerization with different ratios of APS and TMEDA were tested (Table 4-12) for crosslink and comonomer. 0.1mol% APS was the ratio Shea used for MIPs[21], but it didn't work well by us. When the ratio was increased to 0.4 mol% and 1 mol%, apparent polymerization could be observed in several minutes. However, after functional monomers and templates were added, even 1mol% APS didn't initiate the polymerization. To the end, the amount of APS and TMEDA were increased to 4mol%.

4.7.1.6 Design of polymer libraries

Our research was performed in two steps. Firstly, each monomer was used individually to make polymers with crosslinker and comonomer in order to investigate their MIPs effect, and meanwhile to find an optimal crosslinker percentage. The second step is still ongoing. In this step, MIPs will be prepared under the optimal condition with designed monomer combinations and will be screened in order to find the best for IgG recognition.

In the first step two 96-well microplate of polymers were prepared for T1 and T3 respectively. Since T2 was only a part of T1, it wasn't used in the first screening. Each polymer was made in a well with ethylenebisacrylamide (crosslinker), methacrylamide (comonomer) and one of our functional monomers in 10 mM hepes buffer. In each well, 4 μmol of templates, 20 μmol of functional monomers and 400 μmol of MA with EDA were added. Therefore the ratio among the template, functional monomers and comonomer plus crosslinker was 1: 5: 100. The crosslinker percentage for each monomer varied from 20 mol%, 50 mol% to 70 mol%, with the total percentage of crosslinker EDA and commoner MA as a constant (Table 4-12). For comparison NIPs (imprinted polymers without template) were made with the same recipe as MIPs at the same time.

Except of the template difference, different monomers were used in the wells from position G1 to G6 in the two plates. Monomer **5** was a monomer special to histidine and only used in the plate for T3. Instead of **5**, monomer **57** was used for T1 without special purpose. The design of polymerization on microplates was showed in table 4-13.

	Polymer formulation components (μmol)			
mol% cross-linker	template peptide	functional monomer	MA	EBA
70	4	20	120	280
50	4	20	200	200
20	4	20	320	80

Table 4-12 *Recipe in each well for MIPs.*

P1(P2)	1	2	3	4	5	6	7	8	9	10	11	12
	MIPs			NIPs			MIPs			NIPs		
	20%	50%	70%	20%	50%	70%	20%	50%	70%	20%	50%	70%
A	3	3	3	3	3	3	MA	MA	MA	MA	MA	MA
B	2	2	2	2	2	2	51	51	51	51	51	51
C	1	1	1	1	1	1	52	52	52	52	52	52
D	46	46	46	46	46	46	53	53	53	53	53	53
E	7	7	7	7	7	7	54	54	54	54	54	54
F	8	8	8	8	8	8	55	55	55	55	55	55
G	57(5)	57(5)	57(5)	57(5)	57(5)	57(5)	4	4	4	4	4	4
H	10	10	10	10	10	10	56	56	56	56	56	56

Table 4-13 *Plates design a) P1 for template T1, b) P2 for template T3. 20%, 50% and 70% percent represent the crosslinker percentage in each well. MA is the comonomer methacyloyl amide.*

4.7.2 Synthesis

Stock solutions of the substances (Table 4-14) were prepared by dissolving them in 10mM degassed Hepes buffer (PH 7), and each of them was degassed with argon for another 3 minutes.

	Weight /mg	Solvent	Volume /μL
T1	271.5	buffer	1300
T3	192.5	buffer	3600
M1	154.7	buffer	600
M2	65.8	buffer	600
M3	156.5	buffer	600
M4	69.1	buffer	600
M5	119.4	buffer	600
M6	57.7	buffer	600
M7	102.3	buffer	450
M8	478.0	buffer	600
M9	35.4	buffer	600
M10	34.5	buffer	600
M11	179.5	buffer	600
M12	179.6	buffer	600
M13	181.9	buffer	600
M14	105.8	buffer	600
M15	60.6	DMF	600
M16	149.5	DMF	600
M17	52.7	DMF	450
APS	210.5	buffer	2400
TMEDA	42.1	buffer	2400
	EDA /mg	MA /mg	buffer /mL
For 70%	3296	715	16.7
For 50%	2355	1192	8.4
For 20%	942	1906	8.4

Table 4-14 *Stock solution preparation for templates, functional monomers, initiator and mixtures of crosslinker and comonomer.*

As showed in table 4-15, pre-polymerization mixture was prepared by pipetting degassed stock solutions in a sequence of templates, functional monomers, mixture of crosslinker and comonomer, initiator, and porogen to the wells of a PTFE 96-well microtiter plate covered with a silicone rubber sealing mat. In the case of monomer **5** in plate P2, same equivalent of $NiSO_4 \cdot 6H_2O$ was added into the wells from G1 to G6 after the addition of T3. Each pipetting step was accompanied by **5** seconds degas with argon. Afterwards the microplates were sealed with Viton rings and PTFE covers and then heated in the oven at 50ºC for 24h.

	In each well in the microplate (μL)					
cross-linker	template peptides	functional monomers	MA+ EDA	APS	TMEDA	Porogen
70%	20/60*	30	210	80	80	300
50%	20/60	30	120	80	80	210
20%	20/60	30	120	80	80	210

Table 4-15 *Stock solution dispersing scheme for each well. * 20 μL peptide is used for T1 and 60 μL for T3.*

Solid polymers could be observed in microplate wells after polymerization. Generally the polymerization went very well, except of the right half part in the second plate. The possible reason might be that, after the robot worked for some time, the argon outlet was blocked. Therefore the polymerization wasn't under inert atmosphere any more and this led to the failure. These polymers were redone successfully with the same recipe later.

4.7.3 Template release

The removal of target molecules from MIPs is a critical factor in the imprinting capability of the MIPs.[2] The most efficient washing solvents all have in common their ability to solvate efficiently linear homopolymers of the constituent monomers. Furthermore, a match between the porogen and the wash solvent seems important for achieving higher recoveries.[124] Template removal from polyacrylamide hydrogels synthesized in the presence of bovine hemoglobin has been achieved with an aqueous solution consisting of varying ratios of sodium dodecyl sulfate (SDS) and acetic acid (HOAc).[125] However, it has been found that

while increasing the amount of SDS improved template removal, the rebinding effect is clearly compromised. Another obvious choice for template removal in these systems would be the use of proteolytic enzymes (proteases) which are capable of cleaving peptide bonds and subsequently destroying the structure of imprinted proteins or peptides.[126] Peptide fragments could then be removed from the cavity by simply being rinsed with buffer solution. The protease trypsin, for example, has been investigated as a template removal agent. However, after washing of an MIP with a trypsin solution, the rebinding efficiency suffers as cleaved protein fragments block binding sites within the imprint cavity.

Considering above examples, to avoid the influence from other parameters, simple 10 mM of HCl (PH 2) was selected as the washing solution. After polymerization, polymers were transferred to a 96-well filter plate, and incubated with 600 μL of buffer for 24 hours. Afterwards they were washed by successive 50 times with 500 μL 10 mM of HCl solution, and incubated again with 600 μL of buffer. The concentration of the free template in the two batches of buffer was determined with a BCA assay or with a reversed-phase HPLC. Every single case was measured for two times and the average value was used for evaluation. Calibration curves were also made at the same time. The results indicated that, in the first incubation with buffer, approximate 1/4 to 1/3 of templates were released; after 50 times washing with HCl, nearly no template could be observed in the second incubation.

After the washing step polymers were not dried as traditionally, because it was afraid that our polymers made with much less crosslinker than traditional MIPs might shrink and subsequently most of the binding sites became inaccessible any more. Indeed, such shrinkage had been observed by Shea.[34] According to a swelling test, we believed that all the polymerization had a very high conversion degree, and therefore their theoretical weights were used for evaluation.

4.7.4 Rebinding

In rebinding experiments 750 μL of T1 or T3 solution in 10 mM Hepes buffer (PH 7.0) was added into each well of the two filter plates containing T1 or T3 respectively. Then the filter plate was sealed on top and bottom with PTFE-coated silicon closures. After the solutions were incubated in the plates for 24 hours, the closures were removed and the solutions were sucked under vacuum into microplates, from which samples were taken for subsequent

measurements. In the positions from G1 to G6 on the filter plate containing T1, before rebinding, 1 μmol solution of $NiSO_4 \cdot 6H_2O$ was used to wash the polymers in order to let the histidine binding sites saturated with nickel ion.

Two values were calculated to evaluate the MIPs. They are partition coefficient K and imprinting factor IF ($K= (M-M_{free})/W$; $IF= K_{MIP}/K_{NIP}$). M is the total template molar amount; M_{free} is the molar amount of the template in the supernatant; W is the weight of the polymer in each well. As explained above, the theoretical weight of a polymer was used here. K can reflect the affinity of the imprinted polymers to the template and IF reflect the selectivity of the MIPs relative to the NIP references.

Three different template concentrations were used to make the rebinding. They were 50 μM, 500 μM and 5000 μM. The total template in the case of 5000 μM was same as the original amount used in polymer preparation. Rebinding with 500 μM showed some monomer effects, however rebindings with 50 μM and 5000 μM didn't lead to any obvious conclusion.

4.7.4.1 Rebinding with 500 μM of template solutions

In the left half part of T1(Figure 4.40), the polymer made of monomer **1** (C) or **46** (D) showed a saturated K value (5.0), which was not strange since these two monomers had strong affinities to the lysine residue on the template. However, their MIPs had no imprinting effects (IF = 1.0). The highly possible reason was that, monomers used in the imprinting were five times more than templates, and this much excess of these strong binding monomers made the unspecific affinity become very pronounced. MIPs made of monomer **2** (B), **7** (E) or **8** (F) also reached saturated partition coefficients (K), and at the same time they showed some selectivity compared to NIPs. MIPs made of **3** (A), **10** (H) or **57** (G) showed some selectivities with comparatively low affinities.

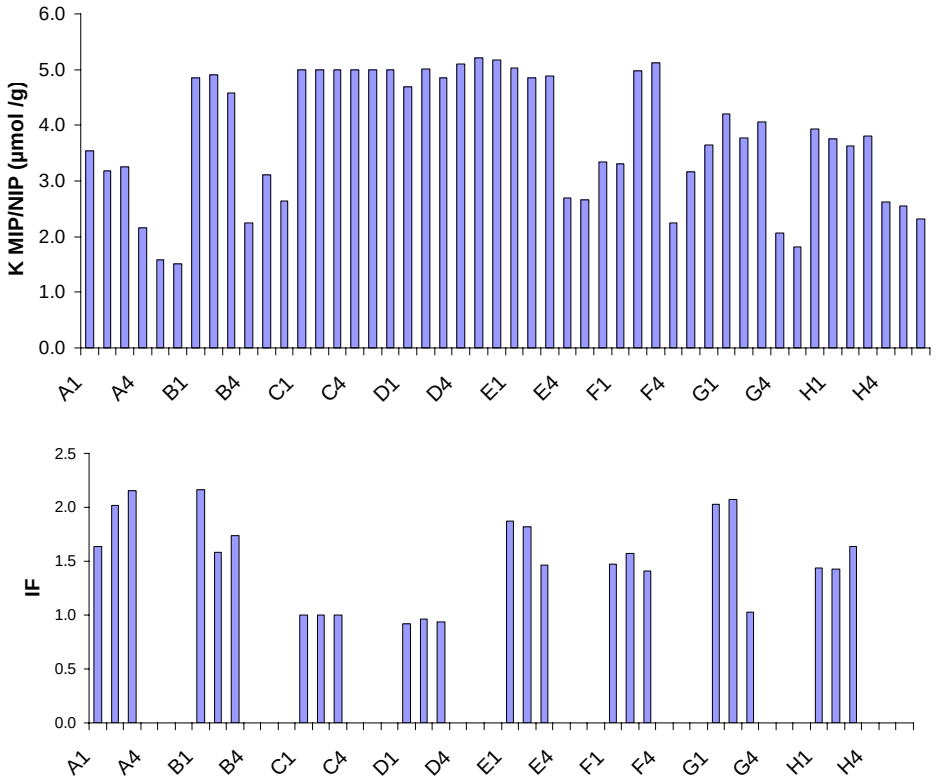

Figure 4.40 *Partition coefficient K and imprinting factor IF in left half part of P1.*

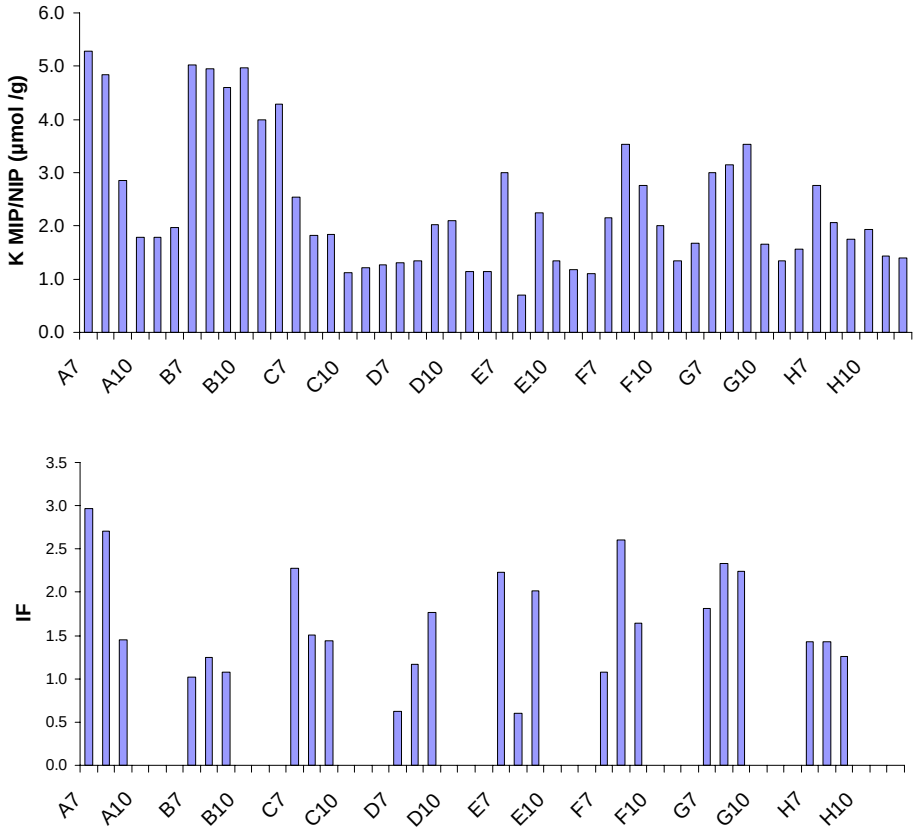

Figure 4.41 *Partition coefficient K and imprinting factor IF in the right half part of P1.*

Compared to the MIPs in the left half part of P1, MIPs in the right half part showed general lower affinities, except of MIPs made of monomer **51** (B) and of MA (A) (Figure 4.41). However, MIPs made with **51** didn't show any selectivity.

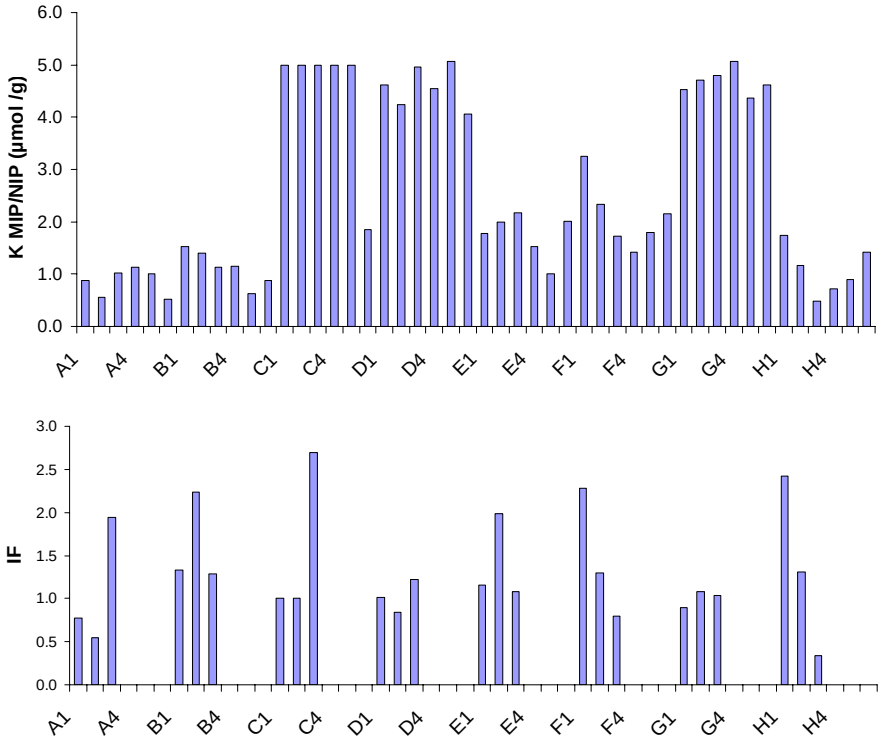

Figure 4.42 *Partition coefficient K and imprinting factor IF in the left half part of P2.*

In the left half part of P2 (Figure 4.42), most of the MIPs didn't show apparently good selectivities. MIPs made of monomer **1** (C) /**46** (D) showed high affinities to T3. The same phenomenon happened to MIPs made of monomer **5** (G), a NTA molecule with a high affinity to the histidine residue in T3 by metal ligand interaction. However, none of them showed selectivities. Obviously the guandinium monomer **2** (B) and ammonium monomer **3** (A) were not good candidates for these MIPs. The highly possible reason was the repulsion between them and the arginine residue in T3.

In the right half part of P2 (Figure 4.43), only polymers containing monomer **51** (methacryloyl acid) showed strong affinities, however they didn't show selectivities. Other MIPs made by cationic monomers seemed not good choices for T3.

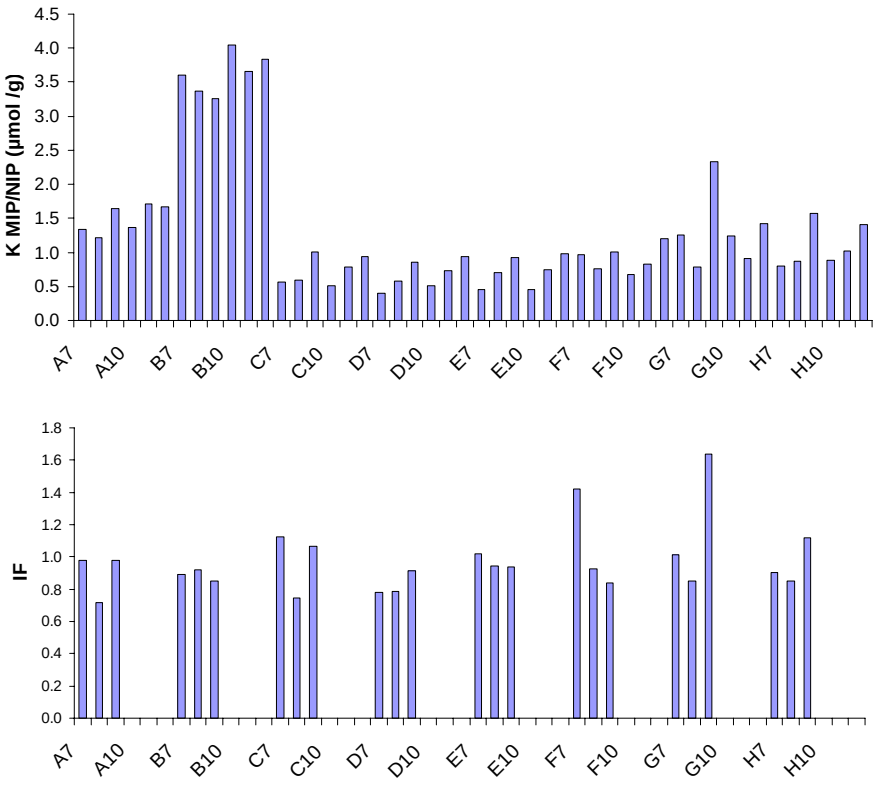

Figure 4.43 *Partition coefficient K and imprinting factor IF in the second right half plate.*

Some conclusions could be derived from above results. Some monomers seemed good candidates for T1: MIPs made of **1**, **46** and **51** had strong affinities, but no selectivities. Their affinities might be obtained by decreasing functional monomer ratios to T1. **2**, **7** and **8** showed both affinities and selectivities. **3**, **10** and **57** showed selectivies, but weak affinities. Combinations of these three kind of monomers might provide efficient MIPs in both sides. For T3, MIPs made of **1**, **5**, **46** and **51** showed good affinities, but no selectivities. As mentioned above for T1, their affinities might be obtained by decreasing functional monomer ratios to T3.

No obvious effect was observed for different crosslinker percentages. In several single case, MIPs made of one crosslinker percentage did have better effect than others, however, there was no apparent trend. In the view of template size, MIPs for the bigger T1 had generally better effect than the smaller T3, even though there were three very specific binding residues to our functional monomers on T3: argine to **3**, histidine to **5** and tyrosine to **10**.

Based on above discussion, in the future, MIPs will be made only for the comparatively large template T1, with a combination of several good monomer candidates. The functional

monomer content for each MIP will be decreased from 5:1 (a monomer to a template) to 1:1 (a monomer to a binding amino acid residue on the template). To reduce the workload, only 50% crosslinker percentage will be used as a compromise.

5 Conclusion and Outlook

5.1 Conclusions

In this work, protein surface recognition by polymers has been widely studied with the concept of multivalency. As basic binding sites of polymeric receptors, monomers with different functionalities specific for some amino acids have been developed. Polymers have been prepared in several forms: dendrimers, linear polymers, grafted polymers on PET membrane and crosslinked polymer materials as protein absorbers. The binding events between these polymers and proteins have been studied either in solution or at interface. In the following, details will be discussed by projects.

Project 1. Dendrimeric bisphosphonates for multivalent protein surface binding

By reductive amination based on different polypropyleneimine (PPI) generations, the lysine and arginine binder was incorporated on the periphery of dendrimers. The binding events between proteins/peptides and dendrimers were studied in buffered aqueous solution by three different spectroscopic methods (PFGLED, UV/Vis, and fluorescence). Results showed that the single weak binder (Ka in pure water <10 M^{-1}) was turned into powerful dendrimer receptors for basic proteins (K_D <250 nM for the hexadecamer and histone H1).

The fluorescence labeled octamer bind basic proteins roughly following the PI scale. This octamer showed preference to lysine rich proteins (lysine-rich histone, trypsin), in contrast of the arginine selectivity of the single binder. A possible explanation involved unfavorable coulomb repulsion between the approaching guandinium cation of arginine and the secondary benzylammonium group on the PPI backbone. Transition from the octamer to the larger hexadecamer did not lead to a drastic increase in affinity, and in some cases, Ka values even decreased. The reason might be that the more rigid structure of the hexadecamer made its binding sites couldn't wind around as freely as the octamer did, and thus rendered its induced fit to basic domains on a protein surface problematic.

The octamer and hexadecamer bind nearly all the used basic proteins with 1:1 or 1:2 stoichimetry, except of the large hemoglobin. This was an indication that dendrimers search

for the basic domains on a protein surface, and therefore the stoichimetry didn't depend on protein sizes, but on the size and distribution of basic domains.

Project 2. A Fluorescent Polymeric Heparin Sensor

As a test, a small linear copolymer library was developed and its binding events with proteins were screened with fluorescence microreader and UV microreader. It was observed that the micro-screening results were unreliable, which might attributed to the polydispersity of these linear polymers. However, during the research, a series of polymers selective to heparin were found.

This series of linear copolymers were decorated with o-aminomethylphenylboronates for covalent ester formation and/or alkylammonium ions for noncovalent Coulomb attraction. These water-soluble polymers showed exceptionally high affinities for a series of glycans: heparin, chondroitin-4-sulfate, hyaluronic acid and dextran. Heparin, a constant repeat of a 1, 4-glycosidic sugar dimer, carrying hydroxycarboxylates (iduronic acids) and hydroxysulfates (glucosamine), could be quantitatively detected with an unprecedented 30 nM sensitivity.

From this result, we proposed a new 7-member-ring binding scheme between the boronate and a sulfated ethylene glycol or aminoethanol unit, and this propose was studied by NMR titration and computer modeling with D-glucosamine 2-sulfate sodium salt (a fragment of heparin) and 1:1 complex of phenylboronic acid and piperidine.

Although the mechanism of heparin binding involved covalent boronate ester formation, it could be completely reversed by protamine addition, similar to heparin's complex formation with antithrombin III. Furthermore, the binding event could be quantitatively observed in a medicinally useful concentration range between 30 and 250 nM, which could be used as a biosensor for heparin monitoring.

Project 3. Protein adsorbers from surface-grafted copolymers with specific binding sites

With a "synergist immobilization method", two polymers (a homopolymer and a copolymer) were grafted onto PET membrane with controlled density and length. The polymer formation

was examined with solid state ^{31}P NMR spectrum, contact angle and water permeability measurements.

Static binding evaluated by BCA assay showed the favorite of the copolymer grafted membrane to the basic proteins. Due to specific -cation interactions between arginines and *m*-xylylene bisphosphonate binding sites, the neutral copolymer membrane was able to distinguish between basic proteins. Langmuir type adsorption isotherms revealed a 15-fold higher K_a value for lysozyme (1.33×10^7 M^{-1}) than for cytochrome C (10^6 M^{-1}), which were very similar as those in solution. Lysozyme could be separated from a 1:1 mixture of both proteins by static equilibration and subsequent elution without leaving a trace of detectable cytochrome C in elute.

This technique ensured the polymer immobilization on surface with a "vertical architecture" compared to the before "horizontal architecture", and thus keep the high flexibility and functionality of the linear polymers on a substrate. The other potential advantage of this grafted polymer compared to the non-covalent route for immobilization of the affinity polymer is the higher stability of the composite, for example under high-salt conditions used for the elution of bound proteins. These new polymeric materials might serve in sensor and separation applications, e.g., as membrane adsorbers or as chromatographic beads.

Project 4. Epitope MIPs for immunoglobulin G recognition in aqueous buffer

With IgG as a final recognition target, an exposed 9-mer fragment from its C-terminal was used as the template in MIPs preparation. 96 polymers were synthesized on a microplate with the aiding of a liquid-handling robot. Each polymer was made with ethylenebisacrylamide (crosslinker), methacrylamide (comonomer) and one of our 16 functional monomers in 10 mM hepes buffer. For each functional monomer, 6 polymers were prepared. Three of them were MIPs (with template in polymerization) with different crosslinker percentages (20%, 50% and 70%), and the other three were corresponding NIPs (without template in polymerization) as references. At the same time, to see the monomer effect more detaily, the other 96 polymers were prepared for a peptide template which was shorter, but with more effective binding amino acid residues (arginine, histidine and tyrosine).

Rebinding experiments were performed at three concentrations, 50 μM, 500 μM and 5000 μM. The total template amount in 5000 μM solution was same as the original used in polymer preparation. After each rebinding, polymers were washed by HCl solution (PH 2) until no template signal was observed. All the experiments were monitored by HPLC and BCA assay.

Results showed that several monomers had comparatively good imprinting effects for the two templates. The larger template showed a better effect than the shorter one. No apparent difference was observed for the three crosslinker percentages. These results provided us much information for the further MIP development for IgG.

Project 5. Microgel receptors with picromolar protein affinities

Functionalized microgel particles were made with 10 mol% crosslinker, 80 mol% *N*-isopropylacrylamide and 10 mol% monomers with functionalities from sodium methacrylate to tetrazole, to bisphosphonate dilithium salt. ITC titrations showed that they could recognize protein guests in buffered aqueous solution at neutral pH with K_a values of up to 10^{11} M^{-1} (averaged affinity towards each single protein). Switching between the functionalities allowed distinction between basic proteins of similar PI and size. Nearly all the other bindings was entropy driving. Intriguingly, the doubly charged bisphosphonate was superior to the carboxylate and tetrazole by one to three orders of magnitude, pointing to the important role of electrostatic attraction for association.

Project 6. Protein recognition by liposomes

Several functional monomers based on 10, 12-tricosadiyne structures were successfully prepared. The monolayer formation of one monomer **14** and the polymerization of this monolayer were monitored by pressure-area-isotherms on a film balance. Some effects were observed when monomers were incorporated with DMPC in the polymer matrix formed by 10, 12-tricosadiynoic acid. The liposome comprising of monomer **14** seemed to inhibit the chromatic transformations induced by positive small molecules and basic proteins; the liposome comprising of monomer **18** responsed more effectively to polysaccharide than small sugars; the liposome comprising of monomer **16** preferred substrates with more aromatic residues.

5.2 Outlook

The combinatorial, high throughput synthesis and evaluation seem promising ways for us to find good polymer candidates for giving proteins. However, traditional radical polymerizations and purifications make the preparation of polymer libraries very time-consumed. Two ways which might be used to get over this problem are a polyaddition and a polymer post-modification.

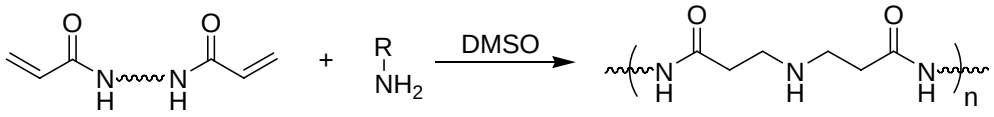

Figure 5.1 *Synthesis of polymers by polyaddition.*

Figure 5.1 shows a polyaddition which has been used for making a polymer library for gene delivery[127]. Due to the nearly 100% polymerization degree, polymers could be prepared easily in DMSO at 50 ºC without the need of further purification. The shortage of this method is the broad molecular weight distribution of the formed polymers. The other possible way to make a library is the modification of succiimide activated polyesters. Polymers with narrow molecular weight distributions could be prepared in large scales, and their modifications in microscales could be performed in a mild condition very cleanly (Figure 5.2).

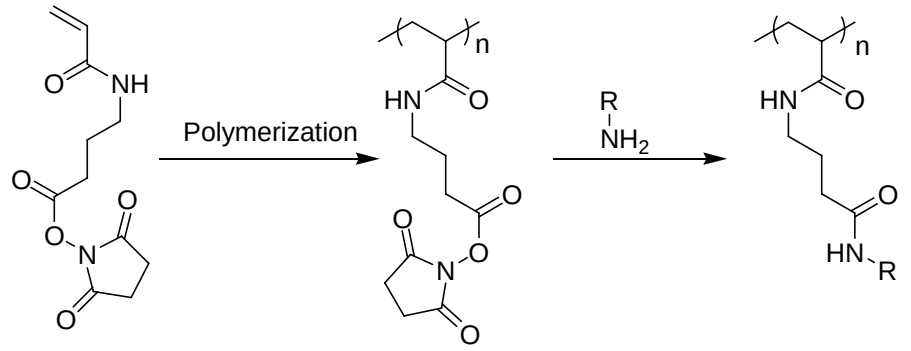

Figure 5.1 *Polymer synthesized by a modification of a succiimide activated polyester.*

In the previous study, I have found that, in our case, fluorescence and UV titrations on microreaders can't give reliable results for screening polymers with proteins. Possible replacers might be RIFs (**R**eflectometric **I**nter**f**erence **S**pectroscopy) or SPR (**P**lasmon

Resonance **S**pectroscopy) with the assistance of autosamplers. In RIFs, immobilization of proteins by a monolayer of polymeric binders fixed (non)covalently onto a SiO_2 surface, could be monitored in a time-resolved manner by RIfs in a flow-through system. The binding affinity could be evaluated by a series of measurements with different protein concentrations. Since one of our final targets is to find polymer candidates for inhibiting enzymes, we could also jump over the step of evaluating the binding affinity between polymers and proteins, and go to screen polymers by enzyme assays directly. Actually, my colleague *K. Wenck* is working in this way.

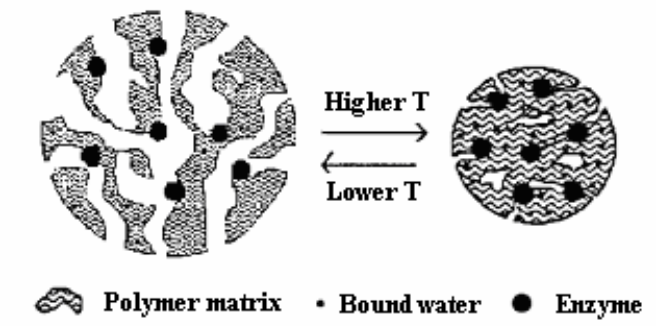

Figure 5.3 *Schematic diagram of pore structure in a swollen and collapsed thermally reversible hydrogel with an absorbed enzyme.*

The water-soluble microgel with protein selectivity found in my work, could be further developed into a smart material. The microgel composed with 80% N-isopropylacrylamide, which is a well-known composite to make the polymer exhibit thermally induced precipitation, might be used for protein purification (Figure 5.3).[128]

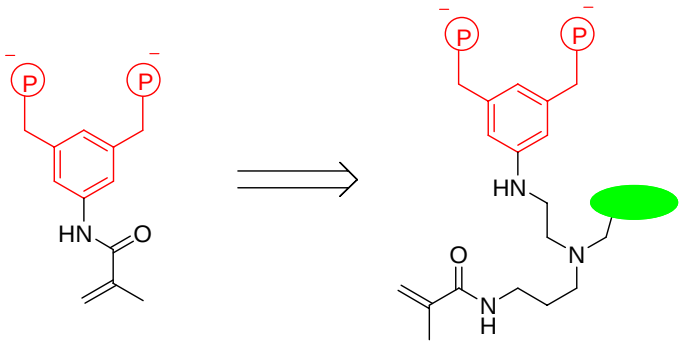

Figure 5.4 *A modification of monomer with a fluorescence label. Left: monomer 1. Left: a possible modification of this monomer*

Molecularly imprinted polymers (MIPs) could be used as protein purification materials. The efficient MIPs might also be developed into biosensors with incorporated optical labels. A fluorescence label could be incorporated into MIPs if one fluorescence monomer is used for MIPs preparation, or the functional monomer is labeled by a fluorophore (Figure 5.4). In the second case, when the binding sites of MIP materials interact with targets, it is very possible that only the template molecule could give an obvious optical signal.

6 Experimental section

6.1 Chemicals and equipments

Chemicals. All the commercial chemicals are purchased from Acros Organics, Sigma - Aldrich, Lancaster, Merck and Fluka. Pepitides used in the molecualr imprinting are from Gene-script.

Solvent. All the technical level organic solvents are distilled before use. Dry solvents are prepared with standard methods.[129, 130] The deionized water is obtained with an ELGA Purelab UHQ system and the ultra pure water is obtained from a Milli-Q unit.

Chromatography. Thin layer chromatography (TLC) with Merck silica-gel 60 F254 plates are used to monitor reactions. The detection is performed under 254 nM or 366 nM UV light. In the case of the non-fluorescent molecule, CAM reagent (2 g ceriumsulfate, 50 g ammonium molybdat and 50 mL concerntrated sulforonic acid in 400 mL water) or Ninhydrine reagent (0.3 g ninhydrine, 3 mL acetic aicd in 100 mL methanol), is used to color the molecule spot on the TLC plate.

Flash chromatography is performed with silicagel 60 (200-400 mesh) from Merck. The eluting solvent and R_f value depend on the substance.[131]

HPLC is performed by two types of instruments. Normally a Merck–Hitachi system with an L-7150 analytical pump, a K-1800 preparative pump, an L-7400 or K-2501 UV detector, and an L-7614 solvent degasser, is used. For the MIPs project, a Hewlett-Packard instrument (HP 1050) equipped with a quaternary pump, an autosampler, a diode array detector is used.

NMR spectroscopy. NMR spectra are recorded at 300 K on Bruker advance AC 200, Bruker AMX 300, Bruker DRX 500. The signals of some commonly used deuterated solvents are reported in literatures[132], and used for calibrations. Chemical shifts are reported in ppm relative to tetramethylsilane. Multiplicities are indicated by s (singlet), d (doublet), t (triplet), m (multiplet), and br (broad).The unit of the coupling constant is herz (Hz).

UV-Vis spectroscopy. UV-vis spectum are obtained at 25 °C on a Jasco V550 spectrophotometer. The UV screening is performed using a multifunctional plate reader SAFIRE from Tecan Deutschland GmbH.

Fluorescence spectroscopy. Fluorescence experiments were performed at 25 °C on a Jasco FP-6500 spectrofluorometer with a stirring unit and a Haake water-temperating unit.

Mass spectroscopy. Electron-spray-ionization (ESI) mass spectra are recorded on a Finnigan MAT 95S spectrometer. MALDI-TOF mass spectrum are measured by using a Bruker Flex III, and 2, 5-dihydroxybenzoylacid or 3, 5-dimethoxy-4-hydroxy-*trans*-3-phenylacrylacid is used as the matrix.

Elemental analysis. Elemental analysis is performed on a Varian elementer from Elementar Analysesysteme GmbH.

Filmbalance experiment. A NIMA 601 BAM filmblance with Wilhelmy plates is used to record the pressure-area isotherm.

Liquid sample handler. Automatic solution pipetting for making the polymer library is performed on a system from Zinsser Analytic GmbH (Germany) with the 96-well PTFE microtiter plate and PTFE coated closures from Radleys (U.K.). Quartz-glass microtiter plates are obtained from Hellma Worldwide (Germany).

Molecular modelling. The molecular modelling is performed with a programm MacroModel V 7.2 from Schroedinger Inc. For aqueous enviroment, Amber solvation model is used. [133,134] The complex structrue is firstly drawed and energy-minimized with the software Spartan, and the following Mente-Carlo simulation give the most stable structure.

6.2 Synthesis

6.2.1 Synthesis of monomers based on methacylate amide

Synthesis of 3, 5-bis-hydroxymethylnitrobenzene[135]

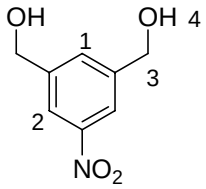

A mixture of 5-nitrophthaloylacid (2.00 g, 9.48 mmol) and PCl_5 (3.95 g, 19.0 mmol) was heated at 120 ºC for 1.5 h. Formed $POCl_3$ was distilled off and the residual acid chloride was dried resulting a colorless syrupy liquid (2.10 g, 90%). A solution of this acid chloride in 10 ml diglyme was added dropwise with stirring at 0 ºC to a solution of $NaBH_4$ (923 mg, 24.2 mmol) in 20 ml diglyme. After the addition, the mixture was stirred at room temperature for 6 h. It was treated with 0.5 N HCl at 0 ºC and the resulting mixture was concerntrated, extracted with ethyl acetate to afford a syrupy liquid, which was chromatographed over silica gel (EtOAC: Hexane=2:1, R_f=0.39) to afford a light yellow solid.

Yield: 1.49 g, 86%.**^{1}H-NMR (300 MHz, DMSO-d$_6$)**: δ (ppm) = 4.62 (d, *J* = 5.5 Hz, 4H, H-3), 5.51 (t, *J* = 5.5 Hz, 2H, H-4), 7.69 (s, 1H, H-1), 8.04 (s, 2H, H-2). **^{13}C-NMR (75 MHz, DMSO-d$_6$)**: δ (ppm) = 62.7, 119.8, 131.3, 145.7, 148.7.

Synthesis of 3, 5-bis-bromomethylnitrobenzene[135]

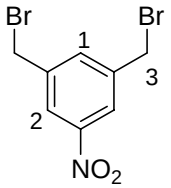

A solution of PBr_3 (1 ml, 10.5 mmol) in 20 ml diethyl ether was added slowly to a stirred solution of 3, 5-bis-bromomethylnitrobenzene (960 mg, 5.24 mmol) in 30 ml diethyl ether at

0 ºC. The mixture was stirred for further 6 h at 0 ºC and at room temperature overnight. Then it was poured onto ice and extracted with diethyl ether. The organic phase was washed with saturated $NaHCO_3$ solution and dried. Removal of the solvent gave a white solid.

Yield: 2.98 g, 92%. **^{1}H-NMR (300 MHz, $CDCl_3$)**: δ (ppm) = 4.52 (s, 4H, H-3), 7.75 (t, *J* = 1.5 Hz, 1H, H-1), 8.19 (d, *J* = 1.5 Hz, 2H, H-2). **^{13}C-NMR (75 MHz, $CDCl_3$)**: δ (ppm) = 30.6, 123.6, 135.2, 140.4, 148.6.

Synthesis of 3, 5-bis-aminomethyl nitrobenzene 19[136]

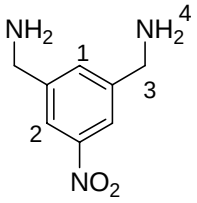

3, 5-Bis-bromomethyl nitrobenzene (6.00 g, 19.4 mmol) and sodium azide (2.91 g, 44.7 mmol) were dissolved in 200 ml DMF and refluxed overnight. After the solvent was removed, the crude product was dissolved in 200 ml CH_2Cl_2 and washed with 50 ml water for 5 times. The organic phase was dried over $MgSO_4$ and the solvent was distilled off. The crude was dissolved in 150 ml THF and triphenyl phosphine (10.0 g, 40.8 mmol) was added slowly at 0 ºC. After the mixture was stirred overnight at room temperature, water was added and the mixture was kept stirring for another 10 minutes. Aquaous phase was acidified with acetic acid to PH=2, and washed with CH_2Cl_2. Then it was basified to PH=10 and extracted with CH_2Cl_2. The solvent was distilled to afford the product.

Yield: 2.71 g, 81%. **^{1}H-NMR (300 MHz, CD_3OD)** δ (ppm) = 3.90 (s, 4H, H-3), 7.71 (s, 1H, H-1), 8.03 (s, 2H, H-2).

Synthesis of 3, 5-bis-(N, N'-bis-Boc-guanidinyl)methyl nitrobenzene 20[137]

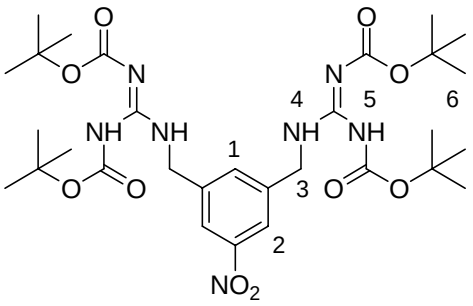

3, 5-Bis-aminomethyl nirobenzene (**19**, 1.40 g, 7.73 mmol), N,N'-bis-Boc-2-methylthiourea (**18**, 4.48 g, 14.7 mmol), triethylamine (2.00 ml, 15.1 mmol) and silver nitrate (2.50 g, 14.7 mmol) were dissolved/suspended in 100 mL CH_2Cl_2. The mixture was stirred for 5 days at room temperature. During this period the colour changed from yellow to dark brown. The precipitation was filtered and the solvent was removed. The crude product was chromatographied over silica gel with ethyl acetate ester and hexane as the eluent (1:3, R_f=0.3) to afford a white solid.

Yield: 720 mg, 14%. **^{1}H-NMR (300 MHz, $CDCl_3$)**: δ (ppm) = 1.49-1.52 (m, 36H, H-6), 4.77 (s, 4H, H-3), 7.81 (s, 1H, H-1), 8.12 (s, 2H, H-2), 8.92 (s, 2H, H-4), 11.6 (s, 2H, H-5). **MS (ESI pos., CH_2Cl_2)**: calcd for $C_{30}H_{48}N_7O_9$ $[M+H^+]$ m/z 666.3463, found 666.2; $C_{30}H_{47}N_7NaO_{10}$ $[M+Na^+]$ m/z 688.3282 found 688.3.

Synthesis of 3, 5-bis-(N, N'-bis-Boc-guanidinyl)methyl aniline 21

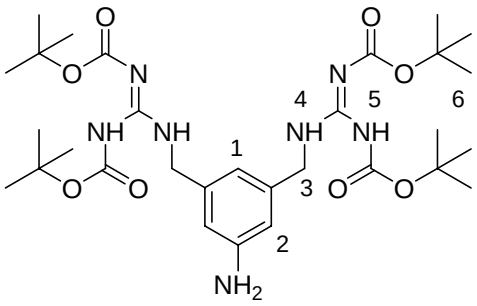

3, 5-Bis-(N, N'-bis-Boc-guanidinyl)methyl nitrobenzene (**20**, 4.52 g, 6.86 mmol) was dissolved in 50 ml absolute methanol, and catalytic amount of Pd/C was added into this

mixture. The mixture was stirred at room temperature under hydrogen atmosphere for four hours. The solvent was removed to afford a light yellow solid.

Yield: 4.36 g, 100%.**^{1}H-NMR (300 MHz, $CDCl_3$)**: δ (ppm) = 1.46-1.50 (m, 36H, H-6), 4.52 (s, 4H, H-3), 7.27 (s, 1H, H-1), 7.90 (s, 2H, H-2), 8.51 (s, 2H, H-4), 10.5 (s, 2H, H-5). **HRMS (ESI pos., CH_2Cl_2)**: calcd for $C_{30}H_{50}N_7O_8$ [M+H$^+$] m/z 636.4, found 636.2; calcd for $C_{30}H_{49}N_7NaO_8$ [M+Na$^+$] m/z 658.4 found 658.4.

Synthesis of 3, 5-bis-(N, N'-bis-Boc-guanidinyl)methyl phenylmethacrylamide

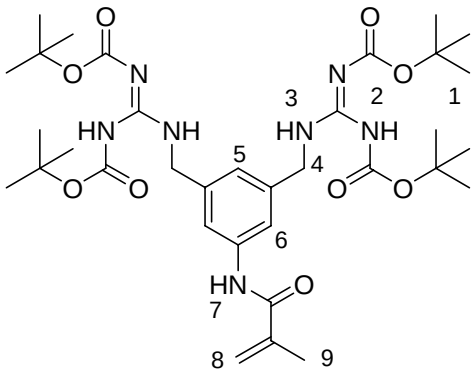

3, 5-Bis-(N, N'-bis-Boc-guanidinyl)methyl aniline (**21**, 4.00 g, 6.29 mmol) and triethylamine (1.75 ml, 12.6 mmol) were dissolved in 100 mL CH_2Cl_2, and methylacroyl chloride (1.22 ml, 12.6 mmol) in 50 ml CH_2Cl_2 was added dropwisely at 0 ºC. After the addition, the mixture was stirred for three hours and the solvent was removed. The product was chromatographied over silica gel (ethyl acetate ester: hexane 3:1, R_f=0.2) to afford a white solid.

Yield: 3 g, 76%. **^{1}H-NMR (300 MHz, $CDCl_3$)**: δ (ppm) = 1.45-1.50 (m, 36H, H-1), 2.02 (s, 3H, H-9), 4.59 (d, *J* = 4.59 Hz, 4H, H-4), 5.44 (s, 1H, H-8), 5.79 (s, 1H, H-8), 6.94 (s, 1H, H-5), 7.46 (s, 2H, H-6), 7.83 (s, 1H, H-7), 8.62 (s, 2H, H-3), 11.6 (s, 2H, H-2). **MS (ESI pos., CH_2Cl_2)**: calcd for $C_{34}H_{54}N_7O_9$ [M+H$^+$] m/z 704.3983, found 704.2; calcd for $C_{34}H_{53}N_7NaO_9$ [M+Na$^+$] m/z 726.3802 found 726.4.

Synthesis of 3, 5-(bis-guanidinium methyl) phenylmethacrylamide hydrochloride 2

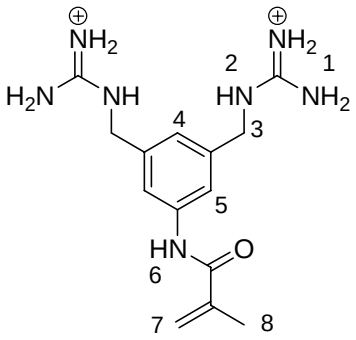

3, 5-Bis-(N, N'-bis-Boc-guanidinyl)methyl phenylmethacrylamide (**22**, 4.00 g, 4.27 mmol) was dissolved in 50mL CH_2Cl_2 and 50 ml 2 M HCl in diethyl ether was added. The mixture was stirred overnight. The precipitation was filtered and dried in vacuum to afford a light yellow viscous solid.

Yield: 1.4 g, 100%. **^{1}H-NMR (300 MHz, CD_3OD)**: δ (ppm) = 2.02 (s, 3H, H-8), 4.43 (s, 4H, H-3), 4.52 (s, 2H, H-2), 5.44 (s, 2H, H-7), 5.53 (s, 1H, H-7), 5.81 (s, 1H, H-7), 7.10 (s, 1H, H-4), 7.37 (s, 1H, H-6), 7.46 (s, 0.4H, H-1), 7.59 (s, 2H, H-5). **^{13}C-NMR (75 MHz, CD_3OD)**: δ(ppm) = 22.7, 124.7, 126.8, 126.9, 142.6, 142.7, 144.1, 161.7, 175.2, 180.3. **HRMS (ESI pos., MeOH)**: calcd for $C_{14}H_{22}N_7O$ $[M+H^+]$ m/z 304.1880, found 304.1879.

Synthesis of N, N'-bis-BOC-2-methyl-2-thiopseudourea 18

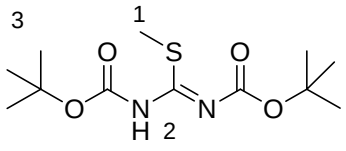

A modification of the Bergeron method was used. A mixture of di-*t*-butyldicarbonate (23.2 g, 106 mmol) and 2-methyl-2-thiopseudourea sulphate (6.21 g, 22.3 mmol) in 100 ml of 1:1 CH_2Cl_2 and saturated $NaHCO_3$ were stirred for 5 days at room temperature. Afterwards it was extracted with dichloromethane (100 ml) and purified by flash column chromatography (15% hexane in $CHCl_3$, then $CHCl_3$) gave a white product**.**

Yield: 10 g, 80%. **^{1}H-NMR (200 MHz, $CDCl_3$):** δ (ppm) = 1.51 (s, 18 H, H-3), 2.41 (s, 3 H, H-1). **HRMS (ESI pos., $CDCl_3$)**: calcd for $C_{12}H_{22}N_2NaO_4S$ [M+Na^+] m/z 313.1198, found 313.1192

Synthesis of 5-nitro-*m*-xylylene bisphosphonic acid tetramethylester 15

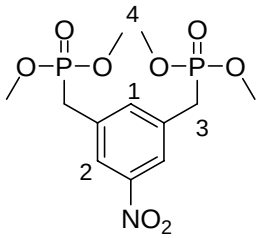

5-Nitro-*m*-xylene (9.52 g, 63.0 mmol) was dissolved in 165 mL of tetrachloromethane. *N*-bromosucciimide (24.8 g, 139 mmol) and a catalytic amount of α,α´-azo-bis-isobutyronitrile were added and the mixture was refluxed for 13 hours. After the insoluble succinimide was filtered, the solvent was removed under a reduced pressure. The remaining yellow oil was recrystallized from 7 mL of ethyl acetate and 15 mL of *n*-hexane. Subsequently the resulting yellowish solid (7.9 g crude product) was dissolved in an excess of trimethylphosphite (9.99 g, 80.5 mmol) and the solution was refluxed for 5 hours. The volatile components were removed in vacuo and the product was purified by chromatography over silica gel eluting with dichloromethane/methanol (14:1, R_f = 0.29).

Yield: 4.10 g, 18 %. **^{1}H-NMR (200 MHz, $CDCl_3$)**: δ (ppm) = 3.25 (d, $^2J_{H,P}$ = 22.0 Hz, 4H, H - 3), 3.73 (d, $^2J_{H,P}$ = 11.0 Hz, 12H, H-4), 7.57-7.62 (m, 1H, H-1), 8.04-8.07 (m, 2H, H-2). **^{31}P-NMR (81 MHz, $CDCl_3$)**: δ (ppm) = 27.3.

Synthesis of 5-amino-*m*-xylylene bisphosphonic acid tetramethylester 16

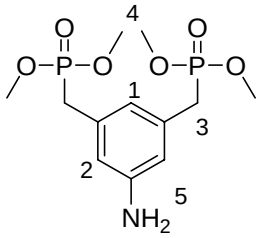

Catalytic amount of palladium on carbon was added to a solution of 5-nitro-*m*-xylylene bisphosphonic acid tetramethylester (**15**, 4.10 g, 11.2 mmol) in 400 mL absolute methanol. The reaction mixture was stirred for 15 hours under a hydrogen atmosphere. After the catalyst was filtered over celite, the solvent was removed under reduced pressure to furnish a yellow solid.

Yield: 3.39 g, 90 %. **^{1}H-NMR (200 MHz, $CDCl_3$)**: δ (ppm) = 3.06 (d, $^{2}J_{H,P}$ = 21.8 Hz, 4H, H-3), 3.06 (sb, 2H, H-5), 3.68 (d, $^{2}J_{H,P}$ = 10.8 Hz, 12H, H-4), 6.53-6.58 (m, 2H, H-2), 6.56-6.61 (m, 1H, H-1). **^{31}P-NMR (81 MHz, $CDCl_3$)**: δ (ppm) = 29.5.

Synthesis of 5-(methacryloylamido)-*m*-xylylene bisphosphonic acid tetramethylester 17

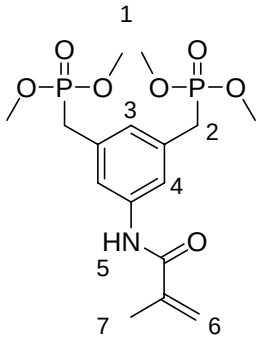

5-Amino-*m*-xylylene bisphosphonic acid tetramethylester (**16**, 900 mg, 2.71 mmol), triethylamine (320 mg, 3.16 mmol) and catalytic amount of 4-(*N, N*-dimethylamino)-pyridine were dissolved in 30 mL of dichloromethane. A solution of methacryloyl chloride (420 mg, 4.02 mmol) in 8 mL of dichloromethane was added dropwisely at 0°C within 1 hour. Stirring was continued for 1 hour at room temperature. Subsequently the organic layer was washed

with 30 mL 0.6 N NaOH and dried in vacuo. The crude product was purified by chromatography over silica gel eluting with dichloromethane/methanol (19:1, R_f = 0.09) to afford a viscous colorlessoil.

Yield: 0.91 g, 83 %. **^{1}H-NMR (200 MHz, $CDCl_3$)**: δ (ppm) = 2.06 (dd, *J* = 1.5 Hz, J=1.0 Hz, 3H, H-7); 3.15 (d, $^2J_{H,P}$ = 22.0 Hz, 4H, H-2); 3.70 (d, $^2J_{H,P}$ = 10.8 Hz, 12H, H-1); 5.47 (s, 1H, H-6); 5.79 (s, 1H, H-6); 6.97-7.01 (m, 1H, H-3); 7.47-7.50 (m, 2H, H-4); 7.69 (sb, 1H, H-5). **^{31}P-NMR (81 MHz, $CDCl_3$)**: δ (ppm) = 28.9. **HRMS (ESI pos., CH_2Cl_2)**: calcd. for $C_{16}H_{25}NNaO_7P_2$ [M+Na^+] m/z 428.1004 found m/z: 428.1011.

Synthesis of 5-(methacryloylamido)-*m*-xylylene bisphosphonic acid dimethylester dilithium salt 1

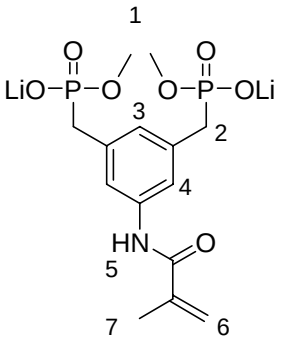

5-(Methacryloylamido)-*m*-xylylene bisphosphonic acid tetramethylester (**17**, 591 mg, 1.46 mmol) was dissolved in 35 mL of absolute acetonitrile under argon. A solution of lithium bromide (283 mg; 3.26 mmol) in 9 mL of acetonitrile was added and the reaction mixture was refluxed for 8 hours under argon. During this period the product precipitates from the reaction mixture. The solvent was decanted and the white solid was washed three times with acetonitrile. A white solid was obtained after being dried in vacuo.

Yield: 576 mg, 96 %. **^{1}H-NMR (200 MHz, D_2O)**: δ (ppm) = 1.99 (s, 3H, H-7); 3.01 (d, $^2J_{H,P}$ = 20.5 Hz, 4H, H-2); 3.51 (d, $^2J_{H,P}$ = 10.5 Hz, 6H, H-1); 5.54 (s, 1H, H-6); 5.79 (s, 1H, H-6); 7.00-7.04 (m, 1H, H-3); 7.18-7.21 (m, 2H, H-4). **^{13}C-NMR (81 MHz, D_2O)**: δ (ppm) = 18.1, 33.7, 52.0-52.2 (m), 121.6-122.0 (m), 128.3-128.6 (m), 135.9-136.2 (m), 136.9-137.1 (m), 140.1, 171.3. **^{31}P-NMR (81 MHz, D_2O)**: δ (ppm) = 26.8.

Synthesis of 2-aminoethyl carbamic acid *t*-butylester 24[138]

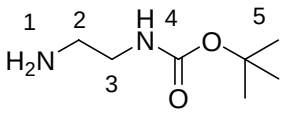

To a solution of 1, 2-ethylenediamine (12.4 g, 206 mmol) in chloroform (100 mL) was added dropwisely a mixture of di-t-butyldicarbonate (5.00 g, 22.9 mmol) in chloroform (40 mL) at 0 °C. The mixture was then stirred overnight at room temperature. Chloroform was evaporated and 100 ml of water was added to the oily crude product. The insoluble bis-substituted byproduct was removed by filtration. The filtrate was extracted three times with 100 ml of dichloromethane and the organic layer was dried over anhydrous Na_2SO_4 and condensed to afford a yellow oily product.

Yield: 2.90 g, 79%. **^{1}H-NMR (300 MHz, $CDCl_3$)**: δ (ppm) = 1.20 (s, 9H, H-5), 2.54 (t, *J* = 6.09 Hz, 2H, H-2), 2.91 (m, 2H, H-3), 3.46 (s, 1H, H-1), 5.54 (s, 1H, H-4). **^{13}C-NMR (75 MHz, $CDCl_3$)**: δ (ppm) = 28.3, 41.6, 43.0, 78.8, 156.2. **HRMS (ESI pos., CH_2Cl_2)**: calc. for $C_7H_{17}N_2O_2$ [M+Na^+] m/z 183.1109 found 183.1112.

Synthesis of *N*-2-((tert-butoxycarbonyl)-amido)ethyl methacrylamide 25[138]

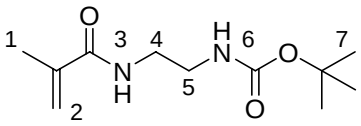

2-Aminoethyl-carbamicacid *t*-butylester (**24**, 2.65 g, 16.5 mmol) and triethylamine (6.67 ml, 47.8 mmol) were dissolved in 30 ml of chloroform. Methacryloyl chloride (1.83 g, 17.5 mmol) was dissolved in 20 ml of chloroform and added dropwise to the above mixture over a period of 2 h at 0 °C. The reaction mixture was stirred for another 2 h at room temperature. The organic layer was extracted five times with 30 ml of water and dried over anhydrous Na_2SO_4. Chloroform was evaporated and the product was recrystallized from a mixture of diethyl ether and hexane (3:5). If it was not pure yet, it could be further recrystallized from chloroform, diethyl ether and hexane (1:55:55) to afford a white solid.

Yield: 3.50 g, 93%. **^{1}H-NMR (300 MHz, $CDCl_3$)**: δ (ppm) = 1.20 (s, 9H, H-7), 1.71 (s, 3H, H-1), 3.00 (t, *J* = 6.09 Hz, 2H, H-5), 3.11 (t, *J* = 6.09 Hz, 2H, H-6), 4.25 (bs, 2H, H-3, 6), 5.13 (s, 1H, H-2), 5.50 (s, 1H, H-2). **HRMS (ESI pos., CH_2Cl_2)**: calc. for $C_{11}H_{20}N_2O_3Na$ [M+Na^+] m/z 251.1372, found 251.1369.

Synthesis of *N*-(2-aminoethyl) methacrylamide hydrochloride 3[138]

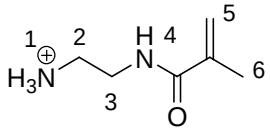

A solution containing *N*-2-((tert-butoxycarbonyl)-amido)ethyl methacrylamide (**25**, 2.07 g, 9.04 mmol) in CH_2Cl_2 (20 mL) and 2 M HCl/Et_2O (20 mL) was stirred at room temperature for 24 h. The hygroscopic salt was filtered and washed with diethyl ether to afford a white solid.

Yield: 1.16 g, 99%. **^{1}H-NMR (300 MHz, D_2O)**: δ (ppm) = 1.89 (s, 3H, H-6), 3.13 (t, *J* = 5.76 Hz, 2H, H-2), 3.53 (t, *J* = 6.09 Hz, 2H, H-3), 5.46 (s, 1H, H-5), 5.72 (s, 1H, H-5). **^{13}C-NMR (75 MHz, D_2O):** δ (ppm) = 19.1, 42.7, 119.8, 140.4, 169.3. **HRMS (ESI pos., MeOH)**: calcd for $C_6H_{13}N_2O$ [M+H^+] m/z 129.1028 found 129.1027.

Synthesis of 2-(*N*-(2-methacrylamido) ethylamino)methyl phenylboronic acid 5

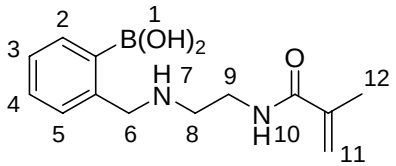

The *N*-(2-aminoethyl) methacrylamide hydrochloride (**3**, 1.00 g, 6.07 mmol), 2-formylboronic acid (0.91 g, 6.07 mmol), triethylamine (6.14 g, 60.7 mmol) and molecular sieve (3 Å) were

dissolved/suspended in 5 ml absolute methanol under nitrogen atmosphere. The mixture was stirred for 2 h at room temperature. Then sodium borohydride (232 mg, 6.07 mmol) was added at once. After an additional 1 h stirring, the mixture was filtered over celite and the filtrate was cooled by ice bath and filtered again. The second patch of filtrate was concentrated and dried in vacuum to afford a white product.

Yield: 1.41 g, 89%. **^{1}H-NMR (300 MHz, CD_3OD)**: δ (ppm) = 1.97 (s, 3H, H-12), 3.05 (t, *J* = 6.31 Hz, 2H, H-8), 3.61 (t, *J* = 6.31 Hz, 2H, H-9), 4.08 (s, 2H, H-6), 5.42 (m, 1H, H-11), 5.72 (m, 1H, H-11), 7.16 (m, 3H, H-3, 4, 5), 7.20 (m, 1H, H-2). **^{13}C-NMR (75 MHz, CD_3OD):** δ (ppm) = 10.2, 18.7, 38.3, 47.4, 55.3, 121.0, 123.9, 127.7, 128.5, 131.5, 141.0, 142.6, 171.7. **HRMS (ESI pos., MeOH)**: calcd for $C_{15}H_{23}BN_2O_3$ [M-2H+2CH_3+H^+] (boronic acid di-methylester) m/z 291.1802 found m/z 291.1878.

Synthesis of 2-methacrylamido-2-deoxy-D-glucose 7[139]

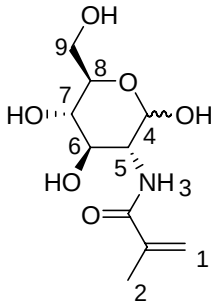

1.5 M sodium methoxide in methanol was added to a stirred solution of 2-deoxy-D-glucosamine hydrochloride (2.50 g, 12.1 mmol) in anhydrous methanol (100 mL) at 0 °C to give a final pH of 8-9. Distilled methacryloyl chloride was added in 1 mL portions (1.08 mL, 1 mmol) over 2 h. After each addition, the pH was adjusted to 8-9 with the sodium methoxide solution. After the addition of methacryloyl chloride was completed, TLC analysis (silica, methanol as eluent) showed 2-methacrylamido-2-deoxy-D-glucose (*R*$_f$ = 0.8) and 2-deoxy-glucosamine (*R*$_f$ = 0.4). The methanol was removed by rotary evaporation and the crude product was chromatographied to give a white product.

Yield: 2.75 g, 92%.**^{1}H-NMR (200 MHz, D_2O):** δ (ppm) = 1.92 (s, 3H, H-2), 3.43-3.97 (m, 6H, H-5, 6, 7, 8, 9), 5.21 (d, *J* = 3.4 Hz, 0.4H, H-4), 5.46 (s, 1H, H-1), 5.69 (s, 1 H, H-1). **^{13}C-NMR (75 MHz, D_2O)**: δ (ppm) = 139.0, 121.2, 121.1, 94.8, 90.8, 75.9, 71.5, 70.5, 70.1, 70.0, 60.6, 56.9, 54.3, 17.8. **HRMS (ESI pos. MeOH)**: calcd for $C_{10}H_{17}NNaO_6$ [M+Na^+].m/z 270.0948, found m/z 270.0947.

Synthesis of methacryloylamido-2-hydroxyl propane 8[140]

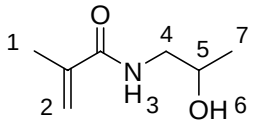

A solution of methacryloyl chloride (2.72 g, 26.0 mmol) in 40 mL of dry dichloromethane was added dropwise to a mixture of 1-aminopropan-2-ol (4.21 g, 56.1 mmol) in 40 mL of dry dichloromethane at 0°C under an argon atmosphere. The precipitating solid was filtered off and the solvent was removed under reduced pressure. After purification by chromatography over silica gel eluting with dichloromethane and methanol (14:1, R_f = 0.32), a white solid was obtained.

Yield: 3.27 g, 88 %. **^{1}H-NMR (300 MHz, $CDCl_3$)**: δ (ppm) = 1.21 (d, *J* = 6.4 Hz, 3H, H-7), 1.98 (dd, ^{4}J = 1.5 Hz, ^{4}J = 1.0 Hz, 3H, H-1), 2.51 (sb, 1H, H-6), 3.18 (ddd, ^{2}J = 14.0 Hz, ^{3}J = 7.5 Hz, ^{3}J = 5.3 Hz, 1H, H-4), 3.51(ddd, ^{2}J = 14.0 Hz, ^{3}J = 6.5 Hz, ^{3}J = 3.0 Hz, 1H, H-4), 3.96 (dqd, ^{3}J = 7.5Hz, ^{3}J = 6.4 Hz, ^{3}J = 3.0 Hz, 1H, H-5), 5.36 (qd, ^{4}J = 1.5 Hz, ^{2}J = 1.4 Hz, 1H, H-2), 5.74 (dq, ^{2}J = 1.4 Hz, ^{4}J = 1.0 Hz, 1H, H-2), 6.38 (sb, 1H, H-3).

Synthesis of N'-(5-N, N-dimethylamino naphthylsulfonylamido) ethylamine 33[141]

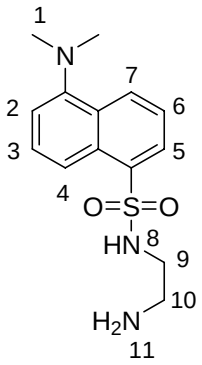

A solution of dansyl chloride (2.50 g, 9.26 mmol) in 40 ml dichloromethane was dropped into 1, 2-ethylenediamine (28.8 mL, 270 mmol) in 100 ml dichloromethane while stirring and cooling over ice. The mixture was stirred further while warming to room temperature, and then it was acidified with 1 N HCl and extracted with dichloromethane (3×20 mL). The aqueous layer was basified (pH 9) using 5 N NaOH and again extracted with dichloromethane (2×20 mL). The organic layer was dried over Na_2SO_4, filtered through a sinter and the solvent was removed under reduced pressure to give a yellow solid.

Yield: 2.58 g, 94%. **^{1}H-NMR (200 MHz, $CDCl_3$):** δ (ppm) = 2.66-2.72 (m, 2H, H-10), 2.88-2.92 (m, 8H, H-1, 9), 7.19 (dd, ^3J = 7.61 Hz, ^5J = 0.59 Hz, 1H, H-2), 7.49-7.60 (m, 2H, H-4, 5), 8.17-8.26 (m, 2H, H-3, 7), 8.51-8.58 (m, 1H, H-6). **^{13}C-NMR (75 MHz, $CDCl_3$):** δ (ppm) = 41.0, 45.5, 45.6, 115.4, 118.9, 123.3, 128.5, 129.7, 129.8, 130.1, 130.5, 134.9, 152.2. **HRMS (ESI, pos. CH_2Cl_2)**: [M+H$^+$] calc. for $C_{14}H_{19}N_3O_2S$ *m/z* 293.1148 found m/z 293.1157.

Synthesis of *N'*-((5-*N*, *N*-dimethylamino) naphthyl sulfonylamido) ethyl-2-methacrylamide 11

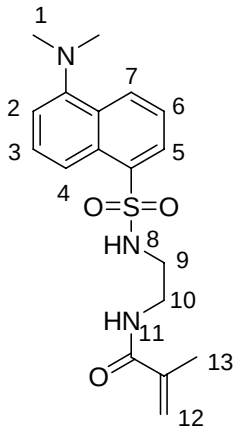

N'-((5-N, N-dimethylamino naphthylsulfonylamido) ethylamine (**33**, 2.55 g, 8.68 mmol) and triethylamine (1.33 mL, 9.55 mmol) were dissolved in 150 ml dichlormethane. To this solution was added methacryloyl chloride (910 µL, 9.55 mmol) in 50 ml dichlormethane dropwisely. After 5 hours the solvent was distilled and the crude product was purified over silica gel eluting with ethyl acetate and hexane (1:1; $R_f = 0.08$) to afford a green-yellow product.

Yield: 2.66 g, 85%. **^{1}H-NMR (200 MHz, $CDCl_3$):** δ (ppm) = 1.86 (s, 3H, H-13), 2.89 (s, 6H, H-1), 3.03-3.11 (m, 2H, H-10), 3.32-3.41 (m, 2H, H-9), 5.28 (s, 1H, H-12), 5.37 (t, $J = 6.01$ Hz, 1H, H-11), 5.61 (s, 1H, H-12), 6.22 (sb, 1H, H-8), 7.19 (dd, $^3J = 7.79$ Hz, $^5J = 0.59$ Hz, 1H, H-3), 7.49-7.61 (m, 2H, H-4, 6), 8.21-8.25 (m, 2H, H-2, 5), 8.48 (d, $J = 8.80$ Hz, 1H, H-7). **^{13}C-NMR (75 MHz, $CDCl_3$):** δ (ppm) = 18.6, 43.3, 39.7, 45.6, 115.6, 119.1, 120.3, 123.4, 128.6, 129.6, 129.7, 130.0, 130.6, 134.7, 139.4, 169.2. **HRMS (ESI, pos. CH_2Cl_2)**: [M+Na^+] calc. for $C_{18}H_{23}N_3O_3SNa$ *m/z* 384.1352 found m/z 384.1354.

Synthesis of dodecylmethacrylamide 9

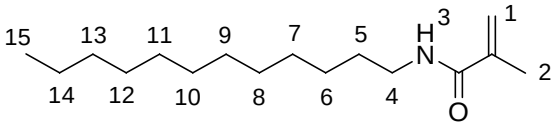

A solution of methacryloyl chloride (311 µL, 3.22 mmol) in 10 ml dichloromethane was dropped into dodecylamine (500 mg, 2.69 mmol) and triethylamine (450 µL, 3.22 mmol) in 50 ml dichlormethane. Then the crude was washed three times with 50 ml 1 N NaOH and three times with 50 ml 1 N HCl. The organic layer was dried over $MgSO_4$ and condensed to give a white product.

Yield: 640 mg, 97%. **^{1}H-NMR (200 MHz, $CDCl_3$):** δ (ppm) = 0.87 (t, ^3J = 6.39 Hz, 3H, H-15), 1.12-1.52 (m, 20H, H-5, 6, 7, 8, 9, 10, 11, 12, 13, 14), 1.96 (s, 3H, H-2), 3.25-3.35 (m, 2H, H-4), 5.30 (s, 1H, H-1), 5.66 (s, 1H, H-1), 5.77 (sb, 1H, H-3). **^{13}C-NMR (75 MHz, $CDCl_3$):** δ (ppm) = 14.2, 18.8, 22.8, 27.1, 29.4, 29.6, 29.7, 29.8, 32.0 40.0, 119.4, 140.3, 168.7. **HRMS (ESI, pos. CH_2Cl_2)**: [M+H$^+$] calc. for $C_{16}H_{32}NO$ *m/z* 254.2478 found m/z 254.2479.

Synthesis of *N*-(2-aminopyridine) methacrylamide 4[142]

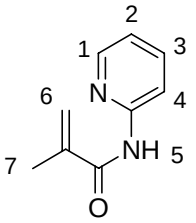

A solution of 2-aminopyridine (2 g, 21.3 mmol) and triethylamine (2.15 g, 21.3 mmol) in 20 mL CH_2Cl_2 was cooled to 0 °C. Methacryloyl chloride (2.23 g, 21.3 mmol) in 10 ml CH_2Cl_2 was added dropwisely. The mixture was stirred at room temperature overnight. After being washed with water, the organic phase was removed and the aquaous layer was extracted twice with chloroform. The combined organic phase was condensed and dried. After chromatography (CH_2Cl_2: MeOH=100:1, R_f = 0.15), the product was recrystallized in hexane to give a white solid.

Yield: 3 g, 87%. **^{1}H-NMR (200 MHz, $CDCl_3$):** δ (ppm) = 2.07 (s, 3H, H-7), 5.53 (s, 1H, H-6), 5.90 (s, 1H, H-6), 7.06 (m, 1H, H-3), 7.71 (m, 1H, H-2), 8.26 (m, 2H, H-1, 4), 8.28 (bs, 1H, H-5). **HRMS (ESI, pos. CH_2Cl_2)**: [M+H^+] calc. for $C_9H_{10}N_2O$ *m/z* 162.0793 found m/z 162.0789.

Synthesis of 4-(methacrylamido)butanoic acid[50]

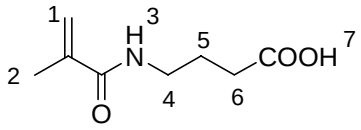

γ-Amino butylacid (5.00 g, 48.5 mmol) was dissolved in 12.5 ml 5 M NaOH and cooled to 0 °C. Methacryloyl chloride (5.57 g, 53.3 mmol) in 12.5 ml 5 M NaOH were added dropwise and simultaniously. The reaction mixture was stirred at room temperature for an additional hour, acidified with conc. hydrochloric acid to pH 2 and the resulting oil was extracted with dichloromethane. Removal of the solvent afforded a white solid.

Yield: 7.31 g, 88%. **^{1}H-NMR (300 MHz, $CDCl_3$):** δ (ppm) = 1.87-1.95 (m, 5H, H-2, 5), 2.44 (t, *J* = 6.96 Hz, 2H, H-6), 2.44 (m, 2H, H-4), 5.34 (s, 1H, H-1), 5.71 (s, 1H, H-1), 6.23 (bs, 1.2H, H-3, 7). **HRMS (ESI, pos. CH_2Cl_2)**: [M+Na^+] calc. for $C_8H_{13}NNaO_3$ *m/z* 194.0793 found m/z 194.0790; [M-H^+] calc. for $C_8H_{12}NO_3$ *m/z* 170.0817 found m/z 170.0811.

Synthesis of N-succiimide activated 4-(methacrylamido)butanoic acid 13

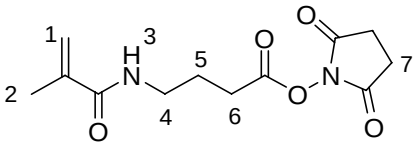

To a solution of 4-(methacrylamido)butanoic acid (2.00 g, 11.7 mmol) in 5 ml dichloromethane, N-hydroxy succiimide (1.48 g, 12.8 mmol) was added followed by EDC (2.46 g, 12.8 mmol). The reaction mixture was stirred at room temperature overnight. The organic phase was washed with water, dried and removed to afford a white solid.

Yield: 2.95 g, 94 %. **^{1}H-NMR (300 MHz, $CDCl_3$):** δ (ppm) = 1.96 (s, 3H, H-2), 2.04 (m, 2H, H-5), 2.68 (t, *J* = 7.2 Hz, 2H, H-6), 2.85 (s, 4H, H-7), 3.42 (m, 2H, H-4), 5.33 (s, 1H, H-1), 5.69 (s, 1H, H-1), 6.17 (bs, 1H, H-3). **^{13}C-NMR (75 MHz, $CDCl_3$):** δ (ppm) = 51.8, 56.3, 58.5, 62.9, 63.1, 97.5, 156.7, 177.6, 206.5, 208.0, 210.5. **HRMS (ESI, pos. CH_2Cl_2)**: [M+H^+] calc. for $C_{12}H_{17}N_2O_5$ *m/z* 269.1137 found m/z 269.1132, [M+Na^+] calc. for $C_{12}H_{16}N_2NaO_5$ *m/z* 291.1035 found m/z 291.0955, [2M+Na^+] calc. for $C_{24}H_{32}N_4NaO_{10}$ *m/z* 559.2016 found m/z 559.2019.

Synthesis of 2-(*N*-(2-methacrylamido) ethylthioureido) fluorescein 12

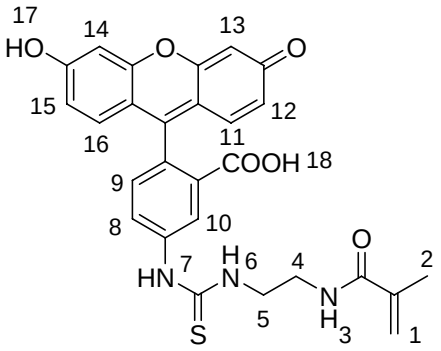

N-(2-Aminoethyl) methacrylamide hydrochloride (**3**, 17.8 mg, 108 µmol), fluorescein isothiocyanate (ITC, 42.0 mg, 108 µmol) and triethyl amine (180 µL, 323 µmol) were dissolved in 5 ml DMF. The mixture was stirred at room temperature overnight and the solvent was removed. The crude product was chromatographied over silica gel (dichloromethane: methanol = 9:1, R_f = 0.44) to give a yellow solid.

Yield: 48.6 mg, 87%. **^{1}H-NMR (300 MHz, CD_3OD):** δ (ppm) = 1.95 (s, 3H, H-2), 3.52 (m, 2H, H-4), 3.81 (s, 2H, H-5), 5.39 (s, 1H, H-1), 5.76 (s, 1H, H-1), 6.53 (d, *J* = 8.73 Hz, 1H, H-12), 6.55 (d, *J* = 2.37 Hz, 1H, H-12, 15), 6.68 (m, 4H, H-11, 13, 14, 16), 7.16 (d, *J* = 8.13 Hz, 1H, H-9), 7.78 (d, *J* = 10.0 Hz, 1H, H-8), 7.78 (d, *J*= 1.71 Hz, 1H, H-10), 8.20 (bs, 1H, H-7). **^{13}C-NMR (75 MHz, CD_3OD):** δ (ppm) = 9.3, 19.0, 39.7, 40.0, 40.5, 45.2, 103.6, 111.5, 113.7, 121.1, 125.9, 129.1, 130.4, 141.2, 142.4, 154.3, 161.4, 171.2, 171.8. **HRMS (ESI, pos. MeOH)**: [M-H^+] calc. for $C_{27}H_{22}N_3O_6S$ *m/z* 516.1229 found 516.1231.

Synthesis of 6'-Deoxy-6'-N-(2-aminoethylamino)-ß-cyclodextrin 32

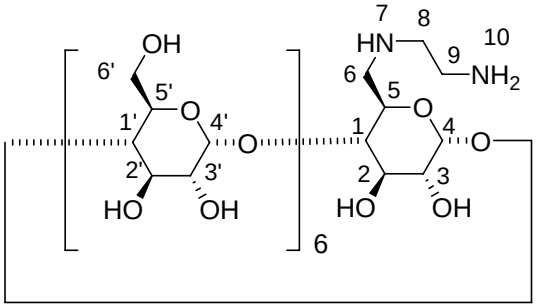

6'-o-(p-Tolylsulfonyl)-ß-cyclodextrin (200 mg, 155 µmol) was dissolved in ethylene diamine (1.03 ml, 15.5 mmol) and the mixture was refluxed at 70 °C under argon atmosphere overnight. After the excess amine was distilled, 10 ml ethanol was added and the mixture was refluxed for another 30 min. The precipitation was filtered and dissolved in 10 ml water. The aqueous solution was washed with 10 ml dichloromethane for three times and followingly condensed to about 0.5 ml. Ethanol was added dropwise to precipitate a white product, which was further washed with hexane.

Yield: 131 mg, 72%. **^{1}H-NMR (300 MHz, D_2O):** δ (ppm) = 2.75-3.0 (m, 4H, H-8, 9), 3.49-3.67 (m, 14H, H-1, 1', 3, 3'), 3.74-4.0 (m, 28H, H-2, 2', 5, 5', 6, 6'), 5.04 (s, 7H, H-4, 4'). **^{13}C-NMR (75 MHz, D_2O):** δ (ppm) = 40.5, 51.0, 61.2, 72.7, 72.8, 73.0, 73.9, 82.0, 84.5, 102.7. **HRMS (ESI, pos., H_2O)**: [M+H^+] calc. for $C_{44}H_{77}N_2O_{34}$ *m/z* 1177.4358 found 1177.4380; [M+Na^+] calc. for $C_{44}H_{76}N_2NaO_{34}$ *m/z* 1199.4177 found 1199.4191.

Synthesis of 6'-Deoxy-6'-(*N*-(2-methacrylamidyl) ethylamino)-ß-cyclodextrin 10

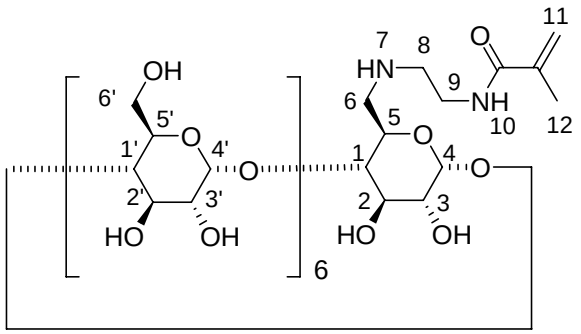

6'-Deoxy-6'-N-(2-aminoethylimino)-ß-cyclodextrin (1.00 g, 850 µmol) and triethylamine (0.14 ml, 1.02 mmol) were dissolved in 50 ml DMF. To his solution methylacroyl chloride (1.81 ml, 1.87 mmol) in 10 ml DMF was added dropwise at 0°C. The mixture was stirred overnight and DMF was distilled under vacuum. The solid was dissolved in 1 ml water and precipitated with 10 ml ethanol. If the precipitation was too fine, some hexane could be added. The whit solid was filtered and dried.

Yield: 529 mg, 50%. **^{1}H-NMR (300 MHz, D_2O):** δ (ppm) = 1.95 (s, 3H, H-12), 2.75-3.0 (m, 6H, H-8, 9), 3.49-3.67 (m, 14H, H-1, 1', 3, 3'), 3.74-4.0 (m, 28H, H-2, 2', 5, 5', 6, 6'), 5.05 (s, 7H, H-4, 4'), 5.51 (s, 1H, H-11), 5.76 (s, 1H, H-11). **HRMS (ESI, pos. H_2O)**: [M+H^+] calc. for $C_{48}H_{81}N_2O_{35}$ *m/z* 1245.4614 found 1245.4679.

Synthesis of *N*-benzyloxycarbonyl *N'*-bis(2-methoxy-2-oxomethyl) L-lysine methylester 26[124]

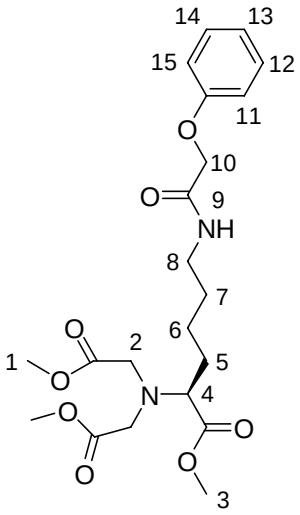

To a solution of *N*-benzyloxycarbonyl L-lysine methylester (3.00 g, 9.07 mmol) in acetonitrile (75 mL) was added methyl bromoacetate (15.1 g, 90.7 mmol) followed by finely ground K_2CO_3 (25.1 g, 181 mmol). The reaction mixture was heated at reflux for 18 h and then filtered through Celite and concentrated. Chromatography of the resulting oil using hexanes and ethyl acetate (1:2) provided the product as a light yellow oil.

Yield: 1.23 g, 31%. **^{1}H-NMR (300 MHz, $CDCl_3$):** δ (ppm) = 1.50 (m, 2H, H-6), 1.68 (m, 4H, H-5, 7), 3.18 (m, 2H, H-8), 3.42 (t, 1H, *J* = 7.56 Hz, H-4), 3.64 (s, 4H, H-2), 3.67 (m, 9H, H-1, 3), 5.09 (s, 2H, H-10), 7.36 (m, 5H, H-11, 12, 13, 14, 15). **HRMS (ESI, pos. CH_2Cl_2)**: [M+H$^+$] calc. for $C_{21}H_{31}N_2O_8$ *m/z* 439.2080 found 439.2099, [M+Na$^+$] calc. for $C_{21}H_{30}N_2NaO_8$ *m/z* 461.1900 found 461.1906.

Synthesis of *N*-(2-methyl-1-oxopropenyl)-*N'*-bis(2-methoxy-2-oxoethyl)-L-lysine methylester 28[124]

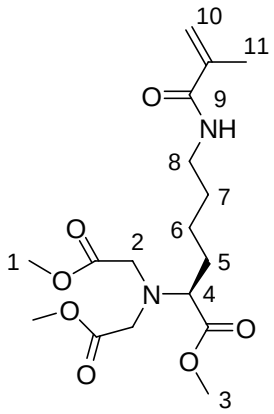

10% Pd/C (10 mg) was added to a solution of *N*-benzyloxycarbonyl *N'*-bis(2-methoxy-2-oxomethyl) L-lysine methylester (1.50 g, 3.42 mmol) in methanol (50 mL). This solution was stirred vigorously under H_2 (1 atm) for 2 h until no starting material could be seen by TLC (3:1 EtOAc/ hexane). The reaction mixture was filtered through celite and concentrated in vacum. The resulting residue was dissolved in THF (50 mL). To this solution was added triethylamine (692 mg, 6.84 mmol) followed by dropwise addition of methacryloyl chloride (358 mg, 3.42 mmol) in THF (10 mL). After the reaction was stirred for 30 min at 0 °C and then for 8 h at 25 °C, the mixture was concentrated. Chromatography of the resulting oil (2:1 EtOAc/hexanes) provided the methacrylamide as a light yellow oil.

Yield: 980 mg, 77%. **^{1}H-NMR (300 MHz, $CDCl_3$):** δ (ppm) = 1.40-1.76 (m, 6H, H-5, 6, 7), 1.96 (s, 3H, H-11), 3.35 (m, 2H, H-8), 3.43 (t, 1H, *J* =7.98 Hz, H-4), 3.63 (s, 4H, H-2), 3.67 (s, 9H, H-1, 3), 5.29 (s, 1H, H-10), 5.69 (s, 1H, H-10), 6.06 (bs, 1H, H-9). **HRMS (ESI, pos. CH_2Cl_2)**: [M+H^+] calc. for $C_{17}H_{29}N_2O_7$ *m/z* 373.1975 found 373.1969, [M+Na^+] calc. for $C_{17}H_{28}N_2NaO_7$ *m/z* 395.1794 found 395.1789.

Synthesis of *N*-(2-methyl-1-oxopropenyl)-*N*'-bis(carboxymethyl) L-lysine trilithium salt[124]

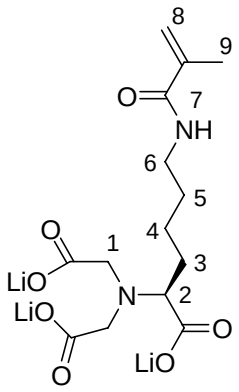

To a solution of *N*-(2-methyl-1-oxopropenyl)-*N*'-bis(2-methoxy-2-oxoethyl)-L-lysine methylester (**28**, 893 mg, 2.40 mmol) in 10 mL tetrachloromethane was added trimethylsilyl iodide (4.80 g, 24.0 mmol). The reaction was stirred at room temperature for 1 h, and LiOH (625 mg, 7.20 mmol) in water was added. The solvent was removed in vacuo to afford a light yellow solid.

Yield: 818 mg, 98%. **^{1}H-NMR (300 MHz, D_2O):** δ (ppm) = 1.32-1.67 (m, 6H, H-3, 4, 5), 1.89 (s, 3H, H-9), 2.99-3.25 (m, 7H, H-1, 2, 6), 3.90 (s, 0.2H, H-7), 5.38 (m,1H, H-8), 5.62 (m, 1H, H-8). **HRMS (ESI, pos. H_2O)**: [M+H^+] calc. for $C_{14}H_{20}Li_3N_2O_7$ *m*/*z* 349.1746 found 349.1757, [M+Na^+] calc. for $C_{14}H_{19}Li_3N_2NaO_7$ *m*/*z* 371.1565 found 371.1583, [M+Li^+] calc. for $C_{14}H_{19}Li_4N_2O_7$ *m*/*z* 355.1828 found 355.1835.

6.2.2 Synthesis of monomers based on 10, 12-tricosadiyne

Synthesis of succimide activated 10, 12-tricosadiynoic acid ester 34

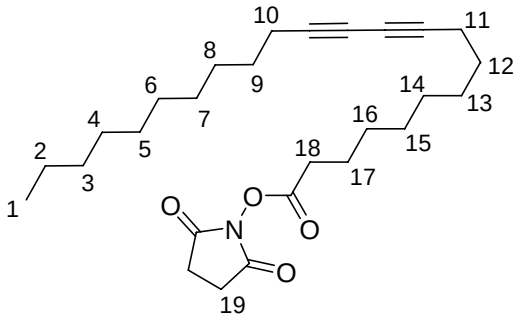

Prior to use, the commercial 10, 12-tricosadiynoic acid was dissolved in chloroform and filtered through Nylon membrane filters (0.8 um, Whatman). The solution was condensed to afford a white powder which was the 100% pure 10, 12-tricosadiynoic acid. To the solution of TRDA (182 mg, 525 µmol) in 5 mL dry dichloromehane, N-hydroxysucciimide (67.2 mg, 583 µmol) was added followed by N-ethyl-N'-(3-dimethylaminopropyl)-carbodiimide hydrochloride (EDC, 112 mg, 583 µmol). The reaction mixture was stirred at room temperature overnight. After the dichloromethane was removed, the residue was extracted with diethyl ether and water. The organic phase was dried over magnesium sulfonate and evaporated to afford a white solid

Yield: 229 mg, 98%.**^{1}H NMR (300 MHz, $CDCl_3$)**: δ (ppm) =0.80 (t, *J* = 6.45 Hz, 3H, H-1), 1.74-1.25 (m, 28H, H-2, 3, 4, 5, 6, 7, 8, 9, 12, 13, 14, 15, 16, 17), 2.24 (t, *J* = 6.81 Hz, 4H, H-10, 11), 2.60 (t, *J* = 7.38 Hz, 2H, H-18), 2.84 (s, 4H, H-19). **^{13}C-NMR (75 MHz, $CDCl_3$)**: δ (ppm) = 14.2, 19.3, 22.8, 24.6, 25.7, 28.4, 28.5, 28.8, 28.9, 29.0, 29.1, 29.2, 29.4, 29.6, 29.7, 31.0, 32.0, 65.3, 65.5, 168.8, 169.3. **HRMS (ESI, pos. CH_2Cl_2)**: $[M+H]^+$ calc. for $C_{27}H_{42}NO_4$ *m*/*z* 444.3114 found 444.3108, $[M+Na]^+$ calc. for $C_{27}H_{42}NO_4Na$ *m*/*z* 466.2933 found 466.2833.

Synthesis of 5-(10, 12-tricosadiynylacryloylamido)-*m*-xylylene bisphosphonic acid tetramethylester 35

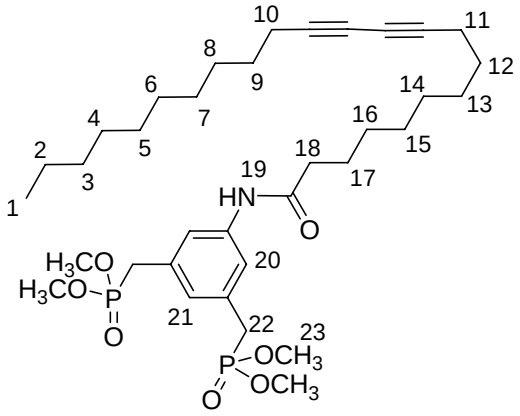

5-(Methacryloylamido)-*m*-xylylene bisphosphonic acid tetramethylester (284 mg, 842 µmol) und 10, 12-tricosadiynoic acid (263 mg, 758 µmol) were dissolved in 40 mL dry dichloromethane. To this mixtrue 530 µL T3P-solution (52% in ethyl ester) (322 mg, 1.01 mmol) and N-Methylmorpholine (469 mg, 4.63 mmol) were added. The reaction was stirred overnight and the solvent was condensed. The residue was washed with diethyl ether (10 mL) for three times and the ether phase was dried over Na_2SO_4. After the solvent was removed, the crude product was purified by column chromatography (R_f= 0.30, CH_2Cl_2: MeOH=30:1) to afford a white solid.

^{1}H-NMR (300 MHz, $CDCl_3$): δ (ppm) = 0.83 (t, *J* = 6.45Hz, 3H, H-1), 1.21-1.40 (m, 20H, H-3, 4, 5, 6, 7, 8, 13, 14, 15, 16), 1.41-1.46 (m, 4H, H-9, 12), 1.48-1.65 (m, 2H, H-17), 2.16-2.29 (m, 6H, H-10, 11, 18), 3.05 (d, ^2J = 21.7 Hz, 4H, H-22), 3.67 (d, ^2J = 20.5 Hz, 12H, H-23), 6.87 (s, 1H, H-21), 7.38 (s, 2H, H-20), 8.23 (s, 1H, H-19). **^{13}C-NMR (75 MHz, $CDCl_3$)**: δ (ppm) = 13.9, 19.1, 22.5, 25.3, 28.2, 28.8, 29.5, 29.6, 31.5, 31.8, 33.3, 37.3, 52.9, 65.2, 119.7, 126.1, 132.1, 139.0, 171.7. **^{31}P NMR (81 MHz, $CDCl_3$)**: δ (ppm) = 29.9. **HRMS (ESI, pos., CH_2Cl_2)**: $[M+H]^+$ calc. for $C_{35}H_{58}NO_7P_2$ *m*/*z* 666.3689 found 666.3694, $[M+Na]^+$ calc. for $C_{35}H_{57}NO_7P_2Na$ *m*/*z* 668.3508 found 668.3495.

Synthesis of 5-(10, 12-tricosadiynylacryloylamido)-*m*-xylylene bisphosphonic acid dimethylester dilithium salt 14

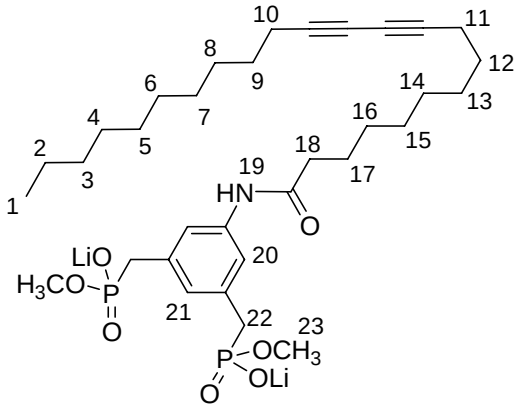

5-(10,12-tricosadiynylacryloylamido)-*m*-xylylene bisphosphonic acid tetramethylester (60.0 mg, 901 µmol) was dissolved in 2 mL dry acetonitrile and LiBr in actonitrile (117 µL, 1.71 mol) was added. After the mixture was heated at 80 °C overnight, the white precipitation was filtered and dried.

Yield: 88.1 mg, 98%. **^{1}H-NMR (300 MHz, D_2O)**: δ (ppm) =0.80 (t, *J* = 6.09 Hz, 3H, H-1), 1.20-1.40 (m, 24H, H-2, 3, 4, 5, 6, 7, 8, 9, 13, 14, 15, 16), 1.58 (m, 2H, H-17), 2.13 (dd, *J* = 6.94 Hz, *J* = 6.89 Hz, 4H, H-10, 11), 2.23 (t, *J* = 7.47 Hz, 2H, H-18), 2.83 (d, ^{2}J = 20.7 Hz, 4H, H-22), 3.40 (d, ^{2}J = 10.42 Hz, 6H, H-23), 6.92 (s, 2H, H-20), 7.23 (s, 2H, H-21). **^{13}C-NMR (75 MHz, D_2O)**: δ (ppm) = 13.0, 18.3, 22.3, 25.6, 28.1, 28.4, 28.6, 28.7, 28.9, 29.1, 29.2, 31.6, 33.3, 35.1, 36.7, 50.7, 50.8, 65.0, 76.4, 118.9, 127.0, 135.8, 135.9, 137.7, 173.0. **^{31}P NMR (81 MHz, D_2O)**: δ (ppm) = 20.9. **HRMS (ESI, pos., H_2O)**: $[M+H]^+$ calc. for $C_{33}H_{52}Li_2NO_7P_2$ *m*/*z* 668.3508 found 668.3495, $[M+Na]^+$ calc. for $C_{33}H_{52}Li_2NO_7P_2Na$ *m*/*z* 666.3689 found 668.3694.

Synthesis of 10, 12-tricosadiynoic (2-aminoethyl) amide 37

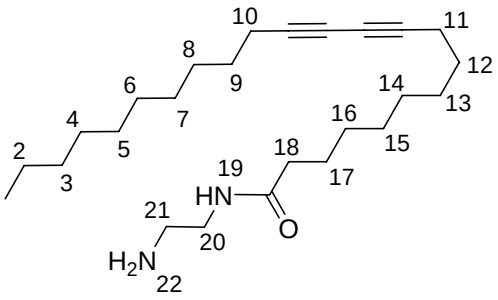

The solution of ethylene diamine (1.35 g, 22.5 mmol) and trimethylamine (502 mg, 4.92 mmol) in 10 mL dichloromethane was added to the suciimide activated 10,12-tricosadiynoic acid ester (**34**, 2.00 g, 4.51 mmol) in 50 mL dichloromethane. After the addition the reaction mixture was stirred overnight. The precipitation was filtered and the solvent was removed under vacumm to afford a white solid.

Yield: 703 mg, 79%. **^{1}H-NMR (300 MHz, $CDCl_3$)**: δ (ppm) = 0.87 (t, *J* = 6.5 Hz, 3H, H-1), 1.25-1.53 (m, 26H, H-2, 3, 4, 5, 6, 7, 8, 9, 12, 13, 14, 15, 16), 1.53 (m, 2H, H-17), 2.16-2.25 (m, 6H, H-10, 11, 18), 2.84 (t, *J* = 6.0 Hz, 2H, H-21), 3.32 (t, ^3J = 6.0 Hz, 2H, H-20), 5.67 (s, 0.2H, H-22), 6.04 (s, 0.8H, H-19). **HRMS (ESI pos., CH_2Cl_2)**: calc. for $C_{25}H_{45}N_2O$ [$M+H^+$] m/z 389.3532, found 389.3535.

Synthesis of 2-(10, 12-tricosadiynoic amido ethylamino) methyl phenylboronic acid 18

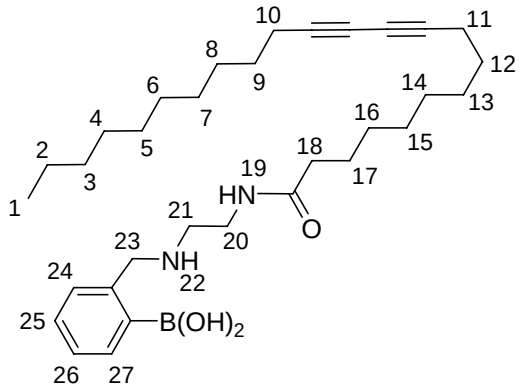

10, 12-tricosadiynoic 2-aminoethyl amide (**37**, 200 mg, 515 µmol), 2-formylboronic acid (74.1 mg, 515 µmol), triethylamine (521 mg, 5.15 mmol) and molecular sieves (3 Å) were dissolved/suspended in absolute methanol (5 mL) under a nitrogen atmosphere. The mixture was stirred for 2 h at room temperature. Then sodium borohydride (19.5 mg, 0.515 mmol) was added. After an additional 1 h stirring, the mixture was filtered over celite, concentrated and dried in vacuum to afford a yellow product.

Yield: 258 mg, 96%. **^{1}H NMR (300 MHz, CD_3OD)**: δ (ppm) = 0.84 (t, *J* = 6.63Hz, 3H, H-1), 1.68-0.94 (m, 28H, H-2, 3, 4, 5, 6, 7, 8, 9, 12, 13, 14, 15, 16, 17), 2.18 (m, 6H, H-10, 12, 18), 2.95 (t, *J* = 6.07Hz, 2H, H-21), 3.47 (t, *J* = 6.07Hz, 2H, H-20), 3.90-4.11 (m, 2H, H-23), 7.08-7.20 (m, 4H, H-24, 25, 26, 27), 7.39 (m, 1H, H-19). **^{13}C NMR (75 MHz, CD_3OD)**: δ(ppm) = 14.4, 19.6, 23.3, 26.4, 29.1, 29.3, 29.5, 29.7, 29.8, 29.9, 30.1, 30.2, 30.3, 32.6, 36.8, 37.6, 54.8, 66.1, 66.2, 123.5, 127.5, 128.2, 131.1, 141.9, 176.7. **HRMS (ESI, pos., MeOH)**: $[M+H]^+$ calc. for $C_{32}H_{52}BN_2O_3$ *m/z* 523.4071 found 523.4090, $[M+Na]^+$ calc. for $C_{32}H_{51}BN_2O_3Na$ *m/z* 545.3891 found 545.3918.

Synthesis of N-(2-bis-(BOC-guandinyl) ethylamino) 10, 12-tricosadiynoic amide 38

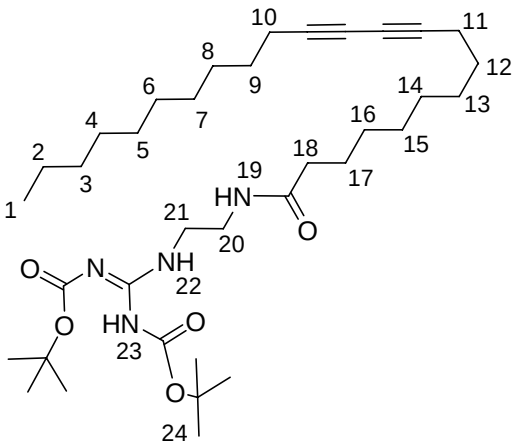

10, 12-tricosadiynoic 2-aminoethyl amide (744 mg, 1.99 mmol), triethylamine (222 mg, 2.19 mmol) and N, N'-bis-*t*-Boc-2-methyl-2-thiopseudourea (**18**, 578 mg, 1.99 mmol) were dissolved in 20 mL dry dichloromethane. After silver nitrate (0.372 g, 2.19 mmol) was added to the solution, the colorless solution became pale brown immediately. The mixture was

stirred at room temperature for five days. Then the precipitation was filtered and the solvent was removed under vacuum. The crude was chromatographied over silica gel (R_f = 0.32, CH_2Cl_2: MeOH = 100:1) to afford a colorless solid.

Yield: 1.14 g, 91%. **^{1}H NMR (300 MHz, $CDCl_3$)**: δ (ppm) = 0.88 (t, *J* = 6.67 Hz, 3H, H-1), 1.21-1.67 (m, 46H, H-2, 3, 4, 5, 6, 7, 8, 9, 12, 13, 14, 15, 16, 17, 24), 2.14-2.28 (m, 6H, H-10, 11, 18), 3.35-3.46 (m, 2H, H-21), 3.56 (m, 2H, H-20), 7.51 (s, 0.5H, H-22), 8.65 (s, 0.5H, H-19), 11.4 (s, 0.5H, H-23). **HRMS (ESI, pos., CH_2Cl_2)**: $[M+H]^+$ calc. for $C_{36}H_{63}N_4O_5$ *m/z* 631.4793 found 631.4821, $[M+Na]^+$ calc. for $C_{36}H_{62}N_4O_5Na$ *m/z* 653.4612 found 631.4636, calc. for $C_{72}H_{124}N_8O_{10}Na$ *m/z* 1283.9338 found 1283.9384.

Synthesis of (bis-guandino ethyl) 10, 12-tricosadiynoic amide

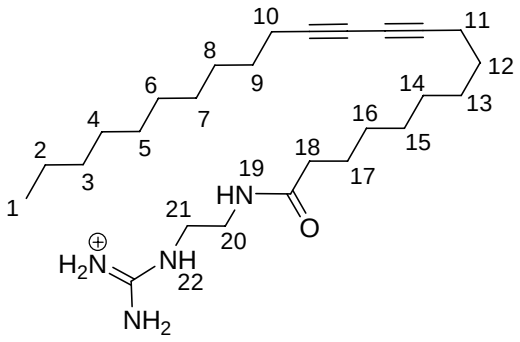

TRDA-Guandinium: The N-(2-bis-(BOC-guandino) ethylamino) 10, 12-tricosadiynoic amide **38** was dissolved in 1 M HCl in diethyl ether and the mixture was stirred overnight. Afterwards the solvent was condensed to afford a white solid. This solid was unstable and became red after several hours (polymerization).

HRMS (ESI, pos., MeOH): $[M+H]^+$ calc. for $C_{26}H_{47}N_4O$ *m/z* 431.6776 found 431.6612.

Synthesis of 6'-Deoxy-6'-(*N*-(2-10, 12-tricosadiynamido) ethylamino)-ß-cyclodextrin 34

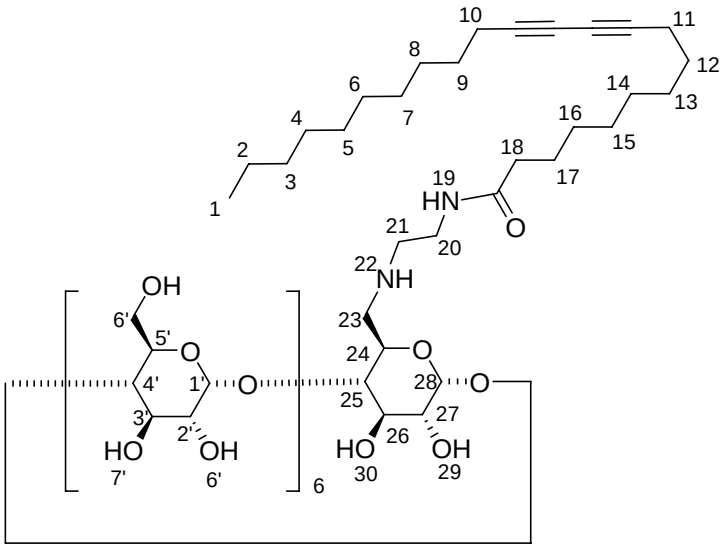

6'-Deoxy-6'-N-(2-aminoethylamino)-ß-cyclodextrin (**32**, 400 mg, 340 µmol), suciimide activated 10, 12-tricosadiynoic acid ester (**34**, 181 mg, 408 µmol) and triethylamine (56.8 µL, 408 µmol) were dissolved/suspended in 10 mL dry DMF and stirred overnight at room temperature overnight. Then the mixture became well soluble in DMF. The solvent was removed under vacuum and the product was dissolved in 20 mL water and washed with dichloromethane (10 mL) for three times. The water phase was condensed to afford a vicous solid with light grown color.

Yield: 174 mg, 34%.**^{1}H NMR (300 MHz, DMSO):** δ (ppm) = 0.88 (t, *J* = 6.62 Hz, 3H, H-1), 1.21-1.67 (m, 28H, H-2, 3, 4, 5, 6, 7, 8, 9, 12, 13, 14, 15, 16, 17), 2.04 (m, 2H, H-18), 2.26 (dd, *J* = 5.67 Hz, *J* = 5.67 Hz, 4H, H-10, 11), 2.58 (s, 4H, H-20, 21), 3.19-3.71 (m, H-2', 3', 4', 5', 6', 7', 29, 30 and water), 4.48 (s, 2H, H-25, 27), 4.73 (s, 4H, H-23, 24, 26), 5.61-5.83 (m, 7H, H-28, 1'). **HRMS (ESI, pos., H_2O)**: $[M+H]^+$ calc. for $C_{67}H_{113}N_2O_{35}$ *m*/*z* 1506.6065 found 1506.6211.

Synthesis of *N*-(10, 12-tricosadiynylacryloylamido)-*N*'-bis(carboxymethyl) L-lysine methylester 35

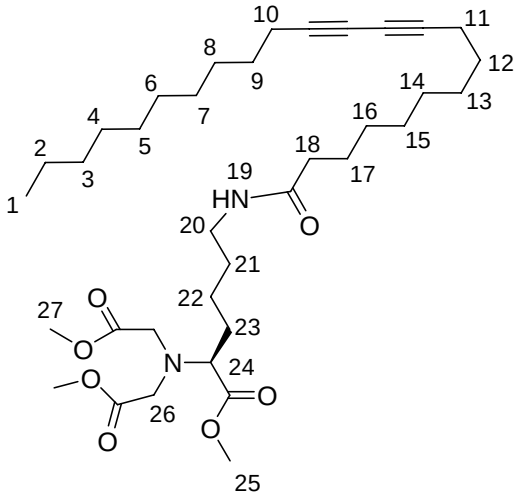

To the solution of 10, 12-tricosadiynoic 2-aminoethyl amide (**37**, 264 mg, 867 μmol) and triethylamine (174 μL, 1.25 mmol) in 10 mL dichloromethane, suciimide activated 10, 12-tricosadiynoic acid ester (**34**, 371 mg, 834 μmol) in 10 mL dichloromethane was added slowly and the mixture was stirred overnight at room temperature. The crude was chromatographied (dichloromethane: methanol=10:1, R_f=0.34) to give a white solid.

Yield: 394 mg, 72%. **^{1}H NMR (300 MHz, $CDCl_3$)**: δ (ppm) = 0.88 (t, *J* = 6.33 Hz, 3H, H-1), 1.25-1.73 (m, 34H, H-2, 3, 4, 5, 6, 7, 8, 9, 12, 13, 14, 15, 16, 17, 21, 22, 23), 2.17-2.25 (m, 6H, H-10, 11, 18), 3.24 (t, 2H, *J* = 5.88 Hz, H-20), 3.42 (t, 1H, *J* = 7.77 Hz, H-24), 3.62 (s, 4H, H-26), 3.68 (s, 9H, H-25, 27), 5.82 (s, 0.8H, H-19). **^{13}C NMR (75 MHz, $CDCl_3$)**: δ(ppm) = 14.0, 19.0, 22.5, 22.7, 25.7, 28.2, 28.5, 28.6, 28.7, 28.8, 28.9, 29.1, 29.2, 29.4, 29.5, 29.6, 31.8, 36.6, 39.0, 51.3, 51.5, 52.4, 53.4, 60.5, 64.2, 65.4, 68.7, 76.7, 171.7, 173.0, 173.3. **HRMS (ESI, pos., CH_2Cl_2)**: $[M+H]^+$ calc. for $C_{36}H_{61}N_2O_7$ *m*/*z* 633.4479 found 633.4504, $[M+Na]^+$ calc. for $C_{36}H_{60}N_2O_7Na$ *m*/*z* 655.4298 found 655.4324.

Synthesis of *N*-(10, 12-tricosadiynylacryloylamido)-*N*'-bis(carboxymethyl) L-lysine trilithium salt 15

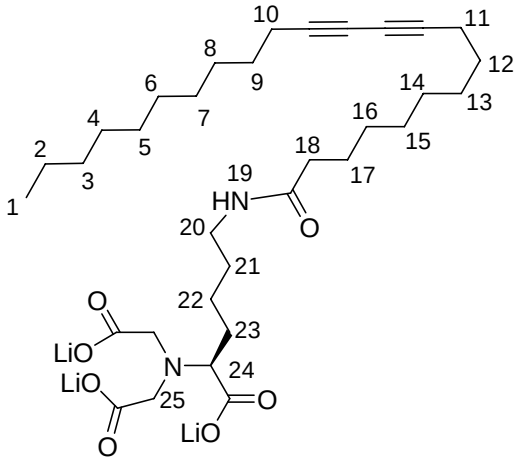

To a solution of *N*-(10, 12-tricosadiynylacryloylamido)-*N*'-bis(carboxymethyl) L-lysine methylester (**35**, 186 mg, 294 μmol) in 2.5 mL acetone and water (4:1 v/v), LiOH (70.4 mg, 2.94 mmol) was added. After the mixture was stirred for 3 days, the solvent was removed to afford a white solid.

^{1}H NMR (300 MHz, D_2O): δ (ppm) = 0.89 (s, 3H, H-1), 1.29-1.53 (m, 34H, H-2, 3, 4, 5, 6, 7, 8, 9, 12, 13, 14, 15, 16, 17, 21, 22, 23), 2.26 (m, 6H, H-10, 11, 18), 2.96-3.22 (m, 6H, H-20, 25), 3.90 (s, 0.4H, H-19), 3.91 (s, 1H, H-24). **HRMS (ESI pos., H_2O)**: calcd for $C_{33}H_{52}Li_3N_2O_7$ [M+H$^+$] m/z 609.4251 found 609.4259, Calcd for $C_{33}H_{51}Li_3N_2NaO_7$ [M+Na$^+$] m/z 631.4071 found 631.4055, for $C_{33}H_{51}Li_4N_2O_7$ [M+Li$^+$] m/z 615.4334 found 615.4386.

6.2.3 Synthesis of fluorescence labeled dendrimers

Synthesis of 3,5-bis(bromomethyl) benzyl alcohol[143]

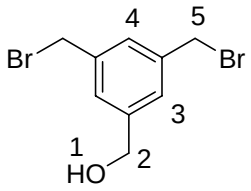

1, 3, 5-Tris(hydroxymethyl)benzol (1.00 g, 340 μmol) and tetrabromomethane (4.68 g, 7.48 mmol) were dissolved in 30 mL absolute acetonitrile. Triphenylphosphine (6.64 g, 7.48 mmol) was added slowly to the solution at 0°C, and the mixtrue was stirred overnight. The crude was chromatographied over silicagel with hexan and ethylacetate (3:2, R_f = 0.26) to afford a solid with pale yellow.

Yield: 935 mg, 54%. **^{1}H-NMR**: **(200 MHz, $CDCl_3$)**: δ (ppm) = 4.48 (s, 4H, H-5), 4.71 (s, 2H, H-2), 7.34 (s, 3H, H-3, 4). **^{13}C-NMR**: **(81 MHz, $CDCl_3$)**: δ (ppm) = 32.6, 64.6, 127.4, 128.7, 138.8, 142.3.

Synthesis of 3,5-bis(brommethyl)benzaldehyde [143]

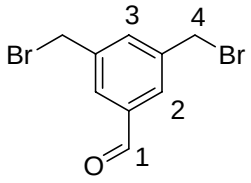

3, 5-Bis(brommethyl)benzylalcohol (700 mg, 2.38 mmol) was dissolved in 25 mL dichloromethane and mangan oxide (2.16 g, 24.8 mmol) was suspended in this solution. The mixtrue was stirred at room temperature over night. After the byproduct was filtered and the solvent was distilled, the crude was chromatographied over silicagel with hexan and ethylacetate (8:1, R_f = 0.14) to furnish a white soid.

Yield: 628 mg, 90%. **^{1}H-NMR**: **(200 MHz, $CDCl_3$)**: δ (ppm) = 4.53 (s, 4H, H-4), 7.69 (t, $^{4}J_{H,H-2}$ = 1.7 Hz, 1H, H-3), 7.84 (d, $^{4}J_{H,H-3}$ = 1.7 Hz, 2H, H-2), 10.01 (s, 1H, H-1).**^{13}C-NMR**: **^{13}C-NMR**: **(81 MHz, $CDCl_3$)**: δ (ppm) = 31.4, 129.8, 135.1, 137.5, 139.7, 190.9.

Synthesis of 3, 5-bis(dimethoxyphosphorylmethyl) benzaldehyde

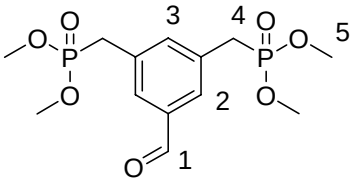

3, 5-Bis(brommethyl) benzaldehyde (620 mg, 2.06 mmol) in trimethylphosphite (631 mg, 4.53 mmol) was refluxed for 5 h. Afterwards the solvent was distilled under vacum and the crude was purified by chromatography with dichloromethane and methanol (19:1, R_f = 0.14) to give a white product.

Yield: 718 mg, 79 %. **^{1}H-NMR**: **(200 MHz, $CDCl_3$)**: δ (ppm) = 3.24 (d, $^{2}J_{H,P}$ = 22.0 Hz, 4H, H-4), 3.71 (d, $^{3}J_{H,P}$ = 10.8 Hz, 12H, H-5), 7.53 (t, $^{4}J_{H,H-2}$= 2.0 Hz, 2H, H-3), 7.71 (d, $^{4}J_{H,H-3}$= 2.0 Hz, 2H, H-2), 9.99 (s, 1H, H-1). **^{31}P-NMR**: **(81 MHz, $CDCl_3$)**: δ (ppm) = 28.2.

Synthesis of dilithium-3, 5-bis (methoxyphosphorylmethyl) benzaldehyde

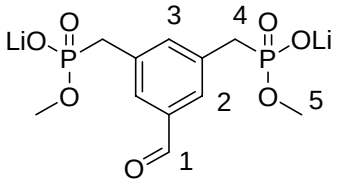

3, 5-Bis (dimethoxyphosphorylmethyl) benzaldehyde (910 mg, 2.06 mmol) was dissolved in dry acetonitrile. Under the nitrogen atmosphere LiBr (390 mg, 4.53 mmol) was added and the mixture was heated at 80 °C over night. A white product was obtained by washing the precipitation with acetonitrile and diethylether.

Yield: 0.65 g, 95%. **^{1}H-NMR (200 MHz, D_2O)**: δ (ppm) = 3.12 (d, $^{2}J_{H,P}$ = 20.4 Hz, 4H, H-4), 3.55 (d, $^{3}J_{H,P}$ = 10.4 Hz, 6H, H-5), 7.49 (s, 1H, H-3), 7.66 (s, 2H, H-2), 9.87 (s, 1H, H-1). **^{31}P-NMR (81 MHz, D_2O)**: δ (ppm) = 30.9. **^{13}C-NMR (81 MHz, D_2O)**: δ (ppm) = 31.1, 50.1, 127.0, 134.2, 134.4, 135.6, 194.7.

Synthesis of fluorescein labeled octamer 40

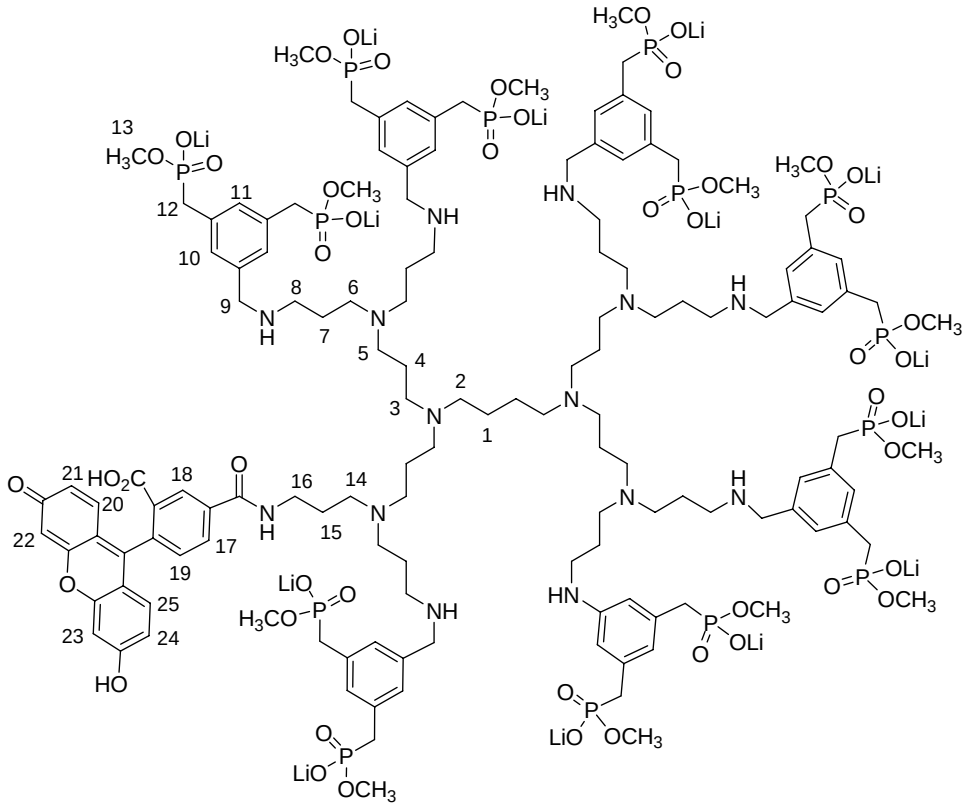

A mixture of PPI dendrimer (DAB-Am8: 50.0 mg, 64.7 µmol) in 2 mL water and fluorescein, activated as N-hydroxysuccinimide ester (40.0 mg, 84.5 µmol) in DMSO (400 mL), was incubated for 4 h. The solvent was removed, and 3, 5-bis(methoxyphosphorylmethyl) benzaldehyde dilithium salt (160 mg, 447 µmol) was added to the residue. The mixture was dissolved in anhydrous methanol (40 mL) and stirred under argon with molecular sieves (3 Å) at ambient temperature. After 24 h, sodium borohydride (20.0 mg, 440 µmol) was added, and the solution was stirred for another 24 h. The pulverized molecular sieves were filtered off, and the solvent was removed in vacuo. The remaining solid was purified by dialysis with water for 4 days.

Yield: 65 mg, 30%. **^{1}H-NMR (300 MHz, D_2O):** δ (ppm) = 1.86 (sb, 28H, H-1, 4, 7), 2.93 (sb, 72H, H-2, 3, 5, 6, 8, 12), 3.50 (d, $^{3}J_{H,P}$= 9.50 Hz, 36H, H-13), 4.13 (sb, 12H, H-9), 7.15 (sb, 18H, H-10, 11), 7.74 (s, 2H, H-21, 24), 7.84 (s, 1H, H-19), 8.05 (m, 4H, H-20, 22, 23, 25), 8.26 (s, 2H, H-17, 18).**^{31}P-NMR (81 MHz, D_2O)**: δ (ppm) = 23.6. **MS (MALDI-TOF)**: m/z = 2404 [$M(BP)_4+H^+$], 2722 [$M(BP)_5+H^+$], 3026 [$M(BP)_6+H^+$], 3344 [$M(BP)_7+H^+$]

Synthesis of fluorescein labeled hexadecamer 41

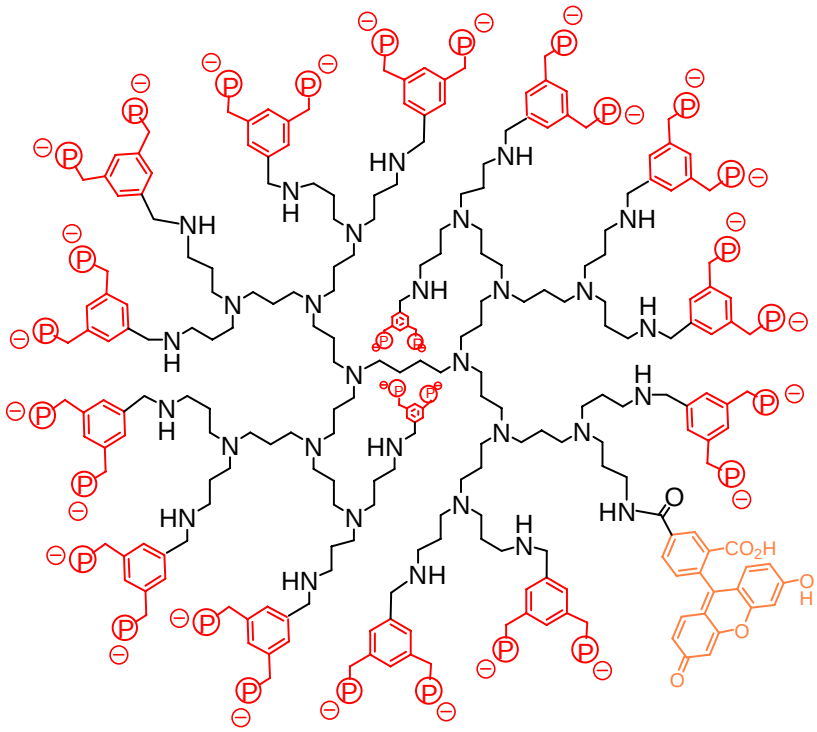

A mixture of PPI dendrimer (DAB Am16: 50.0 mg, 29.6 ummol) in 2 mL water and fluorescein, activated as N-hydroxysuccinimide ester (14.0 mg, 29.1 µmol) in DMSO (100 mL), was incubated for 4 h. The solvent was removed, and 3, 5-bis-(methoxyphosphorylmethyl) benzaldehyde dilithium salt (150 mg, 449 ummol) was added to the residue. The mixture was dissolved in anhydrous methanol (40 mL) and stirred under argon with molecular sieves (3 Å) at ambient temperature. After 24 h, sodium borohydride (20 mg, 440 µmol) was added, and the solution was stirred for another 24 h. The pulverized molecular sieves were filtered off, and the solvent was removed in vacuo. The remaining solid was purified by dialysis with water for 4 days.

Yield: 38 mg, 18%. **^{1}H-NMR (300 MHz, D_2O)**: δ (ppm) = 7.20 (m, 45H), 4.11 (br, 30H), 3.54 (d, $^{3}J_{P,H}$=7.4 Hz, 96H), 3.03 (d, $^{2}J_{P,H}$=19.6 Hz, 106 H), 2.34–2.73 (br, 192 H), 1.60–1.88 (br, 97H), 1.57 (br, 4H). **^{31}P-NMR (81 MHz, D_2O)**: δ (ppm) = 23.5, 24.0.

6.2.4 Synthesis of linear polymers

The general prodecure for polymerization was: a solution containing a combination of monomers and a catalytic amount of initiator (1 mol%) in DMF/methanol/water was degassed and stirred for 24-30 hours at 60 °C. The reaction mixture was diluted with methanol in order to give a maximum concentration of 5% of the initial monomer mass and added dropwise into 5-10 times volume of ethyl acetate. The solid was collected by filtration, washed with ethyl acetate and dried in vacuo. In some cases, the polymers were purified further by dialysis.

The Polymer containing the bisphosphate dianion unit was prepared with monomer **17**, the bisphosphonic acid tetramethylester. Afterwards the neutral polymer was dealkylated: it was dissolved in absolute acetonitrile (approx. 1 mL per 10 mg) under an argon atmosphere. For each bisphosphonic acid tetramethyl ester present in the polymer, 2.2 eq. of dry lithium bromide was added. The clear solution was stirred under argon for 72 hours at 80 °C. During this period the polyanionic product precipitated as poly-(lithiumphosphonate) salt from the reaction mixture. The solvent was decanted and the white solid was washed for three times with acetonitrile. Pure product was obtained after filtration and dried under vacuum.

In selected cases, copolymerization parameters were determined by C. Renner and found to be close to 1.0 for the methacrylate monomers, therotically ensuring a statistical copolymerization. Practically, we could use ^{1}H-NMR spectra to estimate the monomer molar ratios in the polymers. Although the NMR singnals of polymers became broad and intersected each other, some specific peaks could still be observed. For example, signals at 3.6 - 3.9 ppm were from the methylester group in monomer **1**, at 3.9 - 4.1 ppm were from the CH group in monomer **8** and at 8.0 - 8.3 ppm were from monomer **11**. The results showed that, in most cases the monomer ratios in the polymers were very similar to initial recipes.

Synthesis of polymer P1

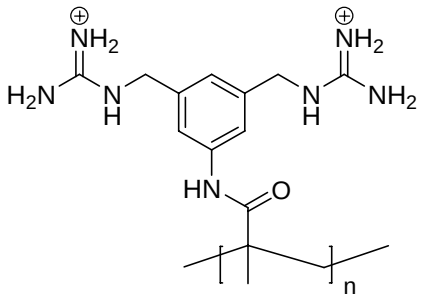

500 mg monomer **2**, 1 mol% V50 in 3 mL water. **Yield**: 190 mg, 38%. **^{1}H-NMR (300 MHz, D_2O)**: δ (ppm) = 1.21 (sb, 3H), 1.90 (sb, 2H), 4.15 (sb, 4H), 4.55 (m, 5H), 7.01 (sb, 5H).

Synthesis of polymer P2

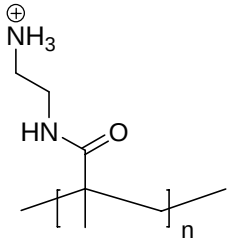

500 mg monomer **3**, 1 mol% AIBN in 3 mL DMF. **Yield**: 400 mg, 80%. **^{1}H-NMR (300 MHz, D_2O)**: δ (ppm) = 1.09-1.85 (sb, 5H), 2.51-3.11 (sb, 5H).

Synthesis of polymer P3

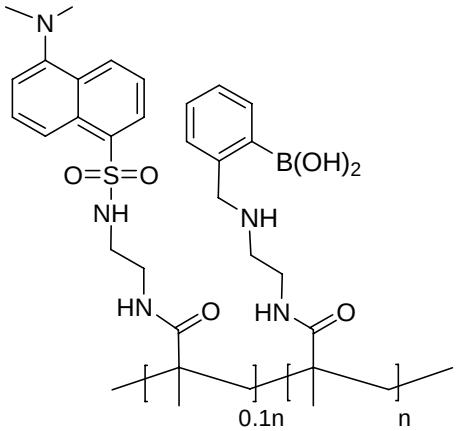

100 mg monomer **6**, 13.7 mg monomer **11**, 1 mol% AIBN in 3 mL DMF. **Yield**: 34 mg, 30%.

^{1}H-NMR (300 MHz, CD_3OD): δ (ppm) = 1.21 (sb, 3H), 1.95 (sb, 2H), 2.31-4.05 (sb, 5H). 7.01 (sb, 1H), 7.40 (m, 3H).

Synthesis of polymer P4

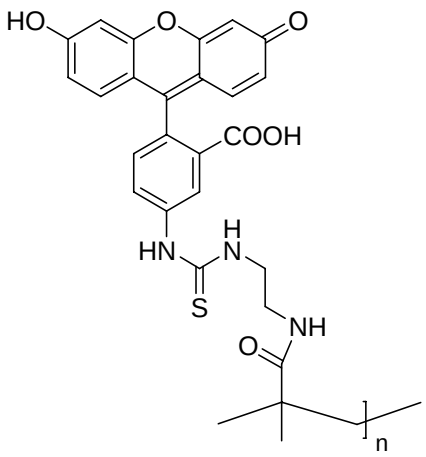

500 mg monomer **3**, 1 mol% AIBN in 3 mL DMF. **Yield**: 105 mg, 35%. **^{1}H-NMR (300 MHz, $CDCl_3$)**: δ (ppm) = 1.09 (sb, 3H), 1.81 (sb, 2H), 3.11 (sb, 4H), 6.01-6.22 (sb, 5H), 7.01 (sb, 1H), 7.46 (sb, 2H).

Synthesis of polymer P5

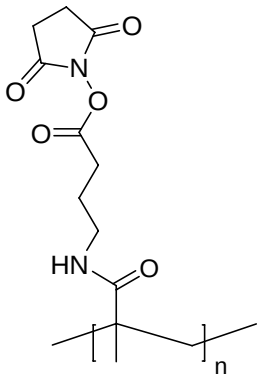

500 mg monomer **3**, 1 mol% AIBN in 3 mL DMF. **Yield**: 45 mg, 9%. **^{1}H-NMR (300 MHz, $DMSO\text{-}d_6$)**: δ (ppm) = 0.99-1.87 (sb, 5H), 1.91-2.65 (sb, 9H), 3.11 (sb, 2H).

Synthesis of polymer P6

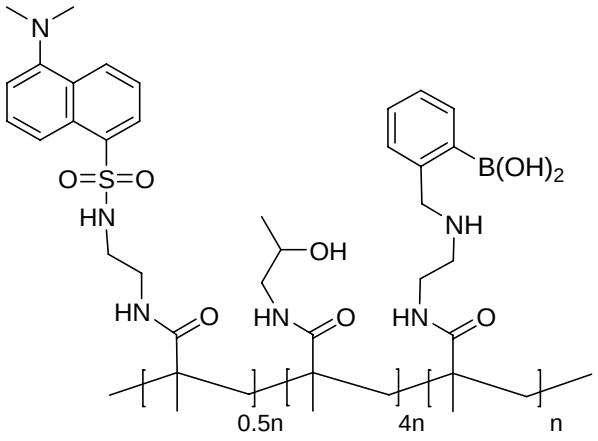

200 mg monomer **3**, 400 mg monomer **8**, 140 mg monomer **11**, 1 mol% AIBN in 5 mL DMF. **Yield**: 495 mg, 67%. **^{1}H-NMR (300 MHz, D_2O)**: δ (ppm) = 0.59 - 1.49 (sb, 14H), 1.50 - 2.10 (sb, 5H), 2.70 - 3.50 (sb, 15H), 3.60 -3.85 (sb, 2H), 3.85 - 4.10 (sb, 1H), 6.93 - 7.51 (sb, 3H), 7.95 - 8.32 (sb, 0.6H). **SEC**: Mw 128530, Mn 51881 (water).

Synthesis of polymer P7

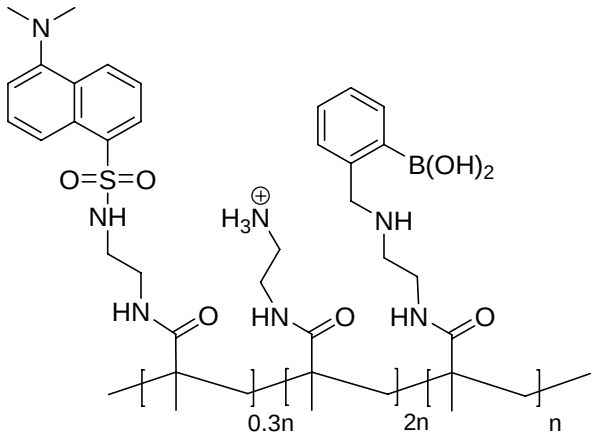

200 mg monomer **6**, 200 mg monomer **3**, 84 mg monomer **11**, 1 mol% AIBN in 5 mL DMF. **Yield**: 180 mg, 37%. **^{1}H-NMR (300 MHz, D_2O)**: δ (ppm) = 0.59 - 1.38 (sb, 10H), 1.45 - 2.22 (sb, 5H), 2.42 - 3.62 (sb, 19H), 3.66 - 4.15 (sb, 2H), 6.80 - 7.50 (sb, 4.4H), 7.95 - 8.32 (sb, 0.5H). **SEC**: Mw 115870, Mn 29665 (water).

Synthesis of polymer P8

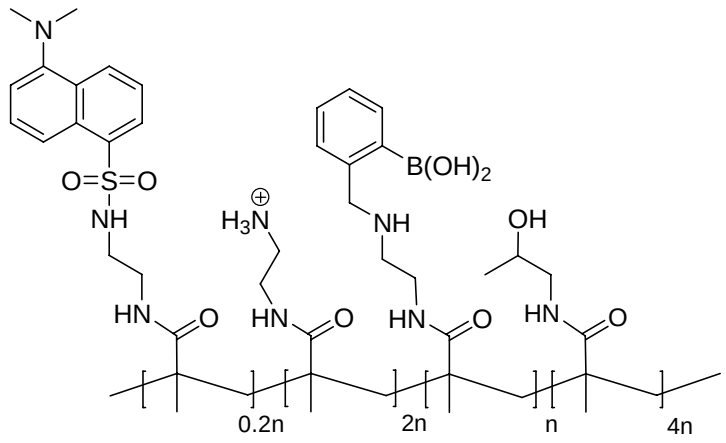

250 mg monomer **6**, 200 mg monomer **3**, 400 mg monomer **8**, 190 mg monomer **11**, 1 mol% AIBN in 8 mL DMF. **Yield**: 426 mg, 41%. **^{1}H-NMR (300 MHz, D_2O)**: δ (ppm) = 0.69 - 1.49 (sb, 16H), 1.50 - 2.25 (sb, 5H), 2.70 - 3.60 (sb, 21H), 3.60 - 3.90 (sb, 2H), 3.95 - 4.15 (sb, 1H), 6.93 - 7.61 (sb, 3.6H), 7.95 - 8.32 (sb, 0.6H). **SEC**: Mw 126400, Mn 49028 (water).

Synthesis of polymer P9

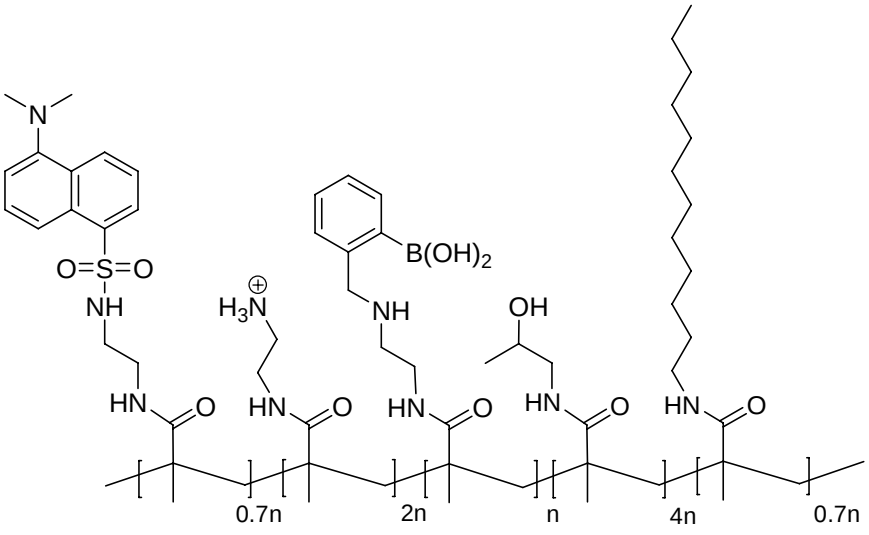

250 mg monomer **6**, 200 mg monomer **3**, 400 mg monomer **8**, 190 mg monomer **9**, 250 mg monomer **11**, 1 mol% AIBN in 10 mL DMF. **Yield**: 1006 mg, 78%. **^{1}H-NMR (300 MHz, DMSO-d_6)**: δ (ppm) = 0.81 - 2.25 (sb, 39H), 2.88 (sb, 21H), 3.64 (sb, 2H), 3.85 (sb, 1H), 7.13 - 7.71 (sb, 4H), 8.01 - 8.42 (sb, 0.7H).

Synthesis of polymer P10

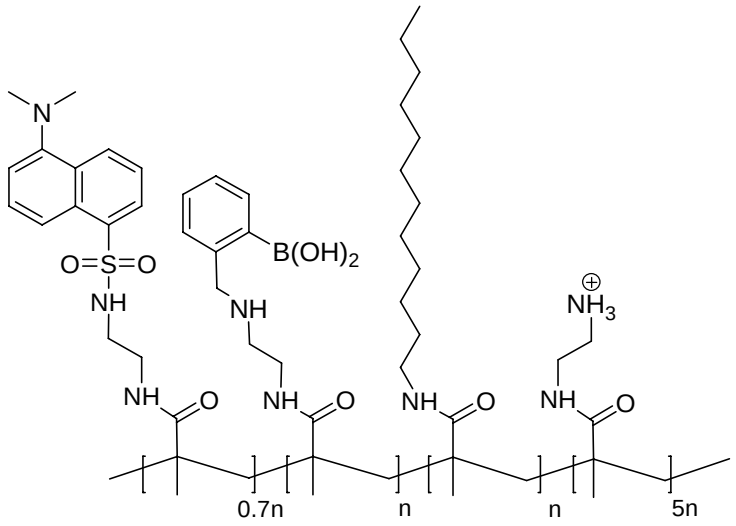

130 mg monomer **6**, 450 mg monomer **3**, 130 mg monomer **9**, 70 mg monomer **11**, 1 mol% AIBN in 3 mL DMF and 2 mL MeOH. **Yield**: 430 mg, 55%. **^{1}H-NMR (300 MHz, D_2O)**: δ (ppm) = 0.88 - 1.61 (sb, 29H), 2.63-3.23 (m, 31H), 3.85 (sb,2H), 6.98-7.51 (m, 4H), 8.09-8.46 (m, 3.5H). **SEC**: Mw 52983, Mn 51563 (water).

Synthesis of polymer P11

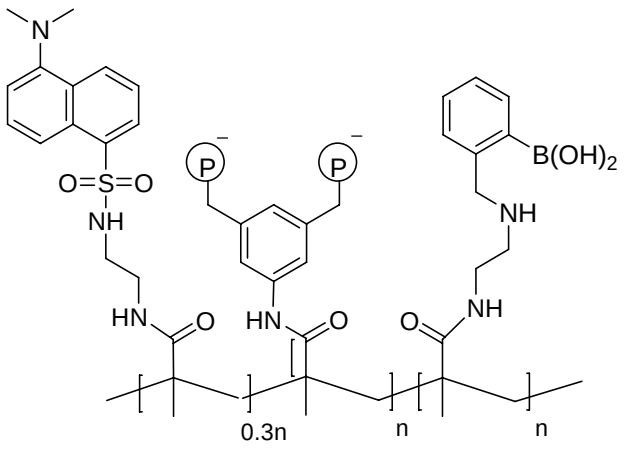

232 mg monomer **1**, 150 mg monomer **6**, 206 mg monomer **11**, 1 mol% AIBN in 4 mL DMF for polymerization and post dealkylation in acetonitrile. **Yield**: 95 mg, 16%. **^{1}H-NMR (300 MHz, D_2O)**: δ (ppm) = 1.12 (sb), 1.95 (sb), 2.81-3.18 (m), 3.62 (sb), 3.93 (sb), 6.99-7.43 (m), 8.14-8.48 (m).

Synthesis of polymer P12

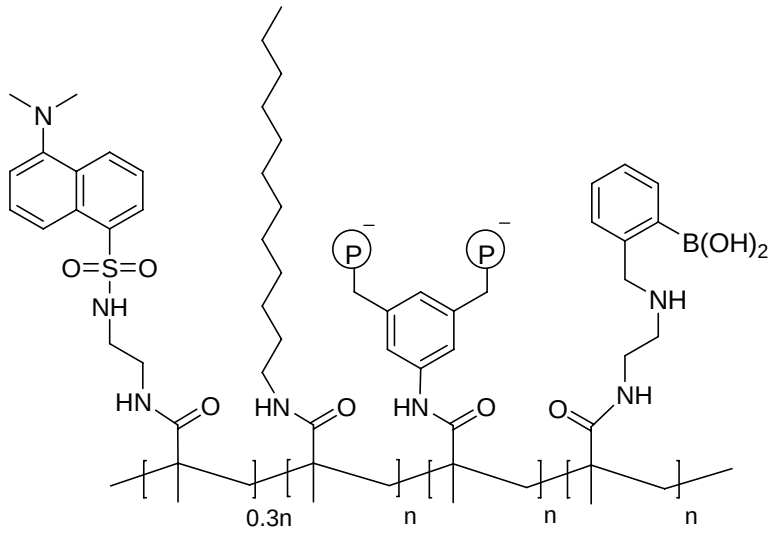

385 mg monomer **1**, 250 mg monomer **6**, 240 mg monomer **9**, 34.3 mg monomer **11**, 1 mol% AIBN in 6 mL DMF for poylmerization and post dealkylation in acetonitrile.**Yield**: 120 mg, 13%. **^{1}H-NMR (300 MHz, D_2O)**: δ (ppm) = 0.80-1.15 (m), 2.50-3.55 (m), 6.70-7.80 (m).

Synthesis of polymer P13

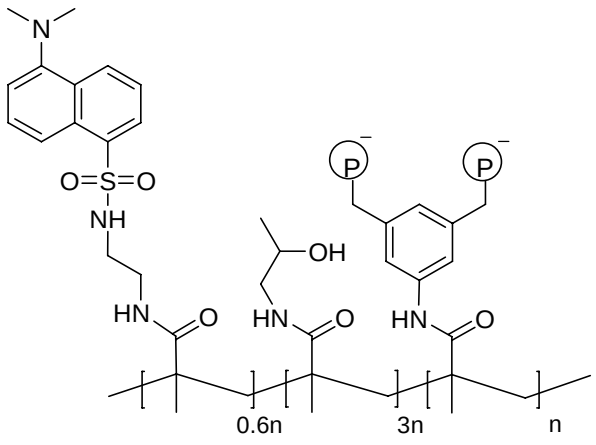

540 mg monomer **3**, 500 mg monomer **8**, 330 mg monomer **11**, 1 mol% AIBN in 8 mL DMF for polymerization and post dealkylation in acetonitrile. **Yield**: 260 mg, 19%. **^{1}H-NMR (300 MHz, D_2O)**: δ (ppm) = 1.10 (sb), 1.98 (sb), 2.98 (sb), 3.50 (sb), 3.88 (sb), 7.07 (sb), 8.18 (sb). **SEC**: Mw 92210, Mn 10076 (water).

Synthesis of polymer P14

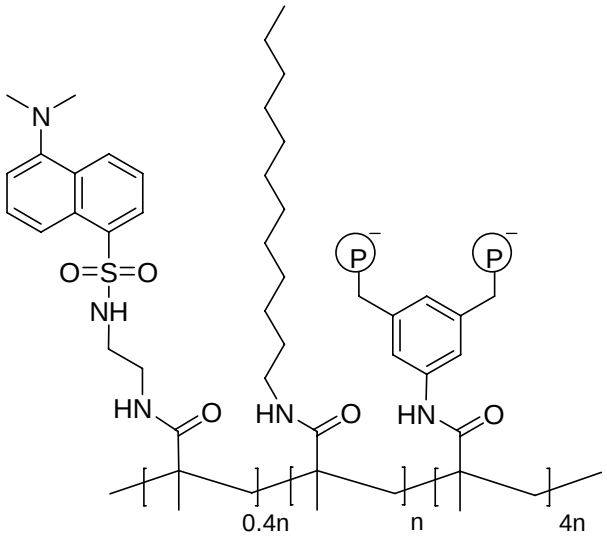

533 mg monomer **1**, 100 mg monomer **9**, 50 mg monomer **11**, 1 mol% AIBN in 4 mL DMF and post dealkylation in acetonitrile. **Yield**: 485 mg, 71%. **^{1}H-NMR (300 MHz, D_2O)**: δ (ppm) = 0.84-2.0 (m), 3.23 (sb), 3.66 (sb), 3.80 (sb), 6.97-7.57 (m), 8.14-8.52 (m). **SEC**: Mw 99805, Mn 23770 (water).

Synthesis of polymer P15

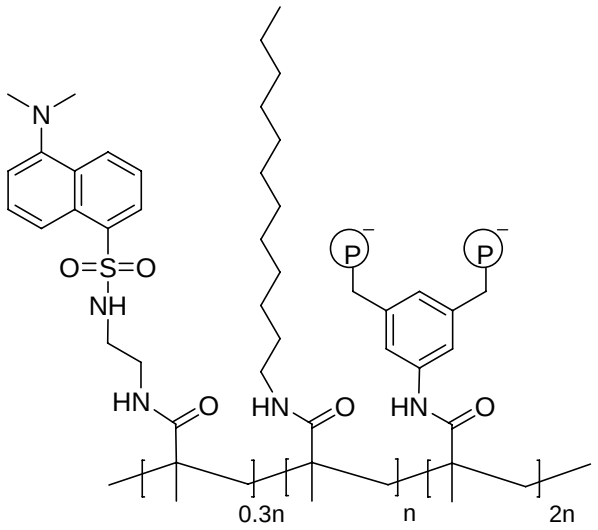

440 mg monomer **1**, 500 mg monomer **9**, 230 mg monomer **11**, 1 mol% AIBN in 8 mL DMF and post dealkylation in acetonitrile. **Yield**: 106 mg, 9%. **^{1}H-NMR (300 MHz, D_2O)**: δ (ppm) = 0.84-2.0 (m), 3.23 (sb), 3.66 (sb), 3.80 (sb), 6.97-7.57 (m), 8.14-8.52 (m). **SEC**: Mw 74459, Mn 26552 (water).

Synthesis of polymer P16

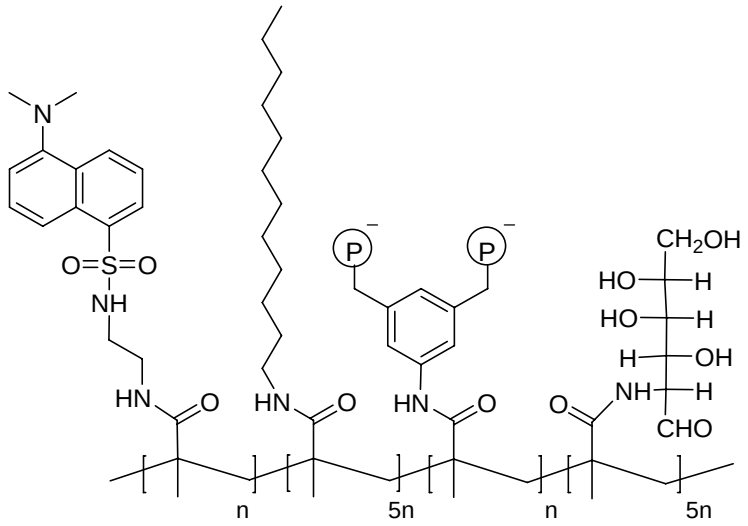

113 mg monomer **1**, 350 mg monomer **7**, 350 mg monomer **9**, 100 mg monomer **11**, 1 mol% AIBN in 8 mL DMF and post dealkylation in acetonitrile. **Yield**: 130 mg, 14%. **^{1}H-NMR (300 MHz, CD_3OD)**: δ (ppm) = 0.90 (sb, 10H), 1.29 (sb, 66H), 1.48 (sb, 6H), 1.92 (sb, 11H), 2.80-3.50 (sb, under the signal from DMF and MeOD), 7.03-7.59 (m, 6H), 8.22-8.75 (m, 2H).

Synthesis of polymer P17

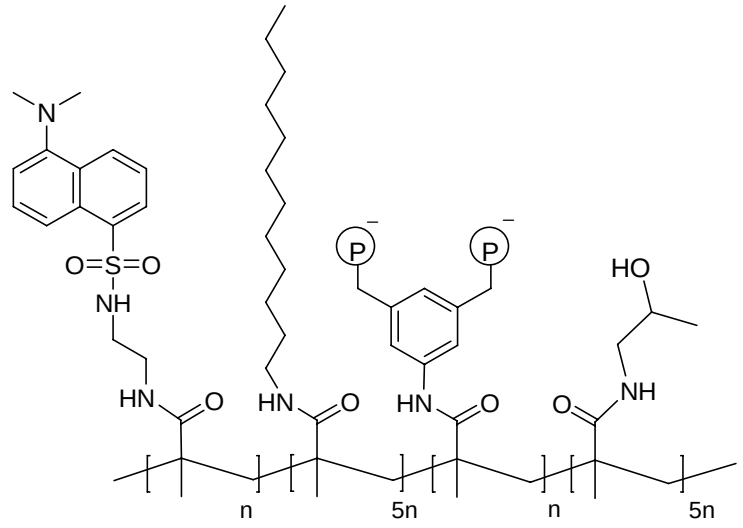

140 mg monomer **1**, 250 mg monomer **8**, 450 mg monomer **9**, 100 mg monomer **11**, 0.6 mol% AIBN in 8 mL DMF and post dealkylation in acetonitrile. **Yield**: 180 mg, 19%. **^{1}H-NMR (300 MHz, D_2O)**: δ (ppm) = 1.22 (m), 2.04 (sb), 2.95 (sb), 3.43-3.57 (m), 7.03 (sb), 7.91-8.44 (m). **SEC**: Mw 27618, Mn 8072 (water).

Synthesis of polymer P19

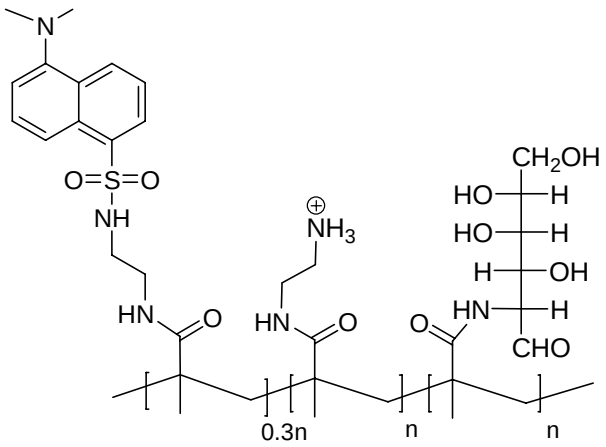

400 mg monomer **3**, 206 mg monomer **7**, 100 mg monomer **11**, 0.7 mol% AIBN in 4 mL. DMF. **Yield**: 140 mg, 22%. **^{1}H-NMR (300 MHz, D_2O)**: δ (ppm) = 0.98-2.06 (m, 18H), 3.14 (sb, 5H), 3.44 (sb, 6H), 7.33-7.76 (m, 2H), 7.33-7.76 (m, 0.3H).

Synthesis of polymer P20

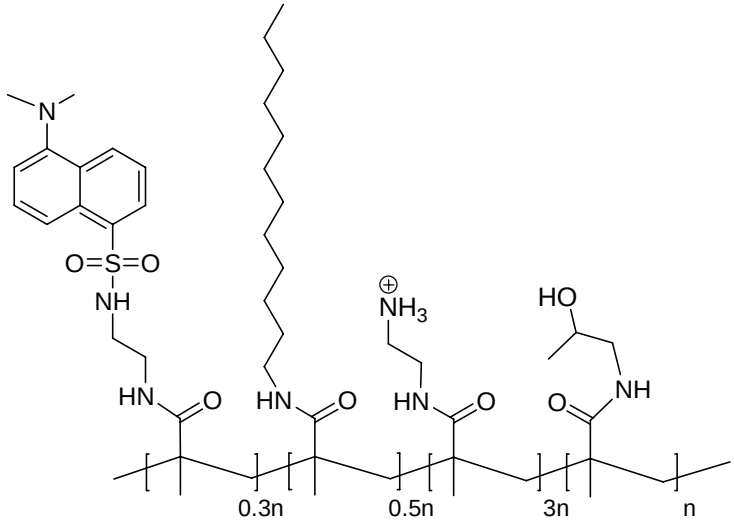

500 mg monomer **3**, 150 mg monomer **8**, 135 mg monomer **9**, 100 mg monomer **11**, 1.3 mol% AIBN in 2 mL DMF and 2 mL methanol. **Yield**: 71 mg, 8%. **^{1}H-NMR (300 MHz, D_2O)**: δ (ppm) = 0.95-1.90 (m, 34H), 2.85-3.29 (m, 12H), 3.91 (sb, 1H), 7.71-8.52 (m, 2H). **SEC**: Mw 231690, Mn 117840 (water).

6.2.5 Synthesis of molecular imprinting polymers

A general procedure to prepare MIPs was: with the assistance of a pipetting robot (Figure 6.1), the polymerization was done with the recipe showed in table 4-17, by pipetting degassed stock solutions to the wells of a PTFE 96-well microtiter plate covered with a silicone rubber sealing mat in a sequence of templates, functional monomers, mixture of crosslinker and comonomer, initiator, and porogen. In the case of monomer **5** in the plate P2, same equivalent of $NiSO_4 \cdot 6H_2O$ as the template **T3** was added into the wells from positions G1 to G6 directly after the addition of **T3**. Each pipetting step was accompanied by 5 seconds degassing with argon. Afterwards the microplates were sealed with Viton rings and PTFE covers and then heated in the oven for 24 h at 50 ºC. After polymerization the polymers were transferred to a 96-well filter plate, ready for washing and rebinding.

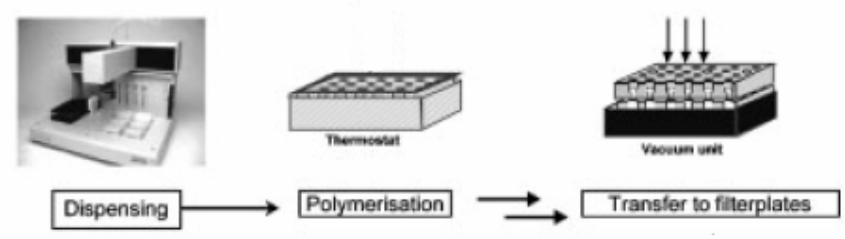

Figure 6.1 *Schematic preparation of MIPs on a 96 well microplate.*

6.3 Binding study

6.3.1 NMR study

Example: NMR study between D-glucosamine 2-sulfate sodium salt and 1:1 aggregate from phenylboronic acid and piperidine

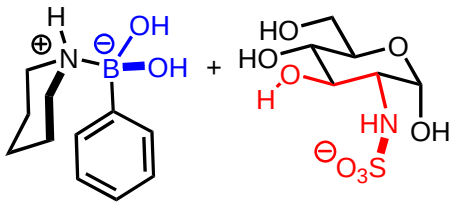

3.21 mg piperidine and 4.60 mg phenyl boronic acid were dissolved in 3.5 mL D_2O as a host solution (1.077 mM). 20 mg D-glucosamine 2-sulfate sodium salt was disolved in 0.5 mL of above solution as the guest solution (14.22 mM). 27 µL (0.5 eq), 53 µL (1 eq), 80 µL (1.5 eq) and 106 µL (2 eq) of the guest solution was added into four NMR tubes filled with 700 µL of the host solution seperately. A new set of signal from the *ortho*-proton of the phenyl boronic acid indicated the formation of the complex.

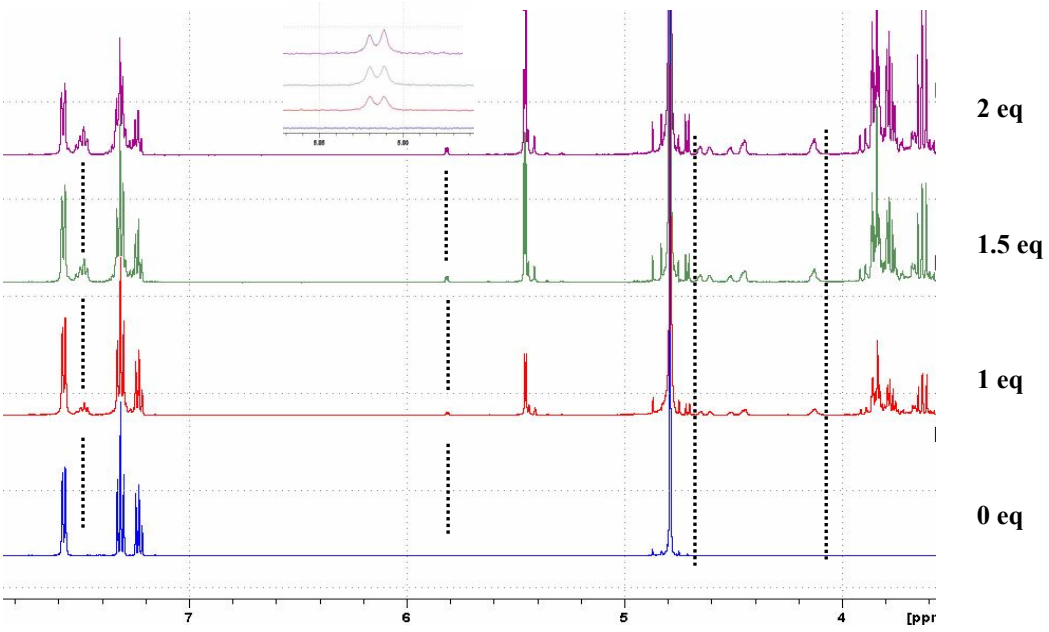

Figure 6.2 *^{1}H NMR spectra of adding glucosamine 2-sulfate sodium salt into 1:1 complex of phenyl boronic acid and piperidine. New sets of signals appear for the*

protons of the host (a) and the guest (b). In the region from 4 – 4.6 ppm, there are also several sets of new signals from the guest.

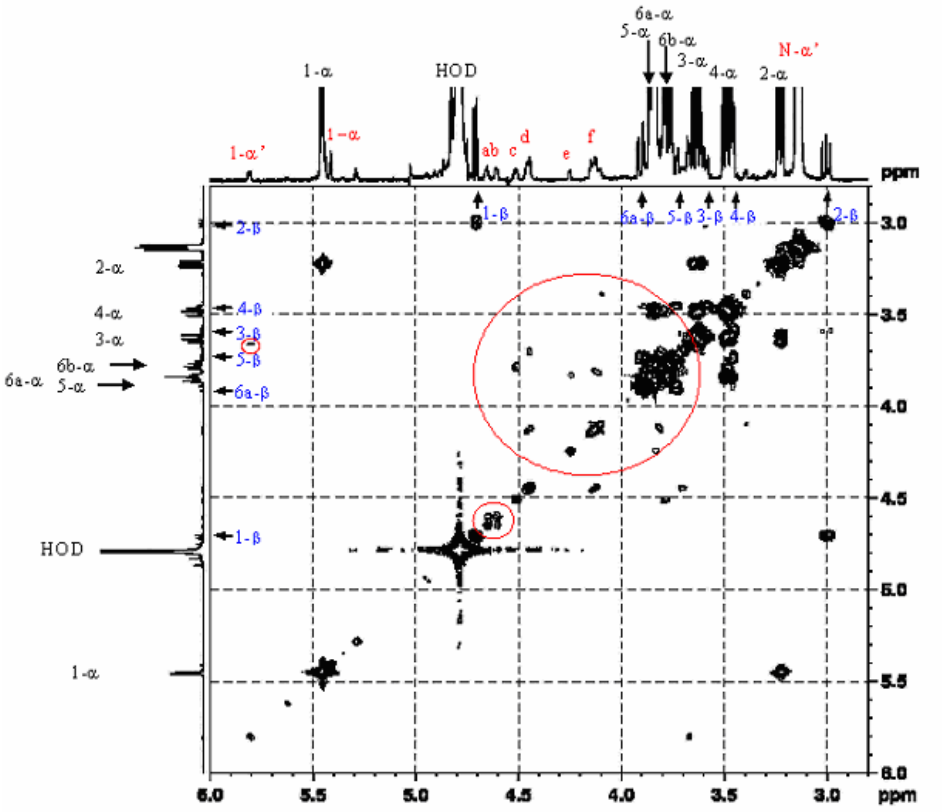

Figure 6.3 *Gs-COSY 90 spectrum of adding 1 eq. of glucosamine 2-sulfate sodium salt into 1:1 complex of phenyl boronic acid and piperidine.*

In the gs-COSY spectrum of 1:1 compex, the new anomeric proton was shifted downfield by 0.4 ppm to 5.8 ppm and couples with a CH proton at 3.7 ppm. This could be the new C-2 in its complex with phenylboronic acid, which was hence also shifted downfield by 0.4 ppm to 3.7 ppm. Several new complex signals also appeared in the region from 4.1-4.7 ppm. They showed couplings among themselves (such as *d/f* ~ 4.4 ppm / 4.1 ppm), and most important, to unshifted CH protons of the sugar (such as *f/6* ~ 4.1 ppm / 3.8 ppm). This might be an indication for the fact, that cyclic esters were formed between all neighboring carbons bearing either free hydroxyls or sulfates. New potential protons could be detected at 5.41 and 5.44 ppm, but they were singlets, suggesting, e.g., deuterium exchange at C-2 with D2O, initiated by free piperidine base. Two new shifted CH protons *a* and *b* displayed a roof effect, and showed mutual crosspeaks in the COSY. However, the HMQC spectrum revealed that they are not shifted diastereotopic methylene protons at C-6, because they belonged to 2 different carbon atoms at 74 and 79 ppm, which was indeed in the range of C-3 to C-5. The large dd at 3.15 ppm could be attributed to the methylene group in piperidine.

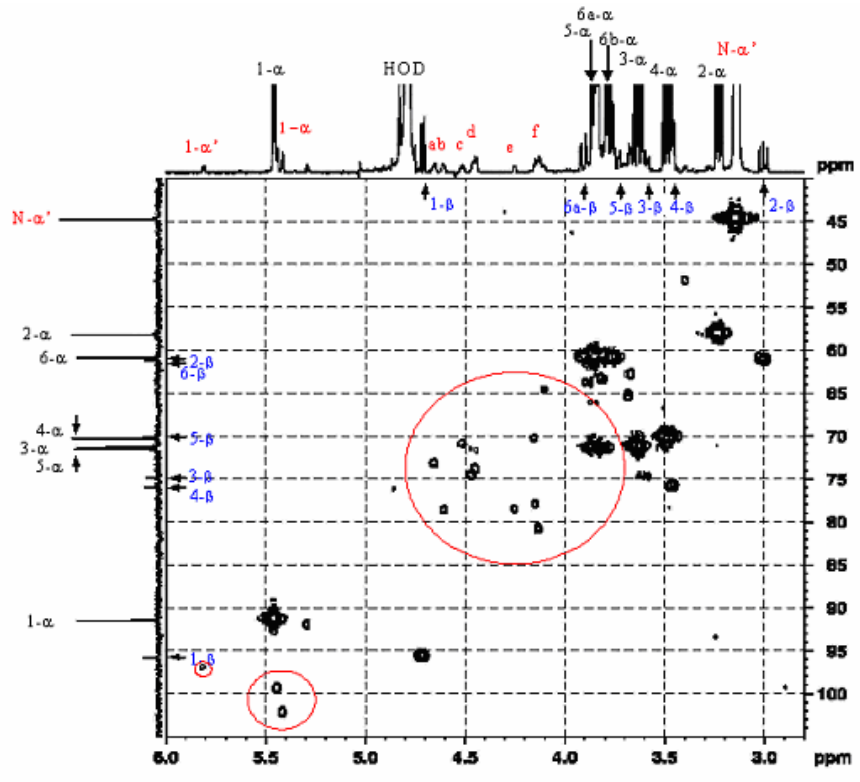

Figure 6.4 *Gs-HMQC spectrum of adding 1 eq. of glucosamine 2-sulfate sodium salt into 1:1 complex of phenyl boronic acid and piperidine*

In the gs-HMQC spectrum of the1:1 complex we find several of the above assumptions confirmed. New singlets NMR signals around the anomeric proton (5.41 and 5.44 ppm) originated from carbon signals in the close vicinity of anomeric proton (100 and 103 ppm). It is thus very likely, that these belong to boronic acid esters, which do not involve the anomeric carbon. The new shifted C-1 (α') in fact showed a small, but distinct crosspeak to a shifted C-1 carbon signal at 97 ppm. The two downfield-shifted proton signals *a* and *b* had already been mentioned above. Several new crosspeaks for *c-f* are found at 70-81 ppm, slightly highered by 1-10 ppm than the original values for C-3 to C-5. Most likely, these were therefore protons attached to these carbons, involved in cyclic boronate ester formation. Unfortunately, we couldn't assign complete sets of signals to all these shifted species, because there were too many of them, with too many "missing links". We therefore summarized, that cyclic esters were formed between hydroxyls and sulfate ions from the sugar, producing new sets of signals with marked downfield shifts. At least the one involving the anomeric proton was characterized. Several effects, however, couldn't be explained at this level and remained unclear.

6.3.2 Fluorescence titration

A general procedure was: a solution of the polymer/dendrimer was prepared in aqueous hepes buffer (25 mM, pH 7.1). The protein or glucan stock solutions were prepared by dissolving them in above solution to guarantee a constant polymer/dendrimer concentration during the entire titration. The polymer/dendrimer solution was filled into a stirrable cuvette and the protein/glucan solution was added stepwise. The samples were excited at a wavelength of 330 nm and the change of the emission intensity at about 510 nm was recorded. For the determination of the stoichiometry, the concentration of the polymer was multiplied with a virtual correction factor, until the Job-Plot[144] showed a 1:1 complex stoichiometry. Binding constants were calculated by non-linear regression methods[145] by a Sigma-Plot program for a 1:1 stoichiometry with the corrected concentrations of the polymer so that an optimal fit was produced. (Non-linear curve fitting with the original uncorrected concentrations gave only small deviations in the binding constant values but increased error values). In seveal cases, the 1:2 or 2:1 complex was evaluated by a WinEQNMR program in order to get a better fitting than the corrected 1:1 case, and to get a better understanding about the binding events.

Example 1. Trypsin vs. fluorescence labeled octamer

$C_{octamer} = 4.80\times10^{-6}$ mol/l, $C_{trypsin} = 1.02\times10^{-4}$ mol/l

$K_{a\,(1:1)} = 1.14\times10^{6}\ M^{-1} \pm 27\ \%$

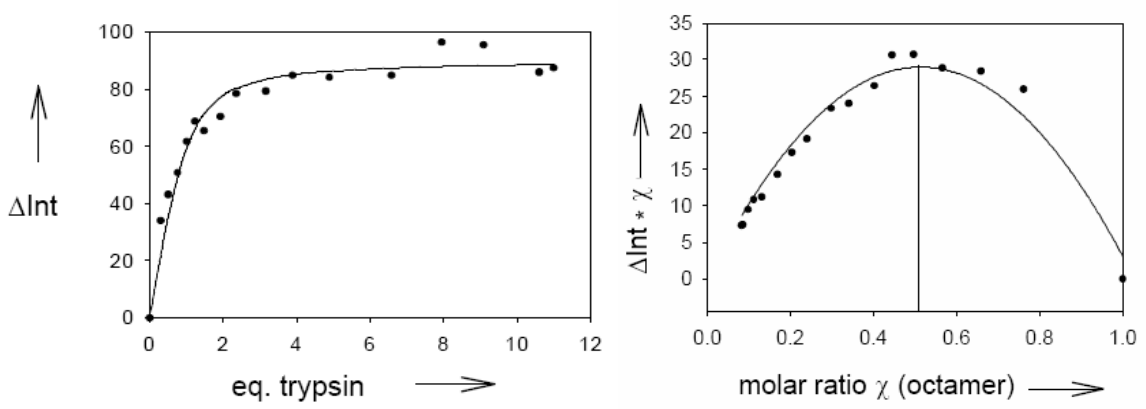

Example 2. Trypsin vs. fluoresence labeled hexadecamer

$C_{Hexadecamer} = 2.93\times10^{-6}$ mol/l, $C_{trypsin} = 1.63\times10^{-4}$ mol/l

$K_{a\,(1:1)} = 1.83\times10^{6}\ M^{-1} \pm 27\ \%$

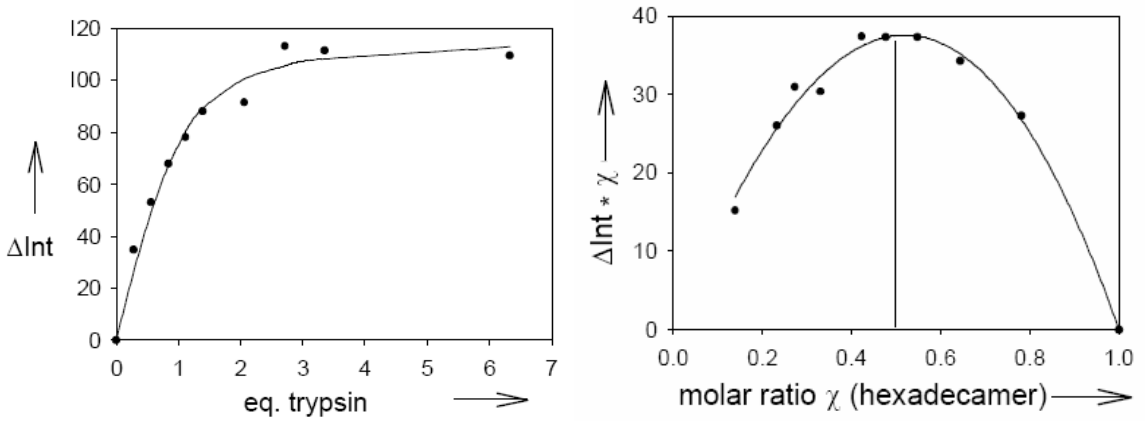

Example 3. Histone (type H1, lysine-rich) vs fluorescence labeled octamer

$C_{octamer} = 4.80\times10^{-6}$ mol/l, $C_{histone} = 2.54\times10^{-4}$ mol/l

$K_{a\,(1:1)} = 1.21\times10^{6}\ M^{-1} \pm 16\ \%$

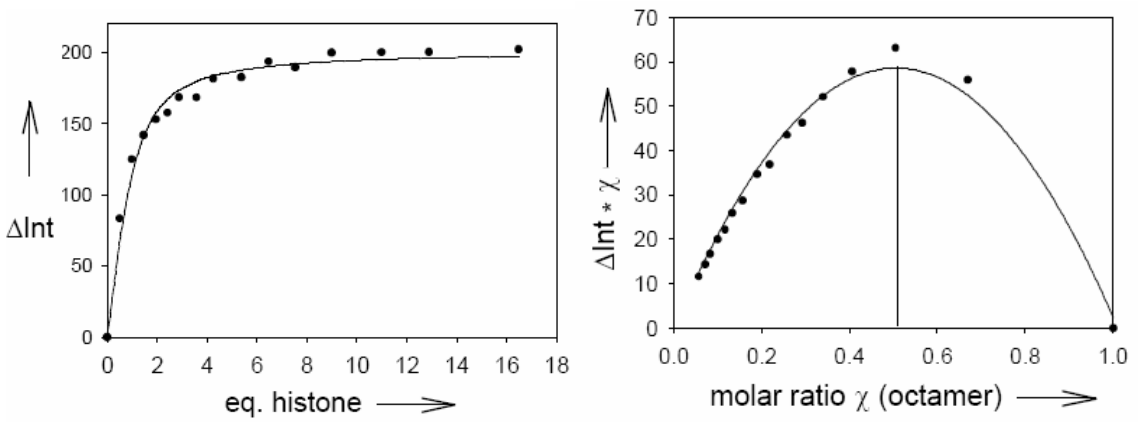

Example 4. Histone (type H3, Arginine-rich) vs. fluorescence labeled octamer

$C_{octamer} = 2.58\times10^{-6}$ mol/l, $C_{histone} = 3.17\times10^{-5}$ mol/l

$K_{a\,(1:2)} = 1.27\times10^{5}\ M^{-1} \pm 6\ \%$

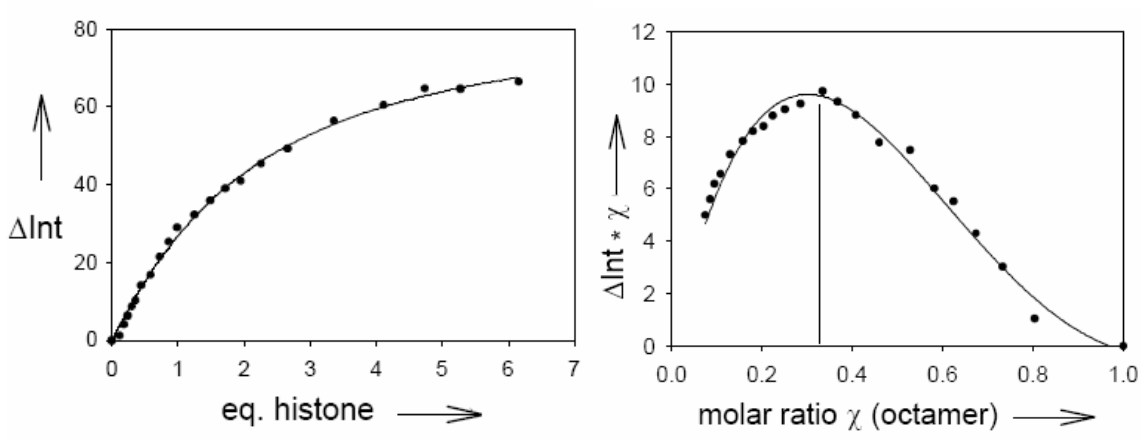

Example 5. Histone (type H3, Arginine-rich) vs. fluorescence labeled octamer 1:2 complex evaluated by WinEQNMR

$C_{octamer} = 2.58\times10^{-6}$ mol/l, $C_{histone} = 3.17\times10^{-5}$ mol/l

$K^1 = 1.43\times10^5\ M^{-1}$, $K^2 = 4.23\times10^3\ M^{-1}$, $K^1\ K^2 = 6.05\times10^8\ M^{-2}$

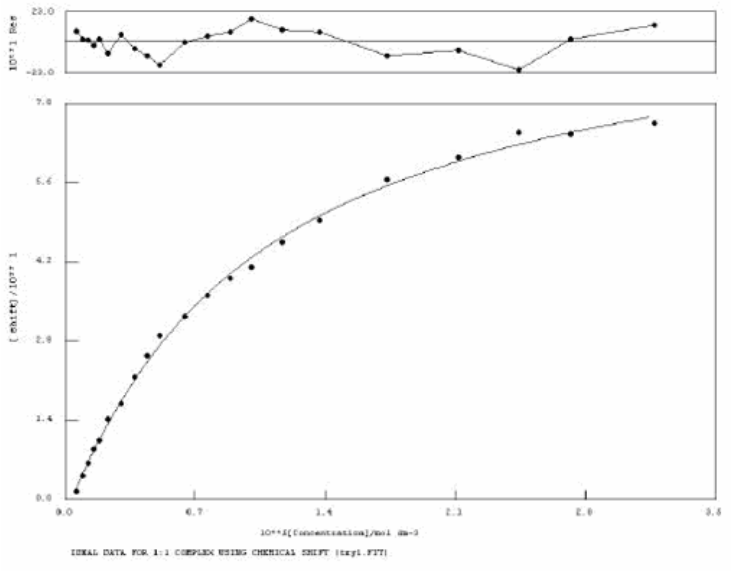

Example 6. Histone (type H3, Arginine-rich) vs. fluorescence labeled hexadecamer 1:2 complex evaluated by WinEQNMR

$C_{octamer} = 5.86\times10^{-6}$ mol/l, $C_{histone} = 6.18\times10^{-5}$ mol/l

$K^1 = 4.78\times10^5\ M^{-1}$, $K^2 = 1.45\times10^3\ M^{-1}$, $K^1\ K^2 = 6.94\times10^8\ M^{-2}$

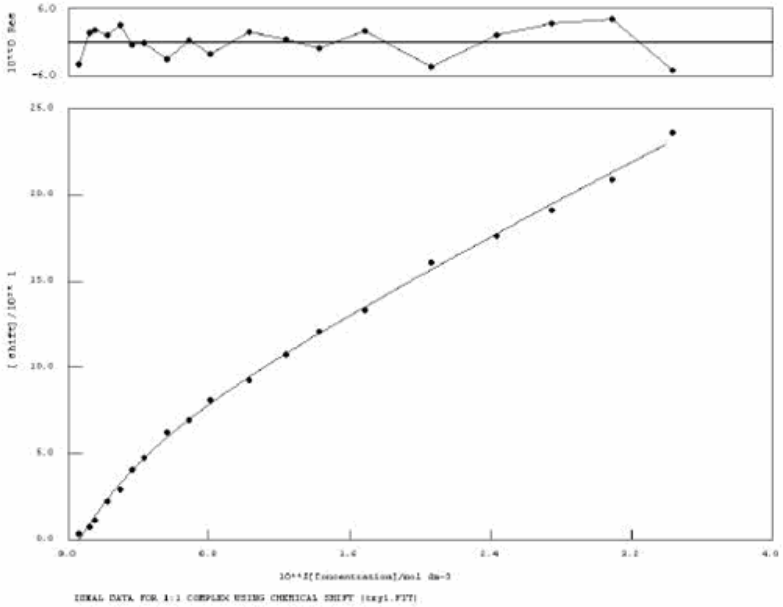

Example 7. Polymer P7 vs. dextran

$C_{polymer} = 4.32\times10^{-6}$ mol/l, $C_{dextran} = 1.31\times10^{-4}$ mol/l

$Ka_{(1:2)} = 3.0\times10^{3}$ M^{-1} ± 37%

$C_{polymer}$ [mol/l]	$C_{polymer}$ (corrected) [mol/l]	$C_{dextran}$ [mol/l]	ratio C_p/C_d	fluorescent intensity at 520 nm	relative intensity change
4,32E-06	8,63E-06	0,00E+00	0,00	305,90	0,00
4,32E-06	8,63E-06	5,24E-07	0,12	300,24	5,66
4,32E-06	8,63E-06	2,58E-06	0,60	294,38	11,52
4,32E-06	8,63E-06	5,06E-06	1,17	287,85	18,05
4,32E-06	8,63E-06	9,74E-06	2,26	277,14	28,76
4,32E-06	8,63E-06	1,41E-05	3,26	270,51	35,39
4,32E-06	8,63E-06	2,19E-05	5,08	253,24	52,66
4,32E-06	8,63E-06	3,03E-05	7,03	232,02	73,88
4,32E-06	8,63E-06	3,76E-05	8,70	204,71	101,19
4,32E-06	8,63E-06	4,93E-05	11,42	171,66	134,24
4,32E-06	8,63E-06	5,84E-05	13,54	157,30	148,60
4,32E-06	8,63E-06	7,17E-05	16,62	135,19	170,71
4,32E-06	8,63E-06	8,09E-05	18,75	118,44	187,46

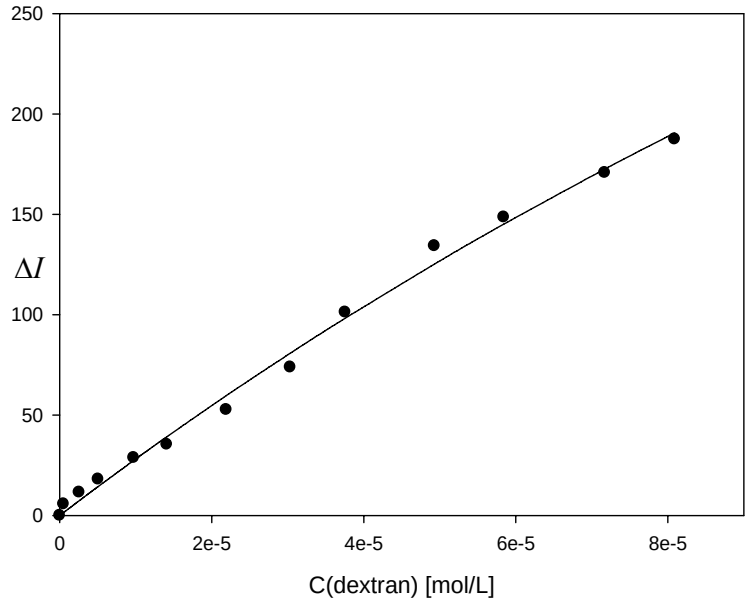

Example 8. Polymer P7 vs. hyaluronic acid

$C_{polymer} = 4.03\times10^{-6}$ mol/l, $C_{hyluronate} = 4.07\times10^{-4}$ mol/l

$Ka_{(1:5)} = 1.6\times10^{3}$ M^{-1} ± 40%

$C_{polymer}$ [mol/l]	$C_{polymer}$ (corrected) [mol/l]	$C_{hyluronate}$ [mol/l]	ratio C_p/C_h	fluorescent intensity at 520 nm	relative intensity change
4,03E-06	2,01E-05	0,00E+00	0,00	400,10	0,00
4,03E-06	2,01E-05	1,62E-06	0,08	401,22	1,12
4,03E-06	2,01E-05	3,23E-06	0,16	405,20	5,10
4,03E-06	2,01E-05	6,41E-06	0,32	407,27	7,17
4,03E-06	2,01E-05	7,98E-06	0,40	410,20	10,10
4,03E-06	2,01E-05	1,57E-05	0,78	420,36	20,26
4,03E-06	2,01E-05	2,30E-05	1,14	431,59	31,49
4,03E-06	2,01E-05	3,70E-05	1,84	453,21	53,11
4,03E-06	2,01E-05	6,79E-05	3,37	480,48	80,38
4,03E-06	2,01E-05	1,16E-04	5,78	520,36	120,26
4,03E-06	2,01E-05	1,53E-04	7,58	550,15	150,05
4,03E-06	2,01E-05	1,81E-04	8,99	590,36	190,26

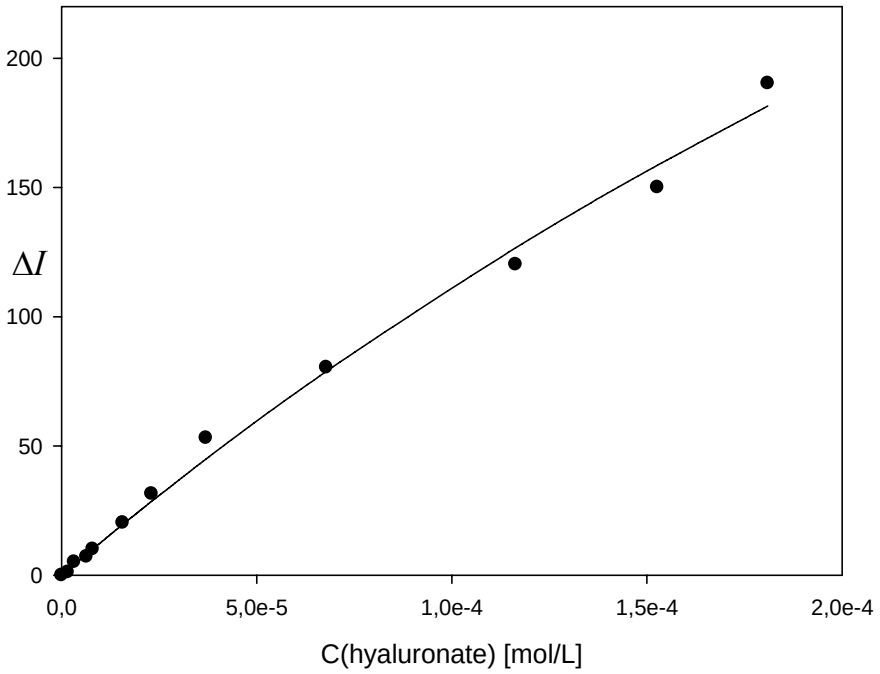

Example 9. Polymer P7 vs. chondrotin

$C_{polymer} = 2.10\times10^{-7}$ mol/l, $C_{chondroitin} = 1.46\times10^{-4}$ mol/l

$Ka_{(1:5)} = 5.8\times10^{6}$ M^{-1} ± 33%

$C_{polymer}$ [mol/l]	$C_{polymer}$ (corrected) [mol/l]	$C_{chondroitin}$ [mol/l]	ratio C_p/C_c	fluorescent intensity at 520 nm	relative intensity change
2,10E-07	1,05E-06	0,00E+00	0,00	582,12	0,00
2,10E-07	1,05E-06	5,71E-07	0,54	618,63	36,51
2,10E-07	1,05E-06	1,14E-06	1,08	656,22	74,10
2,10E-07	1,05E-06	1,70E-06	1,62	664,82	82,70
2,10E-07	1,05E-06	2,26E-06	2,15	663,47	81,35
2,10E-07	1,05E-06	3,63E-06	3,46	675,36	93,24
2,10E-07	1,05E-06	6,30E-06	6,00	689,59	107,47
2,10E-07	1,05E-06	1,14E-05	10,80	681,44	99,32

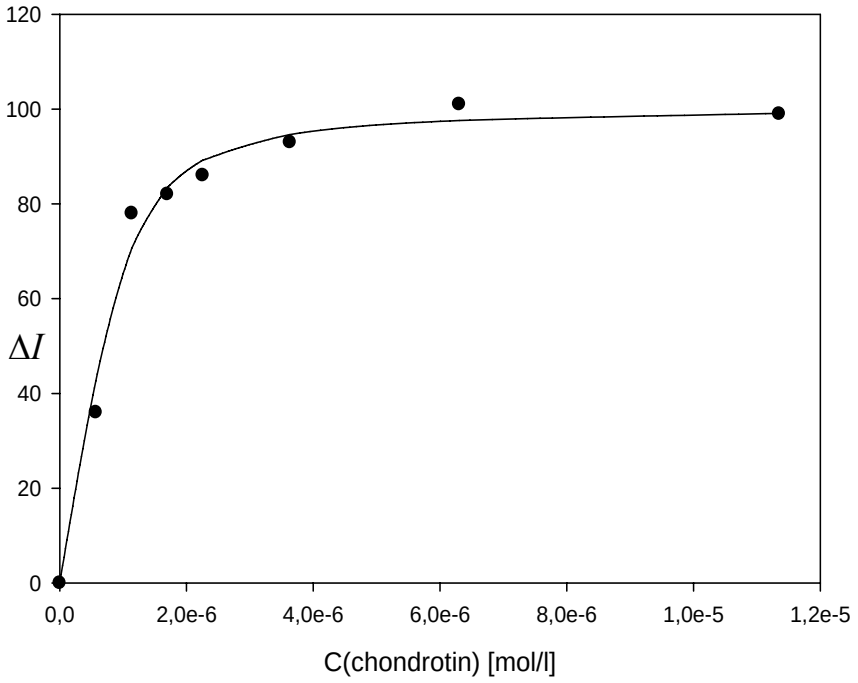

Example 10. Polymer P7 vs. heparin

$C_{polymer}$ = 1.57×10^{-7} mol/l, H_{eparin} =1.47×10^{-5} mol/l

$Ka_{(1:5)}$ = 2.8×10^{7} M

$C_{polymer}$ [mol/l]	$C_{polymer}$ (corrected) [mol/l]	H_{eparin} [mol/l]	ratio C_p/C_h	fluorescent intensity at 520nm	relative intensity change
3,14E-08	1,57E-07	0,00E+00	0,00	224,23	0,00
3,14E-08	1,57E-07	3,67E-08	0,23	218,34	5,89
3,14E-08	1,57E-07	7,32E-08	0,47	212,49	11,74
3,14E-08	1,57E-07	1,09E-07	0,70	206,73	17,50
3,14E-08	1,57E-07	1,46E-07	0,93	190,86	33,37
3,14E-08	1,57E-07	1,82E-07	1,16	180,61	43,62
3,14E-08	1,57E-07	2,71E-07	1,72	176,42	47,81
3,14E-08	1,57E-07	3,59E-07	2,28	171,34	52,89
3,14E-08	1,57E-07	5,32E-07	3,39	172,75	51,48
3,14E-08	1,57E-07	8,65E-07	5,51	170,86	53,37
3,14E-08	1,57E-07	1,63E-06	10,41	169,93	54,30
3,14E-08	1,57E-07	2,94E-06	18,74	171,17	53,06

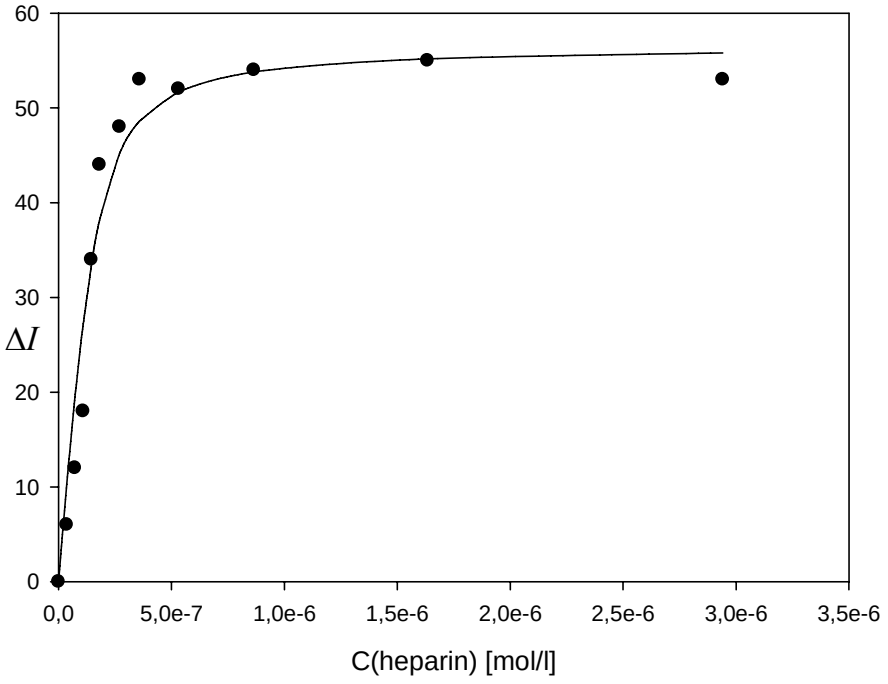

Example 11. Polymer P7 vs. ovalbumin

$C_{polymer} = 2.0\times10^{-7}$ mol/l, $C_{ovalbumin} = 2.93\times10^{-5}$ mol/l

$Ka_{(1:2)} = 1.1\times10^{6}$ M^{-1} ± 7%

$C_{polymer}$ [mol/l]	$C_{polymer}$ (corrected) [mol/l]	$C_{ovalbumin}$ [mol/l]	ratio C_p/C_o	fluorescent intensity at 520 nm	relative intensity change
2,00E-07	6,00E-07	0,00E+00	0,00	369,49	0,00
2,00E-07	6,00E-07	1,46E-07	0,24	353,78	15,71
2,00E-07	6,00E-07	2,90E-07	0,48	344,89	24,60
2,00E-07	6,00E-07	4,32E-07	0,72	320,40	49,09
2,00E-07	6,00E-07	7,14E-07	1,19	294,39	75,11
2,00E-07	6,00E-07	1,06E-06	1,76	277,20	92,29
2,00E-07	6,00E-07	1,39E-06	2,32	264,81	104,68
2,00E-07	6,00E-07	2,66E-06	4,43	232,96	136,54
2,00E-07	6,00E-07	3,82E-06	6,36	224,73	144,77
2,00E-07	6,00E-07	4,88E-06	8,13	204,69	164,80
2,00E-07	6,00E-07	5,85E-06	9,75	196,81	172,68
2,00E-07	6,00E-07	7,98E-06	13,30	191,90	177,59
2,00E-07	6,00E-07	1,13E-05	18,76	187,83	181,66
2,00E-07	6,00E-07	1,37E-05	22,76	188,10	181,39
2,00E-07	6,00E-07	1,55E-05	25,82	187,00	182,49

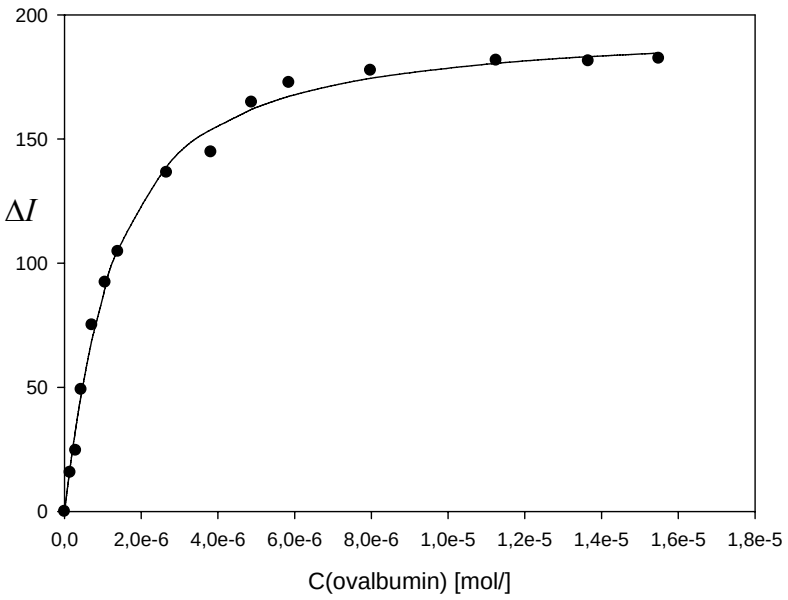

6.3.3 ITC titration

ITC titrations were performed with micro-calorimeter VP-ITC at 25 ºC. The initial volume of the solution in the cell was 1.4211 mL. 10 mM Hepes (PH 7) was used as the buffer. In all the titrations, protein solutions were used as hosts in the cell and polymer/microgel solutions as ligands. The dilution effect of the polymer/microgel was measured as a reference and subtracted from the titrations before evaluating the binding contants. In most cases the incorporated evaluation method “one set of sites” was used, and in some cases the “sequential binding with 2 sites” was used in order to get a good fitting.

Example 1.

MG-Met vs Cytochrome C

Cyto / MG-met = 680

K = 1.16E8±28% M^{-1}

ΔH = 1.04E5±16% kcal M^{-1}

ΔS = 3.50E2 kcal M^{-1} K^{-1}

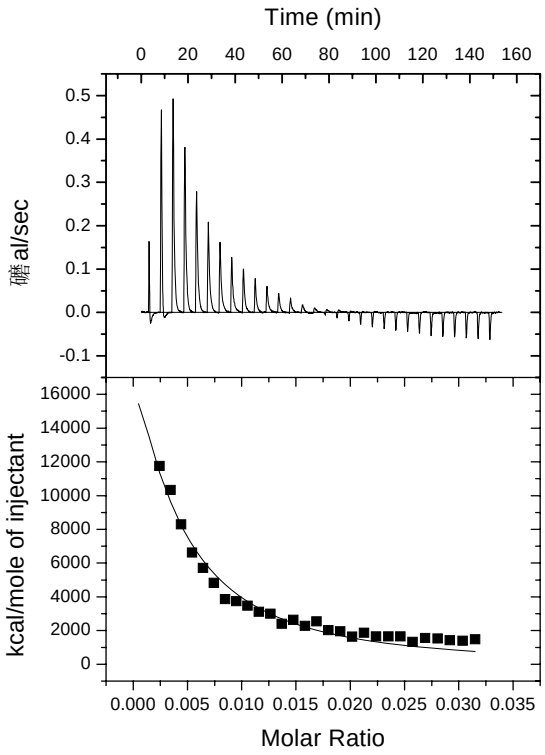

Example 2.

MG-B vs Cytochrome C

Cyto/ MG-B = 1.5E04

K = 3.24E9±31% M^{-1}

ΔH = 1.60E6±46% kcal M^{-1}

ΔS = 5.37E3 kcal M^{-1} K^{-1}

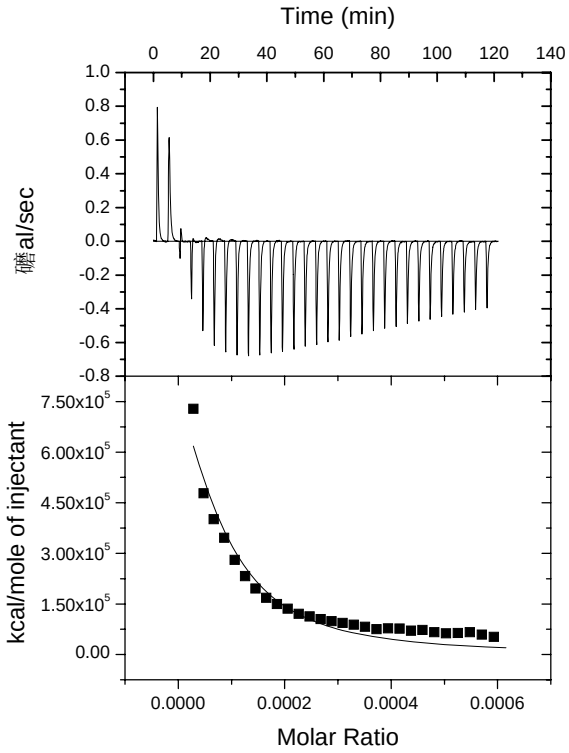

Example 3.

MG-Tet vs Hemoglobin

Hemo/MG-Tet = 1.6E4

K = 3.06E8 ± 22% M^{-1}

ΔH = 7.12E5 ± 9% kcal M^{-1}

ΔS = 2.39E3 kcal M^{-1} K^{-1}

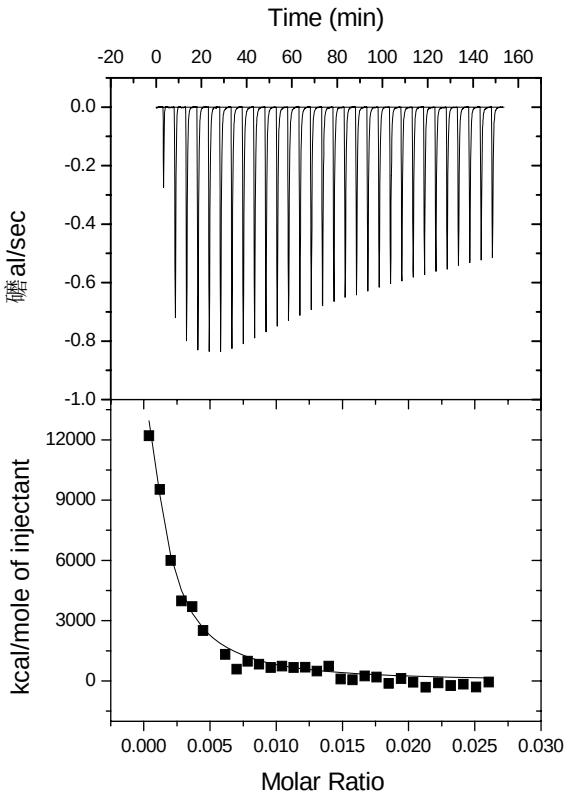

6.3.4 MIPs evaluation by HPLC

After the preparation of MIPs, they were washed followed by rebinding tests. HPLC was used to monitor whether the polymers were washed clean enough for the rebinding and how much templates were absorbed in the rebinding test.

After the polymers were prepared, they were transferred to a 96-well filter plate and dried under vacuum. Afterwards they were incubated in 600 μL of buffer for 24 hours, and the solutions were sucked under vacuum into microplates from which samples were taken for the subsequent measurements. Then the polymers were washed by successive steps with 500 μL 10 mM of HCl (PH 2) solution for 50 times, and incubated again with 600 μL of buffer. The concerntration of the free template in the two batches of incubation solution were determined by a reversed-phase HPLC.

When HPLC showed that there was no any residue in the polymers, they were dried and ready for the rebinding test. 750 μL of **T1** and **T3** in 10 mM Hepes buffer (PH 7.0) was added into the polymers. After 24 hours incubation, the solutions were taken for subsequent measurements. For the polymers made with monomer **5**, before rebinding, 1 μmol solution of $NiSO_4 \cdot 6H_2O$ was used to wash the polymers in order to let the binding sites saturated with nickel ion. Standard solutions of free templates were measured parallarly with the samples, in order to make calibration curves at the used condition (Figure 6.5).

Every single case was measured for two times and the average value was used for the evaluation.

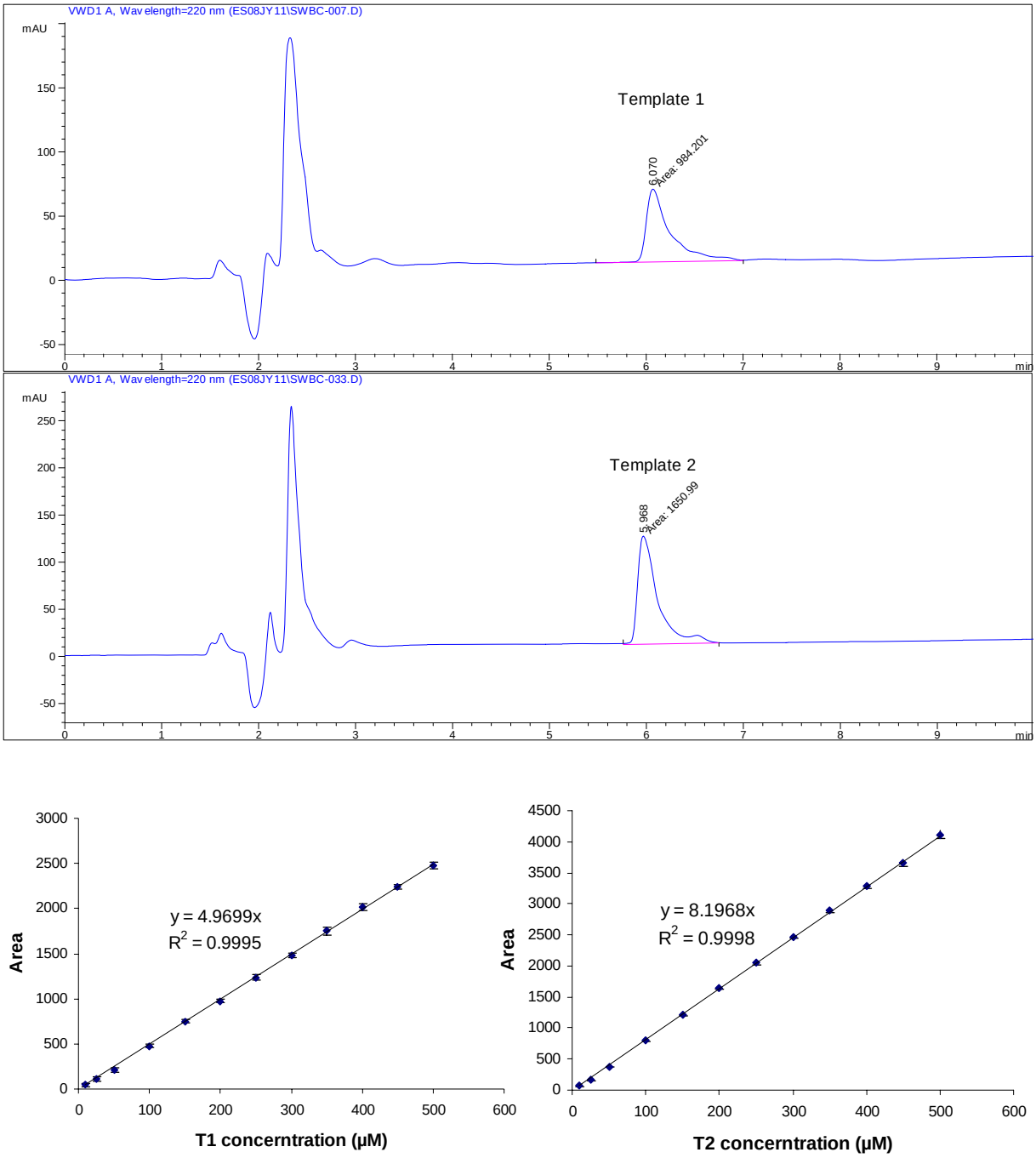

Figure 6.5 *Up) Reversed-phased HPLC analysis of the two templates T1 and T3 by a sequential washing with 0.1% TFA in acetonitrile and 0.1% TFA in water; down) calibration curves with the concerntration of 10, 25, 50, 100, 150, 200, 250, 300, 350, 400, 450, 500 uM made by HPLC.*

6.3.5 BCA assay

The BCA™ Protein assay is a detergent-compatible formulation based on bicinchoninic acid (BCA) for the colorimetric detection and quantitation of total protein. This method combines the well known reduction of Cu^{+2} to Cu^{+1} by protein in an alkaline medium (the biuret reaction) with the highly sensitive and selective colorimetric detection of the cuprous cation (Cu^{+1}) using a unique reagent containing bicinchoninic acid. The purple colored reaction product of this assay is formed by the chelation of two molecules of BCA with one cuprous ion. This water soluble complex exhibits a strong absorbance at 562 nm that is nearly linear with increasing protein concentrations over a range of 20-2000 μg/ml.

All the measurements were performed on the microplate. The BCA working reagent was prepared by mixing 50 parts of BCA reagent A with 1 part of BCA reagent B. 100 μL of the solutions containing proteins or peptides were pipetted into the wells and 800 μL of the BCA working reagent were added to each well. The microplate was covered and incubated on a plate shaker for 2 hours at 37 °C. Then the plate was measured at 562 nm on a UV/Vis reader.

For each measurement a calibration curve must be made parallarly in order to get an exact evaluation, because the color response of the reagent to the peptide or protein has relationship with time. The longer the incubation time was, the deeper the color became.

Example 1: BCA assay mesurement for poly M1-co-M2 membrane and the dealkylated salt analogue, Li-poly- M1-co-M2 membrane

The membranes were incubated in a 1 ml stock solution of the proteins (~ 35 μg/ml) for 12 hours. Then 100 μL of the solutions were taken out and measured in the same way as described above. Afterwards the membrane was washed with 5 ml buffer for three times and incubated in 1M NaCl solution for another 12 hours. The incubation NaCl solution was measured again.

Poly M1-co-M2 membrane with lysozyme

Calibration

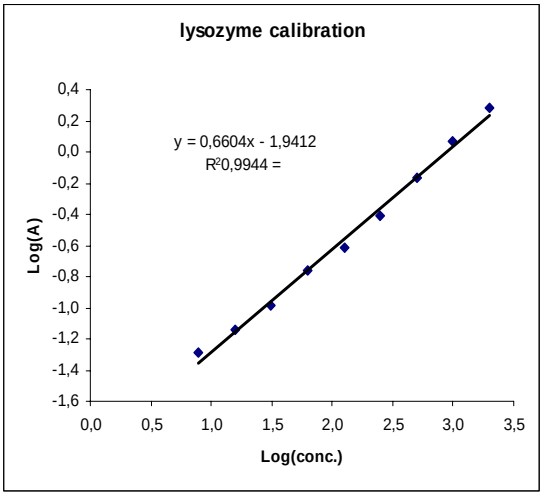

Protein Conc. [µg/ml]	UV Absorbance	Log (P.Conc.)	Log (UV Abs.)
2000	1,9190	3,3010	0,2831
1000	1,1710	3,0000	0,0686
500	0,6890	2,6990	-0,1618
250	0,3925	2,3979	-0,4062
125	0,2435	2,0969	-0,6135
62,5	0,1740	1,7959	-0,7595
31,25	0,1035	1,4949	-0,9851
15,63	0,0715	1,1938	-1,1457
7,81	0,0515	0,8928	-1,2882

Samples

	Stock Solution	36	0,1225	1,5587	-0,9119
1st incubation solution	PolyM1 graftedMembrane	14	0,0640	1,1317	-1,1938
	Poly M1-co-M2 grafted Membrane	34	0,1165	1,5256	-0,9337
NaCl incubation solution	PolyM1 graftedMembrane	7	0,0420	0,8547	-1,3768
	Poly M1-co-M2 grafted Membrane	28	0,1025	1,4414	-0,9893

Lithiated Poly M1-co-M2 membrane with lysozyme

	Stock Solution	101
1st incubation solution	PolyM1 graftedMembrane	85
	Li-Poly M1-co-M2 grafted Membrane	94
NaCl incubation solution	PolyM1 graftedMembrane	3
	Li-Poly M1-co-M2 grafted Membrane	9

Poly M1-co-M2 membrane with cytochrome C

Calibration

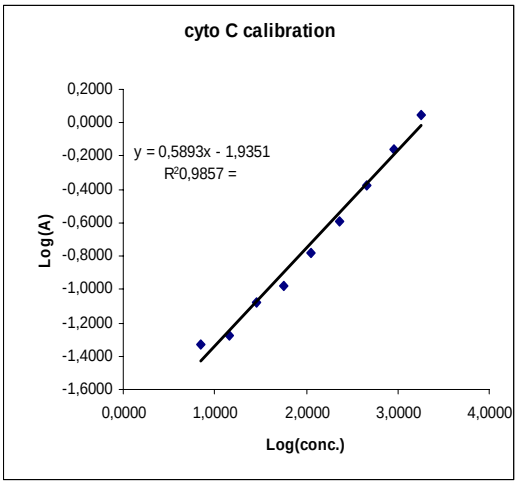

Protein Conc. [µg/ml]	UV Absorbance	Log (P.Conc.)	Log (UV Abs.)
1820	1,1245	3,2601	0,0510
910	0,6945	2,9590	-0,1583
455	0,4195	2,6580	-0,3773
227,5	0,2550	2,3570	-0,5935
113,75	0,1665	2,0560	-0,7786
56,88	0,1060	1,7549	-0,9747
28,44	0,0830	1,4539	-1,0809
14,22	0,0535	1,1529	-1,2716
7,11	0,0470	0,8518	-1,3279

Samples

	Stock Solution	34	0,0935	1,5373	-1,0292
1st incubation solution	PolyM1 graftedMembrane	35	0,0945	1,5451	-1,0246
	Poly M1-co-M2 grafted Membrane	26	0,0791	1,4140	-1,1018
NaCl incubation solution	PolyM1 graftedMembrane	6	0,0337	0,7852	-1,4724
	Poly M1-co-M2 grafted Membrane	5	0,0311	0,7260	-1,5072

Lithiated Poly M1-co-M2 membrane with cytochrome C

	Stock Solution	33
1st incubation solution	PolyM1 graftedMembrane	24
	Li-Poly M1-co-M2 grafted Membrane	24
NaCl incubation solution	PolyM1 graftedMembrane	5
	Li-Poly M1-co-M2 grafted Membrane	7

Poly M1-co-M2 membrane with meoglobin

Calibration

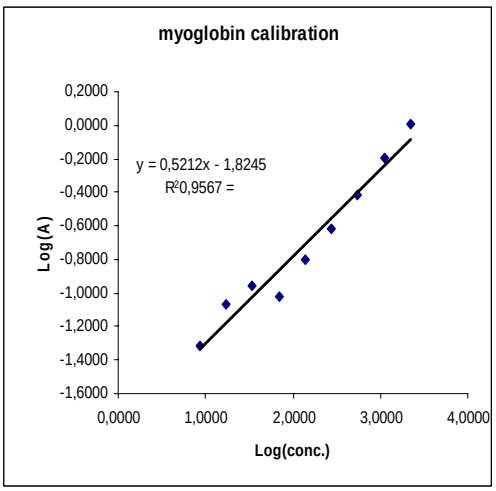

Protein Conc. [µg/ml]	UV Absorbance	Log (P.Conc.)	Log (UV Abs.)
2200	1,0250	3,3424	0,0107
1100	0,6370	3,0414	-0,1959
550	0,3855	2,7404	-0,4140
275	0,2395	2,4393	-0,6207
137,5	0,1565	2,1383	-0,8055
68,75	0,0950	1,8373	-1,0223
34,38	0,1095	1,5362	-0,9606
17,19	0,0865	1,2352	-1,0630
8,59	0,0480	0,9342	-1,3188

Samples

	Stock Solution	35	0,0960	1,5479	-1,0177
1st incubation solution	PolyM1 graftedMembrane	25	0,0795	1,3908	-1,0996
	Poly M1-co-M2 grafted Membrane	28	0,0851	1,4475	-1,0701
NaCl incubation solution	PolyM1 graftedMembrane	3	0,0281	0,5242	-1,5513
	Poly M1-co-M2 grafted Membrane	5	0,0340	0,6830	-1,4685

Lithiated Poly M1-co-M2 membrane with meoglobin

	Stock Solution	40
1st incubation solution	PolyM1 graftedMembrane	48
	Li-Poly M1-co-M2 grafted Membrane	47
NaCl incubation solution	PolyM1 graftedMembrane	3
	Li-Poly M1-co-M2 grafted Membrane	4

7 Abbreviation list

AIBN	Azobis(isobutyronitrile)
Arg	Arginine
BOC	*tert*.-Butyloxycarbonyl
BOC_2O	Di-tert.-butyldicarbonate
BSA	Bovine serum albumin
Cyt C	Cytochrom C
Da	Dalton (1 Da = 1 g/mol)
DBU	1,8-Diazabicyclo[5.4.0]undec-7-ene
DCC	N,N'-Dicyclohexylcarbodiimide
DMAP	4-(*N,N*-Dimethylamino)pyridine
DMF	*N,N*-Dimethylformamide
DMSO	Dimethylsulfoxide
EDMA	Ethylendimetharylamide
EDC	1-Ethyl-3-(3-dimethylaminopropyl) carbodiimide hydrochloride
ESI	Elekrosprayionisation

HRMS	High resolution mass spectrum
ITC	Isothermal titration calorimetry
Lys	Lysin
MMA	Methylmethacrylate
MWCO	molecular weight cut-off
PEI	Polyethylenimine
ppm	Parts per million
RT	Room temperature
SEC	Size exclusion chromatography
SDS	Sodiumodecylsulfate
T3P	Tris-2-propanephosphonic acid anhydride
TFA	Trifluoroacetic acid
THF	Tetrahydrofuran
Z	Benzyloxycarbonyl
V-50	2, 2'-Azobis(2-methylpropionamidine)dihydrochloride

8 Literature

[1] M. W. Peczuh, A. D. Hamilton, *Chem. Rev.* **2000**, *100*, 2479-2493.

[2] H. S. Park, Q. Lin, A. D. Hamilton, *J. Am. Chem. Soc.* **1999**, *121*, 8-13.

[3] R. Zutshi, J. Franciskovich, M. Shultz, B. Schweitzer, P. Bishop, M. Wilson, J. Chmielewski, *J. Am. Chem. Soc.* **1997**, *119*, 4841-4845.

[4] B. D. Ratner, *J. Mol. Recognit.* **1996**, *9*, 617-625.

[5] A. J. Golumbfskie, V. S. Pande, A. K. Chakraborty, *Proc. Natl. Acad. Sci.* **1999**, *96*, 11707-11712.

[6] M. Mammen, S. K. Choi, G. M. Whitesides, *Angew. Chem. Int. Ed.* **1998**, *37*, 2754-2794.

[7] M. R. Eftink, A. C. Anusiem, R. L. Biltonen, *Biochemistry* **1983**, *22*, 3884-3896.

[8] H. Yin, A. D. Hamilton, *Angew. Chem. Int. Ed.* **2005**, *44*, 4130-4163.

[9] N. W. Boyce, S. R. Holdsworth, *Kidney Int.* **1989**, *36*, 537-544.

[10] S. K. Dower, C. DeLisi, J. A. Titus, D. M. Segal, *Biochemistry* **1981**, *20*, 6326-6334.

[11] W. Engelhardt, H. Gorczytza, A. Butterweck, H. Moenkemann, J. Frey, *Eur. J. Immunol.* **1991**, *21*, 2227-2238.

[12] Y. Hamuro, M. C. Calama, H. S. Park, A. D. Hamilton, *Angew. Chem. Int. Ed.* **1997**, *36*, 2680-2683.

[13] Q. Lin, H. S. Park, Y. Hamuro, C. S. Lee, A. D. Hamilton, *Biopolymers* **1998**, *47*, 285-297.

[14] H. Takashima, S. Shinkai, I. Hamachi, *Chem. Commun.* **1999**, 2345-2346.

[15] N. O. Fischer, C. M. McIntosh, J. M. Simard, V. M. Rotello, *Proc. Natl. Acad. Sci.* **2002**, *99*, 5018-5023.

[16] R. Hong, N. O. Fischer, A. Verma, C. M. Goodman, T. Emrick, V. M. Rotello, *J. Am. Chem. Soc.* **2004**, *126*, 739-743.

[17] B. S. Sandanaraj, D. R. Vutukuri, J. M. Simard, A. Klaikherd, R. Hong, V. M. Rotello, S. Thayumanavan, *J. Am. Chem. Soc.* **2005**, *127*, 10693-10698.

[18] S. Koch, C. Renner, X. Xie, T. Schrader, *Angew. Chem. Int. Ed.* **2006**, *45*, 6352-6355.

[19] G. Wulff, *Angew. Chem. Int. Ed.* **1995**, *34*, 1812-1832.

[20] N. W. Turner, C. W. Jeans, K. R. Brain, C. J. Allender, V. Hlady, D. W. Britt. *Biotechnol. Prog.* **2006**, *22*, 1474-1489.

[21] A. Rachkov, N. Minoura, *J. Chromatogr. A.* **2000**, *889*, 111-118.

[22] A. Rachkov, N. Minoura, *Biochim. Biophys. Acta* **2001**, *1544*, 255-266.

[23] H. Nishino, C. S. Huang, K. J. Shea, *Angew. Chem. Int. Ed.* **2006**, *45*, 2392-2396.

[24] S. Rensing, A. Springer, T. Grawe, T. Schrader, *J. Org. Chem.* **2001**, *66*, 5814-5821.

[25] R. P. Dixon, S. J. Geib, A. D. Hamilton, *J. Am. Chem. Soc.* **1992**, *114*, 365-366.

[26] A. Echavarren, A. Galan, J. M. Lehn, J. de Mendoza, *J. Am. Chem. Soc.* **1989**, *111*, 4994-4995; B. Dietrich, D. L. Fyles, T. M. Fyles, J. M. Lehn, *Helv. Chim. Acta* **1979**, *62*, 2763-2767; A. Echavarren, A. Galan, J. de Mendoza, A. Salmeron, J. M. Lehn, *Helv. Chim. Acta* **1988**, *71*, 685-688.

[27] F. P. Schmidtchen, *Tetrahedron Lett.* **1989**, *30,* 4493-4496; G. Mueller, J. Riede, F. P. Schmidtchen, *Angew. Chem., Int. Ed.* **1988**, *27*, 1516-1518; H. Kurzmeier, F. P. Schmidtchen, *J. Org. Chem.* **1990**, *55*, 3749-3755.

[28] D. M. Kneeland, K. Ariga, V. M. Lynch, C. Huang, E. V. Anslyn, *J. Am. Chem. Soc.* **1993**, *115*, 10042-10055

[29] P. A. Frey, W. W. Cleland, *Bioorg. Chem*. **1998**, *26*, 175-192.

[30] M. D. Abul Fazal, B. C. Roy, S. Sun, S. Mallik, K. R. Rodgers, *J. Am. Chem. Soc.* **2001**, *123,* 6283-6290.

[31] W. Bal, J. Christodolou, P. J. Sadler, A. J. Tucker, *Inorg. Biochem,* **1998**, *70*, 33-39; (b) P. J. Sadler, J. H. Viles, *Inorg. Biochem.* **1996**, *35*, 4490-4496.

[32] G. Changa, D. E. Bochkariov, G. G. Jokhadze, J. Hopp, P. Nelson, *J. Chromatogr. A* **1999**, *864*, 247-256; U. Sideneus, O. Farver, O. Jons, B. Gamelgaard, *J. Chromatogr. B* **1999**, *735*, 85-91; M. Y. Wang, Y. Y. Kau, M. S. Lee, S. R. Doong, J. Y. Ho, L. H. Lee, *Biotechnol. Bioeng*. **2000**, *67*, 104-111; H. P. Wu, D. F. Bruley, *Biotechnol. Prog*. **1999**, *15*, 928-931.

[33] K. Ng, D. W. Pack, D. Y. Sasaki, F. H. Arndd, *Langmuir* **1995**, *11*, 4048-4055; C. Dietrich, O. Boscheinen, K. D. Scharf, L. Schmitt, R. Tampe, *Biochemstr* **1996**, *35*, 1100-1105; D. W. Pack, F. H. Arnold, *Chem. Phys. Lipids* **1997**, *86*, 135-152; G. B. Sigal, C. Bamdad, A. Barberies, J. Strominger, G. M. Whitesides, *Anal. Chem*. **1996**, *68*, 490-497; D. Kroger, M. Liley, W. Schiweck, A. Skerra, *Biosens. Bioelectr*. **1999**, *14*, 155-161.

[34] D. W. Pack, G. Chen, K. M. Maloney, C. T. Chen, F. H. Arnold. *J. Am. Chem. Soc.* **1997**, *119*, 2479-2487.

[35] E. Hochuli, H. Dobeli, A. Schacher, *J. Chromatogr.* **1987**, *411*, 177-184.

[36] H. D. James, K. R. A. S. Sandanayake, S, Shinka, *Angew. Chem. Int. Ed.* **1996**, *35*, 1910-1922.

[37] G. Wulff, *Pure Appl. Chem.* **1982**, *54*, 2093-2102.

[38] K. Burgess, A. M. Porte, *Angew. Chem.* **1994**, *106*, 1218-1220; S. L. Wiskur, J. J. Lavigne, A. Metzger, S. L. Tobey, V. Lynch, E. V. Anslyn, *Chem. Eur. J.* **2004**, *10*, 3792-3804.

[39] Y. Yang, P. T. Lewis, J. O. Escobedo, N. N. St. Luce, W. D. Treleaven, R. L. Cook, R. M. Strongin, *Collect. Czech. Chem. Commun.* **2004**, *69*, 1282-1291; H. Otsuka, E. Uchimura, H. Koshino, T. Okano, K. Kataoka, *J. Am. Chem. Soc.* **2003**, *125*, 3493-3500.

[40] C. W. Gray, T. A. Houston, J. org. Chem. **2002**, *67*, 5246-5248.

[41] Dissertation of K. M. Maue, Universität Marburg, **2006**.

[42] C. A. Wartchow, P. Wang, M. D. Bednarski, M. R. Callstrom, *J. Org. Chem.* **1995**, *60*, 2216-2226.

[43] C. Kahle, U. Holzgrabe, Chirality **2004**, *16*, 509-515.

[44] S. A. Piletsky, H. S. Andersson, I. A. Nicholls, *Macromolecules* **1999,** *32,* 633-636.

[45] R. C. Petter, J. S. Salek, C. T. Sikorski, G. Kumaravel, F. T. Lin, *J. Am. Chem. Soc.* **1990**, *112,* 3860-3868.

[46] J. M. Walker, *Methods Mol. Biol.* **1994**, *32*, 321–8; *Methods Mol. Biol.* **1994**, *32*: 329-334.

[47] K. J. Shea, D. Y. Sasaki, *J. Am. Chem. Soc.* **1989**, *111*, 3442-3444.

[48] http://www.sciencegateway.org/resources/fae1.htm

[49] N.S. Finney, *Current Opinion in Chemical Biology*, **2006**, *10*, 238-245.

[50] V. Saudek, J. Kdlal, *Makromol. Chem.* **1976**, *177*, 2833-2848.

[51] G. Wegner, *Z. Naturforsch. Teil B*, **1969**, *24*, 824-832.

[52] W. Chodkiewicz, P.C. Cadiot, *C. R. Hebd. Acad. Sci.* **1955**, *241*, 1055-1057.

[53] T. Clackson, M. H. Ultsch, J. A. Wells, A. M. Vos, *J. Mol. Biol.* **1998**, *277*, 1111-1128; J. A. Wells, *Proc. Natl. Acad. Sci. USA.* **1996**, *93*, 1-6; A. A. Bogan, K. S. Thorn, *J. Mol. Biol.* **1998**, *280*, 1-9; T. Clackson, J. A. Wells, *Science* **1995**, *267*, 383-386.

[54] J. Pontius, J. Richelle, S. J. Wodak, *J. Mol. Biol.* **1996**, *264*, 121-136.

[55] G. M Dykes, *J Chem. Technol. Biotechnol.* **2001**, *76*, 903-918.

[56] O. A. Matthews, A. N. Shipway, J. F. Stoddart, *Prog. Polym. Sci.* **1998**, 23, 1-56.

[57] S. E. Stiriba, H. Frey, R. Haag, *Angew. Chem. Int. Ed.* **2002**, *41*, 1329-1334; R. Haag, *Angew. Chem. Int. Ed.* **2004**, *43*, 278-282.

[58] I. Gössl, L. Shu, A. D. Schlüter, J. P. Rabe, *J. Am. Chem. Soc.* **2002**, *124*, 6860-6865; A.W. Bosman, H.M. Janssen, E.W. Meijer, *Chem. Rev.* **1999**, *99*, 1665-1688; M. Liu, J. M. Frechet, *Pharm. Sci. Technol. Today* **1999**, *2*, 393-401.

[59] B. L. Nilsson, L. L. Kiessling, R. T. Raines, *Org. Lett.* **2001**, *3*, 9-12.

[60] L. Eckardt, K. Naumann, W. M. Pankau, M. Rein, M. Schweitzer, N. Windhab, G. von Kiedrowski, *Nature* **2002***, 420*, 281-286.

[61] H. C. Kolb, M. G. Finn, K. B. Sharpless, *Angew. Chem. Int. Ed.* **2001**, *40*, 2004-2021; R. Manetsch, A. Krasinski, Z. Radic, J. Raushel, P. Taylor, K. B. Sharpless, H. C. Kolb, *J. Am. Chem. Soc.* **2004**, *126*, 12809-12818; N. J. Agard, J. A. Prescher, C. R. Bertozzi, *J. Am. Chem. Soc.* **2004**, *126*, 15046-15047.

[62] X. Li, Z. Y. J. Zhan, R. Knipe, D. G. Lynn, *J. Am. Chem. Soc.* **2002**, *124*, 746-747.

[63] M. J. Hynes, *J. Chem. Soc. Dalton Trans.* **1993**, 311-312.

[64] M. Fineman, S. D. Ross, *J. Polym. Sci.* **1950**, *5*, 259-262.

[65] C. Renner, J. Piehler, T. Schrader, *J. Am. Chem. Soc*. **2006**, *128*, 4831-4841.

[66] Dissertation of Mathius Junkers, Universität Marburg, **2006**.

[67] Z. Zhong, E. V. Anslyn, *J. Am. Chem. Soc.* **2002**, *124*, 9014 – 9015; A. T. Wright, Z. Zhong, E. V. Anslyn, *Angew. Chem. Int. Ed.* **2005**, *44*, 5679-5682.

[68] M. Maue, T. Schrader, *Angew. Chem. Int. Ed.* **2005**, *44*, 2265-2270.

[69] K. Djanashvili, L. Frullano, J. A. Peters, *Chem. Eur. J.* **2005**, *11,* 4010-4018.

[70] J. Hirsh, J. E. Dalen, D. Deykin, L. Poller, *Chest* **1992**, *102*, 337–352.

[71] G. P. Gravlee, L. D. Case, K. C. Angert, A. T. Rogers, G. S. Miller, *Anesth. Analg.* **1988**, *67*, 469-472; J. Umlas, R. H. Taff, G. Gauvin, P. Sweirk, *Anesth. Analg.* **1983**, *62*, 1095-1099; S. Mathison, E. Bakker, *Anal. Chem.* **1999**, *71*, 4614-4621; T. J. Cheng, T.-M. Lin, T. H. Wu, H. C. Chang, *Anal. Chim. Acta* **2001**, *432*, 101-111; N. Ramamurthy, N. Baliga, T. W. Wakefield, P. C. Andrews, V. C. Yang, M. E. Meyerhoff, *Anal. Biochem.* **1999**, *266*, 116-124.

[72] G. Odian, *Principles of Polymerization*, **1991**, John Wiley & Sons, Inc., New York.

[73] R. R. Change, Macromolecules, **1980**, *13*, 396-399.

[74] K. Kato, E. Uchida, E. T. Kang, Y. Uyama, Y. Ikada, *Prog. Polym. Sci*. **2003**, *28*, 209-259.

[75] D. M. He, M. Ulbricht, *J. Mater. Chem.* **2006**, *16*, 1860-1868.

[76] D. M. He, M. Ulbricht, *Macromol. Chem. Phys.* **2007**, *208*, 1582-1591.

[77] T. Schrader, *J. Org. Chem* **1998**, *63*, 264-272.

[78] C. Geismann, A. Yaroshchuk, M. Ulbricht, *Langmuir* **2007**, *23*, 76-83.

[79] F. A. Cotton, G. Wilkinson, *Advanced Inorganic Chemistry*, John Wiley & Sons, Inc. New York, **1988**.

[80] K. N. Plunkett, X. Zhi, J. S. Moore, D. E. Leckband, *Langmuir* **2006**, *22*, 4259-4266; A. Friebe, M. Ulbricht, *Langmuir* **2007**, *23*, 10316-10322.

[81] PROVE program (Protein Volume Evaluation): J. Pontius, J. Richelle, S. J. Wodak, *J. Mol. Biol.* **1996**, *264*, 121-136.

[82] C. Renner, T. Schrader, unpublished.

[83] R. G. Chapman, E. Ostuni, L. Yan, G. M. Whitesides, *Langmuir* **2000**, *16*, 6927-6936.

[84] D. M. He, M. Ulbricht, *J. Membr. Sci.* **2008**, *315*, 155-163.

[85] M. *J.* Stiger, *Chem. Phys.* **2004**, *120*, 6197-6206; X. Wu, R. Pelton, A. Hamielec, D. Woods, W. Mcphee, *Colloid Polym. Sci*. **1994**, *272*, 467-477.

[86] H. Kawaguchi, *Front. Biomed. Biotechnol.* **1996**, *3,* 157-161.

[87] S. Lindman, I. Lynch, E. Thulin, H. Nilsson, K. A. Dawson, S. Linse, *Nano Lett.* **2007**, *7,* 914-920.

[88] A. Tominey, D. Andrew, L. Oliphant, G. M. Rosair, J. Dupré, A. Kraft, *Chem. Commun.* **2006**, *11*, 2486-2492.

[89] A.Taden, A. H. Tait, A. Kraft, *J. Polym. Sci., Polym. Chem.* **2002**, *40*, 4333-4343.

[90] I. Lynch, I. Miller, W. M. Gallagher, K. A. Dawson, *J. Phys. Chem. B* **2006**, *110*, 14581-14589; I. Lynch, K. A. Dawson, *J. Phys. Chem. B* **2004**, *108*, 10976-10983.

[91] K. A. Connors, *Binding constants*, Wiley, New York, **1987**.

[92] G. Maksay, *Neurochem. Int*. **2005**, *46*, 281-291.

[93] D. S. Janiak, P. Kofinas, *Anal. Bioanal.Chem*, **2007**, *389*, 399-404.

[94] B. Sellergren, *Angew. Chem. Int. Ed*. **2000**, *39*, 1031-1037.

[95] M. E. Byrne, K. Park, N. A.Peppas, *Adv. Drug Deliv. Rev*. **2002**, *54*, 149-161.

[96] B. Sellergren, *Trends Anal. Chem.*, **1997**, *16*, 310-320.

[97] L. I. Andersson, K. Mosbach, *J Chromatogr. A*, **1990**, 516, 313-322.

[98] M. Kempe, K. Mosbach, *J Chromatogr. A* **1995**, *691*, 317-323.

[99] B. Sellergren, M. Lepisto, K. Mosbach*, J Am. Chem. Soc.* **1998**, *110*, 5853-5860.

[100] L. I. Andersson, D. J. O'Shannessy, K. Mosbach, *J Chromatogr*. **1990**, *513*, 167-179.

[101] L. I. Andersson, A. Miyabayashi, D. J. O'Shannessy, K. Mosbach, *J Chromatogr.* **1990**, *16*, 323-331.

[102] A.Kugimiya, J. Matsui, T. S. Takeuchi, *Mater. Sci. Eng. C* **1997**, *4*, 263-266.

[103] K. Haupt, A. Dzgoev, K. Mosbach, *Anal. Chem.***1998**, *70*, 628-631.

[104] N. Perez-Moral, M. J. Whitcombe, E. N. Vulfson, *J. Appl. Polym. Sci.* **2000**, *77*, 1851-1859.

[105] N. Perez-Moral, M. J. Whitcombe, E. N. Vulfson, *Macromolecules* **2001**, *34*, 830-836.

[106] S. R. Carter, S. Rimmer, *Abstr. Pap. Am. Chem. Soc.,* **2002**, *224*, 363.

[107] S. R. Carter, S. Rimmer, *Ad*V. *Mater.* **2002**, *14*, 667-670.

[108] M. Han, R. Kane, M. Goto, G. Belfort, *Macromolecules,* **2003**, *36*, 4472-4477.

[109] N. W. Turner, C. W. Jeans, K. R. Brain, C. J. Allender, V. Hlady, D. W. Britt, *Biotechnol. Prog.* **2006**, *22*, 1474-1489.

[110] A. Rachkov, N. Minoura, *J Chromatogr A* **2000**, *889*,111-118.

[111] A. Rachkov, N. Minoura, *Biochim Biophys Acta* **2001**, *1544*, 255-266.

[112] H. Nishino,, C. S. Huang, K. J. Shea, *Angew Chem. Int. Ed. Engl.* **2006**, *45*, 2392-2396.

[113] B. Dirion, Z. Cobb, E. Schillinger, L. I. Andersson, B. Sellergren, *J. Am. Chem. Soc.* **2003**, *125*, 15101-15109.

[114] F. Lanza, B. Sellergren, *Macromol. Rapid Commun.* 2**004**, *25*, 59-68.

[115] L. C. Junqueira, C. J. Carneiro, *Basic Histology,* McGraw-Hill, **2003**.

[116] B. Antes, S. Amon, A. Rizzi, S. Wiederkum, M. Kainer, O. Szolar, M. Fido, R. Kircheis, A. Nechansky, *J Chromatogr B* **2007**, *852*, 250-256.

[117] G. Wolf, *Antioxid. Redox Signal* **2006**, *7***,** 1337-1345.

[118] F. Lanza, B. Sellergren, *Macromol. Rapid Commun.* **2004**, *25*, 59-68.

[119] K. Ariga, T. Kunitake, *Acc. Chem. Res.* **1998**, *31*, 371-378.

[120] H. Shi, W. B. Tsai, M. D. Garrison, S. Ferrari, B. D. Ratner, *Nature* **1999**, *398*, 593-597.

[121] G. Demirel, G. Ozcetin, E. Turan, T. Caykara, *Macromol. Biosci.* **2005**, *5*, 1032-1037.

[122] S. A. Piletsky, H. S. Andersson, I. A. Nicholls, *Macromolecules* **1999**, *32*, 633-636.

[123] B. R. Hart, K. J. Shea, *Macromolecules* **2002**, *35*, 6192-6201.

[124] A. Ellwagner, C. Berggren, S. Bayoudh, C. Crecenzi, L. Karlsson, P. K. Owens, K. Ensing, P. Cormack, D. Sherrington, B. Sellergren, *Analyst* **2001**, *126*, 784-792.

[125] D. M. Hawkins, D. Stevenson, S. M. Reddy, *Anal. Chim. Acta* **2005**, *542*, 61-65.

[126] C. K. Mathews, K. E. V. Holde, *Biochemistry*, Benjamin/Cummings publishing company, **1995.**

[127] D. G. Anderson, D. M. Lynn, R. Langer, *Angew. Chem. Int. Ed.* **2003**, *42*, 3153-3158.

[128] T. G. Park, A. F. Hoffman, *J. of Biomecial Material Research* **1990**, *24*, 21-38.

[129] D. D. Perrin, W. L. F. Armatego, *Purification of Laboratory Chemicals, 3rd. ed.*,

Pergamon Press, New York, **1988**.

[130] H. G. O. Becker, W. Berger, G. Domschke, E. Fanghänel, J. Faust, M. Fischer, F. Gentz, K. Gewald, R. Gluch, R. Mayer, K. Müller, D. Pavel, H. Schmidt, K. Schollberg, K. Schwetlick, E. Seiler, G. Zeppenfeld, *Organikum, 20. Aufl.*, J. A. Barth Verlag, Heidelberg, Leipzig, **1996**.

[131] W. C. Still, M. Kahn, A. Mitra, *J. Org. Chem.* **1978**, *43*, 2923-2925.

[132] H. E. Gottlieb, V. Kotyar, A. Nudelman, *J. Org. Chem.* **1997**, *62*, 7512-7515.

[133] W. C. Still, A. Tempczyk, R. C. Hawley, T. Hendrickson, *J. Am. Chem. Soc.* **1990**, *112*, 6127-6129.

[134] A. R. Leach, *Molecular Modelling*, *2 ed.*, Pearson Education Limited, Harlow, **2001**.

[135] A. Mitra, S. Ghorai, A. Bhattacharjya, A. Basak, R. T. Williamson, *J. Org. Chem.* **2003**, *68*, 617-620.

[136] W. Q. Tian, Y. A. Wang, *J. Org. Chem.* **2004**, *69*, 4299-4308; F. L. Lin, H. M. Hoyt, H. van Halbeek, R. G. Bergman, C. R. Bertozzi, *J. Am. Chem. Soc*, **2005**, *127*, 2686-2695.

[137] S. Han, R. A. Moore, R. Viola, Bioorganic Chemistry **2002**, *30*, 81-94.

[138] T. Reschel, C. Koňák, D. Oupický, L. W. Seymour, K. Ulbrich, *J. of controlled Release* **2002**, *81*, 201-217.

[139] C. A. Wartchow, P. Wang, M. D. Bednarski, M. R. Callstrom, *J. Org. Chem.* **1995**, *60*, 2216-2226.

[140] J. Vacik, K. Ulbrich, J. Exner, J. Kopecek, *Collect. Czech. Chem. Commun*. **1978**, *43*, 1221-1226.

[141] E. L. Doyle, C. A. Hunter, H. C. Phillips, S. J. Webb, N. H. Williams, *J. Am. Chem. Soc.* **2003**, *125*, 4593-4599.

[142] D. Spivak, K, J. Shea, *J. Org. Chem.* **1999**, *64*, 4627-4634.

[143] E. Diez-Barra, J. C. Garcia-Martinez, S. Merino, R. del Rey, J. Rodriguez-Lopez, P. Sanchez-Verdu, J. Tejeda, *J. Org. Chem.* **2001**, *66*, 5664-5670.

[144] P. Job, *Compt. Rend.* **1925**, *180*, 928-930.

[145] H. J. Schneider, R. Kramer, S. Simova, U. Schneider, *J. Am. Chem. Soc.* **1988**, *110*, 6442-6448.

Appendix III: Publication List

Parts of this work are already published or submitted.

1. Dendrimeric Bisphosphonates for Multivalent Protein Surface Binding
   Markus Arendt, Wei Sun, Jens Thomann, Xiulan Xie, Thomas Schrader, *Chemistry Asian Journal*, **2006**, *1*, 544-554.

2. A Polymeric Fluorescence Sensor for Heparin
   Wei Sun, Heinz Bandmann, Thomas Schrader, *Chemistry European Journal*, **2007**, *13*, 7701-7707.

3. A noncovalent switch for lysozyme
   Kirstian Wenck, Sebastian Koch, Christian Renner, Wei Sun, Thomas Schrader, *Journal of the American Chemical Society*, **2007**, *129*, 16015-16019.

4. Protein adsorbers from surface-grafted copolymers with specific binding sites
   Dongming He[†], Wei Sun[†], Thomas Schrader, Mathias Ulbricht, *Journal of Material Chemistry*, **2009**, *19*, 253-260.

5. Selective molecular recognition of proteins using water-soluble receptor microgels
   Alan F. Tominey, Julia Liese, Wei Sun, Thomas Schrader, Arno Kraft, Submitted.

6. Development and evaluation of a fluorescence microplate assay for quantification of heparins and other sulphated carbohydrates
   Susanne Lühn, Thomas Schrader, Wei Sun, Susanne Alban, Submitted.

Appendix VII: Curriculum Vitae

Name: Wei Sun

Place/Date of Birth:
Shenyang, China / 11, Feb. 1976.

Educational Background

2005-2009 (Ph.D.):	Organic Chemistry, University of Duisburg-Essen, Germany.
Supervisor:	Prof. Dr. Thomas Schrader
2003-2005 (M.Sc):	Organic Chemistry, University of Siegen, Germany.
Supervisor:	Prof. Dr. Michael Schmittel
1994-1998 (B.E.):	Organic Chemistry, Tianjin University, China.

Work Experience

1998-2001:	Assistant Engineer
	Research Institute of Petroleum Processing, China
2001-2003:	Engineer
	Mettler-Toledo Instrument Co. Ltd., China